

MSIT Journal of Research –SATYAM

Volume 10 (2021-22)

Patron

Er. Kaptan Singh Ji

Chairman, Surajmal Memorial Education Society

Prof. Prem Vrat

Pro-Chancellor; Professor of Eminence and Chief Mentor, The NorthCap University, Gurugram
Former Director, IIT Roorkee
Former Vice-Chancellor, UPTU Lucknow
Former Professor and Division Chairman, Asian Institute of Technology, Bangkok, Thailand

Prof Ved Prakash

Former Chairman
University Grant Commission

Prof. Saroj Kaushik

Department of computer science & Engineering
IIT, Delhi

Dr Manisha Bharti

Associate Professor, Department of ECE
NIT, Delhi

Dr Kavita Khanna

Campus Director, Delhi Skill and Entrepreneurship
University, Delhi

Col (Dr) Ranjit Singh

Director
Maharaja Surajmal Institute of Technology

Prof Devi Singh

Former Director, IIM Lucknow and MDI Gurgaon
Founding Vice Chancellor, FLAME University, Pune

Dr N.K. Gupta

Member, National executive Council, ISTE, Delhi

Prof. S.D. Joshi

Department of Electrical Engineering
IIT, Delhi

Dr T.V. Vijay Kumar

Professor, School of Computer & Systems
JNU, Delhi

Dr Obbo Chandra Shekhar

HOD, Department of Electrical Engineering
NIT, Delhi

Dr Sushil Chandra

Scientist 'G', DRDO

Dr Amit M. Joshi

Assistant Professor
MNIT, Jaipur

Editor-in-Chief: Dr. Shaifali M. Arora

Faculty Editors: Dr Geetika Dhand, Dr Sakshi Rajput, Dr Parul

Student Editor: Mr. Deepak Sarangi (7th Sem, ECE(M)),

Mr Yash Mani Prakash (3rd Sem, ECE(M))



MSIT Journal of Research – SATYAM

is an annual publication of
MAHARAJA SURAJMAL INSTITUTE OF TECHNOLOGY

C-4, Janak Puri, New Delhi-110058(India)

Phones: 011-45037193/45656183

E-mail: satyamjournal@msit.in, Visit us at www.msit.in

Volume 10 (2021-22)

MSIT Journal of Research – SATYAM (MSITJR)

is an annual publication Surajmal Institute of Technology
C-4 Janakpuri, New Delhi – 110058

Editor-in-chief: **Dr. Shaifali M. Arora**

Copy Right © MSITJR – Vol. 10 (2021-22)

All rights reserved. No part of the material protected by this copyright notice may be reproduced or utilized in any form or by any means, electronic or mechanical including photocopying, recording or by any information storage and retrieval system, without the prior written permission from the copyright owner. However, permission is not required to copy abstracts of papers on condition that a full reference to the source is given.

ISSN 2319-7897

Disclaimer

The opinions expressed and figures provided in this journal are sole responsibility of the authors. The publisher and the editor bear no responsibility in this regard. Any or all such liabilities are disclaimed.

All disputes are subject to Delhi jurisdiction only

Address for Correspondence

Dr. Shaifali M. Arora

Editor-in-chief, MSIT Journal of Research,
Associate Professor, Department of ECE
Maharaja Surajmal Institute of Technology (MSIT)
C-4, Janakpuri, New Delhi-110058
Tel: 011-45037193/45656183
E-mail: satyamjournal@msit.in

Published and printed by Col. (Dr.) Ranjit Singh, Director, Maharaja Surajmal Institute of Technology (MSIT),
C-4, Janakpuri, New Delhi-110058 (INDIA), Tel: 011-45037193/45656183
Email: director@msit.in Visit us at www.msit.in

Contents

1.	Analog Computer: The Future of Technology	1
	<i>Divya Jatain, Ayushman Jha</i>	
2.	Analysis of Level of Education and Its Impact Assessment on Urban Sustainability in Badarpur Slums Area of Delhi	6
	<i>Harikesh Kumar, Yogesh</i>	
3.	Behavioural Finance: Understanding How Biases Impact Decisions	10
	<i>Nishtha Jatana, Drishti Pandita</i>	
4.	Design of Single Stage three Phase Grid Connected Photovoltaic System with MPPT	15
	<i>Shilpam Malik</i>	
5.	NewsDose – The News App	20
	<i>Shaily Malik, Sahil Aggarwal, Yuvraj Gupta, Vipul Goel, Vedansh Varshney</i>	
6.	RGB Image Encryption Algorithm Based on DNA Encoding and Chaos Map	23
	<i>Parul Chaudhary</i>	
7.	Human Pose Estimation and Recognition	26
	<i>Dr. Rinky Dwivedi, Koyel Datta Gupta, Kunal Saini, Apoorv Srivastava, Yugal</i>	
8.	Simulation of Battery Management System of Electric Vehicles	32
	<i>Rakhi Kamra, Annu Dagar, Smile Jandyal, Mohd Arif</i>	
9.	Hackers and Their Techniques	38
	<i>Dr. Kavita Sheoran, Vishrut Rana</i>	
10.	ECG - Analysis of Heart Disease	43
	<i>Geetika Dhand, Ayushi Gahlot, Gowrish Chhabra, Yukta</i>	
11.	Linux for Machine Learning	48
	<i>Krrish Malhotra, Nilay Datta</i>	
12.	Automatic Signature Detection using Image Processing	52
	<i>Sachit Rathee</i>	
13.	Short Deep-fake Video Generation from Text	55
	<i>Sandeep Kumar, Mayank Mani, Sakshi Munjal, D.D.V. Sai Ashish</i>	
14.	Summarization and Speech Synthesis for generating Audiobooks	61
	<i>Koyel Datta Gupta, Rinky Dwivedi, Amar Pratap Singh, Khush Malawaliya, Kshitij Kumar</i>	
15.	Energy Storage Solutions for Low-power Renewable Energy Harvesters: A Review	64
	<i>Suman Mann, Deepshikha Yadav</i>	
16.	Metro Station Infrastructure and Communication Systems	68
	<i>Dr. Jyoti Jain, Manav Pachnanda</i>	
17.	Investigation of Double Diffusive Flow of Nanofluid over a Linearly Stretching Vertical Riga Plate	72
	<i>Nidhi</i>	
18.	Stereoscopic Ray-Tracing for VR using Rasterization	77
	<i>Dr. Shalu, Rahul Kumar Sharma, P Silvanus, Somya Sanu</i>	
19.	Stacked Cylindrical, Rectangular, Cone Multi-layered Dynamic Resonator Antenna with Improved Gain and more Directive Beam	81
	<i>Richa Gupta, Meena Rao</i>	

20.	Axial Ratio Bandwidth and Gain Enhancement of a Stacked Rectangular Dielectric Resonator Antenna	87
	<i>Richa Gupta, Deepshika Yadav</i>	
21.	Periodic Heating System to Investigate Pyroelectric Performance	95
	<i>Deepak Goyal</i>	
22.	Digital Newspaper with Voice Assistant Using Alan AI	98
	<i>Archana Balyan, Deepshikha Yadav</i>	
23.	Future of Software Development Methods and Tools in A Hybrid, Post Covid World	104
	<i>Kirti Dahiya</i>	
24.	Designing of Photovoltaic MPP System with MATLAB Simulation	111
	<i>Monu Malik</i>	
25.	A High-Performance Stand-alone Solar PV Power System for Led Lights	117
	<i>Rakhi Kamra, Monu Malik, Annu Dagar, Shilpam Malik</i>	
26.	High-Efficiency Battery Charging with Switching Resonant Converter	120
	<i>Monu Malik, Rakhi Kamra</i>	
27.	Wireless Charging in Electric Vehicles	124
	<i>Monu Malik, Rakhi Kamra, Jagriti Krishnan</i>	
28.	Verilog Code Tester using Microcontroller	130
	<i>Najeeb Mohammad Khan, Aahan Bhargava, Karan Kumar</i>	
29.	Theorem of L_p-Norm by Linear Combination for Baskakov Durrmeyer Operators	133
	<i>Man Singh Beniwal</i>	
30.	Price Prediction Application on AWS	136
	<i>Sandeep Kumar, Jay Seth, Khushi</i>	
	REVIEWERS	146

Analog Computer: The Future of Technology

Divya Jatain¹, Ayushman Jha²

^{1,2}Department of Computer Science & Engineering
Maharaja Surajmal Institute of Technology, New Delhi
¹divyajatain@msit.in, ²ayushmanjha63553@gmail.com

Abstract-- In this research paper our aim is to revisit digital computing as well as analog computing and see its future in technology. We explore various mathematical aspects to represent an analog computer and define analog computing and find a link between digital computing and analog computing. The gap in the progression that was missing can be filled in an efficient way by using minimal resources and still receiving the same amount of output can be achieved by utilizing analog computing techniques. Digital computing is the trend in society that we are currently abiding by, but it is reaching its limit. and we have to increase that limit in order to continue development and advancement in order to achieve such feats we need to change our strategy. This paper suggests that more people should access analog technology so as to overcome the technological barriers we will be facing soon.

Keywords— General Purpose Analog Computer, Polynomial Circuit, Digital Optical Modules, Conserving energy.

I. INTRODUCTION

Digital technology is widely used in almost everything that runs on electricity. But due to high energy consumption and a position where technological advancement has almost become static, we need to introduce a new strategy and some modifications in the IT industry in order the redemption of rapid technological development. The idea of analog generability could be connected to abstract computability via a computable real function in the coming future.[8]

Analog computing provides the solution for the same problem. It is much more energy efficient and easy for simple problems such as adding two numbers, or solving differential equations and many more simple problems. We need to re-introduce analog technology to people in order to achive this. James Nyce also supported the arugment by saying that user could easily comprehend and relate to analog machines as compared to digital machines [3].

II. HISTORY

Analog computers were introduced way before digital computers, but due to the introduction of digital technology, much more gates to were open to technology and led to a change in focus towards digital technology, instead of analog technology. Though technology was scarce in ancient times, analog computers still existed, even though the terms came into existence afterward.

Though the first major breakthrough was achieved in 1931 by a MIT professor named Vannevar Bush who developed an

electromechanical analog computer differential analyzer to model power networks. He soon saw its value as a general-purpose analog computer. It was capable of solving differential equations up to the sixth order. It was the first practical and reliable device of its kind [1].

This was the next step in the foundation of mathematical analog computers. The concept of GPAC (General Purpose Analog Computer) came into effect in 1941 by a Shannon. He introduced it as a mathematical analog model which was termed as Differential Analyzer [2].

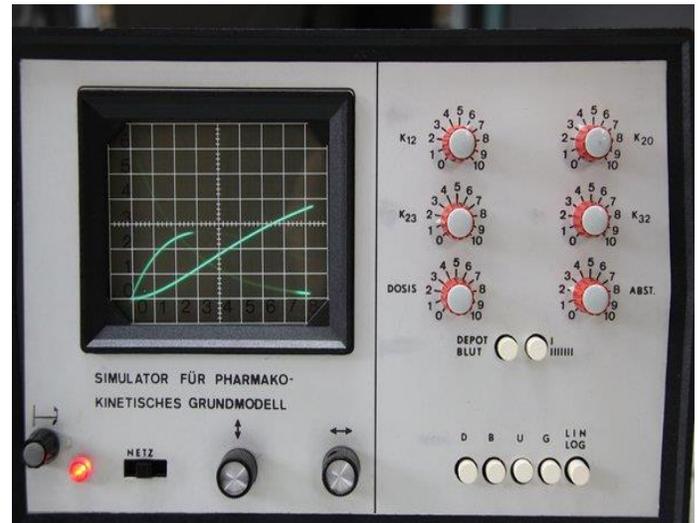


Fig. 1: Analog Computer

III. GOAL

Our goal is to introduce analog technology in the science field in the form of mathematical analog computers like differential analyzer. The gears could be replaced by circuits in order to make the setup cheap and easier to understand. It has the potential to become a very effective educational tool for further advancement in analog technology. A cheap modular computer like Arduino could be developed in order to promote innovation among students.[2][13]

Even those who operate in the digital sector may be drawn to the analogous sector. In order to optimize the advantages of both types of gadgets, it will be fascinating from their perspective to integrate the features of hybrid and digital machines. We will discuss various innovations related to analog technology

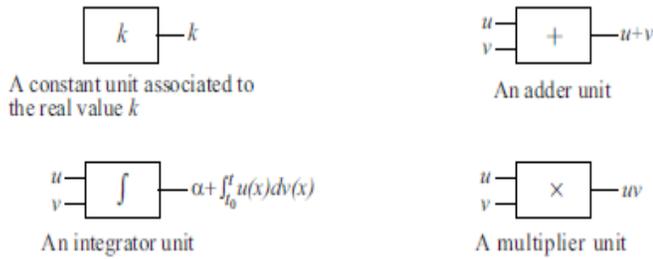


Fig. 2: Different Types of GPAC units

IV. BASIC MODEL

Here we will show one of our basic models. It is a restricted version of Shannon's GPAC [2]. We only need a single input which we refer as 'time'. In some of cases, we might need more than 1 input.

Using constant units, adders, and multipliers, we build acyclic circuits (polynomial circuits) that complete polynomials. We presume that a polynomial circuit might not contain any units at all for computing the identity in this scenario.

Second, use these circuits as the foundation for polynomial GPACs, which are more sophisticated GPACs (PGPAC for short). The next is the construction of a PGPAC. Consider n integrators I_i [7][11]. Next, we employ polynomial circuits to ensure that the following requirements are met:

1. Each of the inputs in the polynomial circuit serves as either an integrator's output or an input to a PGPAC.
2. Each of the inputs in the integrator is an integrand, and each of the output is a polynomial circuit.
3. The input of the PGPAC is each variable of an integrator's integration input.

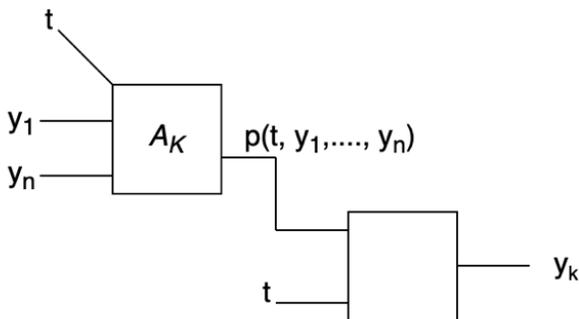


Fig. 3: Schema of inputs and outputs for the integrator in PGPAC.

A polynomial circuit has the following formal definition. Polynomial circuits are thought to be capable of having many inputs. It is up to the reader to provide evidence for the

following lemma.

Lemma 2

A polynomial circuit's output is defined as

$$y = p(x_1, \dots, x_n)$$

where p is a polynomial, and $x_1 \dots x_n$ are its inputs. A polynomial circuit with inputs x_1 through x_n and an output of y exists if

$$y = p(x_1, \dots, x_n)$$

where p is a polynomial[11].

Definition 3 Assume a GPAC U has n integrators, I_1, \dots, I_n , and a single input, t . Assume we can assign a polynomial to each integrator I_i , where $i = 1 \dots n$. Circuit I_i with the characteristic that an output of A_i is connected to I_i 's integrand input. Assume that each input of A_i is coupled to either the input t or the integrator's output. Assume that each integrator's variable of integration input is coupled to the input t . We state that U is a polynomial GPAC (PGPAC) with input t under these circumstances [10].

V. CURRENT USE IN TECHNOLOGY

A. Noise-Cancellation in Bowers & Wilkins:

Analog devices are used to emit frequency and that technology could be used to cancel voice whilst conserving energy at the same time.

Great-end audio maker Bowers & Wilkins, known for their range of signature speaker systems, thinks it has the solution: deliver superior sound engineering, high performance, and low power usage. Bowers & Wilkins overcome difficult technical obstacles with the assistance of their dependable technological partner, Analog Devices (ADI), and were able to reach a larger audience with their distinctive sound.[4][12] The PX5, PX7, and P14 adaptive noise-canceling wireless headphones were developed in partnership by ADI and Bowers & Wilkins to give listeners music in all its splendor.

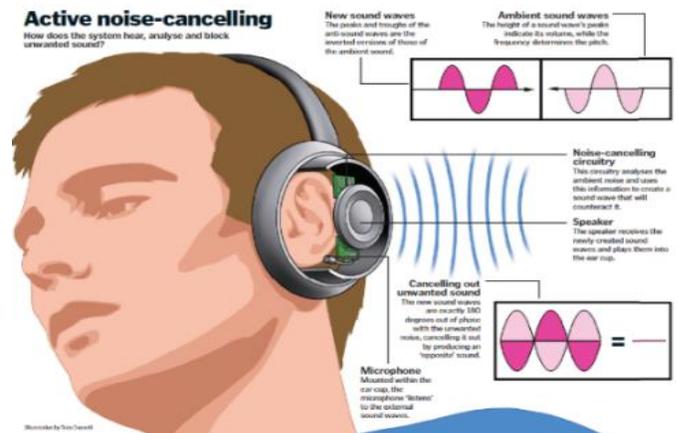


Fig. 4: How Active Noise Cancellation works

Although analog noise cancelling has been around for a while, ADI was among the first to develop a digital hybrid. In this context, the term "hybrid" refers to feedforward and feedback, with one tiny microphone monitoring the sound outside the headphones and another the sound within. The technology was incorporated into Bowers & Wilkins' noise-cancelling headphones. By repeating processes and averaging the outcome, we suggest expanding analogue computing architectures to allow dynamic degrees of precision. This will lessen the impact of noise. We suggest a technique for learning the accuracy of each layer of a pre-trained model without retraining network weights in order to use dynamic precision. Using dynamic precision, we are able to cut energy consumption by up to 89% for computer vision models like Resnet50 and by 24% for natural language processing models like BERT. We test this method on analogue architectures that are exposed to shot noise, temperature noise, and weight noise.[18]

The ANC (active noise cancellation) chip is simultaneously listening through built-in microphones to the noise created by an external source and the sound that is created by the headphone speaker playing into the ears.

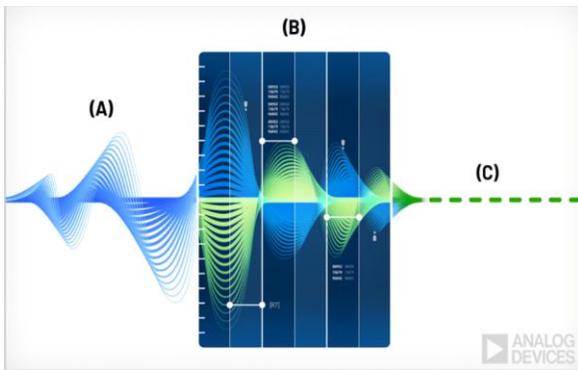


Fig. 5: Waveform of all the Noises considered in a frame

They created unique algorithms, integrated microphones, and an ANC chip that actively "listens" for any voice that could be outside of the domain (A) using the ANC chip, so only the filtered voice(C) could reach our ear. This process uses feedback and feedforward[17]. Digital processing needs to be quick in order to complete this task.

In a similar case, Hyundai motor company also used Analog Technology to Launch First All-Digital Road Noise Cancellation System [14].

B. Neutrino Detector

The largest neutrino detector in the world, IceCube, is permanently encased in solid Antarctic ice in order to gather data from elusive cosmic neutrinos produced by catastrophic astrophysical events like gamma ray bursts and star explosions. Antarctica is one of the most hostile locations for both people and technology, with recorded lows of - 125 degrees Fahrenheit. The IceCube Project, which is supported by the National

Science Foundation, chose converters and amplifiers from Analog Devices to give the digital optical modules (DOMs) of the detector the ability to gather data in this challenging environment. Reliability is essential because the parts of the DOMs should be capable of detecting and signalling data for more than 25 years without requiring maintenance or repair.

The IceCube detector's approximately 5,000 13" glass DOMs are positioned in an array to look for the blue light produced when a neutrino strikes an atom while it is moving through the ice sheet. DOMs are installed via 86 cables utilising a hot water drilling technique at ice depths of 1.5 km to 2 km.[16] When completed in 2011, the IceCube detector will occupy an enormous one cubic kilometer of space.

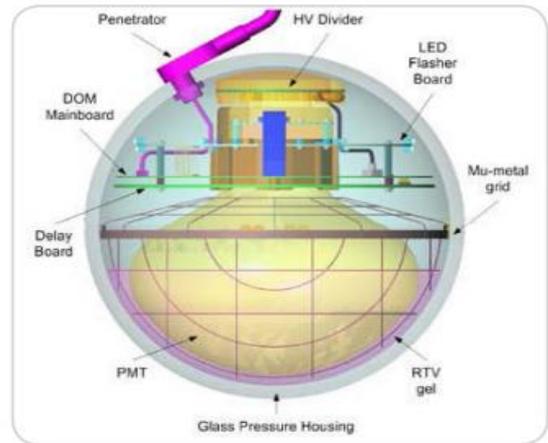


Fig. 6: Diagram of Neutrino Detector



Fig. 7: IceCube (Neutrino Detector)

Each DOM is a stand-alone data acquisition platform with the ability to digitise and record real-time photomultiplier tube (PMT) pulses, store data locally, and communicate digital data to a surface data collection system. A number of ADI components, such as high performance analog-to-digital and digital-to-analog converters, and ultralow power amplifiers, are used by each DOM. To within 5 nanoseconds, the DOMs can precisely calculate the arrival time of each photon.

The success of the project depends on reliability and precision, which makes it difficult for the design engineers to get the design perfect before implementation. IceCube DOM deployments could take 25,000 years to physically reach [18]. The project was a perfect match for Analog Devices' top-notch, thoroughly tested components, extensive and in-depth tools, and documentation [9].

VI. FUTURE OF ANALOG TECHNOLOGY

The multiple rules-based programming languages that are essential to digital computing are changed by analogue computing, which substitutes modifying the configuration of a computer to change the output. Early analogue computers were much more effective and complex than digital computers at the time because they were built to solve specific problems, like those used in the Apollo program. The main factors limiting an analogue computer's performance are its topology and physical limitations. It is prohibitively time-consuming to use analogue computers for complex tasks because each one must be manually programmed.

Analog computers have slowly regained popularity due to its use in replicating complicated processes that may not be achievable with the deterministic logic employed by digital computers, despite analogue computers having mostly been replaced by digital over the years. The best combinations of the two are hybrid systems that enable the analogue computer to perform tasks that the digital computer is unable to. The idea of hybrid computers is not new. For instance, hybrid computers are used in ICUs all around the world to digitise physiologic changes in patients. The idea is much more potent and viable, though, thanks to smaller and more affordable components.

A. Cell-inspired analog circuits

Researchers at MIT and Dartmouth have developed cell-inspired analog circuits that help translate signals between digital and analog systems. With the infinite values that can be generated from an analog computer, this opens doors for simulations of cells or even organisms. The program can implement differential equations at a rate that is far more efficient than a digital computer. Projects like these aim to reintegrate analog designs into modern computing in a way that takes advantage of its rapid processing capabilities. They are also easier to integrate into environments where less energy is available.

The research may pave the way for extremely accurate and efficient analogue models of whole organs, if not entire species.

Analog computers have slowly regained popularity due to its use in replicating complicated processes that may not be achievable with the deterministic logic employed by digital computers, despite analogue computers having mostly been replaced by digital over the years. The best combinations of the two are hybrid systems that enable the analogue computer to perform tasks that the digital computer is unable to. The idea of

hybrid computers is not new. For instance, hybrid computers are used in ICUs all around the world to digitise physiologic changes in patients. The idea is much more potent and viable, though, thanks to smaller and more affordable components.

In contrast, a digital circuit must divide time into thousands, even millions, of tiny intervals and solve the entire set of equations for each one. Additionally, rather of representing a continuous range of values, each transistor in the circuit can only represent one of two values. Sarpeshkar claims that complex differential equations that include the effects of noise can be solved using cytomorphic analogue circuits with a small number of transistors instead of millions of digital transistors and millions of clock cycles.

The digital computing took almost 14-40 seconds per equation which turned out to be fruitless. Analog on the other hand could handle more tasks and took less time.

So analog was preferred instead of digital [6].

B. Three laws and A.I using analog

Artificial intelligence is governed by three laws. The first, known as Ashby's law, after cybernetician W. Ross Ashby, author of *Design for a Brain*, asserts that any effective control system must be as complicated as the system it governs.[5]

According to John von Neumann's second law, a complex system is distinguished by the fact that it is its own purest behavioural description. The organism itself is the most basic and complete model of an organism. The behaviour of the system cannot be reduced to any formal description without increasing complexity, not decreasing it.

According to the third law, a system that is too complicated to understand won't be complex enough to behave intelligently, while a system that is simple enough to understand won't be complex enough to do so.

The third law provides reassurance to those who think we shouldn't be concerned about superhuman intelligence developing in machines until we fully understand it. The third law, however, has a flaw. Without having a thorough grasp of anything, you can still build it. You can create a functioning brain without completely comprehending how it functions. No amount of algorithmic oversight by programmers and their ethical advisors will ever be able to shut this loophole.

Analog computing gives more control to the user and hence the finished product will be in the hands of the user as he/she will be able to understand it. This gives us an edge and helps us prevent the user from losing control from the A.I [15].

REFERENCES

- [1] Bush's "Instrumental Analysis," 1936.
- [2] C. E. Shannon "Mathematical theory of the differential analyzer" J. Math. Phys. MIT, 20:337-354, 1941.

- [3] J. M. Nyce. Guest editor's introduction. *IEEE Ann. Hist. Comput.*, 18:3-4,1996.
- [4] Molnár, B.; Molnár, F.; Varga, M.; Toroczka, Z.; Ercsey-Ravasz, M., A continuous-time MaxSAT solver with high analog performance. *Nature Communications* 2018, 9 (1), 4864.
- [5] Kendall, J. D.; Kumar, S., The building blocks of a brain-inspired computer. *Applied Physics Reviews* 2020, 7 (1), 011305
- [6] Daniel, R.; Rubens, J. R.; Sarpeshkar, R.; Lu, T. K., Synthetic analog computation in living cells. *Nature*, 497 (7451), 619-623, 2013
- [7] M. B. Pour-El. Abstract computability and its relations to the general purpose analog computer. *Trans. Amer. Math. Soc.*, 199:1-28, 1974.
- [8] M. B. Pour-El and J. I. Richards. *Computability in Analysis and Physics*. Springer, 1989.
- [9] Richards, G.. "Pole position [IceCube array]", *Engineering & Technology*, 2009
- [10] M. S. Branicky. Universal computation and other capabilities of hybrid and continuous dynamical systems. *Theoretical Computer Sci.*, 1995.
- [11] M. W. Hirsch and S. Smale. *Differential Equations, Dynamical Systems, and Linear Algebra*. Academic Press, 1974.
- [12] P. Orponen. A survey of continuous-time computation theory. In D.-Z. Du and K.-I. Ko, editors, *Advances in Algorithms, Languages, and Complexity*, pages 209-224. Kluwer Academic Publishers, 1997.
- [13] L. A. Rubel. The extended analog computer. *Adv. Appl. Math.*, 1993.
- [14] "*BOWERS & WILKINS' NOISE-CANCELING HEADPHONES*" Available: <https://www.analog.com/en/signals/articles/bowers-wilkins-noise-canceling-headphones.html>
- [15] "The Third Law" by George Dyson, 2019 Available: <https://onezero.medium.com/the-future-of-computing-is-analog-e758471fbfe1>
- [16] Halzen, Francis & Klein, R. Spencer. IceCube: An instrument for neutrino astronomy. *Review of Scientific Instruments* 81, 081101 (2010)
- [17] Shen, Jiulong ; Lin, Zhi ; Huang, Linqing ; Ruan, Xiukai & Tang, Fang ; A Low-Noise Analog Front End with Interstage Systematically Ambient Interference Cancellation for Pulse Oximeter; *Electronics* 2022, 11(6), 868 (2022)
- [18] Garg, Sahaj ; Lou, Joe ; Jain, Anirudh ; Guo, Zhimu ; J. Shastri, Bhavin ; Nahmias, Mitchell ; Dynamic Precision Analog Computing for Neural Networks Published in: *IEEE Journal of Selected Topics in Quantum Electronics* (Volume: 29, Issue: 2: Optical Computing, March-April 2023).

Analysis of Level of Education and Its Impact Assessment on Urban Sustainability in Badarpur Slums Area of Delhi

Harikesh Kumar¹, Yogesh²

¹Maharaja Surajmal Institute of Technology, Delhi

²Central University of Haryana, Department of Geography, Mahendragarh, Haryana, India

¹kumarharikesh856@gmail.com, ²ykmr9354@gmail.com

Abstract— Slums are one of the major problem to urban development today; In Delhi these are the serious issues of human settlements. This study aims to analyse level of education and its impact on urban sustainability in the Badarpur slum area of Delhi. Badarpur is a historical town located in South East District of Delhi. It is situated close to the Delhi-Haryana state boarder. Commonly known as the Badarpur Boarder. Education is essential in building the foundation for an area's overall socioeconomic growth. The Children's Right to Free and Compulsory Education Act of 2009 ensures that children have the opportunity to enrol in, attend, and complete a free and compulsory primary school education. A mixed-method research design was used to investigate the aforementioned issues. Therefore, both qualitative and quantitative methods of data collection were used for this study. It is based on the primary observations grounded on factor analysis and, attempts to examine the factors which contribute in the educational status and, dropout of school children at secondary level, occupation and consumption patterns of their families and livelihood. Finally, the research makes proposals to enhance the educational attainment among the children living in Badarpur slum area.

Keywords— Education in Slums, Socio-economic, dropout, Occupation, Urban Sustainability.

I. INTRODUCTION

Slums are one of the major problem to urban development today; In Delhi these are the serious issues of human settlements. Badarpur is a historical town located in South East district of Delhi. It is situated close to the Delhi-Haryana state boarder. Commonly known as the Badarpur Boarder. In Delhi slums are commonly called JJ (Jhuggi- Jhopadi) colony. The initial definition of slum living combined the physical, spatial, social and even behavioural aspects of urban poverty. As highlighted in a study by Un-Habitat, the spread of associations has narrowed recently. Indeed, a slum has been re-defined by the United Nations Program on Human Settlements (UN-HABITAT) as “a contiguous settlement where the inhabitants are characterized as having inadequate housing and basic services. A slum is often not recognized and addressed by the public authorities as an integral or equal part of the city” (UN-HABITAT Urban Secretariat & Shelter Branch, 2002).

The definition of Slum as given in the Census of India, 2001 is “a compact area of at least 300 populations, or about 60-70

households of poorly built congested tenements, in unhygienic environment, usually with inadequate infrastructure and lacking in proper sanitary and drinking water facilities”. Slums are described as residential areas that are dilapidated, overcrowded, and unsuited for human habitation due to improper building layout and design, as well as narrowing and lack of air, lighting, or sanitary services, or any combination thereof. These determinants of safety, health, and morality are among these factors. About 93% of Delhi's work force lives in the slum areas. This workforce is a part of about 11% of Delhi's population. Delhi is home to sprawling unauthorized colonies they are classified as slum areas.

II. ORIGIN OF SLUMS IN BADARPUR

Badarpur industrial worker (BIW) slums is an area where people live in the unhygienic conditions. Most of them used to work in the Badarpur Thermal Power Station (BTPS) which was operational from the year 1974 to 2018. BTPS of National Thermal Power Corporation of India was one of the coal based power plants located on Delhi-Mathura road situated in Badarpur. Most of its workers lived and continues to stay in the Badarpur and its surrounding areas/colonies such as Jaitpur, Mithapur, while others are accommodated in other nearby areas including Madanpur khaddar and Jasola. Some of them are also housed, along with smaller blocks to the east of Badarpur such as Ekta Vihar, Harsh Vihar, Shaki Vihar, and Roop Nagar, among others. Furthermore, few of them are also settled in East Badarpur Khadai village situated on the river bank of Yamuna. Most of them migrated from Uttar Pradesh, Bihar, Madhya Pradesh and Odisha in search of Employment. The pull factors due to the livelihood opportunities available at the BTPS; more workers were attracted to make it an industrial hub. As a result it became the cause creating one more slum in Delhi.

The family background such as low educational and socio-economic status of the parents is significantly correlated with the phenomenon of poor quality of the education among the slum dwellers. Most of the sample children dropout school because of financial constraints (Chugh, S, 2011). Lack of financial stability compels people to find education as a luxury and not a necessity. Inadequate funds, unskilled staff, lax

attitude of officials, low classes are some of the reasons that damage the backbone of India's education system (Zedua, articulated, 2019). All Indian states and the central government are responsible for ensuring that all children get a comparable standard of basic education. Unfortunately, increased access is being accompanied with a drop in the quality of elementary education in government institutions. The rise of private fee-charging schools, even for the benefit of slum children, is due to this, (Aggarwal, Y., & Chugh, S. 2003). Kudroli Foundation, in their article, 'The Importance of Education in Developing Countries', (2019), Efforts to emphasize the role of education in eradicating poverty, promoting economic development and increasing the GDP of the country. Which helps to reduce infant mortality and increasing life expectancy of human. Education is an important investment in a country as it pays huge dividends. School going children nowadays are limited to academics and have little exposure of soft skills. The sub-health centre, according to the residents of that region, only offers immunizations and ANC services. Residents of this community must go to Batra hospital in Tigari or Shivalik hospital in Badarpur for any other health needs. It is a certainty, not a fact, that people of this area will have easy access to health care facilities. There is only one sub-health centre, and it is not fully operational. In times of necessity, residents travel to private health care institutions. The RMP charges varies. They charge between 100 and 200 dollars. It covers the cost of the tablets, injection, and consultations. The bulk of residents may only use the government-run Dispensary and Mohalla health clinic. Pregnant women are delivered by the Ayah, who are sometimes trained and sometimes untrained. The residents of this area are involved in working furniture, tools, blacksmith and labours and some people engaged in primary or secondary works. Some of them are worked in the thermal power station. Which is their source of income? In comparison to other areas, the number of children in each home is larger. The fact that practically almost household visited had four or more children demonstrate this. In this location, the concept of family planning is less prevalent. The average monthly household income ranges from Rs. 8000 to Rs. 15,000 rupees. These households' expenditures are typically 20–25 percent higher than their earnings. These individuals are becoming increasingly reliant on loans from local moneylenders and banks.

Research Questions

1. What are factors accountable for low level of education in the area of study?
2. How the education development influences the regional sustainability in the study area?

Objectives of the study

1. To analyse the education status in the study area.
2. To find out the Causes of the low education level in the study area.

3. To find out the level of socio-economic condition in area of study.
4. To evaluate regional sustainability as a function of educational status in the study area.

III. MATERIAL AND METHODS

A mixed method research design employing both qualitative and quantitative techniques of data collection were used for this study. This empirical study adopted observations-based factor analysis in which we visited the areas of study and interacted with respondent for collecting information. Total number of sample selected was 30, for collection of data through well-structured questionnaire or participant's observation, using simple random sampling method. We have adopted the primary field data collection as well as the secondary sources of data collection. A satellite Image has been taken from google earth pro, to the aerial view of the study area. Arc GIS software has been used to prepare the location map of the study area.

For personal Field observation we went to these slums areas in Badarpur Delhi-

- Jaitpur
- Mithapur
- JJ Colony Madanpur khadar

IV. STUDY AREA

Study has been conducted in the Slums Areas of Badarpur in Delhi. Badarpur is a historical town and district in south east Delhi. Situated close to the Delhi Haryana state. Geographically it is located at the intersection of 28°31'00"N, 77°20'00"E. Commonly known as the Badarpur Boarder. People from low-income classes are concentrated in Badarpur and its adjacent areas. It is comprised of many colonies from the surrounding area. This all area is inhabited by the people come from the states, like, Bihar, Uttar Pradesh, Madhya Pradesh and Haryana, etc. There are around 1000 to 1500 families in this region/pocket. There is 9 to10 MCD School and 2 to 3 private Schools

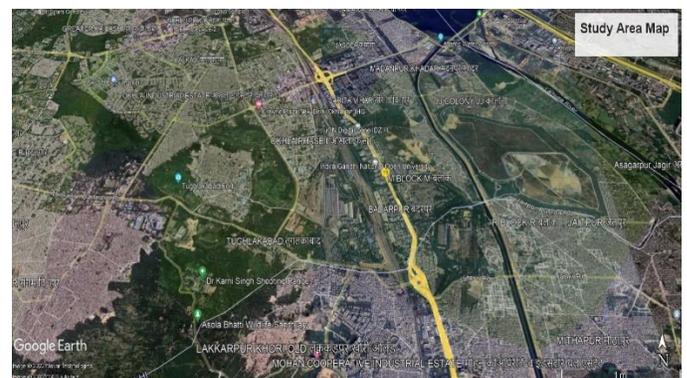


Fig. 2. Satellite view of the study area.

V. DATA ANALYSIS

Both qualitative and quantitative methods of were used in this study for collection of information through a structured questionnaire. We have taken 30 sample sizes to comprehend the level of education in the Badarpur slum areas of Delhi, in which 63% male and 37% female respondents, 63% were below 15, 33% were 15-25 and 3% were above 25 years old. The family/household size is quite larger than conventional. Approx. 33% of families have above 5 family members, combined 53% of families have 4 or 5 members and 14% have 3 members in their family. Some homes are highly congested and 5 to 6 people living in a single room. The large family size of these slum areas indicates the lack of nourishment and unfortunate quality of education for their children. The average monthly income of households range between ₹8000-₹15000. Due to the large family size and the low-income level, they suffer lots of issues related to health and education.

People in these slum regions are mainly daily wage workers. Around 57% of people are unskilled Labour, 20% have their own small business and 23% are involved in other working categories like.

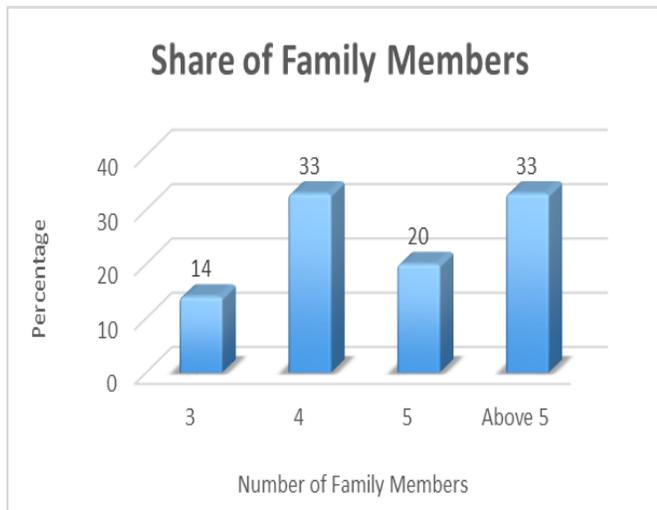


Fig. 3. Share of the family member in the household

Carpenter, electrician, driver, etc. In the light of the above structure, the average monthly income of these slums dwellers is below ₹5000 which consists of 17% of people, 40% earn ₹5000-₹10000 monthly, 27% earn ₹10000-₹15000 and the remaining 16% of people earn above ₹15000.

The occupation structure of the slums indicates that most of them are daily workers which means they have inadequate resources to expend on their child's education. The living standards of these families are not adequate because on an average of 57% of inhabitants have earned less than ₹10000. Also, the family size in these slums is high which directly impacts their living concerns their low earnings.

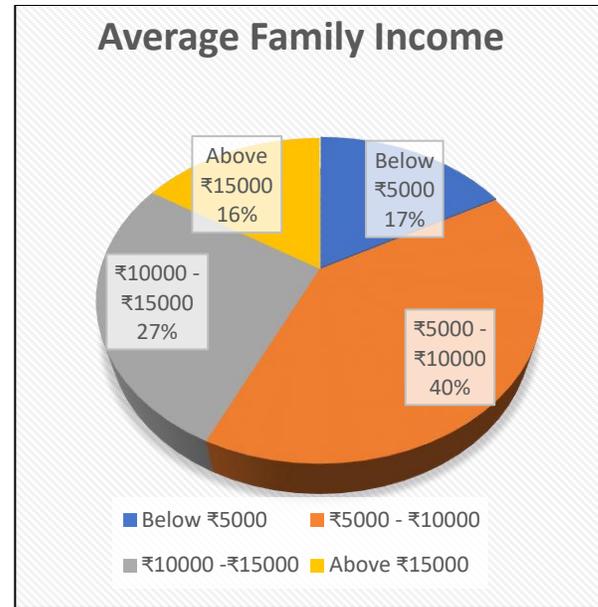


Fig. 4. Monthly family income of the household

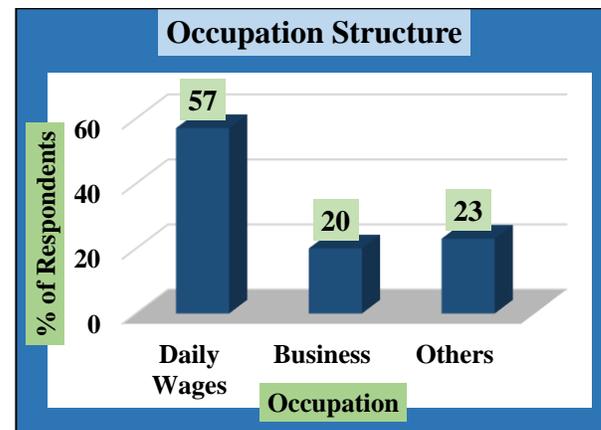


Fig. 5. Occupation structure of the slum dwellers

Education plays a fundamental role in Economic growth. Most of the residents are unskilled labour which directly affects their standard of living. The education level in this area is low and it needs to be enhanced for betterment. As per analysis, 93% of these slum children are going to school and the rest 7% are dropouts or not enrolled in school due to family concerns.

TABLE 1. Level of qualification.

Level of Qualifications	In percentage (%)
Primary Level	40
Secondary Level	47
Graduate	10
None	3

These slums area shows that 40% of children have primary school qualifications, 47% have secondary school

qualifications, and 10 % have graduated and 3% are dropouts. It is primarily due to the low level of family income or some family matters. The dropouts students are working based on daily wages to sustain their families.

The economic dilemma is the main reason why children do not attend school. Only 10 % of students have graduated, which means after secondary school education students cease their studies and become involved in some work to gain a livelihood. There are very low higher education qualifications in this slum area because of a lack of education awareness among slum inhabitants, lacking income and inaccessibility to higher education institutions.

Around 80% of the children are studying in government schools, 13% are in private schools and the remaining 7% households send their children's to both govt. and private schools. As illustrated above 80% of children in this slums area are studying in government schools. It is due to negligible fees in comparison to private schools. Also, 13 % have enrolled in private schools because of additional income or some better living standards than children who are enrolled in government schools. And the rest of the 7% are going to both school's government as well as private.

VI. SUMMARIZE AND CONCLUSION

In the Badarpur slums area, the socio-economic conditions of people are inefficient. Poverty is an intimate part of these slums dwellers. Therefore, the population of these slums are socially and economically backwards. The majority of the population is dependent on the informal sector for their livelihood. More than half of the population are unskilled labour or daily workers i.e., 57%. Also, the average earnings of the family are ₹8000-₹15000 which is insufficient in contrast to a large family size. The low-level income of the household in these slums portrays the low quality of standards of living. They encounter plenty of issues regarding health, education, better environment, etc. 93% of these slums children are enrolled in schools however, 80% the children are in government schools and 7% of children are dropouts due to lack of income and food accessibility. 87% of children have the qualifications up to primary and secondary level qualifications. Only 10% are graduated which shows the major dropout of students after secondary education it is basically due to the lack of educational awareness, low level of income, family issues, inaccessibility to higher education etc.

Government should take initiative to raise educational awareness among the slum dwellers and proper monitoring of dropout students. Better educational infrastructure should be provided in the school of slums area so more accessible to educational resource utility. Unskilled labour should be upgraded to skilled labour, by workshop and professional training and generation of regular source of income so that their income should be increased. A good education helps a child's social, emotional, cognitive, and communication skills grow. Education has positive effects on choosing better livelihoods,

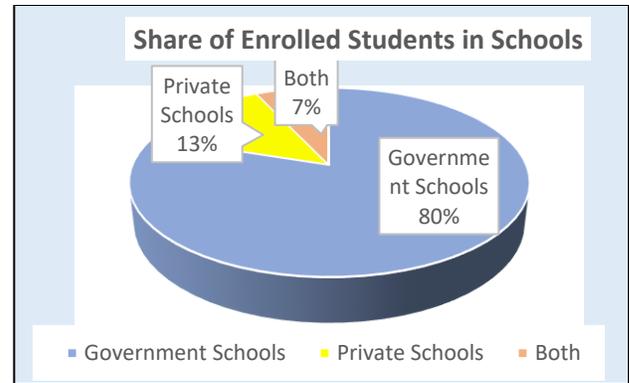


Fig. 6. Types of school in which student enrolled

family income and poverty reduction. Children who have attained higher education or more important quality education can easily give their services to their society. Good education has always been said liberating for individuals of every background, it brings equality in society which determines the standards of living and a sustainable environment for their prosperity. Education is directly linked to economic growth and play a vital role to achieve the sustainability in slums areas. It further improves the standard of living in the area. If people are more economically stable, they will invest in things which make their living better and more comfortable which influence the regional sustainability.

REFERENCES

- [1] United Nations Human Settlements Programme (UN-Habitat), 2003, <https://unhabitat.org/sites/default/files/download-manager/files/The%20Challenge%20of%20Slums%20-20Report%20on%20Human%20Settlements%202003.pdf>
- [2] Census (2001) Office of the Registrar General, India 2A, Mansingh Road, New Delhi with the grant of SER and Planning Commission of India. Response Fund (GOI/32-3/2013, 28.11.2013).
- [3] Chaitanya Mallapur (2015), Slums, Workers Hold Key to Winning Delhi, <https://www.indiaspend.com/slums-workers-hold-key-to-winning-delhi-64550/>.
- [4] Chugh, S. (2011). Dropout in secondary education: A study of children living in slums of Delhi.
- [5] School Dropout Rate in India & the Craze for Ignorance. (n.d.). Retrieved (April 16, 2020), from <https://www.zedua.com/blog/school-dropout-rate-in-india/>
- [6] Aggarwal, Y., & Chugh, S. (2003). Learning achievement of slum children in Delhi. Operations Research and Systems Management Unit, National Institute of Educational Planning and Administration.
- [7] Kudroli. (2019, July 10th). The importance of education in developing countries, Kudroli. Retrieved from <https://www.kudroli.org/blogs/the-importance-of-education-in-developing-countries>.
- [8] Kumar, M., & Gupta, N. Locating Education in the Socio-economic Context of Badarpur Khadar, Delhi, India.
- [9] Awasthi, S., & Aggarwal, S. (2003). Determinants of childhood mortality and morbidity in urban slums in India. *Indian pediatrics*, 40(1), 1145-1160.
- [10] Mandal, R. B. "A Textbook of Urban Geography", Concept Publishing Company.

Behavioural Finance: Understanding How Biases Impact Decisions

Nishtha Jatana¹, Drishti Pandita²

^{1,2}Maharaja Surajmal Institute of Technology, Delhi
nishtha.jatana@gmail.com

Abstract-- Over the past many years, there has been extensive research and study on stock market investments from a rational point of view. A variety of ideas have been put up and developed in this regard. However, they were all contradicted because humans cannot be rational all the time. They are influenced by emotional and psychological biases and use heuristics. The theory of behavioural finance was put forward to cater to the shortcomings in the traditional or conventional models. Behavioural finance is an evolving field that bridges the gap between neoclassical finance and cognitive psychology.

Keywords- *rationality; behavioural finance; traditional finance; efficient market hypothesis; decision-making.*

I. INTRODUCTION

In contrast to economics, which focuses on decisions on what to produce, how to produce, and for whom to produce, finance primarily deals with investment decisions, working capital decisions, dividend decisions, and fund allocation decisions. Similarly, the emerging discipline of behavioural finance addresses the difficult task of decision-making. It takes into account the psychological factors that affect decision-making under uncertain conditions. Decision-making is a complex activity. Behavioural finance provides a new perspective to study the financial markets and also helps to tackle the difficulties faced by the traditional paradigm. It provides models in which all the agents are not rational and there is room for errors and biases.

II. CLASSIFICATION

Financial markets can be classified into two categories – Traditional Finance, also referred to as Conventional Finance and newly emerging Behavioural Finance. According to the traditional theories of the financial market, investors act in a rational manner and all predictions that investors make are completely accurate. The theories of traditional finance majorly revolve around Efficient Market Hypothesis and Harry Markowitz Model. It is based on the assumption that all the decisions that an investor take are rational.

The efficient market hypothesis (EMH) theory – put forward by economist Eugene Fama- claims that the market’s current asset prices accurately represent all the information available – meaning that the assets are efficiently evaluated. So, in theory, it should not be possible for an investor to outperform the market. However, EMH has been challenged from time to time

by investors like Warren Buffet and George Soros who have consistently beaten the market by predicting human behaviour.

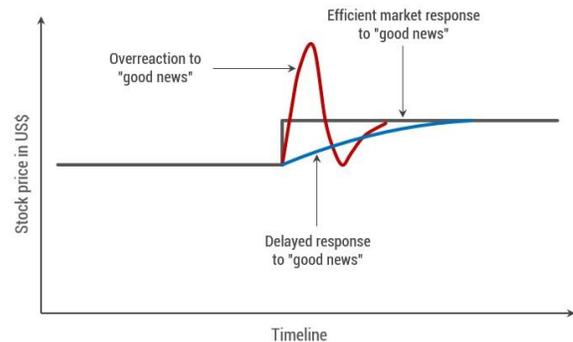


Fig. 1. Stock price relation with investor psychology.

Similarly, Markowitz’s Modern Portfolio Theory provides a means to create and construct a portfolio of assets to maximize returns with the least amount of risk. Harry Markowitz, however, assumed that most investors are risk-averse, rational and when presented with two portfolios, an investor will instinctively choose the one that has the greatest potential for return while posing the fewest risks. It is reliant on variance when it should ideally focus on risk. This makes it prone to contradictions.



Fig. 2 Markowitz’s Modern Portfolio Theory.

III. LIMITATIONS OF CONVENTIONAL FINANCE

A. INVESTORS ARE NOT RATIONAL

Traditional finance is primarily based on the rationality of market participants, but this assumption is the biggest fallback of the theory, studied by various research scholars. The rationality of an investor is analysed in an objective manner and is assessed on the basis of how accurately they use the information that is available to them. The cyclical investment process is, however, fraught with psychological pitfalls. Scholars have criticized investors' psychology when taking rational decisions.

B. INVESTORS ARE EMOTIONAL

Traditional finance downplays the importance of investors' emotions while making an investment decision. Totally neglecting the fact that market agents operate depending on their personal reference point is not apt because decision-making involves emotional components in every element of human life.

C. INFORMATION MAY NOT BE ACCURATE

In the world of investing, there is nearly an infinite amount to know and learn; and even the most successful investors do not master all disciplines [1]. The conventional definition of an efficient market is one in which the prices of financial assets generate and considers all of the information available. It argues that every investor has unlimited access to information about market changes. If this was true, it would have been impossible to predict future market fluctuations. Therefore, investors do not always have all the requisite information for accurate decision-making. And, as it lends credibility and draws investors, informational efficiency is necessary for the successful operation of markets.

D. INVESTORS HAVE DIFFERENT EXPERIENCE LEVELS

Another assumption that traditional finance theories make is that all investors have comparable level of competence and knowledge and can easily forecast and time the market trends based on their experiences and prior market performance. It is false because past performance is not an indicator of future success. Just like any complex problem, the future has too many unknowns to be predicted. Investors can try to make predictions and intelligent guesses but they aren't always accurate and sometimes turn out to be futile.

E. DEMOGRAPHIC FACTORS

Income, gender, age, background, religion, family etc are the various demographic factors that are not considered in conventional finance but play a key role in decision making when making investments. Many researches have been carried out for the same. For example, researches have claimed that overconfidence is a trait that is common to both male and female

psychology, men are however more overconfident than women[2].

IV. EMERGENCE OF BEHAVIOURAL FINANCE

"Economic conditions may differ from period to period, but human psychology is embedded among us and will not change."
- Naved Abdali

Investor irrationality has existed as long as the markets themselves have.

The 1990s saw the emergence of a new field called behavioural finance in several scholarly journals, business magazines, and even neighbourhood newspapers. The foundations of behavioural finance, however, can be traced back to the eighteenth century.

Adam Smith's Theory of Moral Sentiments [3] is packed with insights that presage developments in contemporary behavioural finance. It also promises leads that are yet to be pursued.

The field of behavioural finance as a science originated in 1985 following the publication of two articles in the "Journal of Finance" [4] that discussed the subjective behavioural aspects influencing stock price movements and investor income. Goldberg and Von Nitzsch (1999) described behavioural finance as financial market theory that is behaviour-oriented. Daniel et al., [5] investigated investor psychology and developed a theory behind the pricing of private information and the lack of formal domain evaluation, both of which have a negative influence on long-term investment.

V. COGNITIVE ERRORS: HEURISTICS AND BIASES

Regardless of how rational investors are assumed to be, they often make financial decisions that are coloured by behavioural biases that cause them to act on emotion or make mistakes processing information. There are many areas in which individuals have inconsistent preferences.

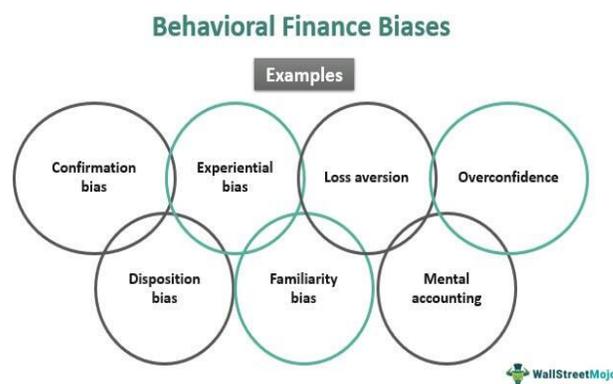


Fig. 3. Examples of behavioural finance biases

The several biases and errors that influence the decision-making process incorporate loss aversion, regret aversion, cognitive dissonance, herding behaviour, limited attention, over-optimism, familiarity bias, status quo bias, prospect theory, mental accounting, anchoring, randomness bias, gamblers’ fallacy, endowment effect. This paper reviews few out of them.

A. THE PROSPECT THEORY

The prospect theory claims that profits and losses are perceived differently. A group of illusions impact the decision-making process of individuals. It revolves around how individuals manage risk and uncertainty. It argues that the people emphasize perceived gains more than the perceived losses and therefore, the decision-making process becomes biased.

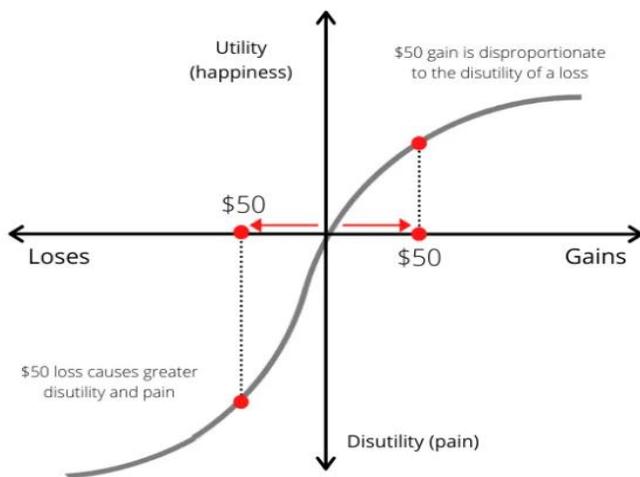


Fig. 4. Graph depicting Prospect Theory

The theory was formulated by Daniel Kahneman and Amos Tversky in 1979. In comparison to the expected utility theory that provides a way of ranking the acts according to how choice worthy they are, the pair claimed that the prospect theory adequately described how decisions are formed.

B. LOSS AVERSION

In behavioural economics, loss aversion refers to the phenomena in which individuals consider an actual or projected loss to be psychologically or emotionally more unpleasant than an equivalent gain. For example, the anguish of losing \$500 is frequently significantly higher than the satisfaction of discovering the same amount. humans perceive losses asymmetrically more acutely than similar benefits humans perceive losses asymmetrically more acutely than similar benefits.

Humans perceive losses asymmetrically more acutely than similar benefits. The asymmetry is widely assumed to arise because individuals anticipate the pain of losing something to outweigh the joy of acquiring it [6].

Loss Aversion Bias

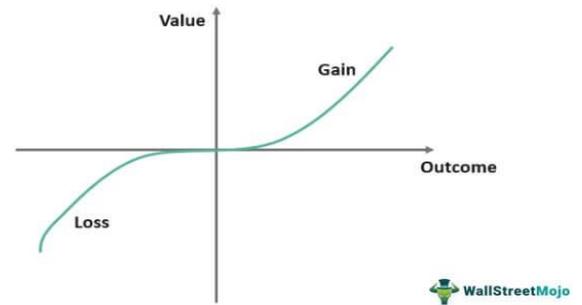


Fig. 5. Graph depicting Loss Aversion Bias

C. REGRET AVERSION

When a decision is taken to prevent regretting an alternative option in the future, this is known as regret aversion [7]. proposed the first definition of regret aversion, stating that it pushes people to avoid future regret. Regret may be a powerless and unpleasant mood, and individuals will occasionally take actions to escape it.

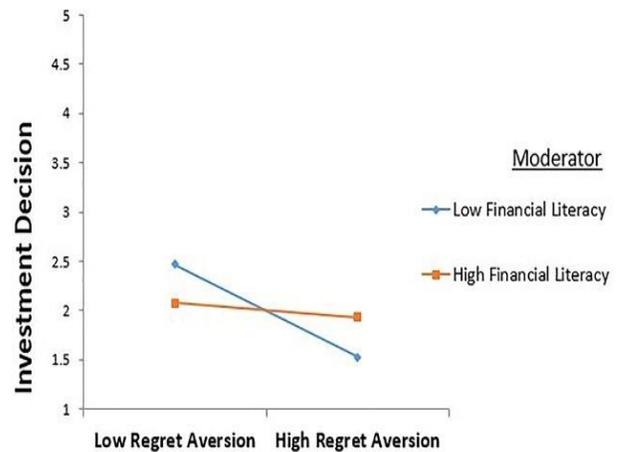


Fig. 6. Graph depicting Regret Aversion

Regret aversion is a situation in which individuals surrender taking a risk and therefore making a possibly incorrect investment commitment to avoid the unpleasant feeling that could arise [8]. Due to regret aversion, investors avoid a market that has recently created losses, even though investing deals may be most readily accessible.

D. MENTAL ACCOUNTING

Mental accounting is the collection of intellectual tasks used by individuals and families to create, analyse, and manage financial transactions. The principle of fungibility of money underpins the theory. This advocates that all money amounts the same, regardless of its source or intended use. The concept of mental accounting was developed by Richard Thaler in his 1999 paper Mental Accounting Matters [9]. He claimed that every

component of mental accounting violates the economic principle of fungibility.

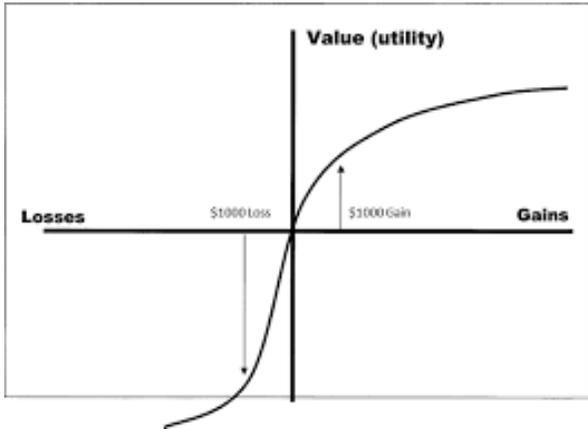


Fig. 7. Graph depicting the influence of Mental accounting

Thaler noticed that while dealing with windfall situations such as bonuses, tax refunds, lottery prizes, and birthday money, people frequently disregarded the fungibility idea. It indicates that "gift money" that is not part of a person's normal salary is spent on lavish items that they cannot explain. As a result, he suggested that people should treat all their money equally and spend windfalls the same way they spend regular income based on a systematic financial plan. Mental accounting, also, leads to the sunk cost fallacy, which is the tendency to engage in an activity for a longer period of time than we should because we feel obligated to make our original investment worthwhile.

E. COGNITIVE DISSONANCE

Leon Festinger published A Theory of Cognitive Dissonance (1957) [10] which has been one of the most influential theories in cognitive finance. Cognitive dissonance is a mental conflict that emerges when a person's actions and beliefs are inconsistent. Individuals altering their beliefs to hold onto their past actions is the key feature of dissonance. It causes psychological problems and mental clashes in individuals when they discover that their convictions and suspicions aren't correct, prompting them to make rash and impulsive financial decisions to resolve their conflicting beliefs so that their thoughts once again become linear and rational.

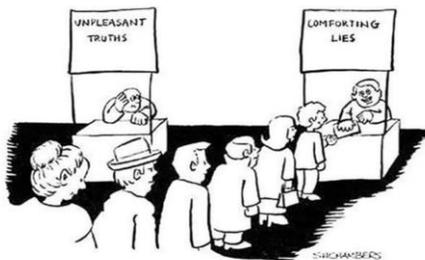


Fig. 8. Picture representing cognitive dissonance in people.

F. STATUS QUO BIAS

The term "status quo bias" was first coined by researchers William Samuelson and Richard Zeckhauser in 1988. Samuelson and Zeckhauser discovered that individuals had a disproportionate preference for decisions that maintain the status quo in a series of controlled studies. Individuals choose one of a known set of alternative choices with certain outcomes in the canonical model of decision-making under certainty.

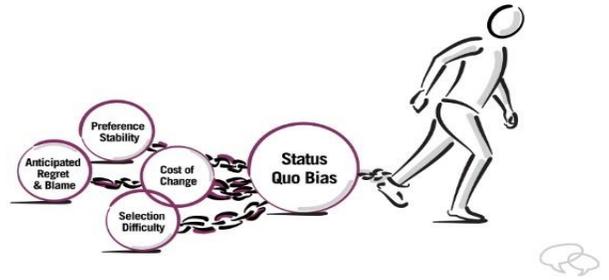


Fig. 9. Picture representing status quo bias

This implies that if an investor is presented with a plethora of alternatives, many of which are difficult and perplexing, they are more likely to select the one that extends their current arrangement.

This happens because humans do not want the hassle of changing and the human brain is wired in a way to save time and brain capacity in the decision-making process.

G. ANCHORING

Amos Tversky and Daniel Kahneman proposed the anchoring heuristic. The anchoring effect is the systematic influence of initially offered numerical values on future evaluations of uncertain quantities, even when the numbers presented are evidently arbitrary and hence unambiguously irrelevant. The anchoring bias is based on the notion that the first or initial information regarding a product's pricing establishes an anchor in our minds. All following information is viewed in light of that anchor.

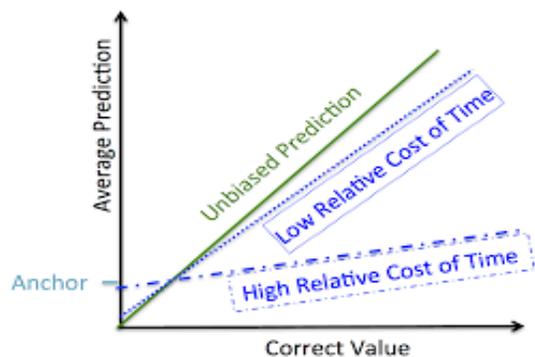


Fig. 10. Graph depicting the application of anchoring effect on market prediction.

This is especially crucial in financial markets, where consumers must evaluate prices and buy and sell on an everyday basis. Anchoring bias is used by businesses all over the world to increase product sales. That is why all over the world, e-commerce portals would publish a higher price, then reveal and discount before finally mentioning the selling price.

REFERENCES

- [1] M. Pompian, *Behavioural Finance and Wealth Management*, United States of America: WILEY, 2006.
- [2] M. A. Lundeberg, P. W. Fox and J. Punčochař, "Highly Confident but wrong: Gender differences and similarities in confidence judgements.," *Journal of Educational Psychology*, 1994.
- [3] A. Smith, *The theory of Moral Sentiments*, Scotland, 1759.
- [4] D. Bondt and R. Thaler, "Does the Stock Market overreact?," *The Journal of Finance*, vol. 40, 1984.
- [5] K. Daniel, D. Hirshleifer and A. Subrahmanyam, "Investor Psychology and Security Market Under- and Overreactions," *The Journal of Finance*, 2002.
- [6] A. P. McGraw and C. Warren, "Benign Violations : Making Immoral Behavior Funny," *Psychological Science*, p. 1441, 2010.
- [7] S. Loomes, "Regret Theory: An Alternative Theory of Rational Choice under Uncertainty," *The Economic Journal*, 1982.
- [8] R. G. Frehen, R. P. Hoevenaars, F. C. Palm and P. C. Schotman, "Regret aversion and annuity risk in defined contribution pension plans," *Insurance: Mathematics and Economics*, vol. 42, no. 3, pp. 1050-1061, 2008.
- [9] R. Thaler, "Mental Accounting Matters," *Journal of Behavioral Decision Making*, 1999.
- [10] L. Festinger, "A Theory of Cognitive Dissonance," *Stanford University Press*, 1957.

Design of Single Stage three Phase Grid Connected Photovoltaic System with MPPT

Shilpam Malik

Department of Electrical and Electronics engineering
Maharaja Surajmal Institute of Technology

Abstract - In remote locations such as villages, islands and hilly areas, there is a possibility of frequent power failures, voltage drops or power fluctuations due to grid-side faults. Grid-connected renewable energy systems or micro-grid systems are preferable for such remote locations to meet the local critical load requirements during grid-side failures. In renewable energy systems, solar photovoltaic (PV) power systems are accessible and hybrid PV-battery systems or energy storage systems (ESS) are more capable of providing uninterruptible power to the local critical loads during grid-side faults. This energy storage system also improves the system dynamics during power fluctuations. In present work, a PV-battery system with DC-side coupling is considered, and a power balancing is proposed to transfer the power to grid/load and the battery. In this system, a solar power conditioning system acts as an interface across PV source, battery and the load/central grid. With the proposed method, the system can operate in following operational modes: (a) in grid-connected mode during regular operation; (b) to charge the batteries and (c) to operate in standalone mode during grid side faults and deliver power to the local loads. The proposed controls are explained, and the system response is described with the help of simulation results.

Keywords: battery; energy storage; MPPT; PV inverter.

I. INTRODUCTION

Nowadays, there is an international trend toward modular structured renewable/distributed system concepts in order to reduce the costs and provide high reliability [1]. Solar PV stations can reduce carbon emissions and provide clean energy but may not be able to supply the load requirements due to sudden changes in weather conditions and when the solar irradiation is weak. The system remains in an idle state during nighttime, which affects the utilization factor of the system drastically. Hence there is much attention to battery energy storage systems along with PV to reduce power disturbances in the system, to improve the stability, for providing continuous power to the load and for improving utilization factor of the system. In such hybrid PV-battery stations, power is transferred from PV array to battery and load during daytime and batteries transfer power to the load during night time. The battery storage system also improves the system dynamics for sudden weather changes [2,3]. Importance of hybrid PV-battery stations and operation strategy is discussed in [4]. A review of energy storage for large-scale PV systems, grid integration issues, stability concerns and the selection of batteries is available in [5]. With the battery storage system in PV applications, the utilization factor of the PCS can also be improved since the

system can be made operational for all the time. To keep the grid power non-negative always, an approach called ‘Solar Plus’s, which is the combination of energy storage, PV, and load controls are presented in [6]. Cost of the battery storage systems is also decreasing over time due to the advancements in the areas of different battery technologies, battery charging and discharging methods. In [7], various battery types such as lithium-ion, lead-acid, aluminium-ion, sodium-sulphur (NaS), flow batteries, etc. suitable for large-scale PV ESS systems are explained and compared. Various discharge strategies are presented for grid-connected hybrid PV-battery applications in [8] and different battery storage technologies suitable for residential applications are also elaborated. In a conventional grid-connected PV power conditioning system, the anti-islanding feature will be incorporated as a feature of protection. But as mentioned earlier, it may be required to operate the PCS in stand-alone mode also when there are frequent disconnections from the grid. In such scenarios, a power management system at a higher level of control architecture needs to isolate the grid from the critical loads. Hybrid PV-battery stations can also be operated in standalone mode; hence it is possible to provide power to local critical loads during grid-side faults or during maintenance on the grid side. Such systems help in catering continuous power supply in remote locations which are not connected to the central grid or which are facing problems of regular power supply failures from the grid. Optimal design for a PV + Diesel + Battery storage hybrid system is presented in [9].

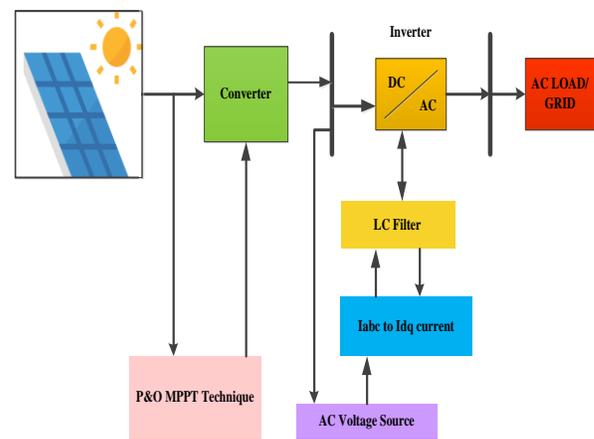


Fig. 1 Detailed model of Single Stage PV system to Grid/ AC load.

As conventional fossil-fuel energy sources diminish and increases the world's environmental concern about acid deposition and global warming, renewable energy sources such as solar, wind, tidal, etc., are attracting more attention as alternative energy sources. Among them solar photovoltaic energy (PV) is being widely utilised in small size applications and is most promising for research and development for large-scale use, as fabrication of less costly photovoltaic devices become a reality. Solar energy is one of the major renewable energy sources and is available everywhere in varied quantities. PV panels do not have any moving parts, operate silently and generate no emissions. Another advantage is that solar technology is highly modular and can be easily scaled to provide the required power for different loads [10]. Interfacing the PV to the grid presents a quite different and challenging scenario because unlike the conventional system, the PV cannot be directly connected to the grid. A power conditioning interface between the PV and grid is required to match the characteristics of PV and the requirements of the grid connections such as voltage, frequency, active and reactive power control, harmonic minimization [11] have presented work on dynamic modelling of PVs which is required for designing appropriate interfacing circuits and controllers for practical PV systems and to investigate PV transient responses with change in solar irradiance and operating temperature. The connection of the PV array to the grid is usually made with a voltage source inverter (VSI), and it may include intermediate DC-DC converter, a transformer, or even both. The presence of a DC-DC converter allows the PV panels to operate over a wider voltage range, with a fixed inverter DC voltage and a simplified system design. On the other hand, the DC-DC converter increases the cost and decreases the conversion efficiency at most operating points [12]. Transformerless and high frequency-transformer topologies are preferred for avoiding bulky low-frequency transformer but are usually limited to single-phase connections with powers of up to a few kW. Hence, PV-conversion schemes including a line-frequency transformer prevails in higher power three-phase systems, ranging from few tens of kW up to MW power ratings [13]. A two stage grid-connected PV system has two control loops. The inner loop modulates the output currents of the inverter, to meet the waveform and phase requirement. The outer loop determines the output power of the inverter according to the maximum power point of PV panels. Conventionally, these two loops are realized respectively in two stages of power conversion, one is a DC-DC converter with maximum power point tracking (MPPT) control and the other is a DC-AC inverter [14]. In single-stage grid-connected PV systems, both loops are realised simultaneously in one power conversion stage, thus, simplifying the system topology. However, to maintain the sinusoidal waveform of output currents, the minimum time period to change the reference output power should be half of the grid voltage period, thus, the outer loop here has a much lower speed than that of the inner loop. To maintain the system stability, the MPPT method should be modified to work at low speed. Due to the utilisation of only one energy conversion stage, the single-stage grid-connected

PV system is simpler, more efficient and economical than its two-stage counterpart; therefore, it is widely gaining acceptance. However, since all, the MPPT control, synchronisation with the utility voltage, output current control with harmonic reduction needs to be considered simultaneously, the complexity of the control scheme is much increased [15]. This paper presents the implementation of a single-stage three-phase grid-connected PV system.

A. Photovoltaic model

This paper, utilizes a single diode solar cell to model the PV system. It consists of current source I_{SC} along with an inverted diode in parallel to it, and a series and parallel resistance ie. R_S and R_P . The photocurrent and output current is given by equations 1, 2, and 3 [12].

$$I_{SC} = \frac{[I_S + K_1(T_C - T_{ref})]\lambda}{1000} \quad (1)$$

$$I_{PV} = N_P I_{SC} - N_S I_S \left[\exp\left(\frac{q(V_{PV}/N_S + I_{PV} R_S/N_P)}{k T_C A}\right) - 1 \right] \quad (2)$$

$$I_S = I_{rs} (T_C/T_{ref})^3 \exp\left[\frac{q E_g \left(\frac{1}{T_{ref}} - \frac{1}{T_C}\right)}{k A}\right] \quad (3)$$

where V_{pv} is output voltage of PV system, I_s presents cell's saturation current, N_p , N_s are number of strings connected in parallel and series, q is the electron charge, T_c , T_{ref} are PV surface and reference temperature, I_{rs} , I_s is the reverse saturation and short circuit current, E_g is the energy band gap of silicon, K_1 is the short circuit temperature coefficient, λ is the irradiation level, K is the Boltzman constant.

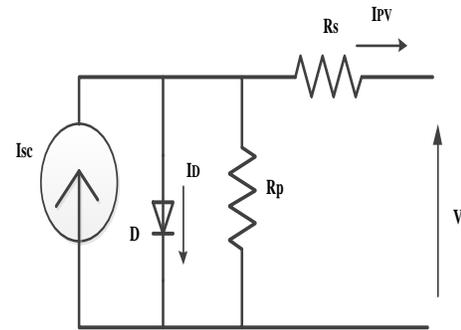


Fig. 2. Model of PV cell.

B. Maximum Power Point Tracking

The solar radiations change with season and during the day and hence it is difficult to obtain maximum power (MP) which enforces the attainment of the MP the whole day and even under changes in solar radiations. The PV system always works on specific value of voltage where global maximum of I-V characteristic is acquired. From the I-V characteristics it is extrapolated that for any specific operating point; MP output can

be obtained from the solar panel and is called the Maximum Power Point (MPP). On the knee of I-V curve of solar panel lies, the MPP. From here it is inferred that on the I-V curve of PV cell a point called MPP always occurs on the knee point of the curve where the generated PV power is maximized. The position of MPP changes constantly at every instant of time as the temperature and irradiation changes [9]. Here, perturb and observation method is employed for obtaining this MPP point and is similar to hill climbing algorithm. This method is most widely adopted for industrial applications due to its robust convergence for MPP. Knowing the direction of sun radiations the output voltage changes thus, adjusting the duty cycle of the converters. Instead of two cases to follow, there are four cases to follow, and are represented by flow chart is given in figure 4.

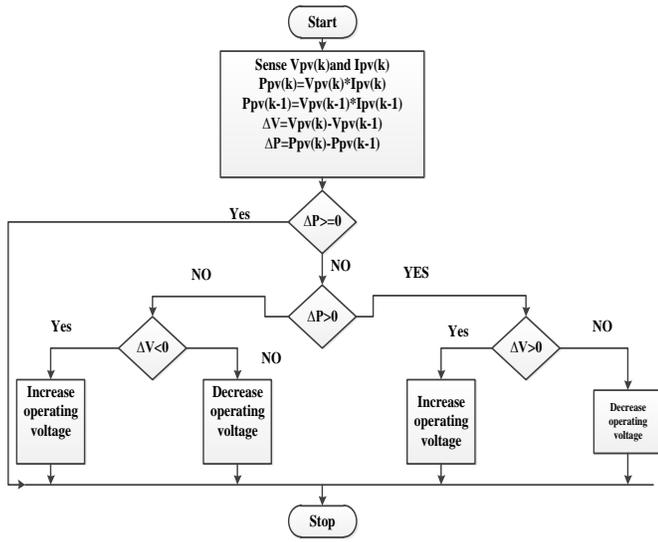


Fig. 3 Perturb and Observation Technique for MPPT.

II. SIMULATION RESULTS AND DISCUSSIONS

To evaluate the performance of PV system and the effectiveness of its control strategy, a detailed model of 200 kW PV system is constructed and simulated in MATLAB-Simulink. Simulation diagram of grid connected solar PV system with MPPT algorithm is shown in figure 4. The various parameters used for simulation are given in Table 2 of the Appendix. The grid is represented by a balanced three-phase source. Simulation results have been presented for the PV system under normal operating conditions with and without variation in solar irradiation.

The current and I-V characteristic of the PV device depends upon the internal characteristics of the device (R_s , R_p) and on external influences such as irradiation level G and temperature T . The solar system with fixed and variable irradiance provides the current and P-V curves which are presented in figure 5(a) and 5(b).

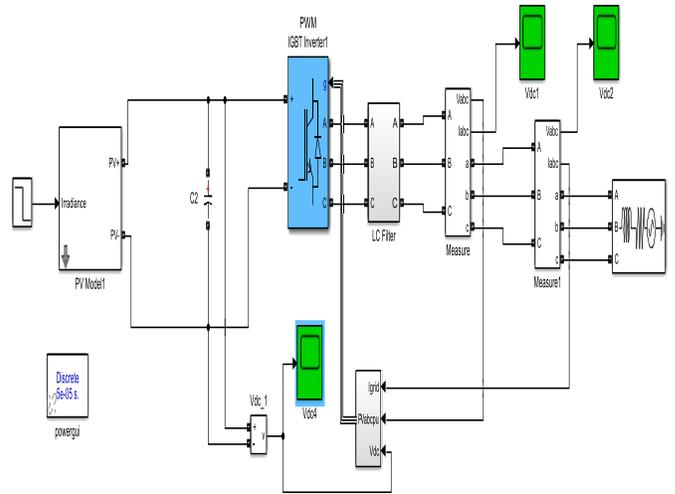


Fig. 4. Detailed model for Single Stage PV Grid connected system for AC supply

The model shown in figure 4 is simulated and the output of PV system i.e the current output and power output of the PV module obtained are presented in figure 5(a) and 5(b). The Perturb and observation technique is implemented for obtaining the maximum power output from the PV module. The voltage obtained from P&O technique is presented in figure 6 when the voltage waveform is filtered using capacitive filter. The three phase ac source provides the voltage V_{abc} presented in figure 8(a) and the zoomed view of the ac voltage is shown in figure 8(b). The AC current from the PWM inverter when supplied to grid consists of two components i.e. direct current and quadrature current which is filtered using three phase LC filter which is depicted in figure 9(a) and 9(b). The three-phase ac current supplied to grid is presented in figure 7.

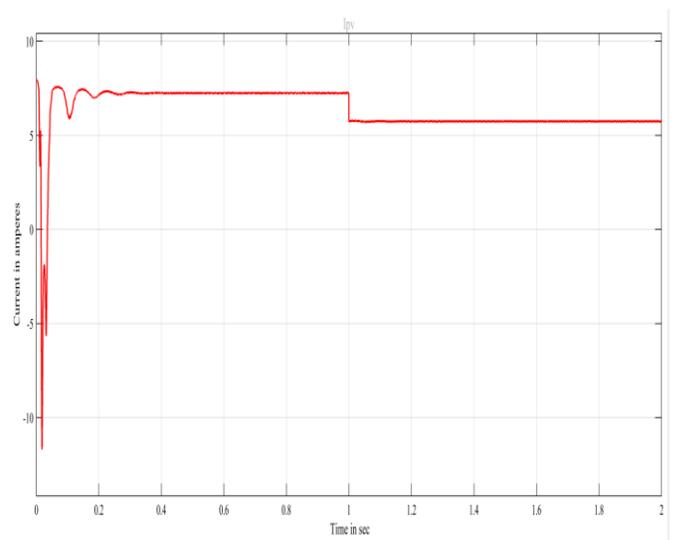


Fig. 5(a) Current output from PV module

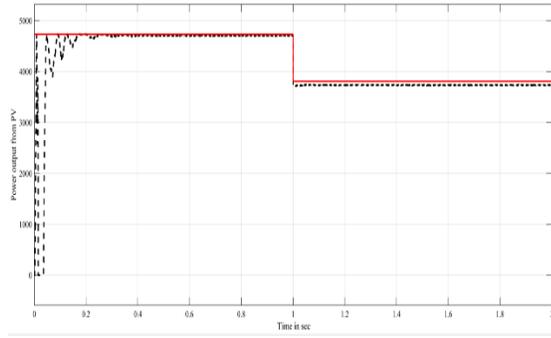


Fig. 5(b) Power output from PV module with reference P_{pv}

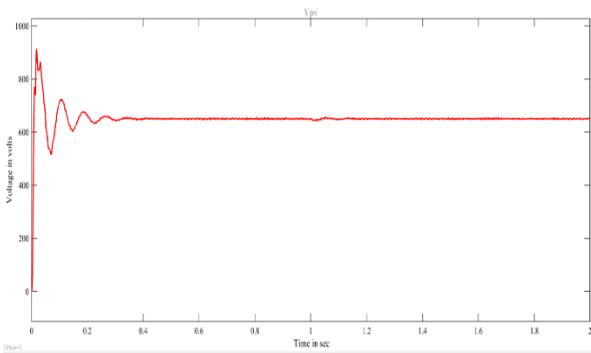


Fig. 6. Output voltage from the PV module

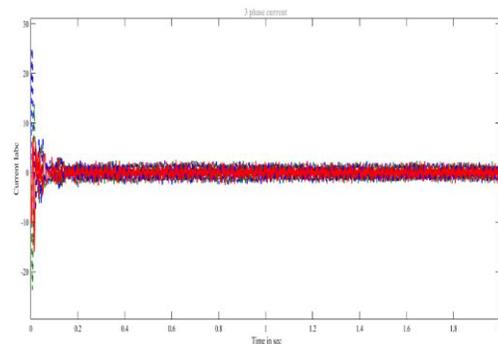


Fig. 7 Three phase AC current to grid

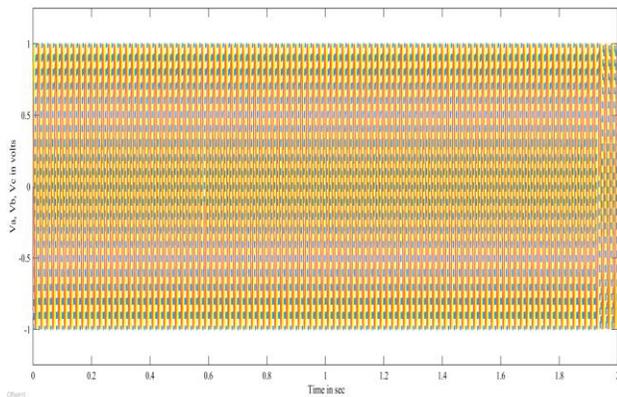


Fig. 8(a) Three phase AC voltage from the source

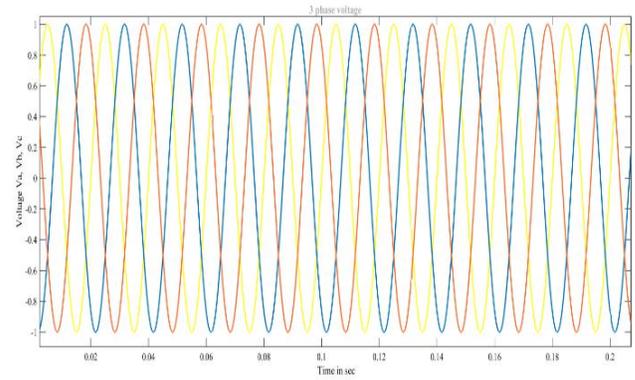


Fig. 8(b) Three phase AC voltage from the source

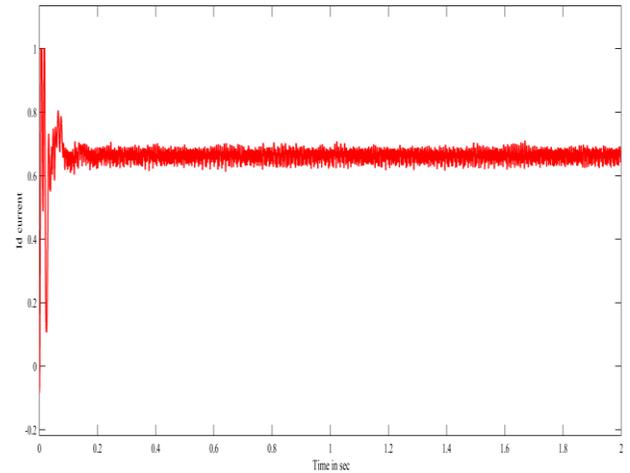


Fig. 9(a) Direct axis AC current

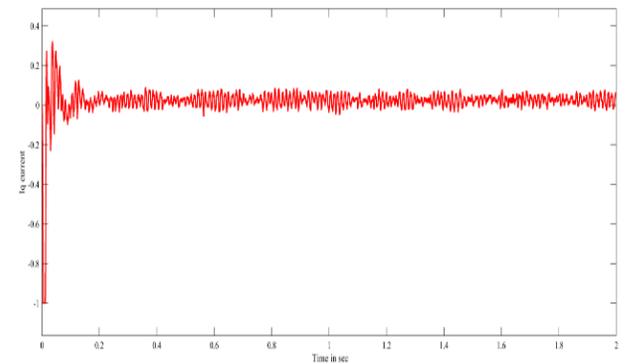


Fig. 9(b) Quadrature axis AC current

III. CONCLUSION

This paper presents the modeling and control of single stage three-phase grid-connected photovoltaic system. A two-loop control scheme is used to control the power delivered from the PV system to the utility grid. The MPPT control and the output current control is realized simultaneously in one power conversion stage thus simplifying the system topology, however increasing the control complexity.

REFERENCES

- [1] Johanna M.A. Myrzlk, " Novel Inverter Topologies for Single-phase Stand-Alone or Grid-Connected Photovoltaic Systems," IEEE PEDS 2001 Indonesia, vol. 1, no. 1, pp. 103 - 108, Oct 2001.
- [2] Chen, L.; Chen, H.; Li, Y.; Li, G.; Yang, J.; Liu, X.; Xu, Y.; Ren, L.; Tang, Y. SMES-Battery Energy Storage System for the Stabilization of a Photovoltaic-Based Microgrid. *IEEE Trans. Appl. Supercond.* 2018, 28, 1–7.
- [3] Rallabandi, V.; Akeyo, O.M.; Jewell, N.; Ionel, D.M. Incorporating Battery Energy Storage Systems Into Multi-MW Grid Connected PV Systems. *IEEE Trans. Ind. Appl.* 2018, 55, 638–647.
- [4] Yang, Y.; Ye, Q.; Tung, L.J.; Greenleaf, M.; Li, H. Integrated Size and Energy Management Design of Battery Storage to Enhance Grid Integration of Large-Scale PV Power Plants. *IEEE Trans. Ind. Electron.* 2018, 65, 394–402.
- [5] Lai, C.S.; Jia, Y.; Lai, L.L.; Xu, Z.; McCulloch, M.D.; Wong, K.P. A comprehensive review on large-scale photovoltaic system with applications of electrical energy storage. *Renew. Sustain. Energy Rev.* 2017, 78, 439–451.
- [6] O’Shaughnessy, E.; Cutler, D.; Ardani, K.; Margolis, R. Solar plus: Optimization of distributed solar PV through battery storage and dispatchable load in residential buildings. *Appl. Energy* 2018, 213, 11–21.
- [7] Zhang, C.; Wei, Y.-L.; Cao, P.-F.; Lin, M.-C. Energy storage system: Current studies on batteries and power condition system. *Renew. Sustain. Energy Rev.* 2018, 82, 3091–3106.
- [8] Olaszi, B.D.; Ladanyi, J. Comparison of different discharge strategies of grid-connected residential PV systems with energy storage in perspective of optimal battery energy storage system sizing. *Renew. Sustain. Energy Rev.* 2017, 75, 710–718.
- [9] Libo, W., Zhengming, Z. and Jianzheng, L. (2007) ‘A single-stage three-phase grid-connected photovoltaic system with modified MPPT method and reactive power compensation’, *IEEE Transactions on Energy Conversion*, Vol. 22, No. 4, pp.881–886.
- [10] Wang, Y-J. and Hsu, P-C. (2011) ‘Modelling of solar cells and modules using piecewise linear parallel branches’, *IET Renewable Power Generation*, Vol. 5, No. 3, pp.215–222.
- [11] Wu, T-F., Chang, C-H., Lin, L-C. and Kuo, C-L. (2011) ‘Power loss comparison of single- and two-stage grid-connected photovoltaic systems’, *IEEE Transactions on Energy Conversion*, Vol. 26, No. 2, pp.707–715.
- [12] Grandi, G., Rossi, C., Ostojic, D. and Casadei, D. (2009) ‘A new multilevel conversion structure for grid-connected PV applications’, *IEEE Transactions on Industrial Electronics*, Vol. 56, No. 11, pp.4416–4426.
- [13] Ghoddami, H. and Yazdani, A. (2011) ‘A single-stage three-phase photovoltaic system with enhanced maximum power point tracking capability and increased power rating’, *IEEE Transactions on Power Delivery*, Vol. 26, No. 2, pp.1017–1029.
- [14] Gitanjali Mehta and S.P. Singh, “Design of single-stage three-phase grid-connected photovoltaic system with MPPT and reactive power compensation control”, *Int. J. Power and Energy Conversion*, Vol. 5, No. 3, 2014.
- [15] U Subramaniam, S Vavilapalli, S Padmanaba, F Blaabjerg, J N D Almkhles, “A Hybrid PV-Battery System for ON-Grid and OFF-Grid Applications—Controller-In-Loop Simulation Validation”, *Energies*, vol. 13, pp no. 755, 2020.

NewsDose – The News App

Shaily Malik¹, Sahil Aggarwal², Yuvraj Gupta³, Vipul Goel⁴, Vedansh Varshney⁵

^{1,2,3,4,5}Assistant Professor, Dept. of Computer Science, MSIT, Janakpuri, Delhi, India

Abstract: In today's 24/7 competitive world, it has become necessary for people to be updated about the latest news happening inside of world. Here comes the role of "NewsDose". This article covers everything you need to know about NewsDose. [1]

I. INTRODUCTION

NewsDose(<https://newsdoseweb.netlify.app/>) is a platform built using react.js[9] which provides you daily news in the form of quick bites for absolutely free. NewsDose is here for you, showing news bites in 7 different categories like health, entertainment, sports, technology, etc. from 13 different countries, that too up to 1 week older!

Not only that, it has more features like:

- Text-to-speech
- Share news with friends on different platforms
- Save news locally for future references



Fig. 1 NewsDose Logo

II. EASE OF USE

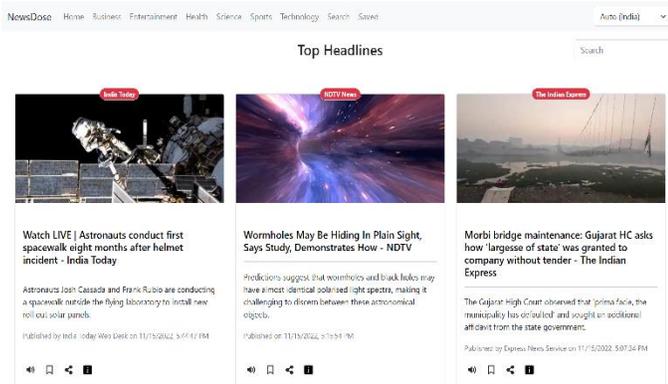


Fig. 2 NewsDose Website

Using NewsDose is as easy as to open a website in a browser. It can be visited independent of the device the user has. It provides

a very simple UI [13] to make the website user friendly and divides the news into 7 different categories so that it becomes easier for the user to read the news they actually want to. It also provides an easy mechanism to save news locally and to share it to friends and family.

III. KEY FEATURES

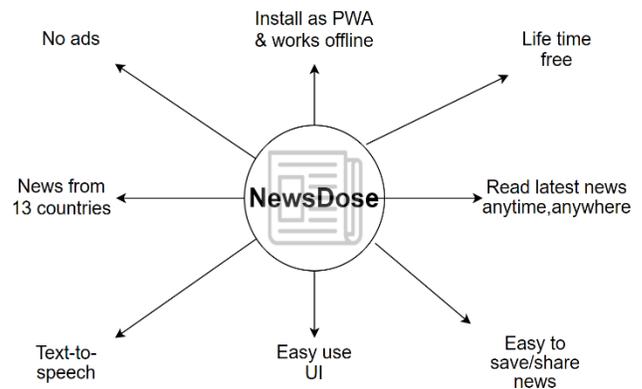


Fig. 3 Key Features of NewsDose

- Read latest news anytime, anywhere
- News from 13 different countries divided into 7 different categories
- Life time free
- No advertisements at all
- Easy to use UI
- Easy to save/share news
- Installable as PWA and works offline
- Supports text-to-speech

IV. RELATED WORK AND COMPARISON WITH OTHER NEWS PROVIDERS

Famous native news apps like Inshorts, Aaj Tak are either paid or contains a lot of advertisements and also are need to be updated very soon as they use their own writers and editors for maintaining and updating the news regularly.

On the other hand, NewsDose uses NewsAPI[10] which updates the news in a regular interval of time automatically and doesn't require any writer or editor to keep the news updated. Also, NewsDose works on a model using which it manages to show the news to the users for free and even without advertisements.

As compared to other apps, we also have a simpler UI as it doesn't contain any ad at all. We also manage to show user the news even when he/she is offline.

WHY NEWSDOSE ROCKS

FEATURES	OTHER WEBSITES	NEWSDOSE
Life time free	✓	✓
24/7 Support	✓	✓
No Advertisements	✗	✓
Text to Speech	✗	✓
Offline Mode	✗	✓
Upto 1 week Older News	✗	✓

Fig. 4 Comparison with other news providers

V. HOW IT WORKS

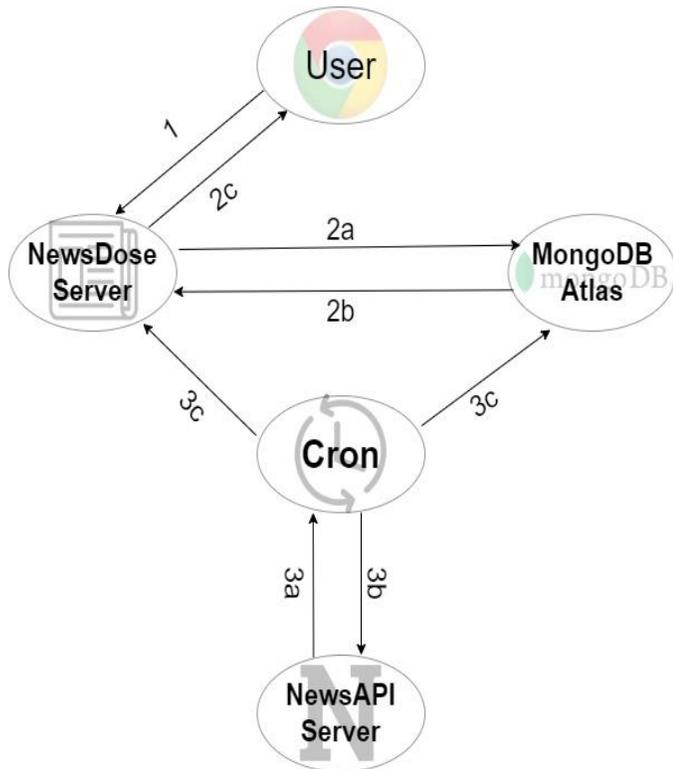


Fig. 5 Working of NewsDose

1. User requests news from NewsDose server.
2. Server operations:
 - a. If news is present in the server locally, the news is sent to the client as a response, else it requests news from MongoDB Atlas and next steps are continued.

- b. MongoDB Atlas returns stored news to the server and saves the news locally.
- c. Server returns the stored news to the user as response.

3. Cron operations [14]:

- a. Every hour, the NewsDosecron sends request to NewsAPI server for latest news.
- b. News API server returns the news as response.
- c. NewsDosecron updates the stored news inside MongoDB Atlas as well as NewsDose server.

VI. PROBLEMS FACED AND THEIR SOLUTIONS

NewsDose use the NewsAPI under the hood to provide the news to its end users.

But, NewsAPI is paid... And in order to provide the news to the people without any money and advertisements, we don't pay to the NewsAPI either, we use its free tier plan.

But, NewsAPI only provides 100 requests per day for free and doesn't show older news too... So how do we manage to show up to 1 week older news independent of how many times someone visits NewsDose? This question came up in our minds also, and we thought it wouldn't be possible to show news for free, but then came a brilliant idea of using a proxy server in between NewsDose and NewsAPI to solve our different problems. The problems we faced and their solutions:

- First problem we faced was dealing with CORS, NewsAPI serves news to only localhost for free. The main reason to create the proxy server was to solve this problem.
- Another problem we faced was only 100 requests available per day. To solve this we generated multiple API keys and stacked them together to increase the daily limit of requests.
- But as we created a proxy server and stacked multiple API keys, we saw another major issue, which was performance. The proxy server added in between caused the request making process too slow (~4-5 seconds). To deal with it, we changed the functionality of our proxy server. Now instead of redirecting the requests, we saved the news inside the local storage of our server and then served news from there, which solved the performance issue.
- Just saving the news to the server storage was not enough, we also had to update the news so that the end user sees the latest news. So we setup another cron server which updated the stored news every hour by fetching latest news from NewsAPI.
- But since the local storage of the server is not persistent, we

were not able to save the older news. To save the news, we used MongoDB Atlas[11] which eventually helped us save older news.

- Being a website, NewsDose was not able to load when user was offline. To solve this issue, we used Workbox [13] inside a service worker to cache the website and the news and update the cached news every time users loads the latest news.

VII. FUTURE WORK

NewsDose is awesome, but we aim to make it even better in the coming future. [1]

We will add features like:

- User signup/login for more personalized news.
- Regional language support.
- Upto 1 month older news.
- More detailed news and advanced searching.
- Notify users when latest news arrives via push notifications.
- Data validation of news.
- Improve the overall performance of the website.

REFERENCES

- [1] Brijesh Joshi, Nehal Patel, "Android News App", International Journal of Applied Engineering Research ISSN 0973-4562 Vol 13, Number 11 (2018) pp. 9310-9315
- [2] Sangeeta Ruth, Srividhya Raghavan V, Smrithi J,Saira Banu. 2016. "Spatial Preference NewsfeedSystem For Android Mobile Users", IJCSITS, Vol6, pp. 3-24
- [3] Carlson D (2003) The history of online journalism. In: Kawamoto K (ed.) Digital Journalism: Emerging Media and the Changing Horizons of Journalism, pp. 31–55
- [4] Boczkowski PJ (2010) Newspaper culture and technical innovation: American newspapers approach their digital future, 1980–2005. In: Neuman WR (ed.) Media, Technology and Society: The Challenges of Digital Convergence. Ann Arbor: University of Michigan Press, pp. 22–38
- [5] Chan-Olmsted S, Kim Y (2001) Perceptions of branding among television station managers: An exploratory analysis. Journal of Broadcasting & Electronic Media 45(1): 75–91
- [6] Bentley, C., B. Hamman, J. Littau, H. Meyer, B. Watson and B. Welsh (2007) 'Citizen Journalism: A Case Study', in M. Tremayne (ed.) Blogging, Citizenship and the Future of Media, pp. 239-259
- [7] Boczkowski, P.J. (2002) 'The Development and Use of Online Newspapers: What Research Tells Us and What We Might Want to Know', in L. A. Lievrouw and S. Livingstone (eds) Handbook of New Media: Social Shaping and Consequences of ICTs, pp. 270-86
- [8] Haris Ali Khan "Youtuber" Code With Harry "React Js Tutorials in Hindi"
- [9] <https://reactjs.org/docs/getting-started.html>
- [10] <https://newsapi.org/docs>
- [11] <https://www.mongodb.com/atlas>
- [12] <https://getbootstrap.com/docs/5.1/getting-started/introduction/>
- [13] <https://developer.chrome.com/docs/workbox>
- [14] <https://www.npmjs.com/package/cron>

RGB Image Encryption Algorithm Based on DNA Encoding and Chaos Map

Parul Chaudhary

Assistant Professor
Maharaja Surajmal Institute of Technology

Abstract-- Based on the peculiarities of RGB images, a new approach is given for encrypting them using DNA encoding and a chaotic map. The method begins by utilizing a DNA sequence matrix controlled by Logistic to encode the RGB image's red, green, and blue components. Next, it uses DNA addition to combine the R, G, and B channels, and last, it uses the DNA sequence matrix's complement to do a complement operation. After decoding, you'll see three grayscale pictures. Further, the encrypted pictures' R, G, and B components are recovered by rebuilding the image pixels disrupted by the Logistic chaotic sequence.

Keywords – Chaos Map, DNA Encoding, Encryption, Matlab, Verilog.

I. INTRODUCTION

With the proliferation of modern computing power, digital images have found numerous applications in many spheres of human endeavour. However, as more people have access to the internet, the security of photos is substantially compromised, making image encryption the most efficient method for transmitting images securely.

Chaos occurs when an otherwise predictable system behaves erratically. A chaotic system is characterized by its ergodicity, boundedness, and sensitivity to beginning circumstances. As a result, the chaotic system may be used for picture encryption while still satisfying some safety standards. Many academic papers warn against the use of encryption algorithms comprised of a single chaos map, despite the fact that chaotic encryption algorithms that use one-dimensional chaos maps, multi-dimensional chaos maps, and ultra-dimensional chaos maps all transform the image's pixel position and pixel values in similar ways.

DNA cryptograms take use of biological technology by encrypting data using DNA as the transport.

II. CONCEPTUAL UNDERPINNING OF THE SOLUTION

The DNA addition operation is carried out using the DNA sequence's encoded matrix, and the picture encryption is implemented using the Logistic mapping function.

A. DNA Encoding

DNA computing is an alternative to typical silicon-based computer technology that makes use of DNA, biochemistry, and

molecular biology to do computations. The field of DNA computing, also known as biomolecular computing, is one of the many subfields of computing that are rapidly expanding.

All data in today's electronic computers are represented in a binary manner, according to the prevailing theory. On the other hand, DNA sequences are the "codes" that carry meaning under the notion of DNA coding. Since each of the four bases in a DNA sequence takes up two bits, we utilise binary numerals to describe the sequence. Based on the complementarity between 0 and 1 in binary systems theory, we may deduce that 00 and 11 and 01 and 10 likewise complement. Since the digits 00, 01, 10, and 11 cover the four possible bases, we have 24 different possible encodings. Because DNA bases are related in a complementary fashion, only eight of the possible twenty-four coding permutations meet the notion of complementary base pairing.

Just to provide one example: According to the first encoding rule, the DNA sequence that corresponds to the value [0 0111010] in a binary picture is [A TGG]. Similarly, the decoding sequence for [11 0 01 01 0] follows the seventh encoding rule. The suggested approach uses a random number generator to select encoding and decoding rules from a pool of eight, with each rule being mapped to a distinct sub-region of the (0,1) interval.

B. The addition and subtraction operation of DNA sequence

To implement matrix computing for the R, G, and B components of DNA sequences, we employ the DNA addition operation. As a classic illustration of how sophisticated chaotic behaviour may emerge from extremely simple non-linear dynamical equations, the Logistic map, a polynomial map (equivalently, recurrence relation) of degree 2, is commonly referenced.

In a major work published in 1976, biologist Robert May popularized the map as a discrete-time demographic model comparable to the Logistic equation developed by Pierre François Verhulst. The most popular chaotic map is the one-dimensional Logistic map.

III. LITERATURE SURVEY

A. *An enhanced DES and chaos-based technique for digital picture encryption, 2009*

Several researchers, including Zhang Yun-peng, Liu Wei, Cao Shui-ping, Zhai Zheng-jun, Nie Xuan, and Dai Wei-di, have studied the effects of combining several types of picture-encryption techniques. As for their approach, it uses a logistic chaos sequencer to generate a pseudo-random sequence, applies it erratically to the RGB channels of a picture, and then encrypts it twice over using an improved DES. The speed and safety of this algorithm's encryption were both excellent.

B. A secure image encryption method based on a chaotic logistic map, 2006.

An image encryption approach based on a chaotic logistic map is presented by N.K. Pareek and Vinod Patidar. Using an 80-bit external secret key and two chaotic logistic maps, this research presents a new strategy for encrypting images. By assigning distinct values to each bit of the external secret key, we can use it to generate the beginning conditions for both logistic maps. Furthermore, eight distinct operations are employed to encrypt the pixels of a picture, and the conclusion of the logistic map determines which operation will be utilised for a given pixel. To make the cypher more secure, the secret key is changed after encrypting each block of sixteen pixels. Experimental, statistical, and key sensitivity testing all corroborate that the picture encryption system is a safe and effective means of transmitting encrypted images in real time.

C. A Method for Securing Images using Random Numbers:2004

Wang Xiu Feng, Zhang Han, to iteratively cycle over the pixel values, we first do a permutation transform and then a nonlinear map. A breakdown in encryption caused by an image's resemblance to itself or other visual psychological features.

D. An Image Encryption Method Based on the Chaotic Domain, 2006.

Inspired by the idea of increased privacy provided by multiple systems, Huang-PeiXiao and Guo-Ji Zang suggested a plan that makes use of two chaotic systems. A random sequence is produced by utilising one of the chaotic systems. Then a threshold function was used, turning the chaotic sequence into a binary flow. A permutation matrix was built using the second chaotic system. To begin, the binary stream has been used as a keystream to randomly alter the pixel values of a simple picture. The second step was to encrypt the revised picture using a permutation matrix.

IV. RESEARCH GAPS

DNA encryption approaches are still not effectively implemented in the encryption sector due to issues such as high costs of experimental equipment, complicated operations, and a lack of familiarity with the biology involved.

V. PROPOSED SOLUTION

Using DNA encoding and a chaos map, we offer a method for

encrypting RGB images that avoids the flaws of both single-chaos and DNA encryption by circumventing the latter through biological experimentation. In order to encrypt photos, the proposed approach uses DNA addition to first scramble the pixel values of the R, G, and B components of the images. Using colour pictures for encryption is straightforward, and the experimental findings demonstrate that this approach is robust against a range of assaults, making it an excellent choice for use in insecure communication. Flowchart of an Image Encryption Algorithm.

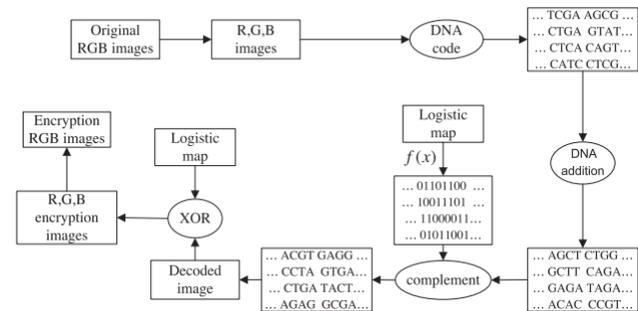


Fig 1: Image encryption algorithm flow chart

A. Algorithm Description

First, we performed an R, G, and B separation on the RGB picture. Second, we convert the R, G, and B channels to DNA code to generate a matrix of three DNA sequences; then, following the rules, we perform an addition operation on the three DNA sequence matrices to scramble the pixels of the various components and complete the DNA sequences with the new, disordered sequences. To finish, we'll decode for three pictures in grayscale, and then use a Logistic chaos map to wreak havoc on the pixels in each of those images. The final step is to combine the R, G, and B channels to produce encrypted RGB pictures. The algorithm's block diagram is seen in Fig. 1.

Specific phases in the encryption procedures are as follows:

First, we take an 8-bit colour picture $A(m,n,3)$ as input, where m and n are the image's row and column dimensions.

(2) Decomposing the RGB picture into R, G, and B matrices, then encoding each component independently using the DNA encoding rules chosen using seed key1 (key1 is a random figure and key1 2 121; 8), yielding three DNA sequence matrices $A_r(m,n,4)$, $A_g(m,n,4)$, and $A_b(m,n,4)$. ($m,n,4$).

(3) For the DNA sequence matrices $A_r(m,n,4)$, $A_g(m,n,4)$, and A_b , we perform an addition operation utilising a DNA pseudo operation ($m,n,4$)

For step (4), you need to produce a chaotic sequence of length $l = 14 \times m \times n \times 8 = 2$. By using Logistic Chaos with g_0 as the starting point and l_0 as the system parameter.

(5) The DNA matrix is supplemented but otherwise unaltered.

Based on the output of step 5, and using the DNA map rules chosen using the seed key2, step (6)

(7) Create a chaotic sequence c of length $m \times n$ using a Logistic chaos map system with g_1 as the beginning value and 11 as the system parameter. The transformation from a numeric vector $(c, 0)$ to a binary matrix $(c, 0)$ is accomplished by mapping the elements of c from $(0,1)$ to $(0,1,2,\dots)$,

(8) Create R_{00} , G_{00} , and B_{00} , three new matrices, by performing an exclusive or operation on c with R_0 , G_0 , and B_0 .

To decrypt colour pictures (RGB) that have been encrypted, step (9) is to retrieve the RGB values.

VI. EXPECTED OUTCOME

The suggested method has a huge secret key space and high secret key sensitivity, as would be seen from the results of a simulation. As a result, it is well suited for RGB picture encryption and can withstand exhaustive assault and statistical attack.

By employing a DNA addition operation, the suggested approach would effectively remove the spatial domain connection between the RGB image's pixels; furthermore, to

boost security, we incorporate a chaotic system to disrupt the value of the pixels. Thus, the security of the algorithm is determined by the chaotic system and the DNA operation to achieve a certain security, and has the dual security. Suitable for use in RGB picture encryption, the simulation experiment and results demonstrate the algorithm's efficacy, simplicity of implementation, vast secret key space, and effective resistance to exhaustive assault, statistical attack, and so on. The technique also has some usefulness as a standard by which to measure the security of encrypted video, audio, and other forms of multimedia.

The proposed algorithm's speed performance is not optimal; however, we use a mathematical model to simulate the algorithm in an electronic computer; and with the advancement of DNA chip technology, it is not difficult that using ultra-large-scale parallel computing power of DNA computing to implement the algorithm, the time cost is negligible.

REFERENCES

- [1] Chong Fu, Zhiliang Zhu, A Chaotic Image Encryption Scheme Based on Circular Bit Shift Method, The 9th International Conference for Young Computer Scientists. (2008) 3057–3061.
- [2] Sun F, Liu S, Li Z, Lü Z. A novel image encryption scheme based on spatial chaos map. *Chaos Solitons Fractals* 2008;38:631–40.
- [3] Vinod P, Pareek NK, Purohita G, Suda KK. A robust and secure chaotic standard map-based pseudo-random permutation-substitution scheme for image encryption. *Optics Commun* 2011;284:4331–9

Human Pose Estimation and Recognition

Dr. Rinky Dwivedi¹, Koyel Datta Gupta², Kunal Saini³, Apoorv Srivastava⁴, Yugal⁵

^{1,2,3,4,5}Computer Science Engineering, Maharaja Surajmal Institute of Technology

¹rinkydwivedi@msit.in, ²koyel.dg@msit.in, ³kunalsaini022@gmail.com

⁴apoorvsri412@gmail.com, ⁵yugal17v@gmail.com

Abstract:- Pose detection is an active area of research in the field of machine learning and offers several real-life applications. Pose can be defined as the arrangement of human joints in a specific manner. Therefore, the problem of Human Pose Estimation can be defined as the localization of human joints or predefined landmarks in images and videos. There are several types of pose estimation, including body, face, and hand, as well as many aspects to it. In this project, we will try to develop one such application and get out hands dirty with pose detection. We learned about pose detection and several models and neural networks that can be used for pose detection. A blaze pose model shall be selected for the purpose and its pros and cons over other models shall be taken into consideration. In the end, a classifier will be built to classify work out poses using the support vector classifier from the sklearn library. We will build our own dataset for this purpose which could further be extended easily using more images. Human Pose Estimation (HPE) is a way of extracting the pose of the human(s), usually in a form of a skeleton, from a given input: an image or a video. It's a fascinating and a rapidly growing field of research that finds applications in a variety of industries. Some of the most common use cases for HPE include sports coaching, computer games, healthcare, and more.

I. INTRODUCTION

With the ever-rising rate of digitalization in the modern age, numerous aspects of our life – be it visual, auditory or even emotional aspects, they are all being stored digitally in computers.

In theory, this is supposed to help in improving our quality of life and to an extent, it does exactly that but there is always room for improvement and innovation. Human Posture Estimation is one such aspect which involves machine learning. It has been more prominent in the recent years with smartphones becoming more accessible to the masses and social media applications getting immensely popular. Human Posture Estimation is defined as the problem of localization of human joints (or key points - elbows, wrists, etc) in images or videos. It is also defined as the search for a specific pose in space of all articulated poses. In traditional object detection, people are only perceived as a bounding box. By performing posture detection and posture tracking, computers can develop an understanding of human body language.

However, conventional posture tracking methods are neither fast enough nor robust enough to occlusions to be viable. High-performing real-time posture detection and tracking will drive some of the biggest trends in computer vision. For example, tracking the human posture in real-time will enable computers to develop a finer-grained and more natural understanding of

human behaviour. Posture estimation is by no means an easy task because strong articulations, small and barely visible joints, occlusions, clothing, and lighting changes make this a difficult problem. Several different models can be chosen from to perform posture estimations. These include – Open pose, Pose net, Blaze Pose, Deep pose, Dense pose and Deep cut.

II. LITERATURE REVIEW

Several recent studies have used various neural networks like the Convolutional Neural Network, Recurrent Neural Network [1] to facilitate pose estimation and detection. Choosing any one model over another may totally depend upon the application. After a thorough study of research studies, we found out about how the classical approaches failed to capture the geometric and motion information from the human body whereas, the neural networks excelled at it [2].

We decided to proceed with the CNN based model, MoveNet Lightning model for multipurpose pose estimation of our project. This model comprises of three models: the backbone layer is made up of MobieNetV2 model [21], the feature extraction layer is composed of a Feature Pyramid Network [22] and the prediction heads is comprised of a CenterNet model [23].



Fig. 1. MobileNetv2 semantic segmentation visualization results on PASCAL VOC 2012 [21]

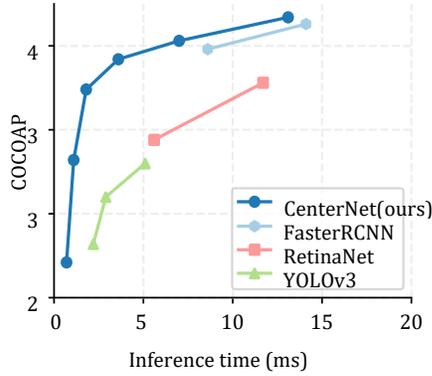


Fig. 2 Speed-accuracy trade-off on COCO validation for real-time detectors. The CenterNet outperforms a range of state-of-the-art algorithm [23].

This Also, the factors like running time, size of the model, and ease of implementation can be various reasons to choose a specific model. So, it is better to know your requirements from starting and choose the model accordingly [3]. There are three types of models using which we can model the human body and hence facilitate the pose estimation. The skeleton-based model, contour based and volume-based model [4]. We are going to use the skeleton-based model (obtained using CenterNet model). The reason behind choosing the skeletonbased model is that, we are keen on obtaining the key-points of the human body joints for which this is the best possible technique based on our research [5][23].

For obtaining the key-points of the human body joints as per the skeleton model, we are going to use a library called media pipe. Media pipe is an open-source cross-platform framework for building multi-model machine learning pipelines [6]. It can be used to implement cutting-edge models like human face detection, multi-hand tracking, hair segmentation, object detection and tracking, and so on.

The detection work can be done both for a 3d image/video or 2d image/video. The OpenCV captures what is being tracked by the camera in real-time [7]. So, we'll be dealing with a 2d input. OpenPose is an open-source real-time system for multi-person 2D pose detection, including body, foot, hand, and facial keypoints [8].

For multi person pose estimation and detection, we propose an extremely lightweight yet highly effective approach that builds upon the latest advancements in human detection and video understanding. Our method operates in two-stages: key-point estimation in frames or short clips, followed by lightweight tracking to generate key-point predictions linked over the entire video [9].

III. SCOPE

- The idea of representing real life objects in general, and particularly, human pose as a graph of parts has been a fascinating topic of research since the early days of

computer vision. To fully utilize the model in majority of real-life scenarios, it needs to be capable of distinguish between multiple subjects when they are present before the screen. If there is occlusion, then there is no realistic way to remedy as far as the model is concerned but in such a case when there are multiple people in front of the camera and there is no obstruction whatsoever, then the model should be able to perform an accurate pose estimation on each of them. This is an important detail which often gets overlooked in a good number of studies related to the field of human pose estimation.

- Majority of the papers related to this field concern themselves with single person pose estimation, which is a vital part of the study but most applications of pose estimation would benefit if one delves deeper into the world of pose estimation and trains a model capable of performing pose estimation on multiple people.
- Moreover, if the camera relies on software level implementation of focus detection and noise reduction then it can cause problems with the pose estimation. While most modern cameras opt for a hardware level implementation of the said functionalities, if we aim to achieve wide compatibility with the model then integrating those features would be helpful in the long run even though it would be time and resource consuming.

IV. METHODOLOGY

A. Data Research

Pose estimation can be done either in 2D or in 3D. 2D pose estimation predicts the key points from the image through pixel values. Whereas 3D pose estimation refers to predicting the three-dimensional spatial arrangement of the key points as its output. The classical approach to articulated pose estimation is using the pictorial structures framework. The basic idea here is to represent an object by a collection of "parts" arranged in a deformable configuration (not rigid). A "part" is an appearance template which is matched in an image. Springs show the spatial connections between parts. When parts are parameterized by pixel location and orientation, the resulting structure can model articulation which is very relevant in pose estimation.

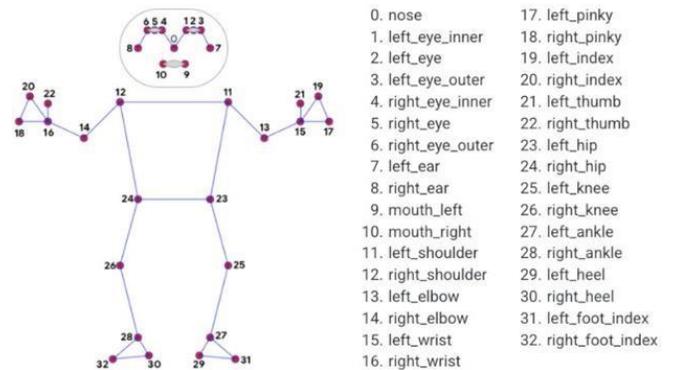


Fig. 3. Pose model for MediaPipe holistics

Pose estimation utilizes pose and orientation to predict and track the location of a person or object. Accordingly, pose estimation allows programs to estimate spatial positions (“poses”) of a body in an image or video. In general, most pose estimators are 2 steps frameworks that detect human bounding boxes and then estimate the pose within each box. The classical pipeline has its limitations and Pose estimation has been greatly reshaped by CNNs. With the introduction of “DeepPose” by Toshev et al, research on human pose estimation began to shift from classic approaches to Deep Learning. Most of the recent pose estimation systems have universally adopted ConvNets as their main building block, largely replacing hand-crafted features and graphical models; this strategy has yielded drastic improvements on standard benchmarks. There are three types of approaches to model the human body:

1. Skeleton-based Model
2. Contour-based Model
3. Volume-based Model

For pose estimation, we would be making use of Skeleton-Based Model.

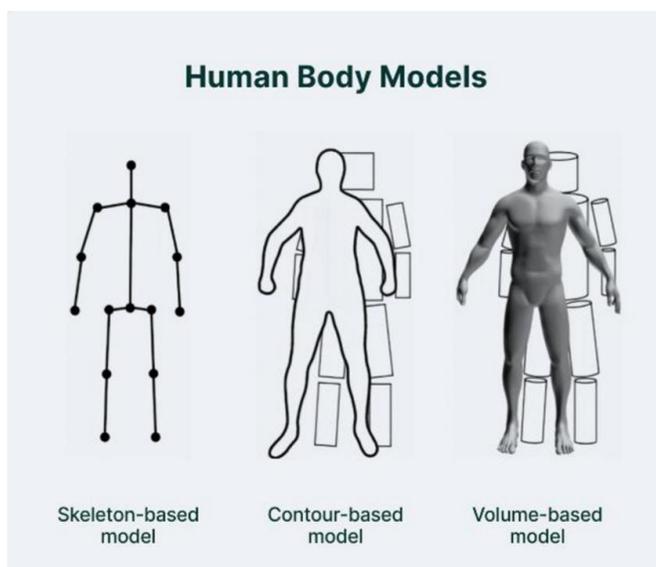


Fig. 4 Human Body Models

Pose estimation operates by finding key points of a person or object. Taking a person, for example, the key points would be joints like the elbow, knees, wrists, etc. There are two types of pose estimation: multi-pose and single pose.

Single pose estimation is used to estimate the poses of a single object in a given scene, while multi-pose estimation is used when detecting poses for multiple objects.

B. Data Analysis

Taking into consideration the various fields in which pose

estimation can be utilised, we can divide our project into two parts –

1. Single-person Pose Estimation
2. Multi-person Pose Estimation



Fig. 5. Single-person pose estimation using skeleton model



Fig. 6. Multi-person pose estimation

To make the flow of project more streamlined we divided the project into two modules, each of them dealing with each of the said two parts.

The first module would be related to singleperson pose estimation and it would serve as the groundwork for second module considering the fact that research done for the first module can be extensively used in the second one since multi-person pose estimation is by and large an extension of single-person pose estimation.

C. Model Training

i. Single-person Pose Estimation

The first module deals with Single-person Pose Estimation. With this, we aim to develop an automated pose detection

system. That system is going to estimate the angle formed between shoulder, elbow and wrist joints). For practical use, this module will help us track our arm movement while we move it up or down. We introduced a counter which keeps track of the number of times our arm has went in either direction.



Fig. 7 Module tracking the arm's 'up' movement



Fig. 8 Module tracking the arm's 'down' movement.

Thus, single person pose estimation (module1 using media pipe holistic) is used to localise human body joints positions when the input is a single person image. This is because the module implemented so far is doing only single person pose estimation. If there are multiple individuals in the vision, then the media-pipe holistic model might not produce skeleton model for more than one individual.

OpenCV reads image in BGR format by default. Moreover, working in RGB colour Scheme takes less memory. So, in the background, we'll be working with the RGB colour scheme and when displaying, we'll convert it to BGR colour scheme.

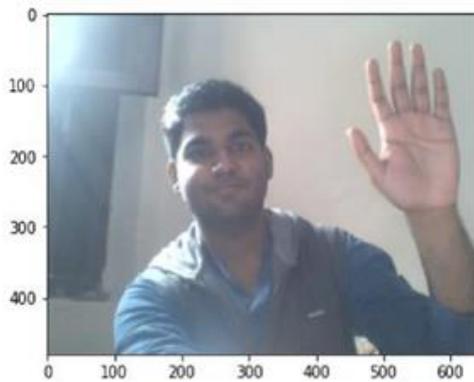


Fig. 9 Image in BGR color scheme



Fig. 10 Image in RGB color scheme

We continued working on the first module extensively till it can estimate the pose in given pictures up to a reasonably accurate degree. After achieving that, we moved on to the second module which deals with pose estimation when multiple people are involved.

ii. Multi-person Pose Estimation

For dealing with scenarios where multiple people are present, we developed a second module that helps us in this very scenario. This module helps in distinguishing between multiple people present on the screen and estimating the pose for each of them individually. In case of live feed, the individuals need to be present at a distance of 5-6 feet from the camera.

For this module we made use of a convolutional neural network-based model called Movenet. We use the Movenet. MultiPose Lightning model which differs from the MoveNet. SinglePose model in the sense that this model is able to detect multiple people in the image frame at the same time while still achieving real-time speed.

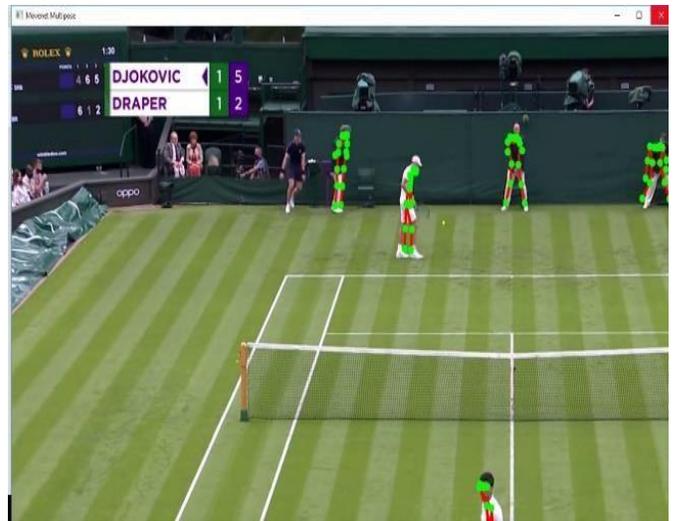


Fig. 11 Multi-person pose estimation

By making use of Movenet, the resulting module is able to detect the players in the tennis match as seen in Fig 6.

b. Model Evaluation

The MoveNet model is comprised of three models: the CentreNet model, MobileNetV2 and Feature Pyramid Network. With this model, we aimed to achieve a light yet robust method of estimating the pose of an individual as well as a group of individuals. We created two separate modules for that purpose, the first for single person pose estimation and the second for multi person pose estimation.

The first module was fed footage through the webcam and it was able to count the number of times there was a movement of user's arms, either upwards or downwards (as seen in Fig 7 and Fig 8). It was also able to convert the image in RGB mode so that the whole operation takes less memory and convert it back to BRG as the output for the user (Fig 9 and Fig 10).

The second module used the clip from a tennis match and it was able to estimate the pose of 5 individuals present on the screen (Fig 11). Although in addition to the players, it predicted the pose of people in the background as well.

V. RESULTS AND DISCUSSION

The modules trained for both single-person pose estimation and multi-person pose estimation perform reasonably well and under the right conditions, they are able to estimate the pose present in the provided media up to a good accuracy, as seen from the resulting images.

That does not mean the modules are perfect as there is some room for improvement present, both in the modules individually and as a whole. As for the first module, it won't work properly in a dark environment. Ample lighting must be present in the room where the module is being tested. Moreover, the colour of the clothes of the person present in front of the camera and that of the background must be different to ensure proper estimation.

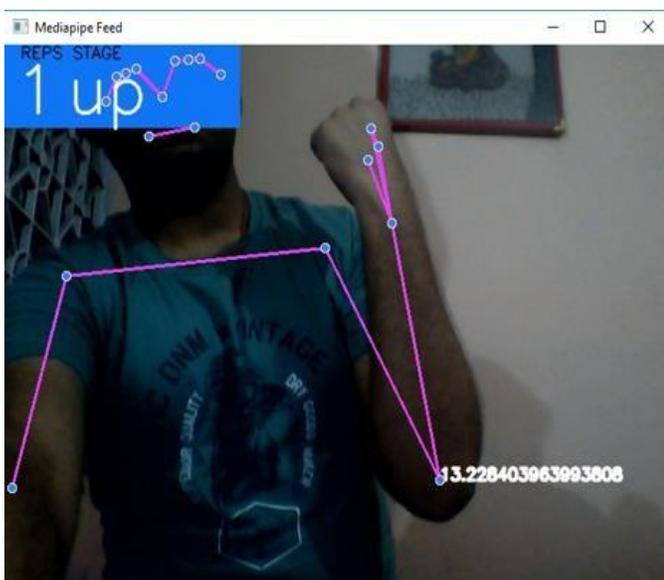


Fig. 12 Single-person pose estimation module up counter.



Fig. 13 Single-person pose estimation module down counter

These drawbacks are shared by the second module. Along with that, the second module also introduces its own limitations. It can only generate the pose of six individuals at a maximum. They also need to be spaced apart, since the model would have problems if the people present are overlapping. It also generates poses of people present in the background without any additional input and that can sometimes be unnecessary.

VI. FUTURE WORK AND LIMITATIONS

The model is able to estimate the pose pretty accurately but it's not without its limitations. There are some drawbacks present in each of the two modules which can be worked on in future.

The module for multi-person pose estimation is able to detect the pose of up to 6 people on the screen. This can be a problem in scenarios where we need to perform pose estimation on a large group of people, especially when it is in a public place. We can further train the module to increase its functionality and make sure it detects more people.

The second module can sometimes detect people that are in the background. This can be problematic when we only need the pose estimation of a limited number of people. As seen in Fig 9, we ran the second module on the clip of a tennis match and the module performed pose estimation on people sitting in the crowd which is not what we required.



Fig. 14. Module generating pose for people in background.

If the person in front of the camera is wearing clothes which have a somewhat similar colour to that of the background, then the pose estimation can get a little bit inaccurate.

The lighting in the piece of media on which the subjects for pose estimation are present needs to be sufficiently good to ensure the proper pose estimation.

VII. CONCLUSION

The model trained during this research is capable of single-person as well as multi-person pose estimation. There are some minor areas in which the accuracy of pose estimation by this model suffers but overall, the results have been majorly successful.

This technology can further be implemented in variety of real-world scenarios. The singleperson pose estimation module thus trained can be helpful in tracking the workout progress of an individual. It can also be used to generate a raw skeleton-based model of the said user present before the camera or in pictures.

The multi-person pose estimation module can be used in tracking the movements of sportspersons during live games and it can also be used to generate models for computer games up to a very high accuracy.

REFERENCES

- [1] Jonathan Tompson, Ross Goroshin, Arjun Jain, Yann LeCun, Christoph Bregler, "Efficient Object Localization Using Convolutional Networks", arXiv:1411.4280v3 [cs.CV] 9 Jun 2017.
- [2] Jiabin Zhang, Zheng Zhu, Wei Zou, Peng Li, Yanwei Li, Hu Su, and Guan Huang. Fastpose: Towards real-time pose estimation and tracking via scale-normalized multitask networks. arXiv preprint arXiv:1908.05593, 2019.
- [3] Zhe Cao, Gines Hidalgo, Tomas Simon, Shih-En Wei, and Yaser Sheikh. Openpose: realtime multi-person 2d pose estimation using part affinity fields. *IEEE transactions on pattern analysis and machine intelligence*, 43(1):172–186, 2019.
- [4] Bowen Cheng, Bin Xiao, Jingdong Wang, Honghui Shi, Thomas S Huang, and Lei Zhang. Higherhrnet: Scale-aware representation learning for bottom-up human pose estimation. In *Proceedings of the IEEE/CVF Conference on Computer Vision and Pattern Recognition*, pages 5386–5395, 2020.
- [5] Ce Zheng, Sijie Zhu, Matias Mendieta, Taojiannan Yang, Chen Chen, Zhengming Ding, "3D Human Pose Estimation with Spatial and Temporal Transformers", arXiv:2103.10455, March 2021
- [6] Jihye Hwang, Jieun Lee, Sungheon Park, and Nojun Kwak. Pose estimator and tracker using temporal flow maps for limbs. *IJCNN*, pages 1–8, 2019.
- [7] Yaadhav Raaj, Haroon Idrees, Gines Hidalgo, and Yaser Sheikh. Efficient online multi-person 2d pose tracking with recurrent spatio-temporal affinity fields. In *CVPR*, 2019.
- [8] Zhe Cao, Gines Hidalgo, Tomas Simon, Shih-En Wei, Yaser Sheikh. "Realtime Multi-Person 2D Pose Estimation using Part Affinity Fields", Cornell University. May 2019.
- [9] Rohit Girdhar, Georgia Gkioxari, Lorenzo Torresani, Manohar Paluri, and Du Tran. Detect-and-Track: Efficient Pose Estimation in Videos. In *CVPR*, 2018.
- [10] C. Chen, R. Ugarte, C. Wu and H. Aghajan, "Discovering Social Interactions in Real Work Environments," in 2011 IEEE International Conference on Automatic Face & Gesture Recognition and Workshops, Santa Barbara, USA, 2011, pp. 933 - 938.
- [11] G. Chittaranjan, O. Aran and D. GaticaPerez, "Exploiting Observers' Judgements for Nonverbal Group Interaction Analysis," in 2011 IEEE International Conference on Automatic Face & Gesture Recognition and Workshops, Santa Barbara, USA, 2011, pp. 734 - 739.
- [12] C. J. Burges, "A Tutorial on Support Vector Machines for Pattern Recognition," *Data Mining and Knowledge Discovery*, Volume 2, Issue 2, p. 121–167, Jun. 1998.
- [13] P. Viola and M. Jones, "Rapid object detection using a boosted cascade of simple features," in *Proceedings of IEEE Computer Society Conference on Computer Vision and Pattern Recognition (CVPR 2001)*, Volume 1, Kauai, HI, USA, 2001, pp. I-511 - I-518.
- [14] L. Breiman, "Random forests," *Machine Learning*, Volume 45, Issue 1, pp. 5- 32, 2001.
- [15] F. De la Torre, J. Hodgins, J. Montano, S. Valcarcel, R. Forcada and J. Macey., "Guide to the Carnegie Mellon University Multimodal Activity (CMUMMAC) Database," Tech. report CMU-RI-TR-08-22, Robotics Institute, Carnegie Mellon University, 2009.
- [16] L. Breiman, J. Friedman, C. J. Stone and R. A. Olshen, *Classification and Regression Trees*, Chapman and Hall/CRC, 1984.
- [17] N. Dalal and B. Triggs, "Histograms of Oriented Gradients for Human Detection," in 2005 IEEE Computer Society Conference on Computer Vision and Pattern Recognition, Volume 1, San Diego, CA, USA, 2005, pp. 886 - 893.
- [18] N. D. Thanh, W. Li and P. Ogunbona, "A Novel Template Matching Method for Human Detection," in 16th IEEE International Conference on Image Processing (ICIP), Cairo, Egypt, 2009, pp. 2549-2552.
- [19] T. Liu, H.-J. Zhang and F. Qi, "A Novel Video Key-Frame-Extraction Algorithm Based on Perceived Motion Energy Model," *IEEE Transactions on Circuits and Systems for Video Technology*, Volume 13, Issue 10, pp. 1006- 1013, Oct. 2003.
- [20] M. Kumar, "Key Frame Extraction From Consumer Videos Using Sparse Representation," in 2011 18th IEEE International Conference on Image Processing (ICIP), Brussels, Belgium, 2011, pp. 24372440.
- [21] MobileNetV2: Inverted Residuals and Linear Bottlenecks, Mark Sandler, Andrew Howard, Menglong Zhu, Andrey Zhmoginov, Liang-Chieh Chen, arXiv:1801.04381v4 [cs.CV] 21 Mar 2019.
- [22] Feature Pyramid Networks for Object Detection, Tsung-Yi Lin, Piotr Dollár, Ross Girshick, Kaiming He, Bharath Hariharan, and Serge Belongie, arXiv:1612.03144v2 [cs.CV] 19 Apr 2017.
- [23] Objects as Points, Xingyi Zhou, Dequan Wang, Philipp Krahenbuhl, arXiv: 1904.07850v2 [cs.CV] 25 Apr 2019.

Simulation of Battery Management System of Electric Vehicles

Rakhi Kamra¹, Annu Dagar², Smile Jandyal³, Mohd Arif⁴

^{1,2,3,4}Maharaja Surajmal Institute of Technology

Abstract: Battery Management Systems (BMS) are used in many industrial and commercial systems to optimize battery-powered and to estimate keeping the battery utmost out of a pernicious state to extend the life of the battery. For this justification, many monitoring strategies to detect the state of charge, temperature and current of the battery. In this paper, a monitoring system for EVs has been executed and tested. This system calculates and shows the battery temperature, charge/discharge current and state of charge (SOC) for the battery model in question. Digital -analog sensors with Microcontrol unit (MCU) are used for monitoring purposes. Received results explaining the main feature of the system are presented in figures and results are demonstrated on the hardware screen.

Keywords: Battery management systems, Monitoring techniques, State of Charge (SOC), State of Health (SOH), Open circuit Voltage (OCV).

I. INTRODUCTION

A Battery Management System (BMS) is a technology designed to handle a battery pack, which is accumulation of battery cells that are electrically arranged, i.e.

- Battery monitoring
- Providing battery protection
- Estimation of the operating state of the battery
- Continuous optimization of battery performance
- Reporting of operating status by an external device.

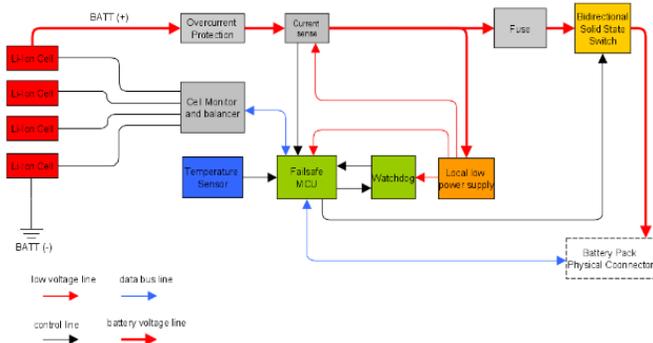


Fig. 1 BMS Block Diagram

The word "battery" includes the complete set; however, monitoring and control functions are particularly implemented to individual cells or groups of cells called modules in the overall battery pack assembly. Battery management system

(BMS) comprise of software and hardware to increase the discharge cycle battery to maximize battery life. For explanation battery management systems (BMS), there are two variables that should be considered. The first variable is the battery SOC, which refers to the amount of charge present in a battery during a charge/ discharge cycle. The second variable is the SOH. In the next section, function of BMS is explained.

II. FUNCTION OF BMS

Protects the security of the host utility operator; perceive dangerous operating situations and reacts Save battery cells from harm in cases of abuse or failure. Extends battery life keeps battery in a state where it can meet its practical layout necessities.

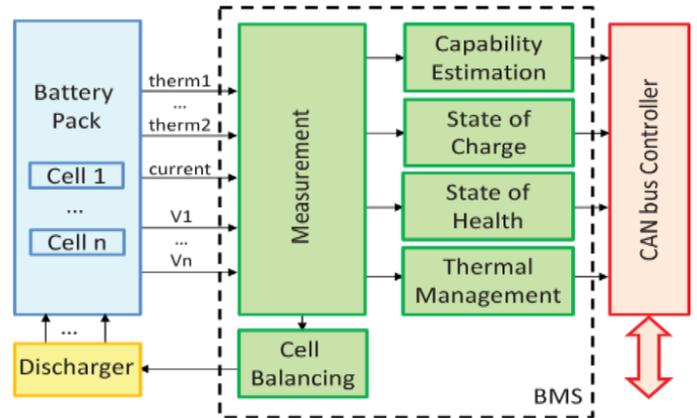


Fig. 2 BMS for Electric Vehicles

The general functionality of the BMS is connected to all components of the battery pack and to the host application control computer. The functionality can be divided into various categories: High voltage sensing and control, Protection, Interface, State-of-charge (SOC) estimation, as shown in Fig.2.

A. Series and parallel cells

Design, determined by economic, safety factors. Require 100V for safety (sometimes 50V) Require 600V to minimize power electronics costs. These considerations limit. For efficiency you want to minimize current to reduce losses (by using a thin higher conductor to reduce copper costs). This consideration limits so sets often designed using 100V modules which are then connected in series for a high voltage set, however there are also

reasons for connecting the modules in parallel, e.g. a "2P3S" module has 2 parallel, 3 serial articles.

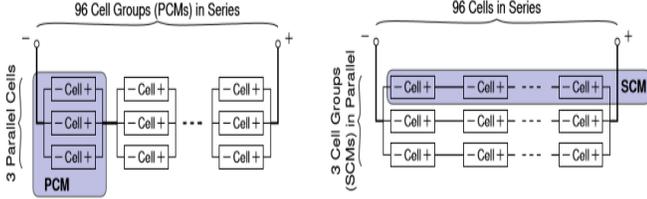


Fig. 3 Modular Design of BMS

III. PROTECTION AND ESTIMATION

A. Protection

The BMS needs to provide monitoring and manipulation to protect:

Cells from insupportable comprehensive operating situations users from the effects of battery failure excessive-energy batteries can be very risky: If electricity is launched in an uncontrolled manner, it may have catastrophic effects inside the occasion of a short circuit, for the duration of microseconds to broaden masses of amperes, different degrees of protection Failure in a lithium-ion cell can be very serious: explosion/fire Protection is indispensable in the automotive environment.

Protection must address the following adverse events or conditions:

- Excessive current during charging or discharging
- Short circuit
- Overvoltage and undervoltage
- High ambient temperature, overheating

B. Communication via CAN bus

The CAN bus (Control Area Network) is an ISO industry standard for on-board vehicle communication. It is designed to provide robust communication in very harsh automotive operating environments with high levels of electrical noise Two-wire serial bus designed to connect intelligent sensors and actuators; can operate at two speeds: High speed (eg 1M Baud): Used for critical operations such as engine control, vehicle stability, motion control Low speed. Simple switching and control of lighting, windows, adjustment of mirrors and instrument displays (etc.)

C. Log book function

The BMS must communicate critical information to the host application Often done via the CAN-bus protocol Communication needs are application specific but often include, how to control the charger to avoid safety risks? Log entries of atypical/malicious space events, Range estimates (distance or time to -empty), And of course estimates of available energy and power etc. Estimates BMS made are explained in next section.

IV. BMS ESTIMATE SOC AND SOH

A. Energy and power estimation

BMS cannot measure available energy or available power. Instead, these values must be estimated:

- In order to estimate energy, need to be known (at least) all states of charge of the cell.
- In order to estimate performance, at the minimum all SOC and cell resistances have to be known.

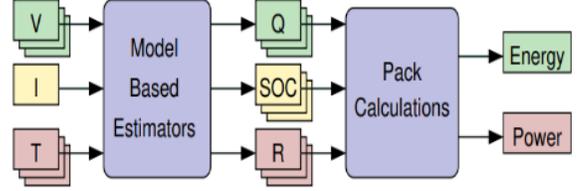


Fig. 4. Modular Design of BMS

B. Cell SOC and battery-pack SOC

The BMS must estimate SOC as input to algorithms that calculate available energy and available power. A good physical/electrochemical understanding of SOC and give information about a discharge/charge cell moves lithium between the negative and positive electrodes. Cell SOC refers to the average concentration in the negative electrode particles

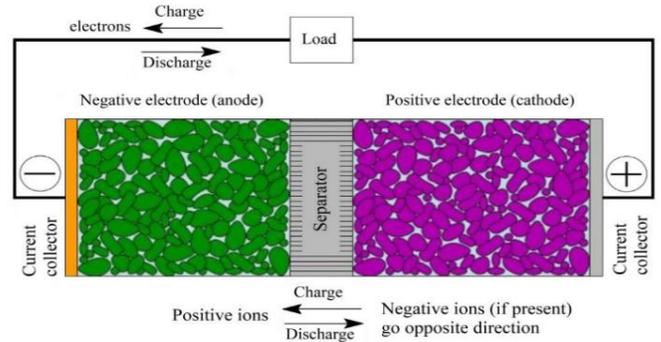


Fig. 5 Detailed structure of the interior of an electrochemical cell of a lithium-ion battery

C. Physical basis for cell SOC

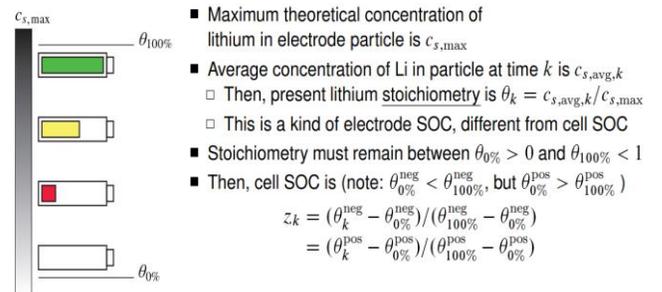


Fig. 6 Cell SOC and Battery-pack SOC

D. Relation Between SOC and Cell Voltage

The cell voltage depends on the surface concentration of Li in the particles that contact the positive and negative current collectors. SOC depends on the average concentrations over the whole electrode: it is not the same. Furthermore, the average concentration unaffected by the change in temperature, which changes the voltage, does not change the SOC. Resting a cell that changes voltage: does not change SOC. The entire current profile vs. net current that changes voltage but not SOC.

E. Relation Between SOC and cell Current

SOC is related to cell current through Cell to the operation of battery deteriorate voltages and charging η is the columbian efficiency of the cell, Q is the total capacity of the cell in coulombs. Note that Q measures the number of vacancies in the crystal structure of the electrode amid of 0 percent to 100 percent that would contain Li (Lithium).It is not dependent on temperature, velocity etc.

F. Cell available energy and power

Energy is the ability to do work, measured in Wh or kWh of the cell's overall energy

$$E(t) = Q \int_{z_{\min}}^{z(t)} \text{OCV}(\xi) d\xi \approx QV_{\text{nom}}\Delta z$$

It is not a dependent on temperature or speed. But it is unfeasible to get overall energy out of the cell at excessive speed and low temperatures.

G. HPPC discharge power

For HPPC discharge power, hybrid pulse power characteristic. For charging power, set $R=R_{\text{chg}}$. Note that this quantity is negative: Can be multiplied (taken absolute value) if needed to be reported as a positive value Usually HPPC will reduce estimates because the equations assume an initial steady state.

$$P_{\text{chg}} = v(t)i(t) = v_{\max} \frac{\text{OCV}(z(t)) - v_{\max}}{R_{\text{chg},\Delta T}}$$

We can now calculate estimates of future time horizon battery power and total battery energy by extending the way we calculated battery power and energy.

V. BATTERY-PACK-AVAILABLE ENERGY AND POWER

A. Computing battery-pack total Power

Recall that the discharge power of the HPPC cells is calculated Computational power in a series multi-cell battery pack, still the terminal V_{\min} . However, it must use a minimum limiting current, multiplied by the number of cells in series. Similarly for

charging (remember charging power is negative)

$$P_{\text{chg}}^{\text{pack}} = \sum_{j=1}^{N_s} \bar{v}_j i_j(t) = N_s v_{\max} \max_j \left(\frac{\text{OCV}(z_j(t)) - v_{\max}}{R_{\text{chg},\Delta T,j}} \right)$$

B. Computing battery-pack total Energy

Calculating battery power is a three-step process:

1. Determine the minimum Ah to discharge any cell to Z_{\min}
2. For this number of discharged Ah, calculate the resulting SOC of all cells.
3. Calculate the total battery discharge energy.

$$E_{\text{pack}}(t) = \sum_{j=1}^{N_s} Q_j \int_{z_{\text{low},j}}^{z_j(t)} \text{OCV}(\xi) d\xi$$

C. State-of-health (SOH)

BMS must report a battery state-of-health, not well defined. Resistance rises by 50% to 100%: (power decay) Estimation and during the operation of the battery will provide life indicators.

D. State-of-life (SOL)

State-of-life (SOL), which tries to predict how much life is left as a percentage.

VI. EXPERIMENT SYSTEM

There are three blocks shown in Fig 6(a):

1. Sensing
2. Discharging
3. Protection

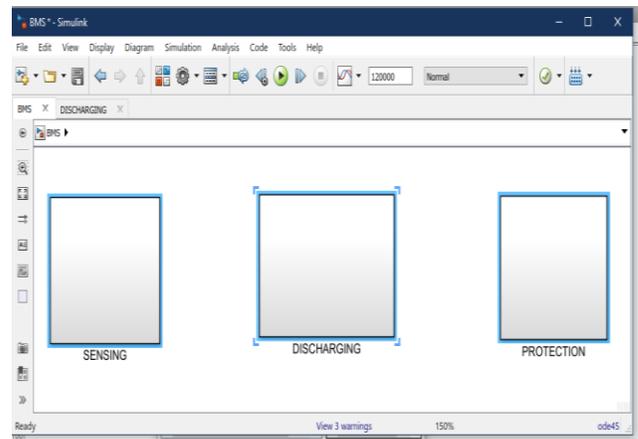


Fig. 6(a) Simulink interface of BMS

A resistive load is attached to the battery and output current (load current) is measured using the current measurement block. (LOAD = 10 Ohm). The measured current is sent to another subsystem using a "Goto Tag" for their specific computing purposes. The output of this subsystem is SOC in real time. The calculated SOC value is inserted into a 1D lookup table to obtain the corresponding OCV values. The measured OCV is fed to another subsystem using a "Goto Tag" for the appropriate calculation

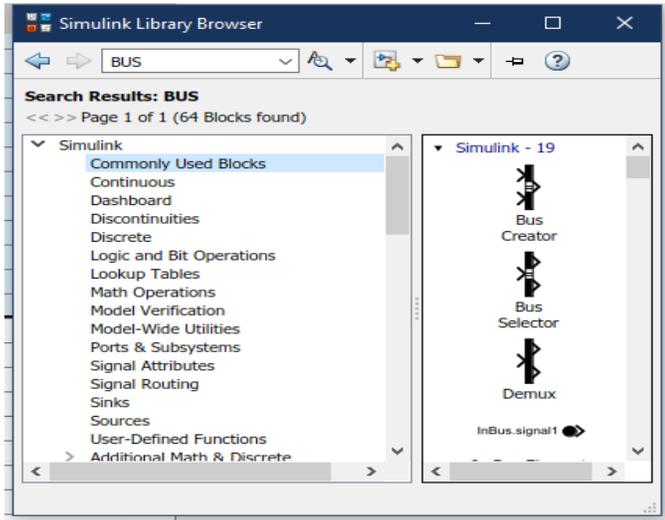


Fig. 6(b) Simulink Library browser

Fig 6(b) shows the Simulink library browser and commonly used blocks.

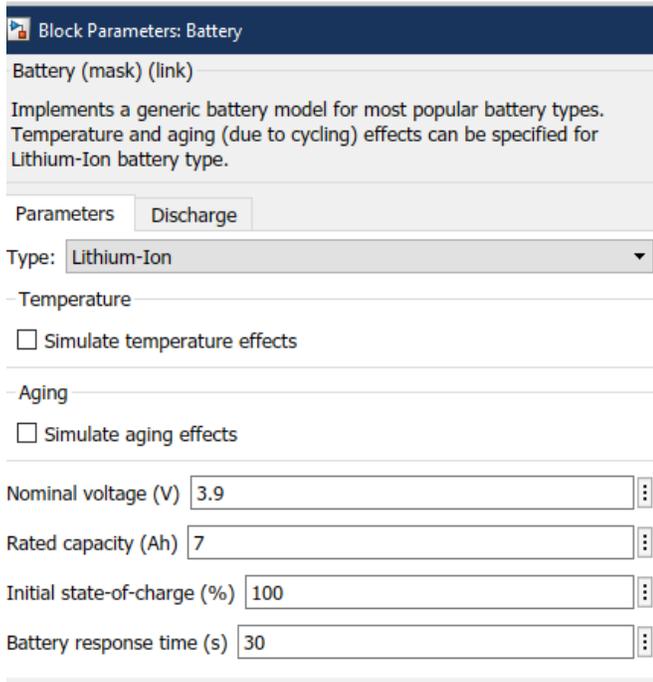


Fig. 6(c) Battery Parameters

Figure 6(c) shows the battery parameters like nominal voltage, rated capacity, initial SOC, Battery response time.

A. Discharging Circuit Diagram

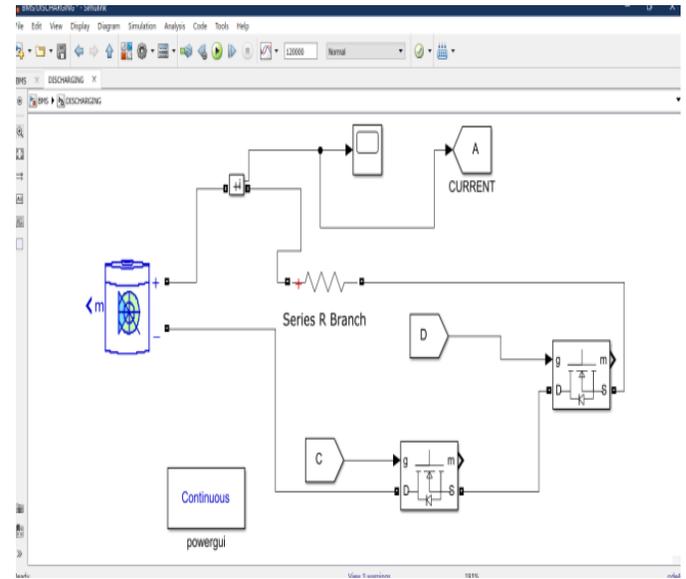


Fig. 6(d) Discharging Circuit model

Fig 6(d) shows a Resistive load is attached to battery and output current (load current) is measured using the current measurement block. (LOAD= 10 Ohm). The measured current is sent to other subsystem using the “ Goto Tag” for their particular calculation purposes.

B. SOC Subsystem

To calculate SOC, the equation is used, where SOC0 is the initial SOC, I represent the current, and alpha u denotes the product of the efficiency at a given temperature and the installed capacity of the cells

$$SOC = SOC_0 - \int \frac{I \times 100}{\alpha U \times 3600} dt$$

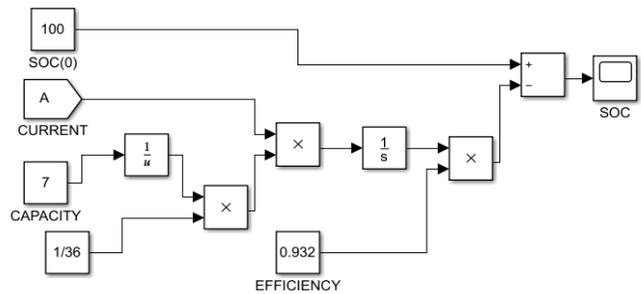


Fig. 6(e) SOC Subsystem

The output of this subsystem is SOC in real time. Fig 6(e) shows the SOC calculation subsystem structure.

E. OCV Subsystem

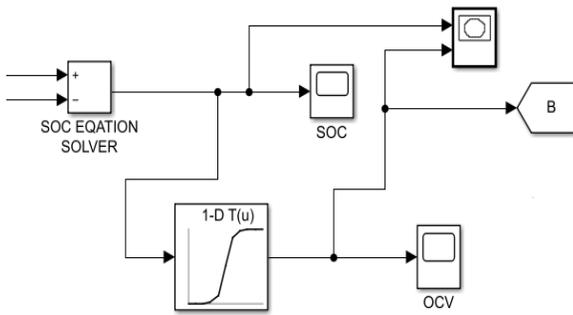


Fig. 6(f) OCV Subsystem

The calculated SOC value is inserted into a 1D lookup table to obtain the corresponding OCV values. The measured OCV is fed to another subsystem using a "Goto Tag" for the appropriate calculation.

F. Sensing Circuit Model

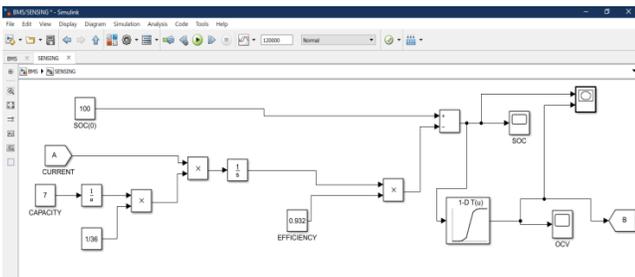


Fig. 6(g) Sensing Circuit Model

G. Protection Circuit Model

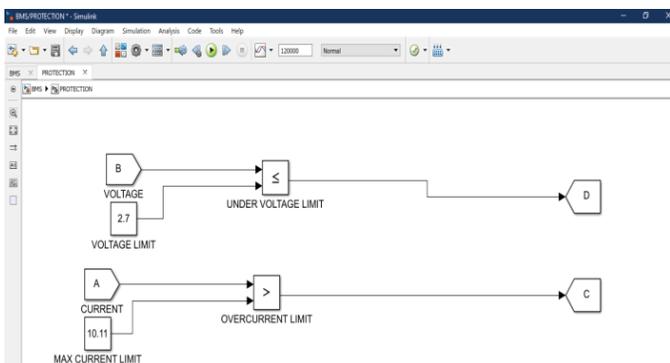


Fig. 6(h) Protection Circuit Model

Fig.6(h) voltage and current values are obtained from the tag, which are then compared with their minimum and maximum value to protect the circuit.

VII. RESULTS

SOC and OCV parameters were estimated and graphs were plotted to show the operation of a simple BMS circuit.

A. Load Current VS Time

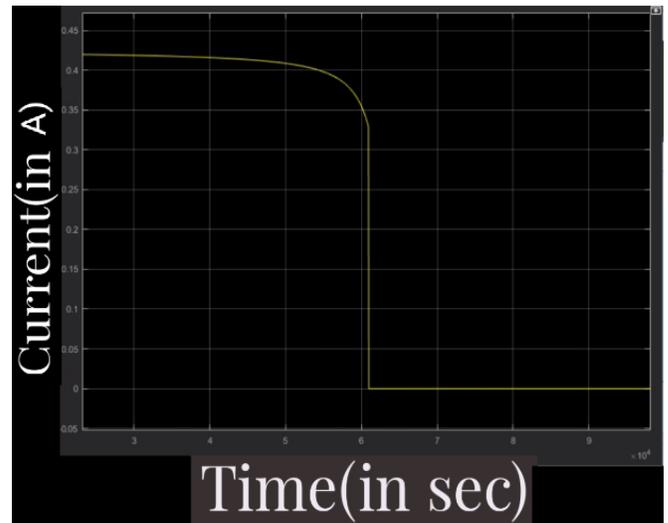


Fig. 7(a) Load current vs Time curve

The efficiency is evaluated according to the operation of battery deteriorate voltages and charging η is the columbian efficiency of the cell, $=1$, but practically ≤ 1

- FOR DISCHARGE: -Deterioratethe cell with a constant current of $C/30$ until the terminal voltage equals $V_{min}=2.75V$
- TO CHARGE: - Charge the cell at a contiuous current rate of $C/30$ up to the voltage at the cell terminals equals $V_{max}=4.33V$

B. SOC Vs Time

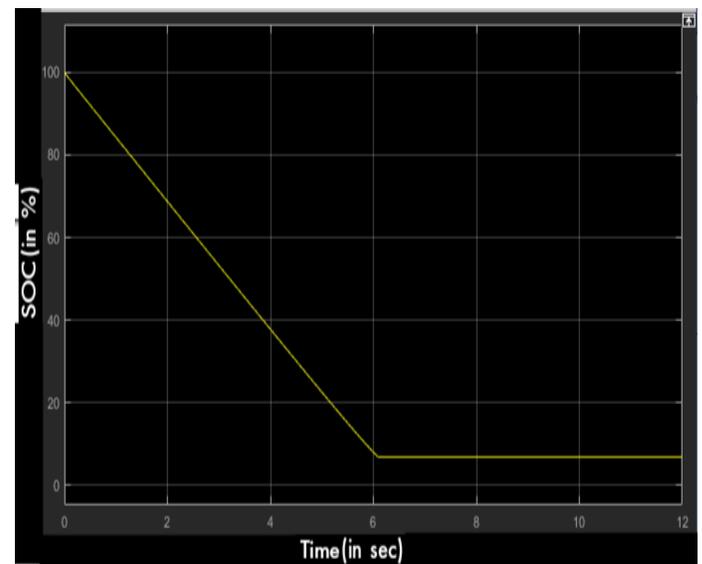


Fig 7(b). SOC vs Time curve

A graph is plotted between SOC and Time and is shown in in 7(b).

H. OCV vs Time

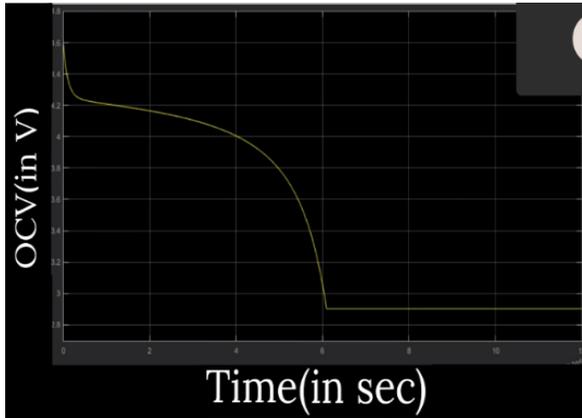


Fig 7(c). OCV vs Time curve

A graph is plotted between OCV and Time and is shown in 7(c).

I. SOC Vs OCV

A graph is plotted between SOC vs OCV as shown in fig7(d):

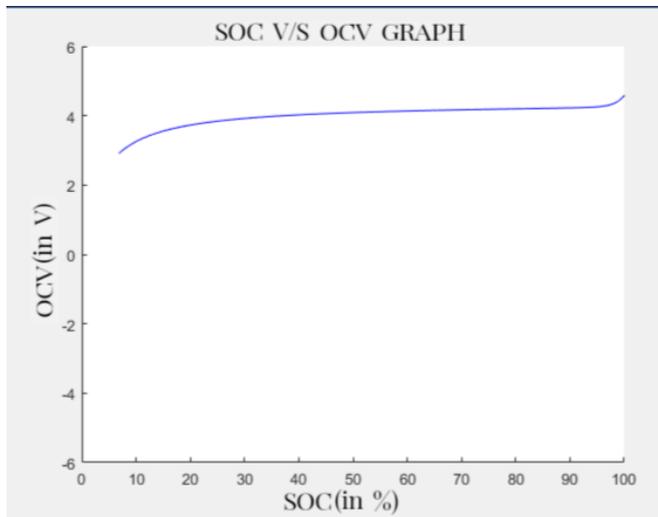


Fig 7(d). SOC vs OCV curve.

VIII. CONCLUSIONS

A simulated model for the carried out battery the usage of Matlab Software is accomplished to decide the SOC, which is the primary purpose of the Battery Control machine, and the model gives good consequences throughout both price and discharge cycles. Additionally, a very easy economical Experimental circuit with the use of MCU is schemed to calculate SOC and calculate battery temperature, the circuit that is designed gives an excellent estimate of SOC and an alarm is acquired when SOC exceeds the least possible or extreme limits an alarm is activated if the temperature transcend the highest set value and those alarms shield battery and make bigger its growth

REFERENCES

- [1] Jiang, J.; Zhang, C. Fundamentals and Applications of Lithium-Ion Batteries in Electric Drive Vehicles, 2015.
- [2] Pop, V. (Ed.) Battery Management Systems: Accurate State-of-Charge Indication for Battery Powered Applications, 2008.

Hackers and Their Techniques

Dr. Kavita Sheoran¹, Vishrut Rana²

^{1,2}Dept of Computer Science, Maharaja Surajmal Institute of Technology, Janakpuri, Delhi, India

¹kavita.sheoran@msit.in, ²vishrutrana0202@gmail.com

Abstract: Nowadays, hacking is a well talked and recognized issue. Because there are so many people in the world, many of whom are hackers, it is difficult to describe and objectively identify. This article is composed to maximize awareness among the different age groups of people/children about the different types of hackers.[1]

I. INTRODUCTION

A hacker is a person with technical computer skills. It is with the person how he uses his skill and for what purposes he uses his skills. There are different types of hackers performing several activities for different purposes. The basic question that arises to the people: How can we defend our system from black hat hackers? What is the average salary package for hackers? What are the types of attacks that an Ethical Hacker can perform on a device? Important steps performed by the Indian government. Which companies require the hackers most? How do we know that our system has been hacked? What was the history of hackers? How powerful could a hacker become in the future?[6]

So let us start our journey to the hackers with a basic technique that a hacker can perform.

II. DIFFERENT TYPES OF HACKERS

Hackers can be classified into many types but basically, there are 3 types of professional hackers (also shown in Fig. 1):

1. White Hat Hackers (Ethical Hackers).
2. Black Hat Hackers (Non-Ethical Hackers).
3. Grey Hat Hackers.



Fig:-1 Types of Hackers

The other types of hackers are:

1. Green Hat Hacker (intermediate hacker):

They are the ones who had just started hacking. They are the ones who perform tracking of IP addresses, packets, etc. [7]

2. **Blue Hat Hackers (revenge hackers):** They are the ones who use their skills for revenge against anyone/any organization.[5]
3. **Red Hat Hackers (aggressive hackers):** They are the ones who had quite a lot of knowledge and skill. They are used to stop the black hat hacker. They are the ones who can destroy the device completely using various dangerous viruses.[4]
4. **Script Kiddie:** A novice hacker who breaches a system using real hackers' tools, scripts, and software. They go by the name Script Kiddie. [5]
5. **Suicide Hackers:** They are those who are not concerned about being caught or receiving any other punishment because their goal is to destroy important infrastructure for a good cause. And many more... [7]

A. WHITE HAT HACKERS (ETHICAL HACKERS)

Many hackers use their skills for the world to be protected and from whom we should feel safe. A white hat hacker is a certified person from a university that uses purely his knowledge on serving the world to be the best in technology and defense. They help the people from the black hat hackers and sometimes grey hat hackers. They are the ones who are respected to be the most by every government agency. They use their skills in making their firewall, password, and smart passwords to be the maximum security and perform different types of penetration. They are the ones that are required the most in the future by every sector. They are quite friendly to us. They use to find the ports that are open in any device.[3]

B. BLACK HAT HACKERS (NON-ETHICAL HACKERS)

They are the ones who use their knowledge in harming the people, government, and world.

They are the ones from whom we should be very careful. As they are the most dangerous community in the world. They are the ones who are not certified and use the knowledge for harming society. They are usually indulged in many illegal activities.

They use many different techniques to access the person's sensitive data, rob money, etc. They are the ones who can even kill a person for not fulfilling their need. They are in huge amounts around the world. [2]

C. GRAY HAT HACKERS

They are the ones who are neither purely black hat hackers nor they are white hat hackers. They are the ones who can do anything they want with anyone's devices. They usually care about the profit they would get. They serve as a link between grey and black hat activities. They frequently scan systems for vulnerabilities without the owner's consent or knowledge. If problems are discovered, they report them to the owner and may ask for a modest charge to correct the issue or for identifying the issue with the code. They work illegally but help the company but after repeated warning to the company they can against black hat hackers. [4]

III. HOW CAN WE DEFEND OUR SYSTEM FROM BLACK HAT HACKERS?

Use the following advice to safeguard your devices and sensitive data:

- 1) **Use a Firewall:** In the present technology, almost all operating systems (OS) are providing a firewall. But the OS with 2007 and below might have to install a firewall. How the firewall defends a system is shown using Fig:- 2 [5].

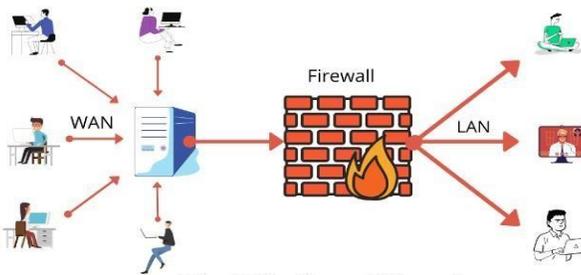


Fig:-2 Working of Firewall

- 2) **Install Antivirus Software:** A person should install an antivirus that can protect the computer from getting hacked. Bitdefender, Panda Free Antivirus, Malwarebytes, Avast, and McAfee are some of the antivirus programs you can utilize.[2].
- 3) **Install an Anti-Spyware Package:** Spyware is a specific kind of software that covertly watches and gathers data from individuals or businesses. Unwanted advertising and search results that are meant to send you to other (sometimes malicious) websites are difficult to spot and deliver. [1]
- 4) **Use Complex Passwords:** The hackers usually hack a device by hit and trial method i.e. by using the global libraries from a source such as GitHub. Try to use such password managing websites that provide you security as well as suggest some strong passwords, such as Dashlane, Sticky Password, LastPass, or Password Boss. For creating strong passwords, you should keep

in mind that the password should not contain any relative person's name, numbers. It should be random. You can use special characters such as '=', '@', '!', contain your mobile number, etc... also the password should not be too short to be guessed.[7]



Fig:-3 Two-Factor Authentication

- 5) **Use Two-Factor Authentication:** Many websites allow you to enable two-factor authentication, which increases security by requiring you to enter a numerical code in addition to your password when logging in. This code is sent to your phone or email address. It is a two-way login process as shown in [5] Fig. 3.
- 6) **Other Measures:** Use a browser that doesn't show any ads or irrelevant ads such as [Brave](#), [Tor](#), [Mozilla Firefox](#), [Vivaldi](#), [Epic](#), or [opera](#), or add an extension such as [DuckDuckGo](#). For Apple or mac users there are additional websites [Apple Safari](#)[3].
- 7) **Camera:** In laptops make sure the camera light is off when you are not using the device camera. If it is not getting off then cover the camera or preferably fold your laptop [5].

IV. AVERAGE SALARY PACKAGE OF AN ETHICAL HACKER

The average salary package of an ethical hacker in India is Rs 6,11,094 per year according to glassdoor.com. The height salary offered in India at present for an Ethical Hacker is from Rs1,21,641 to Rs9,10,630 by the company Infosys Limited [7].

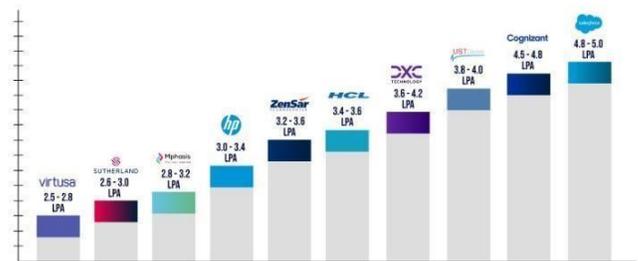


Fig:-4 Package of an Ethical Hackers

The average salary package around the world is between \$67,209 and \$103,583 per annum according to various salary

aggregate websites. The salary distribution on the basis of experience is:

- 0–1 year experience: \$75,027
- 1-3 years experience: \$80,440
- 4-6 years experience: \$89,399
- 7-9 years experience: \$98,991

V. DIFFERENT TYPES OF ATTACKS THAT AN ETHICAL HACKERS CAN PERFORM ON A DEVICE

There are 7 types of Attacks as shown in the Fig. 5

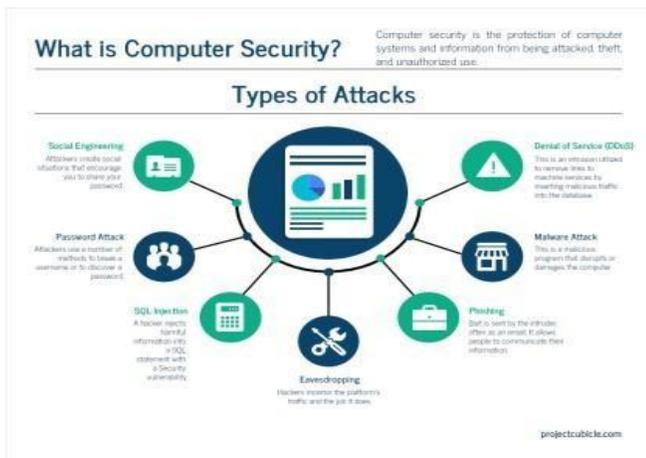


Fig.-5 Types of attacks

There are 10 types of attacks that a hacker can perform:

1. **Malware Attack [Malicious software Viruses]:** It contains trojans, worms, spyware, ransomware, and adware. A valid piece of software is the trojan virus. It restricts access to the vital parts of the network. Software known as spyware grabs all of your private information without your awareness. Adware is software that shows users advertisements on their screens, like any fruit. Malware enters a network and can seriously harm both a human and a device. It happens when a user clicks on a risky link, downloads an email attachment, or uses a pen drive that is contaminated. The rate of malware breaches is as shown in [6] Fig. 5
2. **Phishing Attack:** It is currently one of the most prevalent and pervasive forms of cybercrime. In this scenario, the hacker delivers the victim(s) harmful links via messages or emails. On clicking on such types of link(s) the hacker gains access to confidential information and sometimes account confidentiality through which a person can lose his/her credits from the account.[7]
3. **Password Hacking:** Now a day's password hacking also had become an easy task as hackers most of the time use the inbuilt password libraries and have to implement some of the combinations to crack them. But still while using some strong or difficult password gives the victims some time to stop the hacking. We can get to know whether the device is not responding or showing the filling of the option repeatedly (unless there is an external error)[3].
4. **Man-in-the-Middle Attack (eavesdropping attack):** During the COVID-19 pandemic it has been practiced for quite some time. In this, an attacker intercedes between the two parties. In other words, the attacker interferes with Client(s) and Host's conversation(s) [4].
5. **SQL Injection Attack:** When a hacker modifies a typical SQL query on a database-driven website, it results in a Structured Query Language (SQL) injection attack. It occurs when malicious code is introduced or introduced into the search field, forcing the server to divulge important information. This gives the attacker access to the database's tables for viewing, editing, and deletion. Through this, attackers may also obtain administrative rights. [2].
6. **Denial-of-Service Attack (DOS-attack):** This is a very dangerous attack as it floods the target system using a network resulting in the device to get shutdown or slowing down of the device [1].
7. **Insider Threat:** It is the attack performed by the insider (known person). The person could be dangerous if he is an intermediate as it could be hard or difficult to track the person [2].
8. **Cryptojacking:** These are the attackers who attack to steal/mine cryptocurrency (online currency). They also use online ads in which the JavaScript code was embedded in the emails. The victims are ignorant of this since the Crypto mining code operates in the background; the only indication would be a delay in the execution. [3].
9. **Zero-Day Exploit:** The seller makes the users aware of the vulnerability, but the attackers also learn about it. It depends on time how much time would the vendor and the developer could take. In the meanwhile, the exposed vulnerability is the focus of the attackers. They take care to use the flaw to their advantage even before a patch or other fix is put in place.[7].
10. **Watering Hole Attack:** Here, a specific segment of an entity or area is the victim. Here the attacker targets the website(s) that are frequently used by that group/organization. The Watering Hole Attack technique is done as shown in the [5] Fig. 7.



Fig:-7 Watering Hole Technique

VI. IMPORTANT STEPS PERFORMED BY THE INDIAN GOVERNMENT

According to annual data on cybercrime, the number of security breaches has increased by 69% since 2015 and by 11% since 2018. And hence the Indian government has created a law for the same [10]. Also, the Indian government had spent about \$945 million US dollars to enhance the cybersecurity of the nation.

Certain acts are made by our government:

- The patents(amendment) act, was formed in 1999.
- Trade Marks act.1999
- The copyright act, of 1957
- Information Technology Act

A. THE PATENTS(AMENDMENT) ACT

The 1999 founding of this act. Although such patents were not permitted, this legislation "Provided the filing of applications for product patents in the fields of medications, pharmaceuticals, and agrochemicals." [8]

B. TRADE MARK ACT

The "protection, registration, and prohibition of fraudulent use of trademarks" are the subjects of this law. A trademark is defined as a symbol that may be represented visually and can be used to differentiate one person's goods or services from those of another. This symbol can take the form of an object, its packaging, or a combination of colors. [9]

C. THE COPYRIGHT ACT

This act basically protects the content from getting copied by other [unauthorized] users and display it by just changing the name. In it the content should not be sheared along people using any mode of internet such as social-media, blogs, etc... [8]

D. INFORMATION TECHNOLOGY ACT

It is an Act that was created to give legal legitimacy to transactions that will be carried out through electronic data interchange or other forms of electronic communication, which are collectively known as "electronic commerce." In the year 2000, this law was established. [10]

VII. REQUIREMENT OF HACKERS.

Companies that hire certified ethical hackers in India are IBM, Netsoft Technologies, Prime Infoserve, Deloitte, VISTA Infosec, Standard Chartered, Crypto Mize, and TCS.

VIII. HOW DO WE KNOW THAT OUR SYSTEM HAS BEEN HACKED?

You may experience any of the following signs if your computer has been hacked: frequent pop-up windows, particularly those that direct you to visit other weird websites, some ads that contain viruses, or websites with unsafe links from the main page. Alterations to your homepage Your email account or messages are being used to send bulk emails. It might be even possible for someone to use your device to call another person using IP spoofing [7].

IX. HISTORY OF AN HACKER

In 1955, during a meeting of the Technical Model Railroad Club, the term "hacking" was first employed with technical acumen. Members' modifications to the capabilities of their sophisticated train sets were detailed in the meeting minutes. [9].

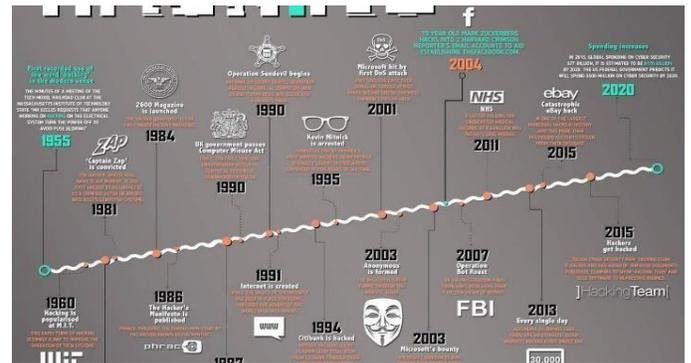


Fig:-8 History of Hacker's

X. POWER OF A HACKER IN THE FUTURE

It is believed that if there would be any war then it could be cyber war as it is quite powerful if a person gets access to any missile (nuclear missiles) so it would be quite dangerous. So according to my perspective, we should be pre-prepared for such types of dangerous things.[9]

XI. CONCLUSION

There are many knowledge in the world but it is within our hand how do we have to become in life and which company can lead

us to a successful as well as a respectful person around the world. Similarly, if there are black hat hackers so to stop them there are white hat hacker who are ready to stop the black hat hackers from defending the systems from getting hacked.

REFERENCES

- [1] Pavan Vadapalli, "Director of Engineering @ upgrade." Upgrade cyber security, AUG 23, 2022.
- [2] Tim Jordan, School of Media, Film, and Music, University of Sussex, SAGA Journals, 2008.
- [3] A handbook of copyright law, copyright government website,1957.
- [4] Authority, "Government of India",9 June 2000.
- [5] Ashish Kumar, "Youtuber" WsCube tech,29 Aug 2021.
- [6] Peter Lipa, co-founder of Sticky Password,2001.
- [7] Motoyuki Isobe, "President and Founder of Techouse", 3 Sep, 2021.
- [8] Krishna Kumar CEO of Simplilearn.com also an engineer graduate from NIT, Surathkal, India and started the company from 2010.
- [9] Kathy database developer and business process engineer and currently the founder of Techouse from 1995.
- [10] Jason McMahon Dual B.S. in Network Security & Digital Forensics, Coleman University (Graduated 2010), 2018.
- [11] Mattia Campagnano Attack & Pen Consultant with Optiv, 2018.

ECG - Analysis of Heart Disease

Geetika Dhand¹, Ayushi Gahlot², Gowrish Chhabra³, Yukta⁴

^{1,2,3,4}Dept. of Computer Science, Maharaja Surajmal Institute of Technology

¹geetika.dhand@msit.in, ²ayushigahlot020@gmail.com

³gowrishchhabra0211@gmail.com, ⁴yuktasolanki360@gmail.com

Abstract-- This article proposes a powerful method for classifying arrhythmias in electrocardiograms (ECGs). Using only the x and y axis, an artificial simple arrangement finds this breakthrough technology by taking into consideration the operation arrangement of various quantities. We transformed an ECG signal into 2-D grayscale images as input data in a CNN model. Various deep learning state-of-arts. This CNN classifier model is optimized with the help of various methods and techniques, some of which are Xavier initialization and data augmentation.

The two very famous CNN models; ALEXNET and VGGNET were compared with our proposed classifier. For the evaluation of the classifier, we used ECG recordings taken from a group or assembly of „MIT- BIH“ arrhythmias. Consequently, the average accuracy of our classifier is 94.05%. With 92.82% average sensitivity. We did ten flood testing to prove our CNN classifier. Also, no noise filtering is required by our proposed 2D CNN model as compared to the previously proposed 1D CNN classifier that uses more data than the one proposed in this project. The reason for this is that in one dimension (1D) the input ECG signal is used, even though the length of the database is improved, so performance improvement is not so significant. Our test findings very precisely showcase ECG images which are interpreted using the proposed CNN classifier without the use of any manual which was before the ECG signals, like noise feature extraction or reduction, and filtering.

I. INTRODUCTION

As recorded by World Health Organization (WHO), a prominent reason for death nowadays 's are cardiovascular diseases (CVDs). Approx. 27 million adults worldwide suffer from congestive heart failure (CHF), which is a burgeoning healthcare problem.

About 17.8 million persons, or 31% of all deaths, were caused by CVDs: according to statics, more than half a percentage of deaths was recorded in middle-income home country as. Any different modification in the normal heartbeat is aimed at Arrhyta, a representative type of CVDs. Congestieart failure; abrupt contraction, ventricular tachycardia, and tachycardia are a few kinds of arrhythmia. [1].

Continuous irregular beats can result in fatal circumstances but a single irregularity in n heartbeat will not substantially make a serious effect. For example: When hypo perfusion happens, heart failure can happen on the spot [2]. Prolonged paroxysmal atria Contraction (PVC) or irregular, fast heartbeats, VT. Thus, to manage and prevent CVDs It's critical to routinely check the heart's rhythms. [3].

II. PROBLEM STATEMENT

The problem states that ECG which means electrocardiogram is a not harmful medico's equipment that helps us display/the output rate of our heartbeat i.e., the status of the current heart. So, in the field of cardiac quick and mechanized detection of abrupt heartbeats by ECG signals is a significant and difficult thing to be done. Computer programs for ECG analysis are being developed and used to reduce the workload. Detecting heart disease early and anticipating its onset beforehand would even give us more and more benefits [4]. Early detection will help to decrease the probable chances of a heart attack. Also, these devices will be able to decrease injuries and avoid losses [5]. The target of the project is to detect these heart diseases early so that proper precaution and treatment gets possible for the patient [6].

III. SOLUTIONS ON APPROACH

A cardiac arrest may not occur if it is discovered early. Furthermore, these devices would be able to prevent injuries and avoid accidents. Noise filtering & feature extraction are no longer needed, after converting 1D ECG signals to 2D images, which helps to prevent the ignored ECG beats during noise filtering & feature extraction. We can augment our training dataset of 2D ECG images for higher accuracy. The malfunctioning of the 1dimension ECG wave may easily negatively affect this classifier as in previous literature data augmentation is hard to be applied [7].

The CNN model can be trained by using different cropping methods; in a particular ECG image various or multiple angles can be added. Because each ECG (electrocardiogram) 1D signal value is always 1 dimensional only, these ECG arrhythmia classification techniques are unprotected from the noise signal. Viewed as having the same degree of categorization. However, it is suggested while getting the relevant feature map CNN model can mechanically neglect the data with noise, in both the convolution and pooling strata when converting this ECG signal to the two- dimensional image. [8].

Hence, this bought-forward CNN model finds application in many ECG instruments for the ECG signal. Varied Models with varied sampling rates and amplitudes are necessary for the many ECG instruments. Images of ECG can be used to detect ECG rates to understand in what way healthcare practitioners get to understand the situation. To explain simply, this system may be used to program a medical robot to monitor ECG signals and

assist specialists in more precisely diagnosing rate conditions [6].

A. REQUIREMENT

Dataset: In reality, the "MIT~bih irregular Heartbeat collection" is made by 24X2 hr and 2 successive ECG data which was extracted by 46 patients who are doing research by the "BIH

Arrhythmia Laboratory" in a span of years 1975 & 1979. In Boston's Beth Israel Hospital. An incorporative percentage of patients' twenty-four- hour anesthetic ECG records are still about 62% and in-patients nearby 45% were gathered. Twenty-three (23) recordings were probably short-listed from this set, and the rest 26 records are probably taken to incorporate medical sufficiency in heartbeats that are not significant otherwise. [10]. All data were subjected to independent review by 2 or perhaps more people. Also, in addition, the database was designed to include each beat's computer-readable reference annotations (a total of about 110,000 annotations)." MIT- BIH Arrhythmia Database" is contained inside this whole directory. Since PhysioNet's launch in September 1999CD- ROM, around half of this database has been made publicly accessible online [11].

B. TOOLS AND LIBRARIES USED

The project has been implemented in python by using sea born, NumPy, pandas, SciPy, MNE, Keras, TensorFlow, OS, Spyder, Jupyter notebook, Arduino, Bread Board, ECG module ad8232, CoolTerm [9].

C. PROPOSED METHOD

Before the compilation of ECG waves and ECG wave classification, there are the steps included in our CNN-based ECG arrhythmia classification procedure. For training and validation, the "MIT~BIH Arrhythmia Database" is being implicated. Due to the CNN model being intended to process pictures, the ECG wave is converted into ECG pics while values preparation. Eight different ECG types are classified in the CNN classifier step [3].

1. ECG data pre-processing

Preprocessing means removing noise from the data to get closer to the true neural signals by converting ECG data into ECG images by mapping each 128 X 128 in a „grayscale“ image as every individual ECG pulse. The fact that every ECG pulse based on Q wave peak time is always sliced is known as "the MIT~BIH Arrhythmia Database. "Additionally, this kind of cardiac can be shown for each beat's identified Q wave peak moment on the ECG.

Hence, by highlighting the Q phase wave and eliminating the initial and final 20 ECGs by the earlier Q phase wave, we were able to create a single ECG beat picture. The ECG beat range is shown as follows:

$$T(Q_{\text{peak}(n-1)} + 20) \leq T(n) \leq T(Q_{\text{peak}(n+1)} - 20)$$

We could derive 100,000 pictures, each one showcasing one of eight from the "MIT~BIH Arrhythmia Laboratory," many ECG beat types are showcased. There are eight multiple kinds of Ecg signals. shown by the following figure with 128 * 128 (units) pictures produced by the ECG value method.

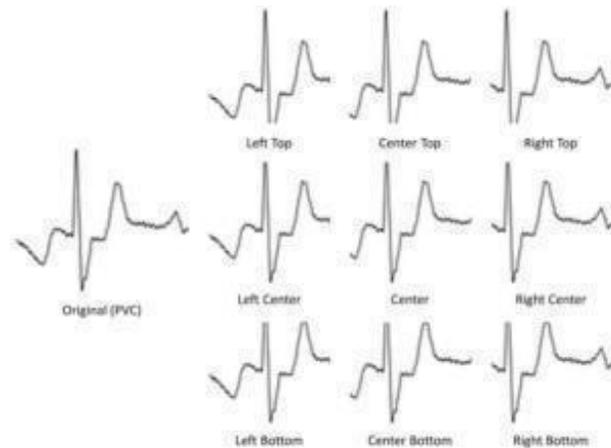


Fig 1: Normal beat and seven ECG arrhythmia beats.

2. ECG arrhythmia classifier

Just like the ECG arrhythmia classifier, we select the CNN. A heartbeat rate disorder known as an arrhythmia incorporates situations including ventricular tachycardia, irregular heartbeats, and heart block, among many more. This allows us to classify and test patients for different cardiovascular arrests or irregular heart rates. "LeCun" invented CNN in an attempt to detect handwritten zip codes, and he initially unveiled CNN in 1989. The current input-taking neutral arrangement is not appropriate for picture differentiation due to no different increase in the number of arguments as the basic picture is shown by not taking into account the architecture of the pictures. [13].

It is feasible to extract different local visual characteristics by using several nonlinear filters. We used 2'D to learn by transforming the ECG wave in an ECG picture because the 2" D complicated and combined strata are much more appropriate for defining the geographical localization of ECG pictures. Due to this, the ability to differentiate ECG arrhythmias is increased. As a result, we derived that by using this 2" D CNN architecture to analyze the ECG picture is comparable to how doctors diagnose arrhythmia.

A contest for identifying and categorizing objects has produced several effective CNN models. At "ILSVRC", AlexNet, which was unveiled in 2012, won first prize as 1st architecture to utilize this CNN architecture and GPU.

Before 2012, the error rate of an image classification model was roughly 25%, but AlexNet startlingly structure filters result since CNN models have greater depth [12]. To demonstrate the

best efficiency for categorizing ECG rhythms, we enhance the Cnn architecture while adhering to the fundamental VGGNet structure. We conducted a difference between the suggested CNN process and AlexNet and VGGNet. To demonstrate the best application of Ecg rhythms categorization, we improve the Cnn process while adhering to the fundamental VGGNet structure. We conducted a difference among the suggested Cnn architecture and AlexNet and VGGNet. The ECG picture used in this study is a straightforward 128x128, therefore nothing is required for different strata.

Increasing the number of data points will lead to more than subpar outcomes. The general layout of the proposed Cnn architecture is seen in Fig. 2 [11].

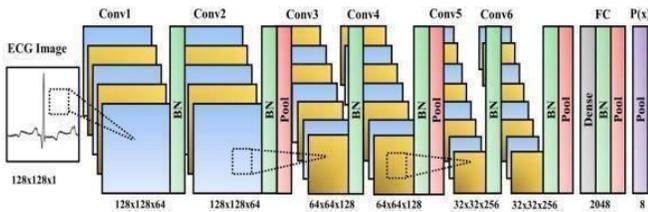


Fig. 2 The proposed CNN model architecture

3. Data Augmentation

Augmentation of data is the process of injecting unobserved samples to enhance the dataset. It's used in physiological 1D signal like the ECG is restricted as well definitely. In contrast to CNN, other classifiers like SVM and FFNN are tree-based algorithms; therefore enhanced data could not be manually supplied. However, our CNN model uses a two-dimensional ECG picture as its input data, cropping and shrinking the image to improve performance rather than degrade it and thereby increase the training data. For medical imaging Crating datasets is not a solution because getting a lot of expertly labeled samples takes a long time.

Here the value of leakage coefficient (α) is '0.3' and the value of hyperparameter (γ) is '1.0' [12].

The augmented network must be more reliable and authentic than the predicted shifts in similar X-Ray pictures. By employing data augmentation, we can increase the dataset number in the subsequent illustration [13].

By enhancing and balancing input data, great specificity and sensitivity may be attained. The seven ECG arrhythmia beats that are enhanced in this work are (1.PVC, 2.PAB, 3.RBB, 4.LBB, 5.APC, 6. VFW, and 7.VEB), the nine various cropping techniques used are: middle, middle->right, middle->left, middle->lowest, middle->lowest, lowest->left, lowest->middle, and lowest->right. The pictures of an ECG are 96 by 96 in size and are produced by the cropping process. There are two to three images in ECG. The images thus are sized to their original size i.e128 by 128 dimensions. The learning progress is sluggish as the time required to copy data inside the main memory and GPU memory during copying images from the disc, therefore, the

images produced inside the model have augmented images [5].

4. Kernel initialization

Kernel initialization is a fancy term for which statistical distribution to use the initializing of weights. A very prominent example of gradient information is that it will depart and fall into the smallest point which is local. Hence, to achieve convergence Kernel initialization is required. Filters (or kernels) signify weights also then a single convolution layer is formed by a group of

Kernels. This method proposed uses Xavier's initialization (According to this Uniform Xavier initialization, each weight is to be chosen at random from this uniform distribution within the range i.e. minus x to x, where x is equal to the square root of 6, multiplied with a measure of the input added to the measure of output for this overall transformation).

In all kernels the scale of the gradients is approximately the same; it is done using initialize balances. The randomly initialized weights have the under-listed range:

$$x = \sqrt{6} \text{ In} + \text{Out}; [-x, x] \quad (2)$$

The kernel weights system's real count of our output and input count is represented by terms In and Out.

According to research, the smaller kernel with more layers performs better than the prior one... As a result, setting our kernel size to 3×3 is more appropriate which is used by current CNN classifiers. After skipping, the image's original size we are including a zero-padding procedure [7].

5. Activation Function

The model's activation function provides the kernel weight as output. Nonlinear activation is easily utilized in contemporary CNN models. CNN is "LReLU" and "ELU" offer data with negation for this proposed activation function ReLU. Also, ReLU reduces all negative values to zero.In comparison to LReLU, ELU shows better performance for ECG arrhythmia classification. By the following equation we can show ReLU, LReLU, and ELU:

$$\text{ReLU}(x) = \max(0, x), \text{LReLU}(x) = \max(0, x) + \alpha_{\min}(0, x)$$

$$\text{ELU}(x) = x \text{ if } x \geq 0, \gamma(\exp(x) - 1) \text{ if } x < 0$$

6. Regularization

Normalization is another name given to regularization. This is a process that helps to lessen over-fitting in the period of training. Dropout and batch normalization are frequently used in most recent deep CNN models which use L1 and L2 normalizing techniques. To reduce the internal covariate shift, Batch normalization is used. Also, the input batch's mean and variance are computed, normalized, scaled, and shifted. The ECG arrhythmia classification is an instance in which it looks much more preferable to insert a batch normalization layer after the

activation function. As a result, we are adding a batch normalization layer after each model's activation function, which also includes the convolution blocks and the fully-connected blocks. To avoid over fitting Dropout is an easy method to perform probabilistic minimization, the reliance across layers by the participation of the nodes of the same layer [4].

As the result of Dropout's deliberate exclusion applied on some networks during learning, the model during training phase creates the voting effect by combining different models. The dropout used in this study can have a probable answer of 0.4, therefore it is represented forth the normalized strata [9].

LearningRate = LearningRate*0.95d (GlobalStep/1000) *e [11].

7. Cost and Optimiser Function

The cost function is the sum of variables that drive the optimization of a schedule. We can use an optimized function with the rate of learning to decrease the value of cost fun to a minimum.

$$C = -\ln X[y \ln(a) + (1-y) \ln(1-a)]$$

Here “n” stands for the quantity of training data, y for the predicted value, and a is the output layer's actual value. Adam, Adagrad, and Adadelta are a few popular optimizer functions. In our tests, we discovered that the Adam optimum places point early if they are being used. As a result, the best can be used Adams algorithm, which had a starting rate of learning 0.001 and a duration of 0.85 per 1,000 points. Additionally, we included the Adam optimizer function in our CNN model with 0.0001 for the early developmental pace and 0.95 for each 1,000 decay step. One method for calculating the learning rate at a specific global step is:

The validation set determines whether a model sufficiently reaches accuracy with a given training.

8. Validation Set

CNN's validation criterion is treated as the loss of value. However, it is witnessed that early model termination which was based on loss value is unable to produce high sensitivity in seven arrhythmias classifications. The confirmation sets and confirmation criteria can both equal the average sensitivity of the testing dataset. We stopped the learning process and started the assessment using the test set because the weighted average sensitivity could not increase over the preceding 500 worldwide steps. [3].

9. Optimized CNN Classifier Architecture

In this study, we propose a “Convolution Neural Network (CNN)” architecture that was optimized for the age categorization task. Comprehensive tests on a variety of them to help them with the breadth and forming of the CNN philosophy and CNN architectures were executed. Error ratios, training

durations, and standard deviations are successful outcomes when the fitness of the age categorization is taken into account. Compared to previous CNN- based designs with a large number of layers, the CNN architecture has 4 convolution layers and 2 fully linked layers. With more than 55,000 photos of faces, we are testing our strategy on them. The overall concept of “Alex Net” as well as of “VGG Net”, which was used by ECG categorization of beats is now a suggested CNN model being used for comparison [8].

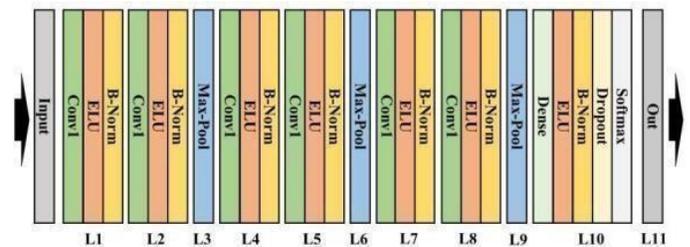


Fig. 3. Proposed CNN Model Architecture

IV. RESULTS

The CNN model applied has an early schedule for being stopped which uses a set that is validated. If beat epoch classification studies are concerned the suggested arrangement performs positively. The accuracy rate for the “MIT~bih” irregular heartbeat data collection training set was nearly 100%, also the curve was comparatively flatter. Also, the accuracies of the set of the test were between 91% and 96%, also once 100 epochs had passed, the accuracy curve was essentially flat. Presents graphs of loss, and average accuracy, showing each arrhythmia type with individual sensitivity until the “10,000” steps globally. In all the graphs, we conclude, around 1,000 steps the loss value begins to converge. Due to Low accuracy and sensitivity loss value is terminated early when the positive and negative classes are distributed inequitably. When using the CNN model to categorize ECG tachycardia and the early stopping strategy considering other metrics such as AUC is recommended [12].

V. CONCLUSION

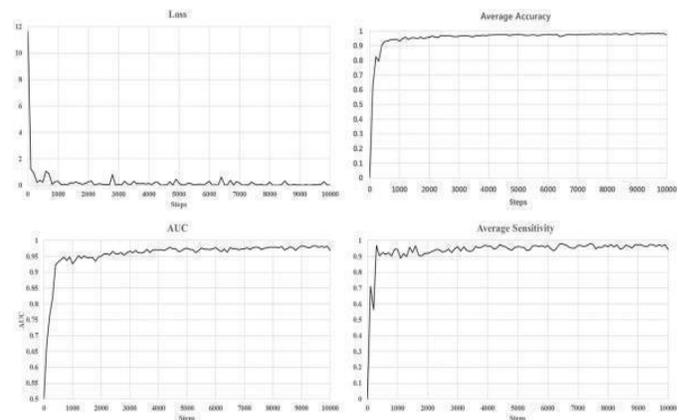


Fig 4: Evaluation Graphs

The ECG signal's low amplitude, complexity, and non-linearity make it challenging to manually classify data quickly and correctly. This calls for the creation of an automated system that can distinguish irregular heartbeats from vast volumes of ECG data for application in the field of health. The findings of our ECG arrhythmia classification report [4] suggest that the identification of heartbeats using ECG pictures also the CNN architecture proves to be a useful method for assisting specialists in the treatment of cardiovascular diseases that can be observed from ECG waves. The scanner or the medical robot that looks over the ECG waves proposed ECG categorization of beats can be used. To alert various doctors about arrhythmia, developing a wholesome ECG approach of classifying discrepancies in which the patient's ECG is scanned using the system and the health robot's pictures.

REFERENCES

- [1] Arif M, Akram MU and Afsar FA "Arrhythmia beat classification using pruned fuzzy k-nearest neighbor classifier." International Conference of Soft Computing and Pattern Recognition pp 37-42, 2009.
- [2] eylan R and zbay Y, "Comparison of FCM, PCA and WT techniques for classification ECG arrhythmias using artificial neural network." Expert Systems with Applications 33(2):286-295, 2007.
- [3] Desai U, Martis RJ and Nayak CG, "Machine intelligent diagnosis of ECG for arrhythmia classification using DWT, ICA and SVM techniques." Annual IEEE India Conference pp 1-4, 2015.
- [4] Dutta S, Chatterjee A and Munshi S, "Correlation technique and least square support vector machine combine for frequency domain-based ECG beat classification." Medical Engineering and Physics 32(10):1161-1169, 2010.
- [5] Gler and beyl ED, "ECG beat classifier designed by combined neural network model." Pattern recognition 38(2):199-208, 2005.
- [6] Haseena HH, Mathew AT and Paul JK, "Fuzzy clustered probabilistic and multi layered feed forward neural networks for electrocardiogram arrhythmia classification." Journal of Medical Systems 35(2):179-188, 2011.
- [7] Jadhav SM, Nalbalwar SL and Ghatol A, "Artificial neural network based cardiac arrhythmia classification using ECG signal data." International Conference on electronics and Information Engineering pp VI-228, 2010.
- [8] Jadhav SM, Nalbalwar SL and Ghatol AA, "ECG arrhythmia classification using modular neural network model." IEEE EMBS Conference on Biomedical Engineering and Sciences pp 62-66, 2010.
- [9] Jun TJ, Park HJ and Yoo H, "GPU based cloud system for high-performance arrhythmia detection with parallel k- NN algorithm." Annual International Conference of the IEEE Engineering in Medicine and Biology Society pp 5327-5330, 2016.
- [10] Jun TJ, Park HJ and Minh NH, "Premature ventricular contraction beat detection with deep neural networks." IEEE International Conference on Machine Learning and Applications pp 859-864, 2016.
- [11] Kiranyaz S, Ince T and Gabbouj M, "Real-time patient- specific ECG classification by 1-D convolutional neural networks." IEEE Transactions on Biomedical Engineering 63(3):664-675, 2016.
- [12] Linh TH, Osowski S and Stodolski M, "On-line heart beat recognition using Hermite polynomials and neuro- fuzzy network." IEEE Transactions on Instrumentation and Measurement 52(4): 1224-1231, 2003.
- [13] Kohli N, Verma NK and Roy A, "Arrhythmia classification using SVM with selected features." International Conference on Computer Communication Technology:pp486-490, 2010.

Linux for Machine Learning

Krrish Malhotra¹, Nilay Datta²

^{1,2}Computer Science Department
Maharaja Surajmal Institute of Technology, New Delhi, India
krrishmalhotra12@gmail.com

Abstract: Several developers trying to get started with ML have a tough time deciding the right environment for their venture. Even though Linux is recommended by mentors as a superior environment, a clear outlook on its advantages isn't provided. This paper focuses on educating newcomers about Linux based operating systems and helping them choose the right distribution for their ideal learning environment.

Keywords: Linux; ml

I. INTRODUCTION

Before ML came into existence, traditional programming was used where the logic was written to get desired output. However, several times writing the correct logic can be very difficult and time-consuming. Thus, ML was first introduced in the 1950s as an attempt to allow the computer to create its logic based on the provided input and desired output.

Over the years, ML gained a lot of popularity and attracted several new developers who weren't as versed with Linux or the open-source community as a whole [5].

Linux user base is expanding at an exponential rate and will soon become the go-to operating system for all developers.

It offers several advantages, especially for ML over other operating systems which are discussed ahead.

II. MACHINE LEARNING

Machine learning is the ability to find the algorithm based on the given inputs and outputs. Unlike traditional programming, the computer creates its logic based on input data and corresponding output data and applies it to other data [4].

A. Machine Learning Environment



Fig. 1. Structure of a Machine Learning Environment

It is an environment where machine learning training can happen. The most commonly used machine learning environment is Anaconda or Miniconda. Because of these environments, we can implement machine learning programs [4].

B. Modules in Machine Learning

Common modules that are installed are Pandas, Scikit Learn, TensorFlow, Numpy, Matplotlib, Pyplot, and Jupyter Notebook [4].

- Pandas

It is used to perform operations on a set of data. These include reading, changing or selecting a part of data.

- Scikit Learn

It is used to implement various models. These models will be used to create logic for the ML model based on the data.

- Numpy

It is used to create or perform operations on an array. We need this as data is stored in an array (tensors).

- Matplotlib.pyplot

It is used to create graphical plots of data. This helps us to analyze our given data.

- Jupyter notebook

It is used as an online environment which allows the user to compile the chunks of code with minimal effort.

C. Iterative Procedure in Machine Learning

- Problem Definition

In this, we analyze the problem we are dealing with and create a suitable model accordingly. The problem is categorized keeping certain factors in mind to generate the best possible outcome [5].

- Data

It includes the inputs and outputs that are used as learning material for Machine Learning. The data should be organized and chosen carefully to ensure a stable and effective solution.

- Evaluation

It is the process of determining if the procedure developed

works efficiently and proceeding accordingly. Careful evaluation isn't necessary however it is a good habit to maintain even for smaller projects.

- Features

It includes analyzing the type of data that should be provided.

- Modelling

Modelling is the process of deciding on a model to be used for the problem. The model is chosen based on several factors to ensure maximum accuracy.

- Experiment

It is the process of experimenting with data and models to find the most accurate outcome.

III. LINUX

Linux is an open-source operating system released under the GNU General Public License (GPL). As long as it is by the same license, anyone is free to run, examine, edit, and redistribute the source code. Even though it is an open-source project, it is completely legal to sell copies of modified code.

Being an open-source project, it keeps on evolving. Hence, the support for new technology and even non-mainstream tools is way more readily accessible.

An operating system is something that manages a system's hardware and resources. An operating system provides a method for stable communication between hardware components like CPU, memory and storage. It acts as a mediator between all of your software and hardware resources to effectively run the entire system.

Linux was originally designed as a better clone of UNIX and over time, it evolved to run on all modern-day devices from smartphones to supercomputers [2].

Every Linux-based operating system involves the Linux Kernel. A kernel can be considered the most essential unit of an OS [6]. It acts as the main underlying layer between the OS and the hardware resources. All the generic tasks such as networking, device control, memory and process management are effectively controlled by the kernel. Linux kernel is unique in its way due to its ability to adapt properly in any engineering environment [6].

The Linux kernel achieves many of the portability benefits that would otherwise need an abstraction layer without suffering from the performance hit associated with microkernels by building a general kernel model using components that are shared by all standard architectures [6].

Professional and amateur developers from all over the world contribute to the Linux kernel by introducing new features, identifying and resolving bugs and security holes, live patching, and offering fresh concepts while giving back to the community.

Any common Linux-based operating system includes several other major components aside from the kernel. One of them being the GNU tools. The system is essentially the GNU system with Linux added. The GNU tools provide a way to manage the resources provided by the kernel, configure performance and security settings, install additional software and much more.

Most of the operating systems also ship with a desktop environment. A desktop environment is a bundle of several components like a window manager, icons, toolbars, wallpapers and much more which form the entire Graphical User Interface of a distribution. Unlike other operating systems, desktop environments in Linux are highly customizable and dynamic. It is even possible to switch to other desktop environments quite easily. This allows the user to make the best out of their operating system ensuring great productivity and usability.

Linux which was considered mostly a hobby for enthusiastic engineers and developers in general has today grown into one of the most used operating systems worldwide [2]. Even though it is mostly used for networking and server management, over the years it has grown into an amazing daily driver alternative.

Linux was always declared as a tool based on good design principles and a sustainable development model. The original goal of its development was to make it widely portable and available. All these factors including the enormous contributions made by the open-source community led to the modern-day success of Linux [2].

IV. ADVANTAGES OF LINUX FOR ML

- Linux is completely open source making it entirely free to use. Being open source, it houses a massive community of developers. Hence, any issues you report would be treated with much more attention than any other privately-owned project.
- Linux also provides you with an overall better performance than any other operating system. Since the installation is highly customizable, you can easily limit the amount of bloatware in your environment. It also provides several lightweight desktop manager alternatives which will be talked about later. Overall, your ML applications will work a lot smoother on Linux with no extra hardware modifications.
- When using Linux, you have much more freedom when it comes to tweaking your system which is essential for developers. With just a single command, you can switch to a Super User allowing you to have complete control over your operating system.
- Support for GPU CUDA is easily better on Linux-based operating systems than on windows. Linux allows you to execute GPU-based commands effortlessly backed up with an adequate amount of guidance available on the internet.
- Several libraries like Tensorflow and PyTorch have limited support on windows since it requires custom compiling of

the software. Comparatively, running such libraries on Linux is way easier.

- Linux overall offers better security than windows due to its robust nature. Running exe files on windows can potentially be dangerous if the source isn't trusted. Whereas, Linux offers a much safer route for the same by centralizing the entire installation process through package managers. Package Managers allow you to conveniently install your software of choice with a single terminal command [3].
- Unlike windows, Linux provides greater stability since it doesn't force reboots during updates and other major changes. It is also better when it comes to random blue screens of death and other such glitches.
- Canonical, the organization which developed Ubuntu (one of the most popular Linux distros of all time) collaborated with Google to develop a tool named Kubeflow, which allows easier installation of ML tools and frameworks, as well as making it easier to use GPUs.

V. TERMINAL EMULATORS

One of the key features of all Linux Distributions is a Terminal Emulator. Each distribution is by default shipped with a custom terminal emulator. It is a software which replicates the functionalities of classic computer terminals.

It can be considered as a way to directly access the computer system. It allows the user to perform hardware actions that GUIs can't ask for.

It is easily the most powerful tool available once you get used to it. Even though it's similar to the Command Prompt in windows, it is way more functional and easier to use.

Because of the vast number of functionalities, new users might have a tough time getting used to it. However, it is worth it. There are several terminal utilities available which make compiling your programs a lot faster and easier.

Some commonly used Terminal Emulators include:

- Xterm

It is one of the oldest terminal emulators that is still used in several xorg-based systems to date. It was developed in the mid-1980s and is extremely lightweight.

- Gnome Terminal

It is the default terminal emulator shipped with a Gnome desktop environment. It is highly functional and extremely easy to customize. Since Gnome is shipped with several mainstream distributions, Gnome Terminal is usually the first emulator used by most.

- Konsole

Konsole is the default terminal shipped with the KDE desktop environment. Similar to Gnome Terminal, it is very convenient

to use and comes along with several personalization features.

- Alacrity

It is one of the few terminal emulators which use GPU specifically OpenGL for some of the processing. It is extremely fast and is written in Rust. Alacrity is currently one of the most commonly used terminal emulators since it appeals to a vast audience.

- Kitty

It is one of the newer terminals and was first released in 2017. Similar to alacrity, it uses OpenGL and is based on Python. Kitty also provides several unique features like embedding media into the terminal window and much more. Overall, it is a great choice for beginners as well as advanced users.

VI. LINUX DISTRIBUTIONS

A Linux Distribution (commonly known as distro) is ready to use operating system which has a compilation of several software along with the Linux Kernel.

Each distribution has its own set of pre-installed tools, a desktop manager, and a window system. Therefore, every distro is unique in its way and has its uses.

Hence, choosing a distribution is the first step when it comes to installing a Linux-based operating system.

Most of the mainstream Linux Distributions available today eventually evolved from one of the five main initial distributions developed during the early days. Each one of them served its unique purposes and later branched into modern-day distributions with a similar goal.

- Slackware Linux

It was initially known for its simplicity since it resembled the original UNIX the most. It is most popular among experienced experimenters and those seeking a more straightforward and straightforward distribution.

- Debian

Debian is to date a good alternative as a daily driver. However, it is mostly used for servers and other networking-based applications. It is extremely stable and formed the foundation for some of the most popular distributions currently available namely Ubuntu, Elementary OS, Linux mint, Kali Linux and much more.

- Red Hat

Red Hat offers the technology needed to develop and deploy applications more securely across a hybrid cloud. It heavily focuses on the importance of security across the entire infrastructure, application stack, and life cycle. It is considered the parent distribution of Fedora which is one of the most popular daily driver distributions today.

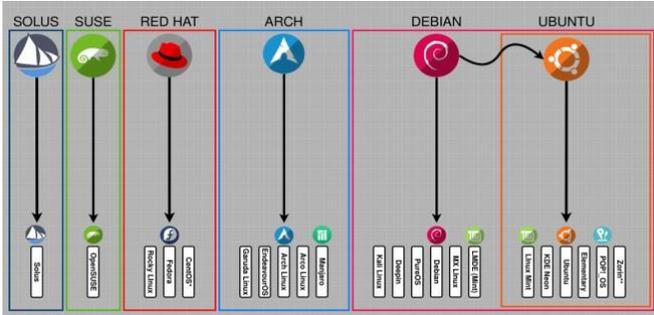


Fig. 2. Linux Distributions Family Tree

- Suse Linux

It was designed for use in mainframes, servers and workstations. Suse is an overall balanced distribution and is actively managed to date.

- Arch Linux

Arch Linux is an independently created general-purpose distribution that uses a rolling-release methodology to deliver the most recent stable versions of most software [1]. It mostly caters the advanced users and is usually not recommended for beginners. However, it is the parent distribution of several popular advanced distributions such as Manjaro Linux, Arco Linux, Endeavour OS and a lot more.

VII. BEST DISTRIBUTION FOR ML

Choosing the right Distro for your ML needs might be complicated since everyone has different requirements as well as different hardware configurations. If it is your first time using a Linux Distro, it is advised to stick to the mainstream ones. A few of them are listed below along with their key features.

- Ubuntu

It is easily the most popular Linux Distribution to date because of its ease of use. Ubuntu is a great choice for beginners since it provides you with several pre-installed utilities and a convenient desktop manager (Gnome).

It is shipped with an apt package manager which allows you to install all your ML-related packages with ease [3]. Ubuntu is a dynamic and secure option because of its consistent support and release.

Moreover, Ubuntu offers official support for KubeFlow, Kubernetes and several other ML-related tools along with one of the biggest communities ready to engage all your doubts.

- Linux Mint

Very similar to Ubuntu, Mint provides you with an easy-to-use working environment especially if you are migrating from windows. It is considered as a great lightweight alternative for

ubuntu making it an incredible choice if you have hardware restrictions.

- Fedora

It is a great choice especially if you want faster releases and have a passion for working with the latest software. Fedora is way quicker when it comes to releasing support updates for newer technologies and the overall introduction of the latest version of packages through the red hat package manager [1]. The user base of fedora is increasing rapidly and it was even chosen as an optimal distribution by Linus himself.

- Arch Linux

Arch Linux is known best for catering the needs of advanced linux. It allows you to basically build your own operating system from scratch and have complete control over every software and service installed from the very beginning.

Since the community isn't as big and mainly consists of users who can tinker their way through problems using the documentations, it might be tricky for new users to get into.

It is not something you would want to try if you aren't as versed with Linux.

VIII. CONCLUSION

Optimally, Linux would definitely be considered as the ideal operating system for one's ML needs as long as there is sufficient support for the individual hardware configuration.

It is essential for developers to learn the basic shell commands for a Terminal Emulator to fully utilize the potential of the distribution.

Choosing a distribution isn't as complicated as it is usually portrayed and it is completely fine to go with a mainstream choice.

Services like KubeFlow should be used effectively to setup the entire ML environment after a fresh install.

REFERENCES

- [1] Damien Legay, Alexandre Decan, Tom Mens, "On Package Freshness in Linux Distributions" in 2020 IEEE International Conference on Software Maintenance and Evolution (ICSME), September 2020.
- [2] Linus Torvalds, "The Linux Edge" in Communications of the ACM, Volume 42, Number 4, 1999, pp 38-39.
- [3] Andrey Falko, "Package Manager: The Core of a GNU/Linux Distribution", Simon's Rock College, 2007.
- [4] M.I. Jordan, T.M. Mitchell, "Machine Learning: Trends, perspectives and prospects", Science, Volume 349, Number 6245, July 2015.
- [5] Foster Provost, Ron Kohavi, "On Applied Researching in Machine Learning", Machine Learning, vv, 1-6, 1998.
- [6] J. Sincero, H. Schirmeier, W. Schröder-Preikschat, and O. Spinczyk, "Is the Linux Kernel a Software Product Line?" in Workshop SPLC- OSSPL 2007.

Automatic Signature Detection using Image Processing

Sachit Rathee

Department of Electrical and Electronics Engineering
Maharaja Surajmal Institute of Technology
Janakpuri, New Delhi-54

Abstract: Biometrics (or biometric confirmation) alludes to the course of distinguishing proof of people by their attributes or characteristics. Biometrics is utilized in software engineering as a type of distinguishing proof and access control which is one of the most dependable strategies to keep people protected. Biometric can be arranged into two classifications: conduct (signature confirmation, keystroke elements, and so on) and physiological (iris attributes, unique finger impression, etc.). A signature has been a distinctive element for individual recognizable proof. Indeed, even today, an expanding number of exchanges, particularly identified with monetary and business are being approved through marks. Subsequently, the need to have techniques for programmed signature confirmation should be created in case legitimacy is to be checked and ensured effectively and consistently. At the point when countless archives, for example, Bank checks, must be validated in a restricted time, the manual confirmation of record holders' marks is regularly unreasonable. Mark gives a secure method for validation and approval. In this way, there is a need for programmed signature checks and recognizable proof frameworks. Written-by-hand marks are not the same as other printed types since individuals for the most part don't utilize text in it; rather they draw a shape as their mark. Accordingly, an alternate methodology ought to be considered to deal with such marks. The current examination work is done in the field of disconnected mark acknowledgement framework by separating some uncommon provisions that make a mark hard to produce. In this exploration work, existing mark acknowledgement frameworks have been completely examined and a model is intended to create a disconnected mark acknowledgement framework.

Keywords: signature recognition, matlab, accuracy recognition.

I. INTRODUCTION

Biometrics alludes to the programmed acknowledgement of people dependent on their physiological and conduct attributes. The world is shouting out for less difficult access controls to individual confirmation frameworks and it appears as though biometrics might be the appropriate response. Rather than conveying a bundle of keys, every one of those entrance cards or passwords you heft around with you, your body can be utilized to remarkably distinguish you. Moreover, when biometrics measures are applied in the mix with different controls, for example, access cards or passwords, the dependability of verification controls moves forward. The different applications utilizing biometrics are international IDs, driving licenses, banking, shunning frauds hacking into networks, taking sends and so on. The conventional security frameworks are token-based frameworks, in this, fakers are kept

from getting to ensured assets utilizing id cards, keen cards and so on, information-based frameworks, in this character is demonstrating by utilizing data like client id and secret phrase related with the framework. In some frameworks, both the previously mentioned approaches are utilized. The fundamental benefit of a biometric framework over ordinary methodology is dependability, it can't be taken or lost. In a biometric framework, different biometric highlights are separated after catching the biometric pictures of the client and confirming the person by checking against the formats recently put away in the information base. How a person is verified relies on the utilization of the biometric framework is utilized. The sorts of working methods of the biometric framework are checked and recognizable proof. To date numerous biometrics strategy arisen and been proposed yet in the monetary areas, organization and legitimate areas transfer more on the mark. A ton of investigations have been performed on the mark biometric framework yet more such frameworks can be applied all around.

II. SIGNATURE RECOGNITION

In some frameworks, both the previously mentioned approaches are utilized. The fundamental benefit of a biometric framework over ordinary methodology is dependability, it can't be taken or lost. In a biometric framework, different biometric highlights are separated after catching the biometric pictures of the client and confirming the person by checking against the formats recently put away in the information base. How a person is verified relies on the utilization of the biometric framework is utilized. The sorts of working methods of the biometric framework are checked and recognizable proof. To date numerous biometrics strategy is been proposed yet in the monetary areas, organization and legitimate areas transfer more on the mark. A ton of investigations have been performed on the mark biometric framework yet more such frameworks can be applied all around. The plan of any mark check framework for the most part requires the arrangement of five sub-issues: information obtaining, pre-handling, including extraction, correlation process and execution assessment. Disconnected mark check essentially utilizes picture handling ideas. The framework utilized tool compartments given by Matlab climate.

III. MATLAB

The plan of any mark check framework for the most part

requires the arrangement of five sub-issues: information obtaining, pre-handling, including extraction, correlation process and execution assessment. Disconnected mark check essentially utilizes picture handling ideas. The framework utilized tool compartments given by matlab climate. This permits you to tackle numerous specialized registering issues, particularly those with the framework and vector definitions, in a small amount of the time it would take to compose a program in a scalar non-intuitive language like c or Fortran. The name Matlab represents grid lab. Matlab was initially composed to give simple admittance to grid programming created by the Linpack and eispack projects. Today, Matlab motors consolidate the lapack and blas libraries, installing the best in class programming for grid calculation. Matlab has advanced over a time of years with input from numerous clients. In college conditions, it is the standard informative device for starting and progressing courses in math, design, and science. In industry, Matlab is the instrument of decision for high-usefulness examination, advancement, and investigation. Matlab highlights a group of extra application-explicit arrangements called tool compartments. Vital to most clients of Matlab, tool compartments permit you to learn and apply specific innovations. Tool stash is a complete assortment of Matlab capacities (m-documents) that stretch out the Matlab climate to tackle specific classes of issues. Regions in which tool kits are accessible incorporate sign handling, control frameworks, neural organizations, fluffy rationale, wavelets, recreation, and numerous others. There are many inherent capacities in Matlab. The assist order with canning is utilized to distinguish Matlab capacities, and how to utilize them. For instance, composing help at the brief in the order window will show a rundown of help subjects that are gatherings of related capacities. This is an extremely extensive rundown; the most rudimentary assist themes with showing up toward the start.

For instance, one of these is recorded as matlab\elfun; it incorporates rudimentary number-related capacities. One more of the primary assistance subjects is matlab\ops, which shows the administrators that can be utilized in articulations.

IV. PROJECT METHODOLOGY

this section describes our approach to solving the problem as I divided it into five steps as shown in the diagram below.

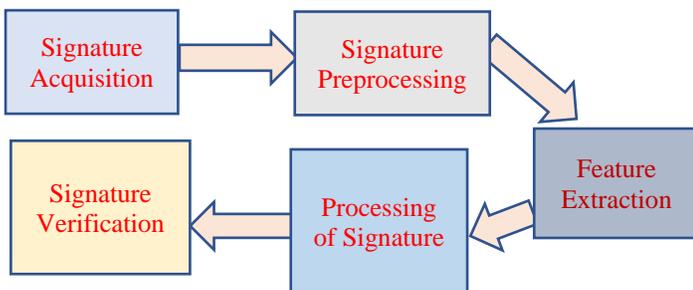


Fig. 1. Project Implementation Block Diagram

A. Signature acquisition

There are two ways to get the signature:

1. Using the tablet provided.
2. By using scanned images of signatures from a scanner or camera.

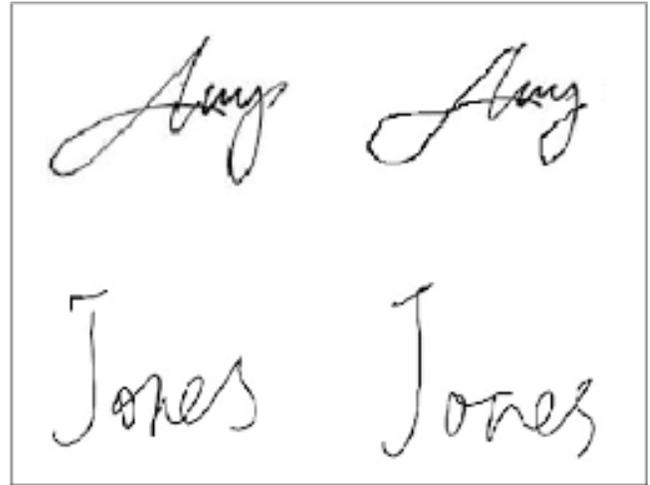


Fig. 2. Different Signature Patterns

B. Signature Preprocessing

Signature preprocessing is a necessary step to improve the latter algorithm's accuracy and reduce its computational needs. The following preprocessing steps are taken into consideration:

1. Transformation from colour to grayscale.
2. Transformation from grayscale to black and white using a suitable threshold.
3. Colour inversion.
4. Apply opening and closing morphological processes with small structure elements to remove the inner and outer noise.

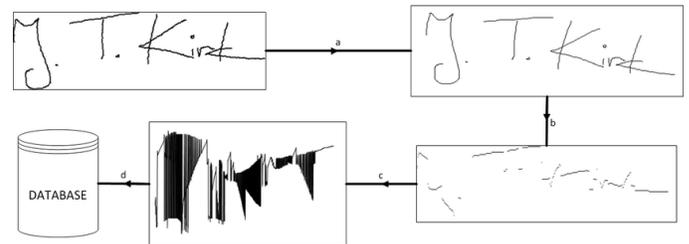


Fig. 3. Process Example.

C. Feature Extraction

The features extracted from handwritten signatures play a vital role in the authentication process. A large number of features are extracted from signatures but not all features can be used in

the feature set. A good feature set would result in a successful system. It is important to have a meaningful feature set for ensuring proper learning by nn. Various features used in the feature set of the proposed method are explained as follows:

1. Eccentricity

It can be thought of as a measure of how much the conic section deviates from being circular. In particular, the eccentricity of a circle is zero. Ellipses, hyperbolas with all possible eccentricities from zero to infinity.

Skewness refers to something that is out of line or distorted on one side. “skewness is a measure of symmetry, or more precisely, the lack of symmetry. A distribution, or data set, is symmetric if it looks the same to the left and right of the centre point”. Skewness can range from minus infinity to positive infinity.

2. Kurtosis

In a similar way to the concept of skewness, kurtosis is a descriptor of the shape of a probability distribution and, just as for skewness; there are different ways of quantifying it for a theoretical distribution and corresponding ways of estimating it from a sample from a population. The measurement of skewness allows us to determine how bowed the lines in each segment of the signature.

3. Orientation

It allows us to know how the signer wrote down the signature. Which letters came first emphasizing the direction of angles and peaks? Orientation' — scalar; the angle (in degrees ranging from -90 to 90 degrees) between the x-axis and the major axis of the ellipse that has the same second moments as the region.

4. Entropy

Entropy is a statistical measure of randomness that can be used to characterize the texture of the input image.

5. Euler number

The Euler number for the binary image bw is the total number of objects in the image minus the total number of holes in those objects. Bw can be numeric or logical and it must be real.

6. Solidity scalar

Specifying the proportion of the pixels in the convex hull that are also in the region. Computed as area/convex area.

7. Mean

Average or mean value of the elements in the image.

8. Standard deviation

The standard deviation of matrix elements is the square root of

an unbiased estimator of the variance of the population from which x is drawn.

D. Processing of signature

Artificial neural networks or ann resembles the human brain in learning through training and data storage. The ann is created and trained through a given input/target data training pattern. During the learning process, the neural network output is compared with the target value and a network weight correction via a learning algorithm is performed in such a way as to minimize an error function between the two values. The mean-squared error (mse) is a commonly used error function which tries to minimize the average error between the network's output and the target value. Five genuine signatures from each signer were taken to train the network and they were enough to give very good results in verification.

In this project, the nn consisted of one hidden layer of 10 neurons and an input of 9 features and output of a vector of 20 numbers and the max of these numbers indicates the signer.

E. Signature verification

In this section, we test the trained network on signature and a classification ratio of about 93% was obtained.

V. CONCLUSION

A reliable signature verification system is an important part of law enforcement, security control and many business processes. It can be used in many applications like cheques, certificates, contracts etc. The integrated signature verification system incorporates database management, noise removal and pre-processing feature extraction, learning and verification modules. The matching is done and decision-making is based on a threshold-based technique that gives near applications. The system showed promising results.

REFERENCES

- [1] Ali karounia, bassam dayab, samia bahlakb, “offline signature recognition using a neural networks approach,” science direct, p. 7, 2010.
- [2] julio martínez-r.,rogelio alcántara-s., “on-line signature verification based on optimal feature representation and neural-network-driven fuzzy reasoning,” ieeec, 2002.
- [3] Harpreet anand,prof. D.l bhombe, “enhanced signature verification and recognition using matlab,” ijirae, vol. 1, no. 4, p. 7, 2014.
- [4] t.y.zhang, c.y. Ceun “a fast algorithm for thinning digital patterns”.communications of acm, march 2011 concepts of image processing.
- [5] s. Mori et. Al, “historical review of ocr research and development”, proceeding ieeec, 80, no 7, pp. 1029-1058, july .
- [6] a. A. Chaudhary, e.a.s. Ahmad, s. Hossain, c. M. Rahman, “ocr of bangla character using neural network: a better approach”, 2nd international conference on electrical engineering (icee 2010), khuln, bangladesh.

Short Deep-fake Video Generation from Text

Sandeep Kumar¹, Mayank Mani², Sakshi Munjal³, D.D.V. Sai Ashish⁴

^{1,2,3,4}Department of Computer Science and Engineering
Maharaja Surajmal Institute of Technology, New Delhi, India

Abstract: This work has been focused on building a pipeline that is capable of consuming short segments of text and using it to generate content to populate the clip. Generative Pre-trained Transformer 3 (GPT-3) has been used for this purpose, which is an autoregressive language model that uses deep learning to produce human-like text. The output content is used as input to the text-to-speech algorithm which creates an audio clip. A suitable short video clip is to be picked from the database. The video is then deep faked to sync the facial movements to the audio clip.

Keywords: Video morphing, deep-fake, lip-sync, text-to-video.

I. INTRODUCTION

With the proliferation of high-speed internet, the consumption of audio-video content all around the globe has been increasing exponentially. Producing high-quality video however is an expensive undertaking, especially for commercial purposes. Moreover, once a video has been shot if the requirements change or a new video is required all the previous work must be redone. This work aims to advance the work in this field to reduce the complexities involved in this process. A lot of research has been done in the field of computer vision in recent years to lip-sync static images and deep-faking videos to look like desired personalities. But doing the same in a dynamic video where the speaker, who could be anybody, is moving their face and already has expressions is a mountain yet to be conquered. This can significantly reduce the overhead required in producing new video content or dubbing videos made in one language to another to expose to an entirely new audience.

An ideal area of application would be for advertisements. A collection of stock videos could be morphed and spliced together to create completely new content at a fraction of the cost. In this work, we aim to take a short description as input and generate a short (less than the 60s) clip of a person talking about the topic. This task consists of three main sub-problems. First, generate the content of the clip using the description/topic provided. In the next step, this content will be converted to audio format. Lastly, a suitable video will be selected from a predetermined selection and the facial movement will be synced to the generated audio clip, they will then be merged to produce the final output video.

II. LITERATURE REVIEW

The text has been processed and used as input for the Generative Pre-trained Transformer model which produces human-like content related to the topic. A comparison of various text-to-speech algorithms was done to select the one best suited to

mimic human speech. It is also a possibility that more than one model will be required to replicate male and female voice and speech patterns. This is an area that has a lot of complexity associated with it. Billions have been spent trying to replicate human speech patterns and the results have certainly improved over time. Yet the goal is still far away. In the context of this paper, the focus was not on developing techniques to further the research in this area, as a result, the best option available has been utilized. Re-inventing this wheel would have made a tall task even taller. We have analysed previous work done in this field using one target speaker to understand the limitations [6]. We have leveraged state-of-the-art Generative Pre-trained Transformer 3 to achieve this. It is an autoregressive language model that leverages deep learning to produce human like-text. We have fine-tuned the parameters to generate output suitable for our use case. We compared various engines including text-davinci-002, text-curie-001 and text-babbage-001. In our testing we found text-davinci-002 to be best at its task, while it does take some extra execution time it is not a restriction in our case. The quality of content is important to give the output a more natural field and as a result, we have selected it as our preferred method going forward.

As our text-to-speech engine, we compared various alternatives like gTTS, IBM Watson and Amazon Polly and decided to move ahead with gTTS in the end. It enables us to select a variety of accents to match the subject of the video while generating the audio. Once the desired audio segment has been generated, we select a video clip to match the audio. To achieve the best results these videos have been curated to include a singular person speaking in front of a mostly uncluttered background.

This makes the task of identifying and modifying the lip movements slightly easier. The model is capable of working even in more complex scenarios, this was just a precaution that was taken to simplify the problem statement. We analysed an LSTM autoencoder, with an attention layer added on top and used it to predict the correct alignment for temporal windows [5].

We are then deep fake this video using a combination of Wav2Lip and GANs. The decision to select this combination instead of just Wav2Lip was made as even though Wav2Lip produces better lip-sync it results in worse video quality. Adding GANs produces an adequate combination of lip-sync and video fidelity. We morph the facial features specifically focusing on the mouth to match the audio segment. These 2 artefacts can then be combined to create the desired output.

III. METHODOLOGY

A. Models And Techniques Used

Models and techniques used for this research includes:

- Neural Networks
- GANS
- GPT3
- Wav2Lip

Neural Networks: Neural networks are also known as artificial neural networks (ANNs). They are a subset of machine learning and are pivotal in deep learning algorithms. Artificial networks are made from layers, the main layer is the input layer, after which there can be at least one secret layer, and a last result layer. If the outcome of any single node exceeds a predetermined threshold, that node is triggered, delivering data to the next tier. If this is not the case, no signal is sent to the network's next tier.

By learning from training data, neural networks can increase their accuracy over time. The weights are assigned after the layered input has been specified. These weights aid in determining the importance of a given variable, with larger inputs contributing much more to the output than smaller ones.

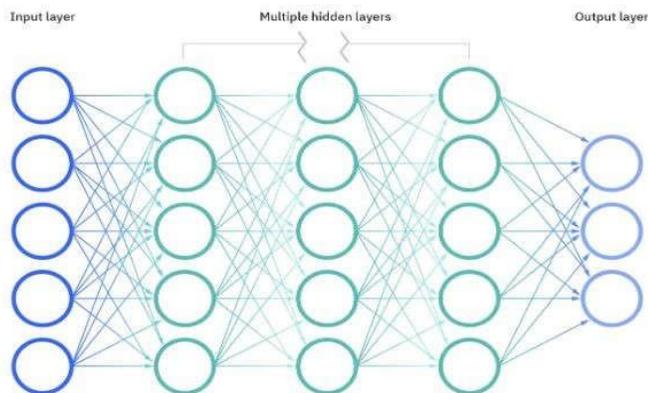


Fig. 1. Neural Network.

Convolutional neural networks (CNNs) [3], like feedforward networks, are used for face recognition, pattern recognition, and/or computer vision. To find patterns in a picture, these networks use ideas from linear algebra (matrix multiplication).

GANS: A generative adversarial network (GAN) is an unsupervised machine learning approach that is implemented by a system of two neural networks competing against each other in a zero-sum game environment. Ian Goodfellow et al. first proposed it in 2014. The discriminative network [9] evaluates candidates while the generative network generates them. The generative network's training objective is to maximize the probability of the discriminative network making a mistake, while the discriminative network's training objective is to minimize the probability of making a mistake. The generative

network can be thought of as a "forger" trying to produce fake data that is indistinguishable from the real data, while the discriminative network can be thought of as a "detective" trying to identify the forged data. This is done until the forger produces data that is indistinguishable from the real data, at which point the process is said to have converged. Once converged, the forger has effectively learned to generate data from the same distribution as the real data. The Generative & Discriminator Model: A fixed-length random vector is fed into the generator model as input and a sample is generated in the domain. The vector is randomly chosen from a Gaussian distribution and used to seed the generating process. Points in the problem domain will correlate to points in multidimensional vector space post-training, resulting in a compressed representation of the data distribution. The domain (real or generated) is sent into the discriminator model, which predicts a binary class label of fake or genuine (generated). A real-world example may be found in the training dataset. The generator model produces the output examples. The discriminator is a well-known classification algorithm. The discriminator model is deleted after the training procedure. The generator can sometimes be reused since it has learnt to extract features from examples in the issue area. Some or all of the feature extraction layers can be used in transfer learning applications using the same or comparable input data. We also experimented with using super-resolution [7] to restore details in the final video without distortion. Speech-assisted frame rate conversion was also analyzed to improve lip synchronization [12]. There is more to creating the final output than just lip-syncing the video the emotions must be conveyed as well and so for this purpose, we have added a layer to recognize the emotion in the content [11].

B. Generating Content

The first step was the generation of content from the short description that is provided. We have leveraged state-of-the-art Generative Pre-trained Transformer 3[1] to achieve this. It is an autoregressive language model that leverages deep learning to produce human like-text. We have fine-tuned the parameters to generate output suitable for our use case. We compared various engines including text-davinci-002, text-curie-001 and text-babbage-001.

C. Generating Audio

The next step is the generation of audio clips using the content generated in the previous step. We have used the very popular Google Text-to-Speech(gTTS) for this purpose. The reasoning was very simple, it is one of the most capable models available with the widest range. There may be some other options that sound closer to human speech but in our testing, we found them to have some other unacceptable downsides. Text-davinci-002: This was the best model available. Even with lesser context it can perform any task the other models can. The only downside is higher execution time. Text-curie-001: This model is faster and has a lower cost than text-davinci-002. It is very capable but lags in some areas. For applications that require light hardware

requirements, this model could be ideal, in our case however the additional surety of better results was enough to swing the needle in text-Davinci-002’s favour. Text-babbage-001: This is a very straightforward model. Very fast with low execution cost but at the same time limited in its capabilities. Text-ada-001: This is the model that is the fastest and has lowest execution cost in GPT-3’s toolbelt. It is also, however, only capable of simple tasks. In our testing we found text-davinci-002 to be best at its task, while it does take some extra execution time it is not a restriction in our case and we have selected it as our preferred method going forward[7]. The content generated here does need to go through a phase of human moderation as sometimes a sentence gets cut-off midway through and such irregularities must be identified as soon as possible. With some fine-tuning, we were able to minimize this phenomenon but it remains as a possibility, albeit a small one. Eliminating it would be ideal. A major one is the lack of abbreviation context. Instead of enunciating an abbreviation how it is meant to them often attempt to ‘pronounce’ it how a human would, except, that’s not what humans do. The only way to deal with this problem at the current stage is to manually replace all the occurrences of the abbreviation from the content. As a result, the trade-off was made to have slightly more robotic-sounding audio in exchange for proper pronunciation of all the words.

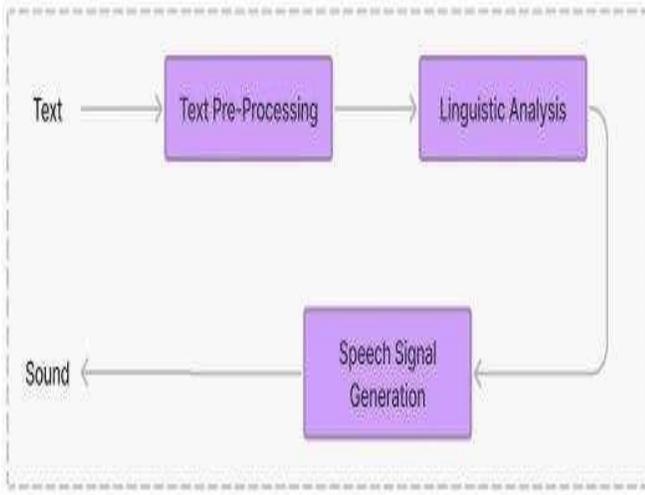


Fig. 2. gTTS Flowchart.

D. Generating the synced video

Despite the growth in work on speech-driven face creation, only a few lip-sync clips with dynamic identities, voices, and languages have been created [12]. Additionally, most of these attempts suffer from some limitations, namely, they work well on static images but fail when applied to dynamic videos. We have identified key factors blocking the task of lip-syncing dynamic, unconstrained videos and have tried to resolve them by learning from a powerful lip-sync discriminator. We have used a sequence of facial landmark detection [13] to generate the talking head video. For resolving lip-sync errors and constructing enormous lip-sync datasets, the SyncNet [4] model

is a common choice. We looked at the existing speaker-independent audio-to-lip creation methods. We evaluated the Connectionist Temporal Classification (CTC) loss model [2] and discovered that these models don’t penalise wrong lip shapes enough. We adopted a robust lip-sync discriminator that pushes the generator to provide genuine lip motion for the given speech constantly. To train our model, we followed two essential phases: Train expert lip-sync discriminator, Train the Wav2Lip model. Once the training process is complete the generator model is used to lip-sync. We have utilized the residual learning framework [8] to improve the training time of our model. We are using a ConvNet to measure the performance of our model.

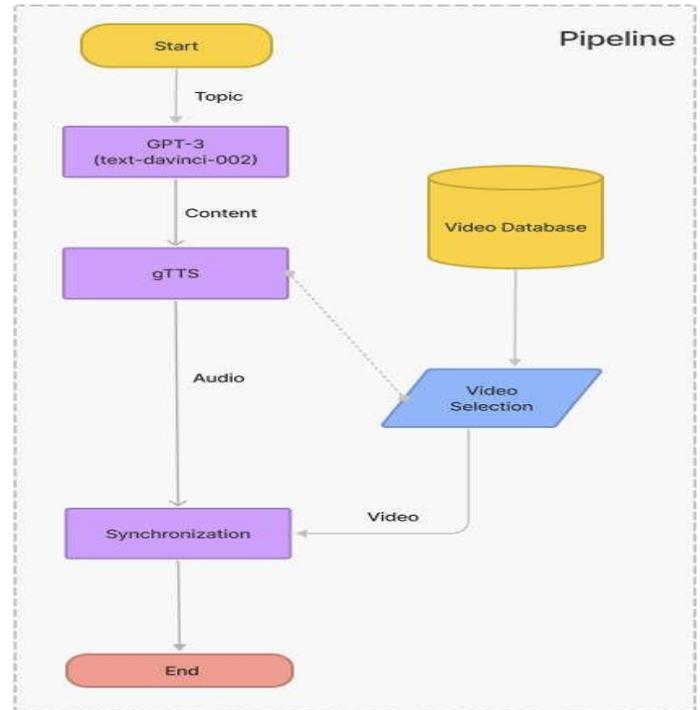


Fig. 3. Process Flowchart.

Algorithm:

- Taking input string from user.
- Using GPT-3’s text-davinci-002 to produce content.
- Utilizing gTTS to generate audio from content.
- Selection of video from database.

Using the generator model from the Wav2Lip variation of the SyncNet model to sync the audio and video.

One of the biggest challenges at the moment is matching the length of the video and the audio without looping the video back. The end of the video should feel natural and in sync with the audio but now there is no good solution to this problem. A set of videos are maintained and the one with the closest length to the generated audio is used. This method needs more refinement to reach its full potential.

IV. RESULTS

In this section, we will share the results and outputs of our research. Fig 1 is a frame capture of the output video generated by our model. Fig 2 is the same frame in the original video.



Fig. 4. Deep-faked Video.



Fig. 5. Original Video.

As you can see the lips are in a different position at the same point in the video. The output video is rendered at a lower video quality to save on processing time but this can be avoided with better hardware/more time. This has been achieved by training our model on the dataset lrs2. Lrs2 is The Oxford BBC Lip Reading Sentences 2 Dataset [9]. The dataset consists of BBC television spoken sentences. All of these sentences are of 100 characters.

TABLE 1: OXFORD BBC LIP READING DATASET.

# utterances	# word instances	Vocab
96,318	2,064,118	41,427
45,839	329,180	17,660
1,082	7,866	1,984
1,243	6,663	1,698

We have also used the DFDC dataset which contains over 1,00,000 clips [9, 10]. We have also created a website where you can try this process out.

We utilized “ReSyncED” to benchmark the performance of Lip-Sync and used the two metrics determined through the SyncNet

model. LSE-D stands for Lip Sync Error Distance and LSE-C stands for Lip Sync Error Confidence. With Wav2Lip + GAN the LSE-D score turned out to be 7.318 and LSE-C score turned out to be 6.851 with an overall experience of 4.13 in comparison to the Wav2Lip with LSE-D 6.834 and LSE-C 7.265 with overall experience of 4.04. Website user interface has been captured and displayed below. This has been implemented to provide an end consumer with ease of use.

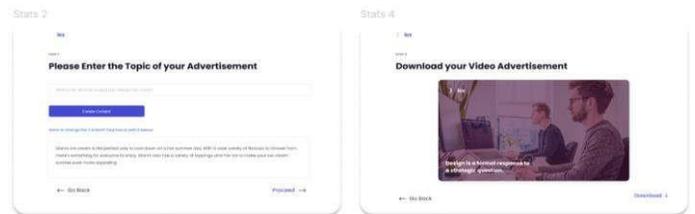


Fig. 6. Homepage.

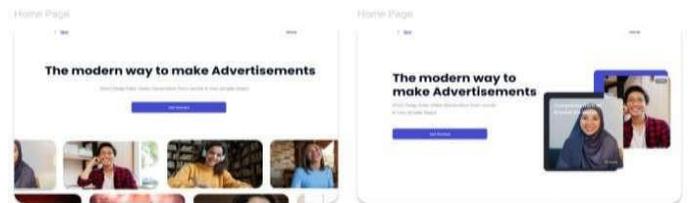


Fig. 7. Stepwise Pages.

React.js has been used to develop the frontend of this application. React is a free and open-source front-end JavaScript library for building user interfaces based on components.

React-router has been used to add page routing for traversing through the different pages.

```
import Navbar from "common/navbar";
import { HomeScreen, StepsScreen } from "screens";
import styled from "styled-components";
import { Routes, Route } from "react-router-dom";

const Container = styled.div`
width: 86vw;
margin: 0 7vw;
padding-top: 10vh;
`;

function App() {
return (
<>
<Navbar />
<Container>
<Routes>
<Route
path="/"
exact
caseSensitive={false}
element={<HomeScreen />}
/>
<Route
path="/steps/:id"
exact
caseSensitive={false}
element={<StepsScreen />}
/>
</Routes>
</Container>
);
}
export default App;
```

Fig. 8. Frontend code.

```

import React from "react";
import ReactDOM from "react-dom";
import App from "./App";
import GlobalStyles from "styles";
import { BrowserRouter } from "react-router-dom";

ReactDOM.render(
  <BrowserRouter>
    <GlobalStyles />
    <App />
  </BrowserRouter>,
  document.getElementById("root")
);

```

Fig. 9. Front-End Code. Fig. 13 Flask API layer.

```

"dependencies": {
  "@testing-library/jest-dom": "^5.16.2",
  "@testing-library/react": "^12.1.4",
  "@testing-library/user-event": "^13.5.0",
  "axios": "^0.27.2",
  "react": "^17.0.2",
  "react-dom": "^17.0.2",
  "react-hook-form": "^7.29.0",
  "react-router-dom": "^6.2.2",
  "react-scripts": "5.0.0",
  "styled-components": "^5.3.3",
  "web-vitals": "^2.1.4"
},

```

Fig. 10. Frontend dependencies.

```

def gpt3(stext):
    openai.api_key = 'sk-UmZR7v4N7QhVIH2zMwzLT3B1bkFJ1SH59Y7yY0fwj'
    response = openai.Completion.create(
        engine="text-davinci-002",
        prompt=stext,
        temperature=0.1,
        max_tokens=1000,
        top_p=1,
        frequency_penalty = 0,
        presence_penalty = 0
    )
    content = response.choices[0].text
    return response.choices[0].text

```

Fig. 11. GPT-3.

Cloudinary has been used to store the videos after modification and it allows us to easily distribute them if need be using a public link. Embedding this video on webpages is also easily achieved. The backend is run in a google colab notebook where we have wrapped the functionality in a flask API layer through which the endpoints can be accessed. This was needed as running the model requires high processing resources.

Ngrok has been used as a tunnelling service to tunnel the requests through to our backend that is running in a google server. It was required as it is not possible to access it directly via IP address or locally.

For accessing GPT-3 we are making use of the version hosted by OpenAI. As mentioned earlier, the text-davinci-002 engine has been used which is the latest version available for the ‘davinci’ family of engines.

```

@app.route("/run", methods=['GET'])
def run():
    EncodedTopic = request.args['topic']
    topic = urllib.parse.unquote(EncodedTopic)
    exec(topic)
    time.sleep(5)
    return jsonify(statusCode=200, message='Ok')

# Start the Flask server in a new thread
threading.Thread(target=app.run, kwargs={"use_reloader": False}).start()

```

Fig. 12. Flask API layer.

```

@app.route("/run", methods=['GET'])
def run():
    EncodedTopic = request.args['topic']
    topic = urllib.parse.unquote(EncodedTopic)
    exec(topic)
    time.sleep(5)
    return jsonify(statusCode=200, message='Ok')

# Start the Flask server in a new thread
threading.Thread(target=app.run, kwargs={"use_reloader": False}).start()

```

Fig. 13. Flask API layer.

The flask app runs in a separate thread to prevent it from blocking execution of the main thread where model is run.

V. CONCLUSION

This research has met and satisfied the expected requirements. The model and pipeline development cycle were challenging, stressful and full of hurdles. Due to its popularity machine learning has leapfrogged in both its scope and applications. Through this work it has been tried to further deepen the knowledge pool in this field and with some refinement in this technology that can someday be deployed and used in real time to make life easier.

REFERENCES

- [1] Brown, T., Mann, B., Ryder, N., Subbiah, M., Kaplan J.D., Dhariwal, P., ... & Amodei, D., "Language Models are Few-Shot Learners", (2020).
- [2] T. Afouras, J. S. Chung, A. Senior, O. Vinyals, and A. Zisserman. Deep Audio-Visual Speech Recognition. In arXiv:1809.02108. (2018).
- [3] Leon A Gatys, Alexander S Ecker, and Matthias Bethge, "Image style transfer using convolutional neural networks" (2016).
- [4] Prajwal, K. R., Mukhopadhyay, R., Namboodiri, V. P., & Jawahar, C. V., "A Lip Sync Expert Is All You Need for Speech to Lip Generation In the Wild" (2020).
- [5] Yoav Shalev, Lior Wolf. End to End Lip Synchronization with a Temporal AutoEncoder. (2020).

- [6] Supasorn Suwajanakorn, Steven M Seitz, and Ira Kemelmacher-Shlizerman. 2017. Synthesizing Obama: learning lip sync from audio. *ACM Transactions on Graphics (TOG)* 36, 4 (2017).
- [7] Deokyun Kim, Minseon Kim, Gihyun Kwon, and Dae- Shik Kim, "Progressive face super-resolution via attention to facial landmarks" (2019).
- [8] Kaiming He, Xiangyu Zhang, Shaoqing Ren, and Jian Sun. Deep residual learning for image recognition. In *Proceedings of the IEEE conference on computer vision and pattern recognition*. 770–778. (2016).
- [9] Brian Dolhansky, Joanna Bitton, Ben Pflaum, Jikuo Lu, Russ Howes, Menglin Wang, and Cristian Canton Ferrer. *The DeepFake Detection Challenge Dataset*. (2020).
- [10] Ruben Tolosana, Ruben Vera-Rodriguez, Julian Fierrez, Aythami Morales, and Javier Ortega-Garcia. *DeepFakes and Beyond: A Survey of Face Manipulation and Fake Detection*. (2020).
- [11] S. A. Al-agma, H. H. Saleh and R. F. Ghani, "Multi- model Emotion Expression Recognition for Lip Synchronization," 2020 1st. Information Technology To Enhance e-learning and Other Application (IT- ELA, 2020).
- [12] T. Chen, H. P. Graf and K. Wang, "Lip synchronization using speech-assisted video processing," in *IEEE Signal Processing Letters*, vol. 2, no. 4, pp. 57-59, 1995.
- [13] Lele Chen, Guofeng Cui, Ziyi Kou, Haitian Zheng, Chenliang Xu. *What comprises a good talking-head video generation?: A Survey and Benchmark*. (2020).

Summarization and Speech Synthesis for generating Audiobooks

Koyel Datta Gupta¹, Rinky Dwivedi², Amar Pratap Singh³, Khush Malawaliya⁴, Kshitij Kumar⁵

^{1,2,3,4,5}Computer Science Engineering Department, Maharaja Surajmal Institute of Technology

Abstract: In this work, recent advancements in NLP have been applied to generate novel audiobooks using WaveNets. The content of the books is also summarized using TextRank technique to generate long-form summaries of the books. There is also an android application that aims to provide a UI to the audiobooks generated by this method for better user experience.

Keywords: Extractive summarization, Speech synthesis, TextRank, WaveNet, Booksum

I. INTRODUCTION

With the advent of mobile phones, the number of mobile phones in the world has seen an exponential growth in the last decade. This sudden boom makes it easier to get information whenever required with a few swipes on the screen. One major source of information is books as they can contain 10 years of experience compressed in 500 pages. Being able to absorb information like that is highly beneficial in today's world. Audiobooks have become a new source of information that aims to make books more accessible.

Currently these books are generated by human readers which is a time-consuming process, also note the fact that a lot of books will have an audiobook version. The authors take it up a notch in this project and use advances in NLP to automate the process of generating audio from books, hopefully close to human levels with the aim that one day these AI generated audiobooks may be indistinguishable to humans reading. This process also makes it possible to generate audiobooks for old books that don't have audiobook versions.

They also use Text summarization to make it possible for the reader to get a gist of the book before actually reading the entire thing or maybe just read a summary if that suits the user.

II. LITERATURE REVIEW

The goal of the project is to generate an audiobook for summarized versions of the book. To achieve this goal there are two major tasks that need to be completed:

1. Text summarization
2. Speech synthesis

There are two types of text summarization - **Extractive** summarization and **Abstractive** summarization. Extractive summarization makes the summary out of the sentences that are present in the original text i.e. it takes the sentences from the

text which summarizes the content and contains most information. On the other hand, Abstractive summarization creates an intermediate representation of the text and then generates new text from the representation that is not taken from the book itself. This can cause problems because the essence of the author's writing is lost or modified. Books, especially fictional books are heavily dependent on the author's writing style which gives the book its uniqueness. Extractive summarization on the other hand keeps the writer's style intact (mostly). Mostly because some of the information may still be lost depending upon the ratio of length of summary generated to the original text. But this comes with the idea of "summarization", trying to convey as much information with least loss while decreasing the size of the text. Extractive summarization was exactly the way to go.

A. Text summarization - TextRank

The TextRank model [1] is a graph-based model for ranking that builds graphs from natural language texts. TextRank originally was developed and tested on two language computing processes comprising of unsupervised learning and sentence selection. TextRank obtained results that were promising with state-of-the-art at the time developed in the area.

Graph-based ranking algorithms are fundamentally dependent on determining the importance of a node within a graph, on the basis of information extracted recursively from the entire graph. The basic idea is that of "voting". Each vertex that points to a given vertex can be understood as casting a vote onto it. Moreover the "importance" of the vertex that is casting the vote is also taken into account.

A factor d is used for incorporating randomness in the selection of nodes which is usually set to 0.85. The process begins by assigning an arbitrary value to each vertex in the graph. The process is repeated until the convergence reaches below an agreed threshold. At the end of execution of the algorithm, a score is assigned to each node which portrays the "importance" of the node within the graph. The graph uses Undirected and Weighted graphs. Let's see why that is.

1. Undirected and Weighted graphs

A recursive graph-based ranking algorithm is usually used for directed graphs. However, the same may be used for directed graphs where the in-degree and out-degree of the graph is

identical. TextRank uses undirected graphs and shows that they achieve similar rates of convergence to directed graphs. It can also be seen that as the connectivity of the graph increases, convergence is usually achieved after fewer iterations.

Considering the web surfing context, a page usually does not include numerous or incomplete links to another page, and hence the original PageRank algorithm assumes the case of unweighted graphs. On the contrary, in TextRank technique, the graphs are built from natural language texts, which might include numerous or incomplete links between units(nodes) that are extracted from text. It may therefore be useful to indicate and incorporate into the model the “strength” of the connection between two vertices and a weight added to the corresponding edge that connects the two vertices

2. *Text as a graph*

One major problem still remains, representing a text with a graph. Regardless of the task at hand, the process of generating graphs from texts mainly comprises of the subsequent steps:

1. Detect the text sections that best express the current task and augment them as nodes to the graph.
2. Next, determine the relations among the text sections, and these relations are used to form edges between Node in the graph. Links can either be directed, undirected, weighted or un-weighted.
3. Repeat the graph-based ranking algorithm until it converges.
4. Order the nodes in terms of their final score. Finally, the values associated to each node is utilized for deciding the ranking.

3. *Sentence Extraction*

In sentence extraction the units/vertices for the graph are complete sentences. For drawing a sentence, the objective is to rank all the sentences. Hence a node is appended to the graph for each sentence in text.

The connection in a graph is defined by a "similarity" relation between the sentences, where "similarity" is assessed in terms of their text content similarity. This type of connection amid two textual samples can be considered as a course of “recommendation”: A sentence that reports certain notions in a text, provides the reader a “recommendation” to denote to the other similar phrases that works on similar ideas, and consequently an edge can be retrieved amid any two such sentences that have similar content.

The connection of two phrases may be identified by comparing the value of shared tokens amid the lexical depictions of both the phrases. In addition, to evade endorsing extended sentences, they also use a normalization factor, and split the shared content of two phrases according to the length of the phrase.

Another work [2] experimented with different similarity functions between sentences that may act as a better notion of similarity than the one used in the original text rank research paper. They tested Cosine Sim, LCS, BM25 and BM25+ as dissimilar means to weight the links for the TextRank graph. The best results were obtained using BM25 and BM25+. They also made their code available through the gensim [3] project which was later used in this project.

B. *Speech synthesis - WaveNet*

WaveNet [4] is a deep neural network model that is used for producing raw audio waveforms. The framework is entirely probabilistic and autoregressive. The model can be proficiently trained using extensive number of samples for each audio. It achieves state of the art results in text-to-speech performance. The model can also be conditioned on the speaker's identity to include features about the speaker's speech.

WaveNet is an autoregressive model based on the PixelCNN [5] architecture. They also use dilated causal convolutions which exhibit large receptive fields. The joint probability of a waveform is factored as a product of conditional probabilities. Hence every audio piece is trained on all the data as previous timesteps. The main ingredient of the model are causal convolutions. Similar to PixelCNNs, the conditional probability distribution is designed by a load of convolutional layers. The output of the technique has equal dimension as the input. But one of the problems of causal convolutions is that they require many layers or large filters to increase the receptive field.

Instead, they use dilated convolutions that increase the receptive field by orders of magnitude, without greatly increasing the computation cost. These stacked dilated convolutions enable the network to have extensive receptive fields with very few layers.

Given an additional input h , WaveNets can model the conditional distribution. By conditioning the model, they can guide the WaveNet's generation to yield acoustic sample with essential characteristics. For instance, a multi-speaker setup can be chosen by applying characteristics about a speaker.

WaveNets for the TTS task were conditioned on linguistic samples/characteristics which were extracted from input texts. To evaluate the performance, subjective paired assessment and mean opinion value tests were conducted and they achieved best results in the MOS tests.

III. PROPOSED METHODOLOGY

A. *Books Source*

To start this project the authors needed to find a source for the books that can be summarized. A quick Google search leads us to a large collection of open-source books that are copyright free "Project Gutenberg" [5]. They provide books in multiple formats like EPUB, HTML, Raw text etc. We use EPUB and raw-text format to generate summaries. They also provide books based on genres which were later used in the application

provided with this work.

B. *Android app*

Accompanied with this work is an android application that showcases an use-case for this work. The app provides a feature-rich user interface to access the audiobooks generated.

C. *Summary and Audio Generation*

The books generated are only a subset of the books available on the Project Gutenberg website. These books follow more or less a predefined format and the current code for Summarization and Speech synthesis works only on these books. However only minor changes to the codebase can make it adaptable to other formats. The books are generated offline because of the long tail of edge cases that may occur with web-scraping and the fact that some of the books don't follow the format exactly.

IV. MATERIALS AND METHODS

A. *Gensim*

Gensim [3] is a Python library for topic modelling, document indexing and similarity retrieval with large corpora. It has a lot of applications available for NLP. The summarization submodule is used for extracting book summaries. An improved version of TextRank has an open-source implementation that was submitted to the gensim project which is used here.

B. *gTTS*

gTTS stands for Google Text-to-Speech is a python library and CLI (Command Line Interface) tool to interface with Google Translate text-to-speech API. It allows users to make calls to the Google Translate text-to-speech API programmatically and generate audiobooks from summary text files.

V. RESULTS AND DISCUSSIONS

TABLE 1: Rouge scores achieved using Textrank on Booksum, Multi-news[8], CNN dailymail[9] datasets

	Booksum-subset	Multi-news test	CNN-daily mail test
Rouge 1	0.063	0.39	0.704
Rouge 2	0.003	0.126	0.271
Rouge L	0.063	0.185	0.453

The low scores shown on the subset of Booksum may be due to the nature of long form summarization. The lengthier the summary, the more ways there are to convey information. Also, since the number of N-grams is large when using long form summarization, it also plays a factor in reducing the score.

Sometimes the audiobooks may have some characters that should have been preprocessed and cleaned but the TextRank implementation does not include them, so the audio generated can have some problems when dealing with these characters.

VI. CONCLUSIONS

For future work, modifications to the Evaluation strategies for long form summarization may be required. Also, Extractive summarization with deep learning-based methods may be more accurate as they can take advantage of large datasets (like Booksum) to learn meaningful patterns to generate a summary closer to the actual summary.

REFERENCES

- [1] Mihalcea, Rada, and Paul Tarau. "Textrank: Bringing order into text." Proceedings of the 2004 conference on empirical methods in natural language processing. 2004.
- [2] Barrios, Federico, et al. "Variations of the similarity function of textrank for automated summarization." arXiv preprint arXiv:1602.03606 (2016).
- [3] Řehůřek, Radim, and Petr Sojka. "Gensim—statistical semantics in python." Retrieved from gensim.org (2021).
- [4] Oord, Aaron van den, et al. "Wavenet: A generative model for raw audio." arXiv preprint arXiv:1609.03499 (2016).
- [5] Oord, Aaron van den, et al. "Conditional image generation with pixelcnn decoders." arXiv preprint arXiv:1606.05328 (2016).
- [6] Project Gutenberg. (n.d.). Retrieved December 17, 2021, from www.gutenberg.org.
- [7] Kryściński, Wojciech, et al. "BookSum: A Collection of Datasets for Long-form Narrative Summarization." arXiv preprint arXiv:2105.08209 (2021).
- [8] Fabbri, Alexander R., et al. "Multi-news: A large-scale multi-document summarization dataset and abstractive hierarchical model." arXiv preprint arXiv:1906.01749 (2019).
- [9] See Abigail, Peter J. Liu, and Christopher D. Manning. "Get to the point: Summarization with pointer-generator networks." arXivpreprintarXiv:1704.04368(2017).

Energy Storage Solutions for Low-power Renewable Energy Harvesters: A Review

Suman Mann¹, Deepshikha Yadav²

¹Department of Information & Technology MSIT, Delhi

²Department of ECE MSIT, Delhi

¹sumanmann@msit.in, ²deepshikha@msit.in

Abstract: *These days, the two key technologies promoting the widespread use of sustainable technologies are energy harvesting and energy management. To faithfully achieve the energy demands of the low-power devices, embed in interconnected networks like the Internet of Things, management of energy harvesting from environmental energy sources such as solar radiations, thermal sources, wind, mechanical etc. is presented in this paper. Powering low-power devices like sensor nodes, energy harvesting, or converting ambient energy to electrical energy, has become popular. This study concentrates on the voltage enhancement and energy-storing techniques that are available, including the cold-start and charge pumps, which are useful when cascaded with small self-powered portable devices and sensors.*

Keywords: *power management; energy harvesting IOT; low power; energy storage, sensors*

I. INTRODUCTION

Recently we have seen a remarkable increase in the usage of wireless sensor networks in a variety of fields, including calamity management, automation, infrastructure observation and surveillance. To create fully autonomous smart structures, automated houses and buildings must incorporate wireless sensors [1]. With the increased dependence on sensor networks around us, it is inevitable to see the internet of things (IoT) being embedded in our daily lives. In the upcoming years, it is anticipated that the Internet of Things (IoT) paradigm will have a significant influence. IoT nodes are expected to be everywhere, which necessitates that they are unchained and independent of power supply. Power autonomy in IoT nodes is managed by generating energy from the ambient environments sources like solar radiations, thermal energy, wind energy etc. using transducers. Instead of focusing on the network's sustainability, research is primarily concerned with the implementation of functionalities in wireless sensor network architecture.

The power supply basis for the wireless sensor node is generally a battery with a limited life span. It becomes extremely challenging to replace the battery of wireless sensor nodes when deployed due to the large number of nodes in wireless sensor networks and their constant distribution in a vastly wide and complex environment [2]. As forecasted, the number of wireless sensors required to support the Internet of things (IoT) will increase two folds by next year thereby

increasing the demand for power sources for an estimated 50 billion wireless sensors [3]. An autonomous wireless sensor network is made possible by two important technologies: energy harvesting and energy management [4]. These systems have become further comprehensively used as a result of a convergence between increasing power output from harvesters and decreasing energy demand from electronic devices. Although batteries have typically been used to power these gadgets, their capacity is limited, and they must be changed or recharged when they run out [5]. For this reason, energy harvesting is a desirable power source since it might supply an endless source of energy if the deployment environment has adequate and suitable energy. Small form factor sources such as energy harvesters, in particular, offer an appropriate solution because of their size comparability with current battery-powered systems and suitability for wearable sensors and smart homes, the two most frequently discussed and searched IoT applications [6].

Another technological paradigm of useful ambient energy harvesting is represented by wearable technology. Numerous researchers have sought to create wearable gadgets that are discreet, tiny, and can enhance users' quality of life [7-10]. They can also be utilized for computer-assisted rehabilitation, emergency notification, and the early detection of medical problems. It is vital to accelerate the research towards the fusion of both energy harvesting and energy management technologies to fully optimize the wireless networks for self-sustainability, rather than merely improving WSN energy management or energy harvesting. This study sheds light on crucial enablers for energy management. in power-demanding networks technologies like self-sustaining and autonomous wireless sensor networks. To provide a quantitative examination of a wider range of alternatives, this study analyses circuits based on their performance of efficiency when compared with input voltage. Limitations of current systems are outlined to drive future research toward finding solutions and enabling the anticipated growth in wireless sensor deployments.

II. DESIGN CONSIDERATIONS

A. Overview of sources

One of the earliest ways of energy harvesting was the conversion of solar energy to electrical energy. This idea has

recently been expanded to include a variety of other energy sources, including thermal energy, piezoelectric energy, and RF energy. Many of these fields are the subject of a wide variety of research. This section includes a quick summary of some of the energy harvesting-related works. Yildiz has studied non-traditional power sources including solar cells (photovoltaic cells) and thermoelectric generators (TEGs) [11- 12]. Lingam et al. [13] have employed pyroelectric nanogenerators to capture thermoelectric energy by converting temperature variations into electrical voltage or current. Utilizing ambient RF energy sources from several wireless sources with different frequency ranges is also possible, such as radar, wireless LAN, TV signal broadcast stations, and mobile base units [14]. With outputs between 4W and 800W, mechanical sources offer a promising alternative for energy harvesting. Mechanical energy sources can manifest in a variety of ways. Vibration energy harvesting is thus a possible technological advancement. However, the majority of recent studies have only managed to obtain 10 mW to 100 mW power, which has just a few applications in wireless sensors that can run on their power and low-power electronics [15].

B. Design issues

Numerous methods may be used to store energy in the power system. It is vital to take into account a variety of pertinent factors, including price, lifetime, dependability, size, storage capacity, and environmental impact, to determine the most pertinent storage solutions [16]. The three primary categories of energy storage technologies are mechanical, electrochemical, and electromagnetic storage shown in figure 1 below.

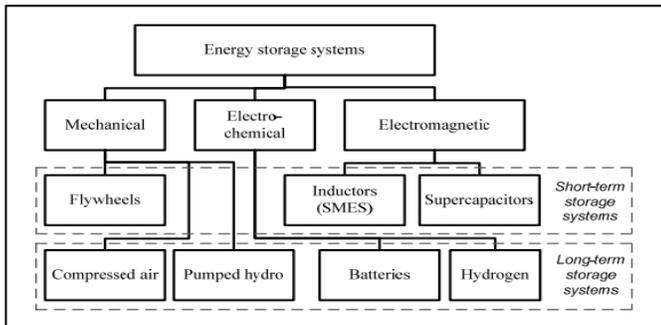


Fig. 1. Energy storage technologies [17]

Examples of mechanical storage include energy storage by compressed air, flywheels and hydrogen-based energy storage pumps. Batteries of all kinds and energy storage systems based on hydrogen are examples of electrochemical storage. Supercapacitors and magnetic energy packing are examples of electromagnetic storage. Energy storages can be divided into short-term and long-term energy storages based on the amount of energy they can hold. Above mentioned flywheels and super capacitance energy storage solutions along with magnetic energy collection are examples of short-term storage technologies. Pumped energy storage based on hydroelectricity, energy stored by compressed air, battery storage solutions and

hydrogen-based energy is some categories for long-term storage systems. The operation of pumped hydro units is similar to that of a hydroelectric power plant. But they also use their generators as motors. The substantial amount of land needed to build the reservoirs and the height necessary between them are the main drawbacks of this design [18]. Compacted air energy storage systems use off-peak electrical energy produced by a conventional load facility or an unconventional renewable energy source to pressurize air at high pressure into a subterranean reservoir or a surface vessel. The reservoir needs to be very big and airtight for a compressed air system to work properly [19]. One of the promising substitutes for using energy carriers is hydrogen. A hydrogen energy storage system's electrolyzer unit is a crucial component, which produces hydrogen from electrical energy by causing water molecules to dissolve, the hydrogen storage system itself, and a hydrogen energy conversion system, which converts the chemical energy stored in the hydrogen back into electrical energy [20]. However, Utilizing hydrogen for the storage and recovery of electrical energy involves several inefficiencies. The storage of hydrogen requires energy. This varies depending on the many energy storage strategies and each technique's effectiveness. In self-powered sensors with energy-harvesting capabilities, supercapacitors can be employed as energy storage in place of batteries. Batteries can be replaced with supercapacitors, which are replenished by energy-harvesting devices. A supercapacitor has a 10-year efficient work life span before its energy capacity degrades and can be recharged more than 500,000 times. The amount of energy that each type of capacitor can store varies greatly from supercapacitors. Supercapacitors have a smaller form factor and a higher energy density for energy storage, making them a better choice for sensor nodes than utilising a capacitor.

C. Cold Start-up

When there is no energy stored in the system and the circuit starts with a discontinuous supply it is referred to as a cold start. Because many dc-dc converters contain switches and/or diodes, a gate-drive voltage greater than the energy harvesting source voltage is often required for the circuit to operate effectively. Cold-start can be dodged by using an uncontrolled charge pump before the boost converter. [21]. The source voltage is enhanced and applied to an oscillator before an SC circuit and high-turn ratio transformer-based systems to store enough energy to power gate-drive circuitry [22-25]. The cold start for the transformer circuits is achieved by resonance between the inductor and capacitor. Energy harvesting devices can become entirely autonomous and independent of outside power sources thanks to these strategies. Since cold-start occurs so infrequently—possibly just once throughout the system's lifetime—it is typically excluded from published efficiency values.

D. Other commercial limitations

Commercially accessible sensor nodes with energy-collecting

power are used for specific applications like industrial environmental control and indoor climate monitoring. There are sensor nodes available that don't require batteries and can run on any energy harvester. Even when energy harvesting is utilized to augment batteries, the problem of having to replace them when they run out still arises. procedure only puts off what must happen. The sensors must be installed in situ (potentially embedded and out-of-reach once they are deployed) and operate for extended periods in applications like structural health monitoring of civil infrastructures. WSNs that run completely on energy harvesting can be implemented by combining low-power electronics, energy-harvesting devices, and supercapacitors. The power levels attainable from cutting-edge energy harvesting devices are in the order of several mW, even though it is very promising for addressing the energy limits of classic WSNs. Still, a lot of scopes exist for improvement in power generation and storage capacity.

III. CHARGE PUMPS FOR POWER MANAGEMENT BECAUSE THE OUTPUT SIGNAL FROM ENERGY HARVESTERS IS SO

strongly dependent on the operating conditions, they are typically unsuitable for feeding directly into the circuit where they are applied. They employ a power management circuit to improve conversion efficiency. The clock generator and DC-DC converter are the two essential components of a power management topology [26-27]. These blocks must also be able to self-start in emergency scenarios, such as those brought on by low voltage and low power levels from external energy harvesters. The DC-DC converter can be built using switched inductor or switched capacitor converter. High-power applications are best served by switched inductor converters, but their implementation necessitates large off-chip inductors.

Switch capacitor-based converters are preferred in low-power and low-area applications because they can be fully integrated on-chip like in IoT nodes [28-30]. Conventionally, switched capacitor converters with voltage increases above one are commonly called charge pumps or multipliers. Charge pumps have traditionally been employed in nonvolatile memories and RAMs, where the design is constrained by settling time and low space, as well as RF antenna switch controllers and LCD drivers, where the main design constraint is the present drivability. Charged pumps are now frequently used to convey the electric energy that is captured from the environment to a storage buffer as well as to alter the voltage levels between two or more functional blocks. Their present set of uses includes energy-autonomous systems like battery-free circuits, biomedical implants, and more recently IoT nodes.

A. Charge pump architectures

The category of inductor-less DC-DC converters includes charge pumps. They use switched capacitors to construct clock circuits. As a result, they are appropriate for full integration and are frequently utilized in solid-state electronic systems.

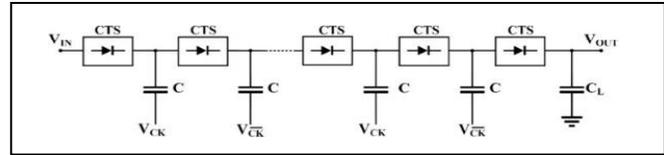


Fig. 2. Charge pump architecture [31]

Figure 2 illustrates the common block diagram of an N-stage CP, with each i-th stage consisting of a charge transfer switch (CTS) and a pumping capacitor, C. The output stage is made up of the final pair, CTS and CL. The CTS is typically made up of one or two primary transistors that operate as switches and have their gates correctly driven by other nodes and other inclusive CTS supporting circuits. In 1980, Dickson suggested and received a patent for the development of the fundamental Dickson topology. The CTS in this example comprises a single NMOS transistor, with the bulk connected to the ground and the gate linked to a forward node to raise the overdrive voltage and thus prevent loss due to the transistor threshold voltage, allowing a reduction in the least required supply voltage. The fact that the CTSs are not completely turned off is its primary flaw.

As a result, the power conversion efficiency is decreased when the CTS is turned off because a non-negligible reverse current flows from the output to the input. As shown in Figure 3b, the traditional Dickson charge pump is improved upon by using PMOS transistors with their bulk connected to the source in place of NMOS transistors. This organization provides for identical inception voltages during turn-on. Additionally, it has a higher value during turn-off, which lowers the opposing inverse current. This method performs well when a standard double well is the only technology available and each NMOS transistor's bulk cannot be separately adjusted. Controlled-switch and non-controlled-switch gate biasing methods can be distinguished. In the first scenario, each transistor's gate is directly coupled to a control signal produced by an auxiliary circuit. In the second instance, the node signals built into the CP itself are connected to the gates of each transistor. Since they allow for lowering the minimum input voltage, gate and body control systems may be an intelligent choice for low- supply-voltage applications like energy recovery from TEGs.

Applications demanding low power consumption can benefit from energy recycling or active/idle mode transition provided by adiabatic charge pumps or adaptive charge pumps, although at the expense of extended settling durations and elevated area overhead. For flash memory, clock-boosted or reconfigurable charge pumps might be a good choice if the main purpose of internal DC-DC converters is to quickly generate a range of voltage levels.

IV. CONCLUSION

Finding a solution to the current issues with the utilisation of renewable energy sources will rely heavily on the use of energy storage technology, including their dependability, stability, and

power quality. With advancements in microelectronics and MEMS, energy harvesting techniques and their applications are growing and becoming more appealing. Power management enables the collection of energy from many sources, which, depending on the application, may provide battery-free direct powering of the application circuit. Energy harvesting technology as it stands now is still unable to continuously power the sensors and nodes with a steady supply of energy. Furthermore, a variety of environmental aspects require more study to comprehend and take advantage of to be able to harvest energy from the environment. We have reviewed the difficulties in developing power storage structures as well as an outline of the research in energy management by charge pumps powered by ambient energy gathering.

Besides energy storage solutions other pathways also promise enhanced energy harvesting capabilities in future endeavours. Using innovative power conditioning circuits and energy storage components, as well as new transducer designs or materials, are just a few examples of it, it is feasible to improve the generated energy. Additionally, the versatility of the device in getting energy under diverse circumstances will be improved by merging numerous energy collection mechanisms into one device.

REFERENCES

- [1] Wan, Z. G., Y. K. Tan, and C. Yuen. "Review on energy harvesting and energy management for sustainable wireless sensor networks." In *2011 IEEE 13th international conference on communication technology*, pp. 362-367. IEEE, 2011.
- [2] Rossi, Maurizio, Luca Rizzon, Matteo Fait, Roberto Passerone, and Davide Brunelli. "Energy neutral wireless sensing for server farms monitoring." *IEEE Journal on Emerging and Selected Topics in Circuits and Systems* 4, no. 3 (2014): 324-334.
- [3] Suci, George, and Ijaz Hussain. "Smart Service Systems: Security and Privacy Challenges in Internet of Things." In *2019 11th International Conference on Electronics, Computers and Artificial Intelligence (ECAI)*, pp. 1-6. IEEE, 2019.
- [4] Seah, Winston KG, Zhi Ang Eu, and Hwee-Pink Tan. "Wireless sensor networks powered by ambient energy harvesting (WSN- HEAP)-Survey and challenges." In *2009 1st International Conference on Wireless Communication, Vehicular Technology, Information Theory and Aerospace & Electronic Systems Technology*, pp. 1-5. Ieee, 2009.
- [5] Chong, Yung-Wey, Widad Ismail, Kwangman Ko, and Chen-Yi Lee. "Energy harvesting for wearable devices: A review." *IEEE Sensors Journal* 19, no. 20 (2019): 9047-9062.
- [6] Lueth, Knud Lasse. "The 10 most popular Internet of Things applications right now." *IoT Analytics* (2015).
- [7] M.-Z. Poh, H. Kim, A. Goessling, N. Swenson, and R. Picard, "Cardiovascular monitoring using earphones and a mobile device," *IEEE Pervasive Comput.*, vol. 11, no. 4, pp. 18–26, Oct./Dec. 2012.
- [8] D. Teichmann, A. Kuhn, S. Leonhardt, and M. Walter, "The MAIN shirt: A textile-integrated magnetic induction sensor array," *Sensors*, vol. 14, no. 1, pp. 1039–1056, 2014.
- [9] A. Dionisi, D. Marioli, E. Sardini, and M. Serpelloni, "Autonomous wearable system for vital signs measurement with energy-harvesting module," *IEEE Trans. Instrum. Meas.*, vol. 65, no. 6, pp. 1423–1434, Jun. 2016.
- [10] D. Dakopoulos and N. G. Bourbakis, "Wearable obstacle avoidance electronic travel aids for blind: A survey," *IEEE Trans. Syst., Man, Cybern. C, Appl. Rev.*, vol. 40, no. 1, pp. 25– 35, Jan. 2010.
- [11] Yildiz, Faruk. "Potential Ambient Energy-Harvesting Sources and Techniques." *Journal of technology Studies* 35, no. 1 (2009): 40-48.
- [12] Yildiz, Faruk, and K. L. Coogler. "Low Power Energy Harvesting with a Thermoelectric Generator through an Air Conditioning Condenser." 121st ASEE Annual Conference & Exposition, Indianapolis, IN, Paper ID. Vol. 10552. 2014.
- [13] Lingam, Devashish, Ankit R. Parikh, Jiacheng Huang, Ankur Jain, and Majid Minary-Jolandan. "Nano/microscale pyroelectric energy harvesting: challenges and opportunities." *International Journal of Smart and Nano Materials* 4, no. 4 (2013): 229-245.
- [14] Cansiz, Mustafa, Dogay Altinel, and Gunes Karabulut Kurt. "Efficiency in RF energy harvesting systems: A comprehensive review." *Energy* 174 (2019): 292-309.
- [15] Sezer, Nurettin, and Muammer Koç. "A comprehensive review on the state-of-the-art of piezoelectric energy harvesting." *Nano Energy* 80 (2021): 105567.
- [16] Rahman, Faizur, Shafiqur Rehman, and Mohammed Arif Abdul- Majeed. "Overview of energy storage systems for storing electricity from renewable energy sources in Saudi Arabia." *Renewable and Sustainable Energy Reviews* 16, no. 1 (2012): 274-283.
- [17] Andrijanovits, A., H. Hoimoja, and D. Vinnikov. "Comparative review of long-term energy storage technologies for renewable energy systems." *Elektronika ir Elektrotechnika* 118, no. 2 (2012): 21-26.
- [18] Faias, S., Santos, P., Sousa, J. and Castro, R., 2008. An overview on short and long-term response energy storage devices for power systems applications. *system*, 5, p.6.
- [19] Choi, S. S., King-Jet Tseng, D. M. Vilathgamuwa, and Trong Duy Nguyen. "Energy storage systems in distributed generation schemes." In *2008 IEEE Power and Energy Society General Meeting-Conversion and Delivery of Electrical Energy in the 21st Century*, pp. 1-8. IEEE, 2008.
- [20] Andrijanovits, Anna, Mikhail Egorov, Madis Lehtla, and Dmitri Vinnikov. "A hydrogen technology as buffer for stabilization of wind power generation." *Water supply* 2 (2010), pp. 62-70
- [21] K. Kadirvel et al., "A 330 nA energy-harvesting charger with battery management for solar and thermoelectric energy harvesting," in Proc. IEEE Int. Solid-State Circuits Conf., 2012, vol. 55, pp. 106–107.
- [22] J. Kim, P. K. T. Mok, and C. Kim, "A 0.15 V input energy harvesting charge pump with dynamic body biasing and adaptive dead-time for efficiency improvement," *IEEE J. Solid- State Circuits*, vol. 50, no. 2, pp. 414–425, Feb. 2014.
- [23] J. P. Im, S. W. Wang, S. T. Ryu, and G. H. Cho, "A 40 mV transformer reuse self-startup boost converter with MPPT control for thermoelectric energy harvesting," *IEEE J. Solid- State Circuits*, vol. 47, no. 12, pp. 3055–3067, Dec. 2012.
- [24] W. Jung et al., "An ultra-low power fully integrated energy harvester based on self-oscillating switched-capacitor voltage doubler," *IEEE J. Solid-State Circuits*, vol. 49, no. 12, pp. 2800– 2811, Dec. 2014.
- [25] K. Kadirvel et al., "A 330 nA energy-harvesting charger with battery management for solar and thermoelectric energy harvesting," in Proc. IEEE Int. Solid-State Circuits Conf., 2012, vol. 55, pp. 106–107.
- [26] Goeppert, J.; Manoli, Y. Fully Integrated Startup at 70 mV of Boost Converters for Thermoelectric Energy Harvesting. *IEEE J. Solid-State Circuits* 2016, 51, 1716–1726.
- [27] Grasso, A.D.; Pennisi, S. Micro-scale inductorless maximum power point tracking DC-DC converter. *Iet Power Electron.* 2013, 6, 1634–1639.
- [28] Le, H.; Sanders, S.R.; Alon, E. Design Techniques for Fully Integrated Switched-Capacitor DC-DC Converters. *IEEE J. Solid-State Circuits* 2011, 46, 2120–2131.
- [29] Tanzawa, T. Innovation of Switched-Capacitor Voltage Multiplier: Part 3: State of the Art of Switching Circuits and Applications of Charge Pumps. *IEEE Solid-State Circuits Mag.* 2016, 8, 63–73.
- [30] Palumbo, G.; Pappalardo, D. Charge Pump Circuits: An Overview on Design Strategies and Topologies. *IEEE Circuits Syst. Mag.* 2010, 10, 31– 45.
- [31] Wu, J.-T.; Chang, K.-L. MOS charge pumps for low-voltage operation. *IEEE J. Solid-State Circuits* 1998, 33, 592–597.

Metro Station Infrastructure and Communication Systems

Dr. Jyoti Jain¹, Manav Pachnanda²

^{1,2}Maharaja Surajmal Institute of Technology New Delhi, India
¹jyotiee@msit.in, ²manav@connect.co.in

Abstract: In 1950, the population of Delhi was 13,19,000 and at present in 2022, the population of Delhi is 32,66,000 yearly populations, which is increasing day by day, to provide transportation facilities for the public of Delhi NCR, mass rapid transit was initiated on 25th December 2002 from Shahdara to Tis Hazari. In this paper, a layout of a metro station and its various areas and their respective components have been explained. Various systems are installed for the functioning of a metro station. Integration of various systems and workflow of such systems and their working procedures in runtime are also presented.

Keywords: ATS; SCR; P.A. System; PIDS Master clock; RASTI; SPL; ACDB; UPS; OCC; BCC.

I. INTRODUCTION

The idea of building electric railway systems emerged in the early, 90s. The idea was to provide completely electric interstate travel for the public, the DMRC (Delhi metro rail cooperation) was registered on 3rd May 1995 under the Companies Act, 1956. However, later the massive increasing population called for more efficient and faster travel in the state. In present times, there are more than 286 stations with over 390 Km of metro rail spanning across Delhi NCR. There have been massive improvements in the field of the electric railway since its beginning, currently; the trains use 25000 volts, 50 Hz of electricity to travel across a train corridor. Many electrical advancements have been made to conserve electricity for the trains e.g. use of regenerative braking. They use traction motors along with the use of isolation transformers for the safe transmission of electricity to ensure the safety of the public travelling through these trains. This idea has transformed into a marvel of electrical and communication technology. Lay out of the metro station is shown in fig1. Metro Station layout has many components as explained.

II. COMPONENTS

The roof is the uppermost layer/surface of a metro station; it is a necessary component as it acts, as a mounting surface for Radio equipment and Surge arresters, also it protects the public/technical components on lower levels from environmental events, such as e.g. heavy rain, hailstorms, heavy sunlight.

A. Platforms

This zone consists of two long platforms running parallel to each

other (Approximately 160-185 meters, depending upon train length) in the between which the train arrives. From here the passengers board the train, the reason for having two platforms on a station is because they act as bidirectional pathways from a particular station i.e. a passenger can choose to go in either direction from a station depending on the platform from which he/she chooses to board the train. Platforms also have some ant Important locations where equipment is installed such as; SCR, TER, PSB, UPS etc.

B. Station control room

The Station Control Room is the room where authorized personnel monitor all the technical systems installed in the station premises, in conjunction with train positioning and activity on track. This level can be termed as the controlling zone of the station, where the station controller is equipped with the necessary equipment to take care of any emergency in case of failure of any systems, and safely execute emergency evacuation procedures

C. Uninterruptible power supply

This room is for power distribution and power redundancy for all zones across the station premises; it consists of an uninterruptible power supply with a massive power bank connected to it. Along with ACDB (Alternating current distribution box). Which distributes power on copper cable throughout the station with proper labelling and sorting of cables.

D. Platform supervision booth

Platform supervision booth houses emergency equipment like an emergency telephone and a PA control desk for live announcements.

E. Ground

The term 'Ground' refers to the grounding system in a station, it collectively means the network of earth terminals throughout the station and the surge arresters installed with the elevated equipment.

F. Telecomm equipment room

The telecom equipment room is one of the most important locations in a station, as all the technical systems such as Public

addressing systems, Master clocks, Public information display systems etc., are assembled and setup in this zone, this Zone is the originating point of all the various systems in the station

G. Concourse

This zone acts as the interchanging, entry and exit pathway for the public, Passengers can enter and exit the station and go to various platforms through the concourse.

H. Viaduct

The viaduct is a channel running throughout the station and with cables connecting all zones altogether, i.e. every zone has connectivity with every other zone through this particular channel. This duct is a very essential part of a station as it allows transmission of wires and ducts within the station, which allows integration of technical systems in different locations in the station and for transmission of power cables in every room in the station.

III. SYSTEMS

A. Public announcement system

This system has a vast connective hold throughout the station, this system consists of various components namely; Control Desks[1] Amplifiers[2], Zone controllers, Speakers, Automatic noise level cancellation devices, Equalizers, Mixers and Servers.

This system is responsible for delivering audio announcements on the stations in all zones, along with announcements regarding train data, emergency, status updates, and other general public announcements, which are executed by the station controllers.

This system acts as a standalone system, in case of failure of the central location as it acts as a completely hardware-based solution [3] for live and restored announcements. The logic behind this system is very simple, firstly the station dimensions are taken and then for the correct placement of speakers, a simulation of the station is built.

The surface of the floor and walls of the platform, their absorbing property for sound and the distance of speakers from these surfaces are taken into account. Mainly two parameters for the optimum placement of speakers are considered (the optimum placement it is meant that the volume of speakers in ideal condition will be safe and audible. In case of noise, it maintains a safe value of decibels also; there will be no such spot on the platforms where an uneven distribution of sound will be present) RASTI (Rapid Acoustics Speech Transmission Index) and SPL (Sound Pressure Level). After the simulation is complete, termination of speaker circuits on the ceiling of the platforms and concourse. The circuits are arranged in a manner that two circuits are present on one platform i.e. in an array of speakers the alternating speakers will be part of the same circuit, such is done to ensure safety in case of damage to one circuit on any platform.

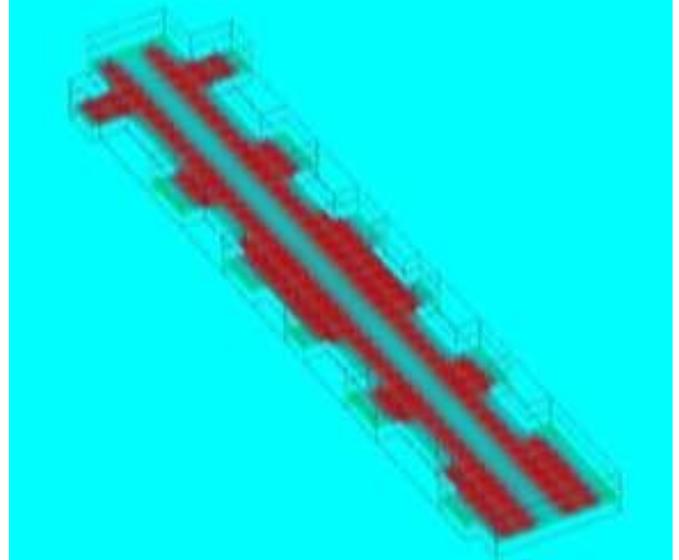


Fig. 2. Simulation of Sound pressure level

The total quantity of speakers is then multiplied with their power consumption (in Watts) to get the total power consumption of one circuit and then, multiplied with the number of circuits (depending on the station size) to get the total power consumption of all speaker.

Now, the selection of the amplifiers for corresponding circuits is done, for example, if the power consumption of a circuit is 200W then a 250W amplifier is optimum for that circuit, to

avoid overloading. Also, for redundancy, a backup amplifier is installed which functions in case of failure of any one amplifier.

B. Public information display systems

This system works in synchronization with PAS, as it holds the key responsibility of displaying train information and emergency messages on platforms and concourse, the train data usually shows; destination of incoming train, time of arrival, along with some fixed messages.

C. Private automatic branch exchange

private automatic branch exchange is the system that is one of the most interactive and most frequently used systems in station, we use this system for internal telephonic linking between all stations that exist previously on that line, and main centers of management which are; OCC (Operation control center) and BCC (Backup control center).

D. Master clock

This system is responsible for providing time information to all existing systems and all clocks present in the system. The idea here is that there exists a Masterclock at the OCC, which provides time information on an I.P. so; all systems that exist have either a sub-master clock or slave clocks, in either case the clocks at the station have to be synced with the master clock and

so, all stations throughout a state show the same time.

E. Closed-circuit television

CCTV system provides a camera feed to the SCR for controllers to monitor every movement at the station and the OCC for security redundancy.

F. Synchronous digital hierarchy

Metro stations are built, on a very basic logic of redundancy of data and functionality i.e. all the data that is being broadcasted to the SCR of any station also be broadcasted to another central location, similarly all functionalities that are being provided to a local controller also be provided to another controller on the same central location.

So, in order to execute this logic, Synchronous Digital Hierarchy is used. On a practical level, at every station an IP address range is assigned, via fiber/copper cables from a network card SDH (Synchronous digital hierarchy). Now, that cable reaches the station, it is terminated into another network card which then extends that network throughout various systems in the station, in this way all data and functionalities are also provided to the Control center.

IV. MMI

MMI stands for man machine interface; this is a software designed to communicate with the PA and PID Systems. This software is present in the SCR (Station control room) and can perform various tasks such as displaying specific messages on the Display and making live announcements at the station. In cases of emergency, the mmi features initiation of an evacuation sequence, announcements, and messages on the displays in the station. This software used for monitoring the status of all PA and PIDS equipment is as it can also detect alarms and provide audible and visual indication of failure. Based on the logic mentioned above, there is also another mmi, which is present at the control center. This mmi holds top most priority in terms of functionalities, for example if a message is being broad casted onto the PA systems and a message is sent from the mmi at control center then, in that case the mmi at control center overwrites the messages projected previously by the local mmi, and the new message will be announced. This MMI at OCC has a slightly different interface as it can be used to control the MMI of all the existing stations on that particular Railway corridor. The MI is a software that allows seamless transaction of commands from the controller to the any level of the station. It houses various features like periodic message scheduling,

So, when the train passes by the AFTC, it transmits a signal to the Control center, from there an ATS Server (Automatic train supervision) projects a hexadecimal string message (this sting message contains the data about the arrival time, coach length, car load, destination, station ID) on an I.P address. Now, at the station level there is an interface system that receives that string and decodes it according to a specified protocol (the message

received is decoded in a way that is understandable to the mmi and the mmi then produces data packets an send them onto the PAS and PIDS) and transmits it on to the MMI. Here, the MMI receives the decoded message and uses the data produced to initiate announcements on Platforms, which contains information about the arrival of the train and form messages in real-time and display the information of the oncoming train onto the PIDS, which include destination and arrival time.

The basic logic of how arrival time is calculated is very simple; the AFTC is mounted onto the rails at regular known intervals. So, when the train passed by it the AFTC send a trigger to the control center. Now, the distance between that AFTC and the platform is known. In addition, the speed of the train is under monitoring. As, we know that,

restoration of logs in various fields; errors, announcements, interface messages, etc. also with

$$time = \frac{Distance}{speed}$$

On simply dividing the two

these features, with the help of MMI prerecorded of special announcements (e.g. for wishing the public on a festival.) can be made and also be looped within a time frame of several week of periodic intervals. The MMI is used to announce and display multilingual messages at the same time and for sequencing an array of several different messages instantly.

The MMI is a very useful tool for the smooth functioning of a metro station and is considered essential at every station that exists.

V. WORKFLOW

Now, that we know about the various Zones and components of the station, we will now move on to the workflow of these components and how are they integrated together for real-time activities.

There also exists a CCTV system, that is provides camera feed to the SCR for controllers to monitor and at the OCC for security redundancy.

A. Integration

Automatic system

Firstly, prior to when a metro train arrives at a station; there is an interlocking system on the rail track, which has Audio Frequency Track Circuits (AFTC) mounted on the rails at regular intervals.

known variables we calculate the arrival time. This data integrates inside the message string that projects to the interface system present at the station.

So, periodically as the train moves on the track, AFTCs keep

sending triggers to the ATS and new Messages are received at regular time intervals, hence the arrival time information on the Display system drops, until the train the arrives.

B. Manual system

The manual systems are the systems or parts of systems that work on manual operation generally; it is the station controller present in the SCR who is authorized to operate these systems. These include telephone and live announcements from the PA system.

Therefore, even though PA system acts automatically on the station there is also hard control available for zone announcement. The control desks available for zone announcements are set up in a manner that multiple zones selected at the same time can initiate live announcements at run time.

Again, for redundancy multiple control desks are present on a station and at the Control center with the same functionalities present.

VI. CONCLUSION

A metro station can be termed as one of the most advanced centers of technology, the amount of precise calculations and accuracy of installation of equipment along with assurance of its safe working, which is needed to build a metro station, is immense. In today’s day and age the technology of electric railway is constantly improving at a rapid speed and with such powerful workforce in this industry, it is inevitable for this technology to reach greater heights.

ACKNOLEGDMENT

This paper would have been possible without the help of my family, and the incredibly supportive staff of DMRC, as they guided me throughout the process of understanding the basic concepts that were involved in the workflow of the structure, as well as making me implement these logics on site. I have had many help from Dr. Jyoti Jain, associate professor at MSIT, New Delhi. As she helped in presenting my research and motivating me to write this paper.

REFERENCES

- [1] <https://buildings.honeywell.com/us/en/products/by-category/voice-and-notification/bi-directional-amplifiers/call-stations>
- [2] [https://buildings.honeywell.com/us/en/products/by-category/voice-and-notification/bi-directional-amplifiers/250 W Amplifier](https://buildings.honeywell.com/us/en/products/by-category/voice-and-notification/bi-directional-amplifiers/250-W-Amplifier)
- [3] <https://buildings.honeywell.com/us/en/products/by-category/voice-and-notification/bi-directional-amplifiers/circuit-protection>

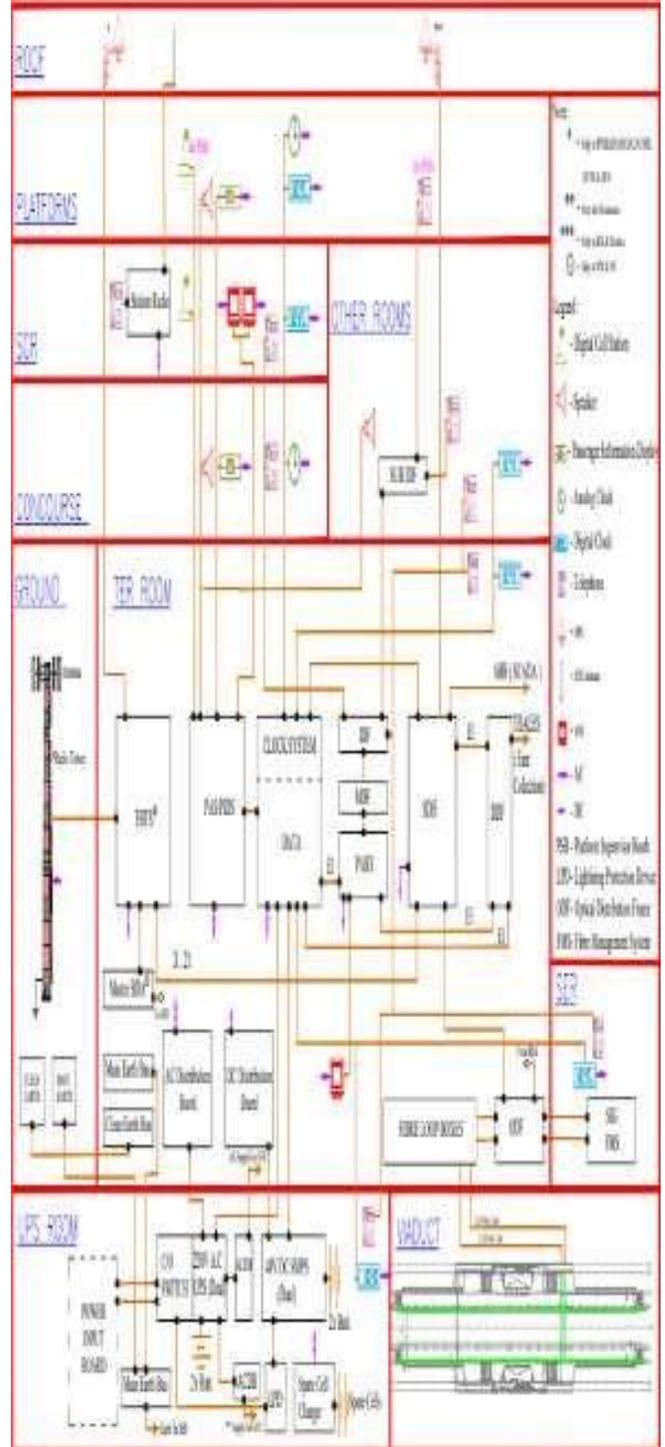


Fig. 1.

Investigation of Double Diffusive Flow of Nanofluid over a Linearly Stretching Vertical Riga Plate

Nidhi

Department of Applied Sciences
 Maharaja Surajmal Institute of Technology
 Janakpuri, New Delhi, 110058, India

Abstract: Current endeavor shows the study of steady 2-dimensional flow of nanofluid past a stretching Riga sheet with convective boundary condition. The Dofour and Soret effect have also been considered in the model developed for transport phenomenon given by Buongiorno[1]. The conservative flow equations have been transformed to the non-dimensional form by applying similarity transformation and then shooting method has been applied to solve the transformed equations. Effect of modified Hartmann number on dimensionless velocity, temperature, solute concentration and nanoparticles concentration has been displayed through graphs.

Keyword: Nanofluids, Riga Plate, Double Diffusive, Mixed Convection.

	<i>Nomenclature</i>
a	Constant
ϕ_s	Solutal concentration of salt
$\phi_{s\infty}$	Ambient solutal concentration of salt
ϕ_{sw}	Solutal concentration of salt at the wall
ϕ_{np}	Nanoparticles volume fraction
$\phi_{np\infty}$	Ambient nanoparticles volume fraction
ϕ_{npw}	Nanoparticles volume fraction at the wall
T	Nanofluid temperature
T_w	Nanofluid temperature at sheet
T_∞	Ambient temperature of the fluid
u, v	Velocity components along x - axis and y -axis respectively
u_w	The stretching velocity of the sheet
x, y	Cartesian coordinates
L	Dimensionless stream function
s	Suction/injection parameter
k	Thermal conductivity
Nu_x	Local Nusselt number
Ra_x	Local Rayleigh number
R	The rescaled nanoparticles volume fraction

Bi	Biot number
d	Dimensionless constant
B	Modified Hartmann number
D_{CT}	Soret diffusivity
D_{TC}	Dufour diffusivity
Pr	Prandtl number
D_B	Brownian diffusion coefficient
D_T	Thermophoretic diffusion coefficient
D_S	Solutal diffusivity of porous medium
Gr	Thermal Grashof number
Gr	Buoyancy force owed by temperature difference
Bc	SolutalGrashof number
g	Acceleration due to gravity
Ln	Nanofluid Lewis number
Ld	Dufour-solutal Lewis number of salt
Le	Regular Lewis number of the salt
Nr	Nanofluid buoyancy ratio
Nd	Modified Dufour parameter
Nb	Brownian motion parameter
Nt	Thermophoresis parameter
Nc	Regular buoyancy ratio of the salt
Nur	Reduced Nusselt number
M	Dimensionless solute volume concentration
	Greek symbol
$(\rho c)_f$	Heat capacity of base fluid
$(\rho c)_p$	Heat capacity of nanoparticles
β_T	Volumetric thermal expansion coefficient of the fluid
τ	Shear stress at surface

σ	Electric conductivity of basefluid
η	Similarity variable
μ	Dynamic viscosity of the base fluid
χ	Stretching/shrinking ratio
β_c	Volumetric solutal expansion coefficient of the fluid
ρ_p	Nanoparticles mass density
ρ_f	Base fluid density
θ	Dimensionless temperature
	Subscript
f	Fluid
∞	Ambient condition
w	Condition on surface

I. INTRODUCTION

Firstly, Choi [2] developed the fluids containing nanoparticles (1 – 100 nm) of metals/non-metals/oxides form and named them as nanofluid. These fluids are powerful heat transfer fluids due to various applications like nuclear system cooling, engine cooling, in car radiators, geothermal energy sources, micro channels, domestic refrigerator [3]–[5] etc. Crane [6] firstly studied the flow of nanofluid over a stretching surface and obtained an analytic solution. Khan and Pop[7] analyzed the stretching sheet flow considering nanofluid numerically. To increase the efficiency, magnetic field has been applied. But for weak electromagnetic fluid, a very strong magnetic field was a challenge. This problem was resolved by Gailitis and Lielausis [8] by developing a Riga plate. Nidhi and Kumar [9] analyzed three dimensional flow of hybrid nanofluid past a Riga plate. In the present study, I have investigated numerically double diffusive mixed convective boundary layer flow of nanofluid past a stretching Riga sheet with convective boundary conditions. I have used Buongiorno model [1] to study the revised model in which nanoparticles volume ratio at the plate is controlled passively [10]-[11].

II. MATHEMATICAL FORMULATION

The model analyzes the steady, 2-dimensional, laminar flow of an incompressible, homogenous, electrically conducting binary nanofluid along a vertical stretching Riga plate, (see Fig. 1) which is stretched by giving a velocity $u = u_w = px$ (p is constant). The base fluid is a dual fluid such as salty water. x -axis is taken along the sheet and y -axis is taken perpendicular to it. The fluid is flowing in the region $y > 0$. Riga plate consists of permanent magnets and electrodes arranged alternatively. The electromagnetic field of the Riga plate produces the wall parallel Lorentz force $\frac{\pi M_0 J_0}{8} e^{-\frac{\pi}{a}y}$. The nanoparticles volume ratio at the surface is controlled passively. The denotations of

physical quantities involved are given in the nomenclature. The steady state conservation of mass, momentum, energy, nanoparticles volume ratio and solutal concentration equations after applying boundary layer approximation are given as

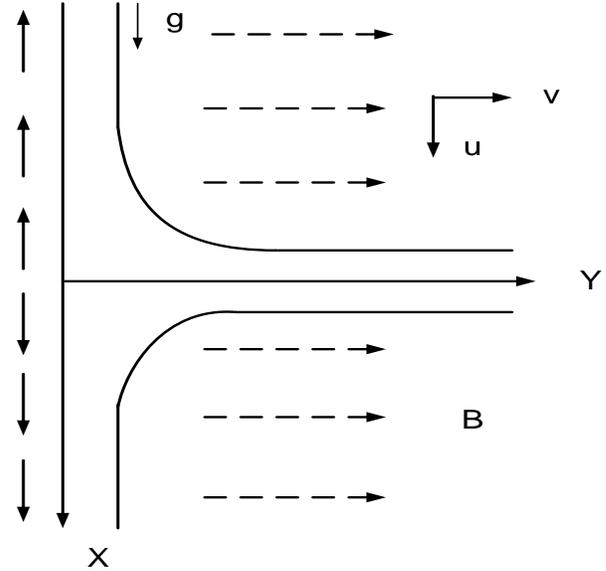


FIGURE 1. Physical Model

Mass Equation

$$\frac{\partial u}{\partial x} + \frac{\partial v}{\partial y} = 0, \quad (1)$$

Momentum Equation

$$\begin{aligned} \frac{\partial P}{\partial x} = & -\rho_f \left(u \frac{\partial u}{\partial x} + v \frac{\partial u}{\partial y} \right) \\ & + \frac{\pi M_0 J_0}{8\rho} e^{-\frac{\pi}{a}y} \\ & + [(\phi_p - \phi_{p\infty})(\rho_p \\ & - \rho_f) + \mu \frac{\partial^2 u}{\partial y^2} \\ & + (1 - \phi_{p\infty})\{\rho_f(1 - \beta_T(T - T_\infty) \\ & - \beta_{c_1}(\phi_s \\ & - \phi_{s\infty}))\}]g, \end{aligned} \quad (2)$$

$$\frac{\partial P}{\partial y} = 0, \quad (3)$$

Energy Equation

$$u \frac{\partial T}{\partial x} + v \frac{\partial T}{\partial y} = \quad (4)$$

$$+\tau \left[D_B \frac{\partial T}{\partial y} \frac{\partial \phi_p}{\partial y} + \left(\frac{D_T}{T_\infty} \right) \left(\frac{\partial T}{\partial y} \right)^2 \right]$$

$$\alpha \frac{\partial^2 T}{\partial y^2} + D_{TC} \frac{\partial^2 \phi_s}{\partial y^2},$$

Solute Concentration Equation

$$u \frac{\partial \phi_s}{\partial x} + v \frac{\partial \phi_s}{\partial y} = D_{CT} \frac{\partial^2 T}{\partial y^2} + D_S \frac{\partial^2 \phi_s}{\partial y^2}, \tag{5}$$

Nanoparticles Volume Concentration Equation

$$u \frac{\partial \phi_p}{\partial x} + v \frac{\partial \phi_p}{\partial y} = D_B \frac{\partial^2 \phi_p}{\partial y^2} + \left(\frac{D_T}{T_\infty} \right) \frac{\partial^2 T}{\partial y^2}, \tag{6}$$

subject to the conditions at the boundary

at $y = 0$,

$$u = px, v = 0,$$

$$-k \frac{\partial T}{\partial y} = h(T_f - T),$$

$$\phi_s = \phi_{sw},$$

$$D_B \nabla^2 \phi_{pw} + \left(\frac{D_T}{T_\infty} \right) \nabla^2 T = 0,$$

as $y \rightarrow \infty$

$$u \rightarrow 0, v \rightarrow 0, T \rightarrow T_\infty,$$

$$\phi_s \rightarrow \phi_{s\infty}, \phi_p \rightarrow \phi_{p\infty}. \tag{7}$$

where

$$\alpha = \frac{k}{(\rho C)_p}, \tau = (\rho C)_p / (\rho C)_f. \tag{8}$$

Removing P and applying the similarity transformations given as:

$$u = axL'(\eta), v = -\sqrt{av}L(\eta),$$

$$\eta = \sqrt{\frac{a}{v}}y, \theta(\eta) = \frac{T - T_\infty}{T_w - T_\infty}, \tag{9}$$

$$M(\eta) = \frac{\phi_s - \phi_{s\infty}}{\phi_{sw} - \phi_{s\infty}}, N(\eta) = \frac{\phi_p - \phi_{p\infty}}{\phi_{pw} - \phi_{p\infty}},$$

we get the subsequent coupled equations

$$L''' + LL'' - (L')^2 + Be^{-d\eta} + Gr(\theta + NcM - NrN) = 0, \tag{10}$$

$$\theta'' + Pr(L\theta' + Nb\theta'N' + Nt(\theta')^2 + NdN'') = 0, \tag{11}$$

$$M'' + PrLeLM' + LdPr\theta'' = 0, \tag{12}$$

$$N'' + PrLnLN' + \frac{Nt}{Nb}\theta'' = 0, \tag{13}$$

subject to the conditions at the boundary

$$L(0) = 0, L'(0) = \chi,$$

$$\theta'(0) = -Bi(1 - \theta(0)),$$

$$M(0) = 1, NbN' + Nt\theta' = 0,$$

$$L'(\infty) = 0, \theta(\infty) = 0, M(\infty) = 0, \tag{14}$$

$$N(\infty) = 0,$$

where

$$Pr = \frac{\nu}{\alpha}, Ra_x = \frac{u_w(x)x}{\nu}, Le = \frac{\alpha}{D_s}, \tag{15}$$

$$Ld = \frac{\alpha D_{CT}(T - T_\infty)}{D_S(\phi_s - \phi_{s\infty})}, Ln = \frac{\alpha}{D_B}, \chi = \frac{p}{a}$$

$$Nd = \frac{D_{CT}(\phi_{pw} - \phi_{p\infty})}{\nu(T_w - T_\infty)}, M = \frac{\sigma B^2}{a\rho_f a^2 x'}$$

$$Gt = \frac{(1 - \phi_{p\infty})\rho_{f\infty} g x^3 \beta_T (T - T_\infty)}{\nu^2},$$

$$Gr = \frac{Gt}{Ra_x^2}, Nb = \frac{(\phi_{pw} - \phi_{p\infty})D_B\tau}{v}$$

$$Nt = \frac{(T - T_\infty)D_T\tau}{vT_\infty}, M = \frac{\pi M_0 J_0}{8\rho}$$

$$Nr = \frac{(\phi_{pw} - \phi_{p\infty})(\rho_p - \rho_f)}{\rho_f(\phi_p - \phi_{p\infty})\beta_T(T - T_\infty)}$$

$$Bc = \frac{(1 - \phi_{p\infty})\rho_{f\infty}g\alpha^3\beta_T(\phi_s - \phi_{s\infty})}{v^2}$$

$$Nc = \frac{Bc}{Gt} = \frac{Br}{Gr} = \frac{\beta_c(\phi_s - \phi_{s\infty})}{\beta_T(T - T_\infty)}$$

$$Br = \frac{Bc}{Ra_x^2}, Bi = \sqrt{\frac{\vartheta h}{ak}}, s = -\frac{v_w}{\sqrt{av}}$$

III. NUMERICAL SOLUTION AND JUSTIFICATION

The equations (10)-(13) along with boundary conditions (14) are firstly converted into initial value problem (IVP) by assuming $(L, L', L'', \theta, \theta', M, M', N, N') = (Y(1), Y(2), Y(3), Y(4), Y(5), Y(6), Y(7), Y(8), Y(9))$.

$$Y(1)' = [Y(2)]$$

$$Y(2)' = [Y(3)]$$

$$Y(3)' = Y(2)^2 - Y(1)Y(3) - GrY(4) - Be^{-d\eta} + NcY(6) - NrY(8)$$

$$Y(4)' = [Y(5)]$$

$$Y(5)'$$

$$= \left(\frac{1}{NdLdPr^2} \right) \begin{pmatrix} PrY(1)Y(5) \\ +NbY(5)Y(9) \\ +NtY(5)^2 \\ -NdPr^2LeY(1)Y(9) \end{pmatrix}$$

$$Y(6)' = [Y(7)]$$

(16)

$$Y(7)'$$

$$= -\left(\frac{LdPr}{LdNdPr^2} \right) \begin{pmatrix} PrY(1)Y(5) \\ -NdPr^2LeY(1)Y(9) + \\ NbY(5)Y(9) + NtY(5)^2 \\ -PrLeY(1)Y(7) \end{pmatrix}$$

$$Y(8)' = [Y(9)]$$

$$Y(9)' = -\left(\frac{Nt}{LdNdNbPr^2 - Nb} \right) \begin{pmatrix} PrY(1)Y(5) \\ -NdPr^2LeY(1)Y(9) + NbY(5)Y(9) + \\ NtY(5)^2 \\ -PrLnY(1)Y(9) \end{pmatrix}$$

with the initial conditions

$$Y^T = \left(0, 1, x_1, 1, x_2, x_3, -Bi(1 - x_3), x_4, (-Nt/Nb)x_2 \right)^T \quad (17)$$

In (17), the values of $Y(3), Y(4), Y(7)$ and $Y(8)$ i.e. $L''(0), \theta(0), M'(0)$ and $N(0)$ are not known. I have assumed their values so as to satisfy the distant conditions i.e. $L'(\infty) = 0, \theta(\infty) = 0, M(\infty) = 0, N(\infty) = 0$, are satisfied. A MATLAB code for RKF45 method is employed to find its solution.

IV. RESULTS ACHIEVED

Effect of modified Hartmann number Bon dimensionless velocity L' , temperature profile θ , dimensionless solute concentration M and dimensionless nanoparticles volume fraction N are described in Fig. 2,3. Other parameters appeared in the equations are taken as $Pr = 6.2, Le = 1, Ln = 10, Ld = 0.1, Nr = 0.5, Nt = 0.3, Nb = 0.1, Nc = 2, Nd = 0.1, d = 0.4, Gr = 1$.

To validate the results found, we have compared the results with the results obtained by Khan and Pop[7] and results are found to be in the good agreement. Therefore, we are confident that the results obtained in the present problem are correct.

TABLE 1. Comparison of Nur with the result obtained by Khan and Pop [7]

Nt	Nb	Nur (Present)	Nur (Khan and Pop[7])
0.1	0.1	0.9523	0.9524
0.3		0.5203	0.5201
0.5		0.3211	0.3211
0.1	0.3	0.2512	0.2522
0.3		0.1356	0.1355
0.5		0.0833	0.0833
0.1	0.5	0.0543	0.0543
0.3		0.0292	0.0291
0.5		0.0178	0.0179

Fig. 2 depicts that as the value of B increases dimensionless velocity profile $L'(\eta)$ get enhanced whereas the temperature

profile $\theta(\eta)$ get decreased. The reason behind is that $B > 0$ indicates an assisting flow phenomenon. The higher value of B rises the external electric field which rises the velocity profile. Moreover, the Lorentz force induced by the Riga-plate parallel to the surface enhances surface tension and results in enhancing fluid velocity.

Fig. 3 shows that with the increase in B , M decreases and hence the boundary layer thickness decreases. Also this figure shows that N firstly increases and then decreases with increase in B . Also it is depicted from the figure that there is negative value of N near the surface as due to higher temperature at the surface than the ambient temperature, the thermophoretic force results in depression of their concentration near the surface.

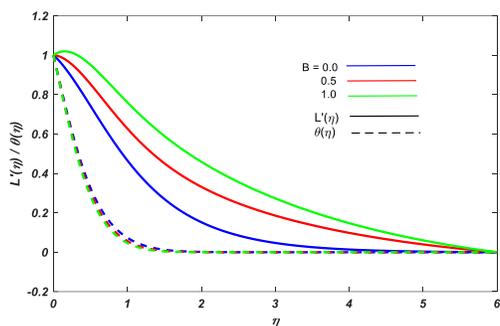


Fig. 2. Variation of dimensionless velocity L' and temperature profile θ with modified Hartmann number

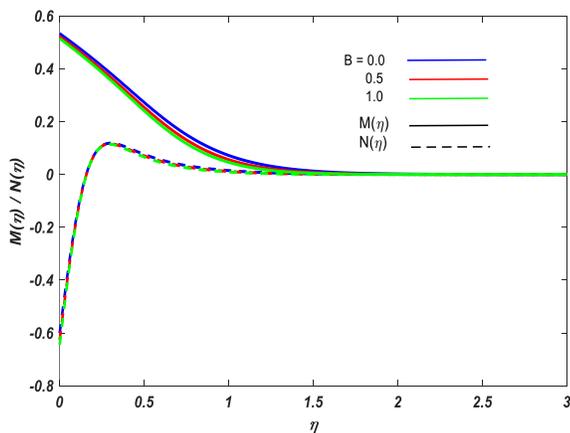


Fig. 3. Variation of solutal concentration M and nanoparticles volume fraction N with modified Hartmann number B

V. CONCLUSIONS

Double diffusive mixed convective boundary layer flow of MHD nanofluids past a stretching Riga sheet is investigated. Dimensionless velocity and nanoparticles concentration are increasing with enhanced modified Hartmann number B , but temperature profile and solute concentration are showing opposite behavior. Also there is negative nanoparticles volume concentration near the surface due to depression effect of thermophoretic force near the surface.

REFERENCES

- [1] J. Buongiorno, "Convective transport in nanofluids," *J. Heat Transfer*, vol. 128, no. 3, pp. 240–250, 2006.
- [2] S. U. S. Choi and J. A. Eastman, "Enhancing thermal conductivity of fluids with nanoparticles," *ASME Int. Mech. Eng. Congr. Expo. Proc.*, 1995.
- [3] K. V. Wong and O. De Leon, "Applications of nanofluids: Current and future," *Adv. Mech. Eng.*, vol. 2, pp. 519659 (1–11), 2010.
- [4] M. Raja, R. Vijayan, P. Dineshkumar, and M. Venkatesan, "Review on nanofluids characterization, heat transfer characteristics and applications," *Renew. Sustain. Energy Rev.*, vol. 64, pp. 163–173, 2016.
- [5] R. Saidur, K. Y. Leong, and H. A. Mohammad, "A review on applications and challenges of nanofluids," *Renew. Sustain. Energy Rev.*, vol. 15, pp. 1646–1668, 2011.
- [6] L. J. Crane, "Flow Past a Stretching Plate," *Zeitschrift Fur Angew. Math. Und Phys.*, vol. 21, pp. 645–647, 1970.
- [7] W. A. Khan and I. Pop, "Boundary-layer flow of a nanofluid past a stretching sheet," *Int. J. Heat Mass Transf.*, vol. 53, no. 11–12, pp. 2477–2483, 2010.
- [8] A. Gailitis and O. Lielausis, "On the possibility to reduce the hydrodynamic resistance of a plate in an electrolyte," *Applied Magneto-hydrodynamics*, Rep. Inst. Phys. Riga, 12 (1961), pp. 143–146.
- [9] J. Nidhi and Kumar, "Cu – Al_2O_3 /Engine oil Williamson hybrid nanofluid flow over a stretching/shrinking Riga plate with viscous dissipation and radiation effect."
- [10] A. V. Kuznetsov and D. A. Nield, "Natural convective boundary-layer flow of a nanofluid past a vertical plate: A revised model," *Int. J. Therm. Sci.*, vol. 77, pp. 126–129, 2014.
- [11] P. Rana, R. Dhanai, and L. Kumar, "MHD slip flow and heat transfer of Al_2O_3 -water nanofluid over a horizontal shrinking cylinder using Buongiorno's model: Effect of nanolayer and nanoparticle diameter," *Advanced Powder Technology*, vol. 28, no. 7, pp. 1727–1738, 2017.

Stereoscopic Ray-Tracing for VR using Rasterization

Faster Ray-tracing through Rasterization and Reprojection

Dr. Shalu¹, Rahul Kumar Sharma², P Silvanus³, Somya Sanu⁴

¹Assistant Professor, Department of Computer Science & Engineering
Maharaja Surajmal Institute of Technology, Delhi, India

^{2,3,4}Undergraduate in B-Tech(CSE)

Maharaja Surajmal Institute of Technology, Delhi, India

¹shalu.mehta@msit.in, ²rahul.kumarkv1@gmail.com, ³selvasilvanus@gmail.com, ⁴somyasanu2805@gmail.com

Abstract: *Virtual Reality (VR), sometimes called Virtual Environments (VE) attracted a lot of attention a few years ago. The wide spread of the media is causing this interest to grow rapidly. Very few people, however, really know what VR is, what its basic principles are and its open problems. This paper presents a historical perspective on visual facts, basic terms and classes of VR programs listed, following the application of this technology to science, work, and places of entertainment. An in-depth study of typical VR systems is done. All parts of VR usage and communication between them are well evaluated: input, output devices and software. Adding human features and their impact on design issues of VE is discussed. Finally, the future of VR is considered in two respects: technology and social. New research guidelines, technical limitations and potential applications have been identified. The potential positive or negative impact of VR on the lives of ordinary people is considered.*

I. INTRODUCTION

Two main algorithms are used in computer graphics to produce 2D images in 3D rasterization scenes [15] and ray tracking [16, 17]. While built almost simultaneously, rasterization has quickly become the leading method of interactive applications due to its low computer requirements initially (no need for floating point in 2D image space), its increased mobility in hardware, and later, with the growing continuous functionality of dedicated image hardware. The use of space and the calculation of each triangle makes it suitable for a relay pipe. However, managing global outcomes, such as reflection, is complex.

Ray-Tracing, on the other hand, is a powerful way to produce high-quality real-life images. It works by tracing the imaginary line from the camera through the pixels on the screen, and enters the scene itself to see what objects are on track and thus what the pixels should be in color. The depth of the ray trace is how often each ray appears at the scene, including different colors and lighting values from all affected areas for the final brightness of the pixels, a method we will explore to enable VR ray tracing software. solution. A large part of the cost of tracking ray rays in VR comes from having to double each frame, producing the perfect image for each eye. A strategy for making stereoscopic ray-tracing tracking effective using almost all production of one of the required images has long existed [Adelson 1993]. This method works by first tracing the entire rays of the left eye at the scene, and then extracting a large

portion of those pixels from the right eye so that only the undisputed pixels must be re-inserted. followed. To test the effectiveness of this method, we built a CPU-based ray tracer, Javascript, that can work in a browser. Our use was based on an existing open source [MacWright 2019]. We then used a stereoscopic ray tracing algorithm from [Adelson 1993] to our ray tracer. After experimenting, we noticed a significant decrease in the number of ray traces needed to produce the right-eye image. Although, while benefiting from computer efficiency, we also noticed some problems with the duplicate image of the right eye. All in all, we found that out of the box, this method is not suitable for VR due to the deterioration of image quality, and we suggest future work involving Machine Learning to optimize the image so that this method can be an effective way to track VR rays.

In this paper, we focus on the main (camera) rays, i.e. rays of the same origin or related rays because this is the only one covered by rasterization. We consider secondary rays and global light algorithms that work, such as following a path or making a photon map, as orthogonal to our path. Even in the simplest case of the main rays, the rasterization and ray follow-up seems very different. In this paper, we show that a different view of both algorithms based on a less common practice - rasterizing by using 3D edge functions defined in the atmosphere instead of 2D edge functions in an image plane - can compile ray rays, i.e. tracking rays and rasterization into a single 3D rasterization algorithm. In this cohesive context, we can now apply restrictive strategies in one way and another context. In this new setting, the only difference between the two algorithms is the way the triangles can be seen and the coated image samples are calculated. Traditionally, both methods use different acceleration structures, e.g. ray tracing uses a 3D location index almost vertical to reverse the scene with obvious tension and occlusion to calculate only the triangles that may be visible to cover the cover, and rasterization uses a 2D grid of image samples that allows rapid (sequential identification) samples may be covered by a triangle (cf. binning). A combination of both worlds was introduced earlier, e.g. Benthin et al. [18] use parallel traversal and binning in multi frustrate rays setting, and Hunt et al. [15] describe the continuous visibility of algorithms between z-buffer systems with tiles and rays tracking. 3D rasterization enables us to freely explore many additional

compounds formally and to analyze the different transactions between these methods.

II. LITERATURE REVIEW

Effective VR-tracking is not a new concept and is being tried in many ways, including purpose-built computer hardware, deep learning, and older algorithms like the Adelson algorithm.

A study conducted by Windows central shows that 73% of users in the PC community do not have the powerful hardware to support VR output. Due to the entrenched VR environment, and providing live 3D most of the computer hardware is not a well-processed data cable. A simple solution to this problem would be Stereoscopic Ray-Tracing for VR (Rapid Generation Image with Denial) [3]. In this way, we aim to produce one of the two images required for stereoscopic ray-traced rendering, based on an image that is already traced by another eye. For this purpose, we also use and evaluate an algorithm [6] that replicates the pixels from the left-hand image created by the right-hand image, re-tracking only where necessary. We show that this retrofitting algorithm significantly reduces the cost of producing one of the two required images. Ray-Tracing [4] is a powerful way to produce high-quality real-time images. It works by tracing the imaginary line from the camera through pixels on the screen, as well as the scene to see what objects are on track and thus what color the pixels should be. The depth of the ray track is how often each ray appears at the scene, which combines different colors and amounts of light from all the affected areas into the final pixel colors. The high cost of this app comes from all the indicators that must be calculated across the track, depending on the depth. Even completely hidden objects can contribute to the final image as shown in something else, so it is difficult to maintain the calculation as one would do by removing rasterization [5].

2.1. Deep Learning

Platforms similar to NVidia's RTX system are designed to improve the state of the art in terms of ray tracking [Vk 2019]. With a special design capable of performing ray tracing and in-depth learning activities, these tools can produce real-time ray-based images faster than ever before. The in-depth learning component allows audio-based and low-resolution translation to be developed, in real-time, into high-quality reliable images. This development of ray-based image production helps to achieve the dream of tracking VR, as any acceleration in the production of a single ray-based image at a given time doubles when the task is to produce two ray-based images. Simply put, such green energy draws us closer to tracking VR rays at an acceptable level of frames.

2.2. Overview of Adelson algorithm

To test the algorithm from Adelson 1993 [6], we first used a stereoscopic ray tracer and then adjusted it to use the right-generation image algorithm [7]. We then proceeded to test the algorithm by checking the quality of the images generated by

the retrieval algorithm (compared to the full-blown image), and by measuring the maximum benefits in performance. The re-imaging algorithm used was taken directly from Adelson [6], where it is referred to as "the visual space algorithm for creating stereo pairs of ray-followed images". The algorithm works on the principle that, when looking at the point links in the left eye plane, that point can also be compared to the right eye view plane with some simple calculations. We redesigned the algorithm almost as presented in the original paper. As in Adelson [6], we take an integrated left-handed system with a viewing plane located at $0 = 0$. We also take two cameras, located at $(-e / 2, 0, -d)$ and $(e / 2, 0, -d)$ where e is an interpapillary distance and d is the depth of the camera associated with the viewing plane. Then, by looking at the point (xpl, ypl) in the left-eye guessing plane, we can determine the position of this point in the right-sighted plane using this equation,

$$xpr = xpl + e (zp / (d + zp))$$

where zp is the depth of the point to be projected in the scene.

```

1: for each scan-line do
2:   let oldx = -1
3:   for each pixel i in the left eye-image do
4:     Compute intersect of ray through i and scene, (ix, iy, iz)
5:     Calculate color C for left-eye view
6:     Let j = ix + e(iz/(d + iz))
7:     if j < width of screen then
8:       mark j in left image as able to re-use C
9:     end if
10:    if j ≥ width of screen then
11:      set j = M
12:    end if
13:    if j - oldx > 1 then
14:      for each pixel k in right image between oldx and j do
15:        mark k in left image as unable to be re-projected
16:      end for
17:    end if
18:  end for
19:  let oldx = j
20: end for

```

Fig. 1. Adelson algorithm

III. METHOD

To test the algorithm from [Adelson 1993][6], we first used it stereoscopic ray-tracer, then adjusted it to use an algorithm producing almost the right eye image. Then we support-stop testing algorithm by properly checking the accuracy of images generated by the repetition algorithm (considered in the image followed by the full ray), and by mass measurement benefits in performance. The integration of rasterization will help in further reduction of rendering time. The modern rasterization technique includes everything like pixel binning and anti-aliasing. New OpenGL extensions provide ways to query confinement information from the GPU or make conditional group transfers content, which leaves the group through the app. An integrated rendering method such as 3D

rasterization suggests that bandwidth discoveries should be integrated with the main rendering algorithm for GPU.

IV. BENEFITS & LIMITATIONS

The advantage of this approach is obviously the reduction in calculation that a person gains by not having to fully track one of the two images required for stereoscopic delivery. The limitations of this approach lie in the quality of the re-edited image. Out of the box, it is only suitable for domains where some visual errors are acceptable. Due to the discomfort experienced by users in VR when scenes are given incorrectly, this makes it difficult to recommend it in that domain. But in some cases, when a large overhaul of a small loss of quality performance is acceptable, this approach will work effectively.

V. EVALUATION OF THE RESULT

In order to test the repetition algorithm, we have considered both achieved computer performance, as well as the quality of resulting images.

5.1 Performance

To quantify computer performance, we look at the related supply costs, depending on the required ray tracks, in each image. Our instrument code indicates that, as the algorithm is in place, drawing the left eye image occupies approximately 87% of all ray traces per frame, and only the remaining 13% is used to render the image of the right eye. A rearranged image in the right eye requires very little tracking, and very cheap to produce. To put it another way, the image of the right eye is about 85% less radiant than the left eye image, considering that the left eye image is already created. The additional cost of the self-prediction algorithm itself, compared to the number of ray-traces it saves, is ignored.

5.2 Image Quality

There were a few visible problems with the right-hand image that was repeated. First, high-level objects (such as turquoise and purple sphere) met a significant amount of drag, which no longer appears as complete spheres. Additionally, when the light source is not in front, but far to the left or right of the event, the boundary between the recurred and reverted eye-to-eye locations. The image became clear due to light variations. This is most evident in the green and turquoise spheres in the image above. Depending on the application you are requesting, these errors may be allowed if additional performance is more important than image quality. Trading is very good in that case, as it is based on us for example, a duplicate image on the right, while it costs 85% less calculation, certainly did not seem to look very bad at 85%, to say the least. Of course, our place is simple. When looking at the most complex scenes the destruction of the image can be very bad. In VR in particular, the destruction of the image, even our simple scene, can make this approach a bad choice. Such lightning flashes and object dragging as seen in our statistics can be very noticeable in the

VR environment and can break immersion and may cause discomfort.

VI. CONCLUSION & FUTURE WORK

Overall, we find the method from [Adelson 1993][6] to be very effective in terms of making stereoscopic ray-tracing tracking very effective. One of the two required images can be produced for a fraction of the normal cost, significantly reducing computer load compared to fully tracking two images. Despite the increase in performance, the effectiveness of this method in tracking VR rays is questionable due to the deterioration of the re-edited image quality. More work, perhaps involving Machine Learning, is needed to explore ways to “correct” the image quality that has been redesigned to make this technique truly suitable for tracking real-time VR rays.

Tracking and rasterization [13] have long been considered two different ways of delivering. We showed that by doing a little a change that extends the functions of a triangle edge to work in 3D, the two approaches are almost identical in relation to the base rays. This introduces a new approach to rasterization, which is similar to homogeneous 2D rasterization, faster than traditional 2D rasterization, and requires minimal setup and testing tasks. The similarities achieved also allow us to convey ideas of dedication between you both rasterization and radiation. We have introduced a standard algorithm that integrates both worlds and opens up more opportunities for future research, allowing us to explore and compare new ways of delivering.

We also believe that 3D rasterization makes the pipeline supply for the future integrated software that provides piping structures - simpler and more efficient. Obviously, the next step would be to apply 3D rasterization using CUDA within the Laine and Karras software-based rasterization pipeline; depending on the location, 3DR may benefit from avoiding vertex modification and possible 3D acceleration structures. However, we aim to replicate the norm, in particular, a parameter that allows for incremental calculations, not only in the direction of radiation but also in the radiation source. This has a huge number of applications on offer, such as mimicking global impacts that require a second complex radiation to treat it with rasterization, and expensive to incorporate it into radiation.

REFERENCES

- [1] Technobyte blog post, What is VR?, technobyte.org, 2018.
- [2] Geeks for Geeks, Introduction to VR, gfg.org, 2019
- [3] M. Piszczek, Stereoscopic Ray-Tracing for VR, University of Washington, 2018.
- [4] Nvidia developers forum, Implementation of Ray-tracing, developer.nvidia.com, 2018.
- [5] Z. Taylor, A Modern Approach to Software Rasterization, University of California, 2018.
- [6] V. Clay, Eye Tracking in Virtual Reality, University of Osnabrück, 2019.
- [7] D. Period, Simple Implementation of Rasterization using Linear Algorithm, University of London, 1998.
- [8] E. H. Adelson, Perceptual Organization and the Judgment of Brightness, American Association for the Advancement of Science, 1993.

- [9] D. Alhadis, Implementation of Adelson algorithm using javascript, Github.com, 2015.
- [10] M. Bailey, Graphics Shaders, University of Chicago, 2019.
- [11] E. Kim, User discomfort while using a virtual reality headset, University of Singapore, 2021
- [12] Oracle forum, CPU time vs cost, community.oracle.com, 2013
- [13] B. Caulfield, What's the Difference Between Ray Tracing and Rasterization?, Nvidia blog posts, 2018.
- [14] UC Berkeley, CS184/284A, Class Lecture, Topic: "The Rasterization Pipeline", Caltech, 2018.
- [15] J. Pineda. A Parallel Algorithm for Polygon Rasterization. Computer Graphics (Proceedings of SIGGRAPH '88), 22(4):17–20, 1988.
- [16] A. Appel. Some Techniques for Shading Machine Renderings of Solids. In AFIPS '68 (Spring): Proceedings of the spring joint computer conference, pages 37–45, 1968.
- [17] T. Whitted. An Improved Illumination Model for Shaded Display. Communications of the ACM, 23(6), 1980.
- [18] C. Benthin and I. Wald. Efficient Ray Traced Soft Shadows using Multi-Frusta Tracing. In Proceedings of High Performance Graphics, pages 135–144, 2009.
- [19] W. Hunt and W. R. Mark. Ray-Specialized Acceleration Structures for Ray Tracing. In Proceedings of Symposium on Interactive Ray Tracing, pages 3–10, Aug 2008.

Stacked Cylindrical, Rectangular, Cone Multi-layered Dynamic Resonator Antenna with Improved Gain and more Directive Beam

Richa Gupta¹, Meena Rao²

¹Dept. of ECE, Maharaja Surajmal Institute of Technology
Janakpuri, New Delhi, India

¹richaguptamsit@gmail.com, ²meenarao@msit.in

Abstract- A novel distinct beam aperture coupled DRA is projected which resides in a multi-layered cylindrical, rectangular, cone geometry ceramic disk of different permittivity joined collectively to accomplish the requisite height. The operating frequency stretches from 6 GHz to 9 GHz. The stacked rectangular, cylindrical, and conical geometries are inspected for increasing and decreasing stacked permittivity. 10-layer Cylindrical mounting permittivity stacking structure with permittivity shifting from (11,12,....,20) with height 1.5mm each afford narrow beamwidth of 37.38° in frequency assortment 6.27-6.36 GHz with a gain of 5.2 dB

Keywords: Antenna, Rectangular DRA, Cylindrical DRA, Cone DRA, Beamwidth

I. INTRODUCTION

Dielectric resonator antennas (DRAs) encompass a quantity of recompense in the vein of squat loss, easiness of excitation, in addition to ample bandwidth [1]-[3]. Several investigations on dropping the dimension of the DRA have been enfolded by researchers. By approach of higher-order mode, the DRA diminution technique is anticipated in [4]. To augment the gain of the DRA, scores of research have been premeditated in [5–7]. Even though they push gain of the DRA, the volume of the DRA turns out to be immense, put side by side with the conservative DRA. DRA gain is too improved by the production of advanced order modes [8] as well as Hybrid configuration [9], and superstrate composition [10]. A quantity of examining groups premeditated the elevated gain antenna by stacking two dissimilar dielectric sheets seeing that in [11, 12]. The scheme of Stacked DRA with a variety of sizes of the metallic cap is investigated in [13] for gain augmentation. The performance of stacked DRA is converse in [14]. It was exposed in [15-17] that stacking two DRAs on top of each can boost an impedance bandwidth.

The act of DRA is appreciably prejudiced by the material

$$\epsilon_{eff} = \frac{h}{\frac{h_1}{\epsilon_{r1}} + \frac{h_2}{\epsilon_{r2}}}$$

possessions along with the geometrical bond. The vital concern of conservative DRAs is the dependence of their dimension and impedance bandwidth on the dielectric constant of material

worn in antennas. A DRA commencing a small permittivity substance would be comparatively outsized owed to the converse proportionality stuck between effective wavelengths along with the square root of the permittivity. It would disclose a low-down radiation Q-factor in addition to an extensive impedance bandwidth. On the other side, a high permittivity DRA would be miniature in size, amid narrowed bandwidth action [18]. The selection of dielectric constant of material worn in the DRA is momentarily significant for wideband submission. In this exertion dissimilar permittivity DRAs materials are connected mutually in favour of gain and bandwidth enrichment.

Various three-dimensional geometrical structures (Rectangular, Cylindrical, Cone) have been stacked over generic RDRA to present improvement in gain and controlling the beam width of the antenna.

II. SYSTEM DESCRIPTION

A. An Improved-Two Stage Sensing detector

Figure 1(a-c) assembles the geometry of a stacked rectangular DRA, Cylindrical DRA and Cone DRA using FR-4 epoxy substrate with a permittivity (ϵ_r) of 4.4. Ten rectangular layers each of height 1.5mm, making a total height of 15mm and permittivity varying in increasing order from 11,12,13,20 is revealed. The same stacked rectangular geometry is explored in which stacking layer permittivity is diverse in decreasing order of permittivity from 20,19,10,11. In Figure 1(b) rectangular geometry is replaced by stacked cylindrical geometry where each stacked cylinder has a radius of 7.5mm and height of 1.5m of varying permittivity. Fig 1(c) presents stacked conical geometry of varying layers of permittivity. All models are scrutinised for mounting and a declining layer of permittivity. Dimensions for the same have been portrayed in table 1.

The effective permittivity (ϵ_{eff}) of the proposed stacked RDRA is obtained as

The resonance frequency of the rectangular DRA antenna can be anticipated by tapping the estimated plausible expression for

the resonance frequency of $f_o = \frac{c}{2\pi\sqrt{\epsilon_r}}\sqrt{k_x^2 + k_y^2 + k_z^2}$

$$k_x^2 + k_y^2 + k_z^2 = \epsilon_r k_o^2,$$

where,

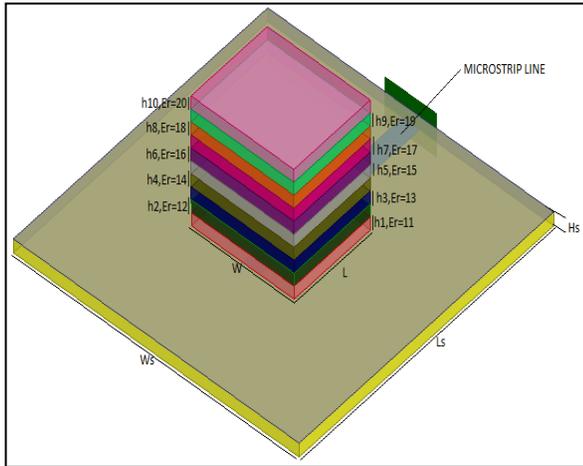
$$k_x = m\frac{\pi}{a}, k_y = n\frac{\pi}{b}, \text{ and } k_z \text{ tag}(k_z d / 2) = \sqrt{(\epsilon_r - 1)k_o^2 - k_z^2}$$

Where ϵ_r denotes dielectric constant of the dielectric resonator antenna, c is the velocity of light, and k_o, k_y and k_z are wave numbers along x, y and z directions correspondingly.

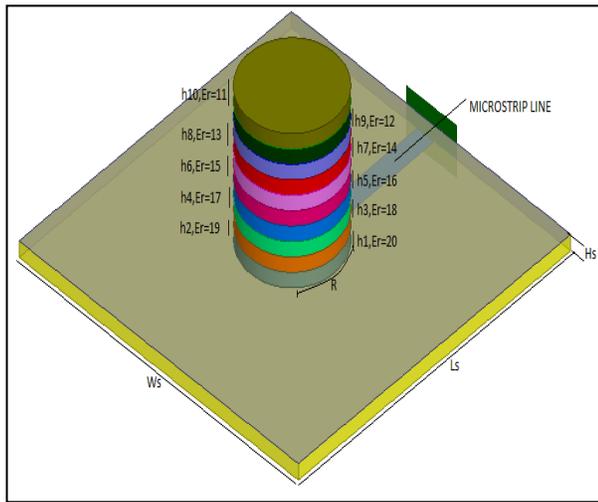
Resonant Frequency in Cylindrical Geometry is $F_r 111 =$

$$\frac{1.841}{2\pi\sqrt{\mu\epsilon}} \frac{1}{R} \left(1 + 2.912 \frac{R^2}{d^2} \right)^{\frac{1}{2}}$$

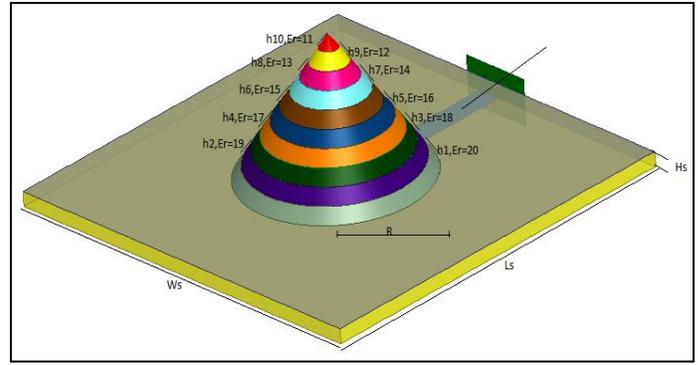
Where R is the radius and d is the height of the cylindrical resonator.



(a)



(b)



(c)

Fig.1. (a-c) Stacked Rectangular, Cylindrical, Cone Geometry.

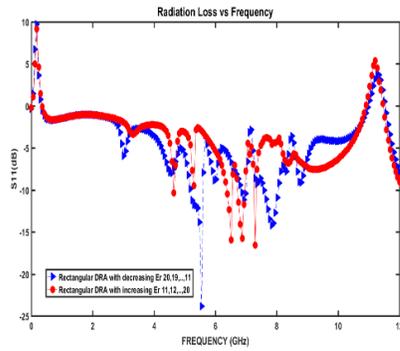
TABLE 1. Design Dimensions

Parameters	Dimensions(mm)
ϵ_r substrate	4.4
Substrate Dimensions	50*50*1.6
Strip Line Dimensions	31*3
Slot Size	1.568*7.84
Stub Size	5.216*3
Rectangular DRA Length	15
Rectangular DRA Width	18
Rectangular DRA Height	1.5mm each (permittivity increasing from 11,12,13.....,20) Total Height 15mm
Radius of cylinder	7.5
Height of cylinder	1.5 (permittivity increasing from 11,12,13.....,20) 1.5 (permittivity decreasing from 20,19, 18, 11.)
The radius of cone DRA	11.175
Height of cone DRA	15mm 1.5(permittivity increasing from 11,12,13.....,20) 1.5(permittivity decreasing from 20, 19, 18,11.)

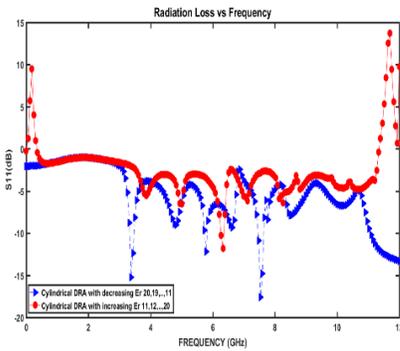
III. NUMERICAL RESULTS AND ANALYSIS

The S_{11} vs frequency response of three geometries are exposed in Figure 2(a-c). The running frequency spreads after 6 GHz to 9 GHz. Supplementary, the directivity radiation pattern for diverse geometries is submitted in figure 3(a-c), which wires a variance in the half power beam width of the radiated beam from 37.38° to 97°. 10 layered Cylindrical growing permittivity from (11,12.....,20) stacking configuration with height 1.5mm each displaying the minimum beam-width of 37.38° is revealed in Figure 3(b). From this Figure, it can be witnessed that the

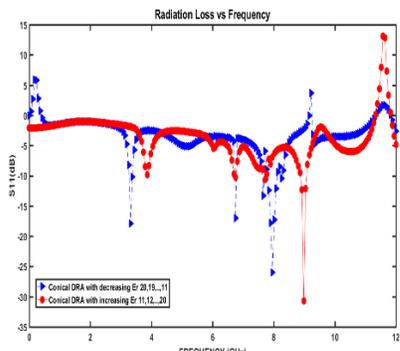
broadside radiation pattern is converted into a directive radiation pattern with diminished beam width. The gain plot for numerous geometries is revealed in figure 4(a-c). 10-layer conical alignment with declining permittivity reveals a gain of 6.26 dBi while 10 layers stacked rectangular geometry with declining permittivity characterizes the highest gain of 6.9 dBi. In Figure 5, gain patterns of numerous geometries Rectangular, Cylindrical, and Cone are exemplified collectively. The radiations pattern of assorted design is embodied in Figure 6. Table 2 illustrates a comparative evaluation of six distinct geometries under study, assessing their appropriate beamwidth, gain, directivity, and efficiency.



(a)

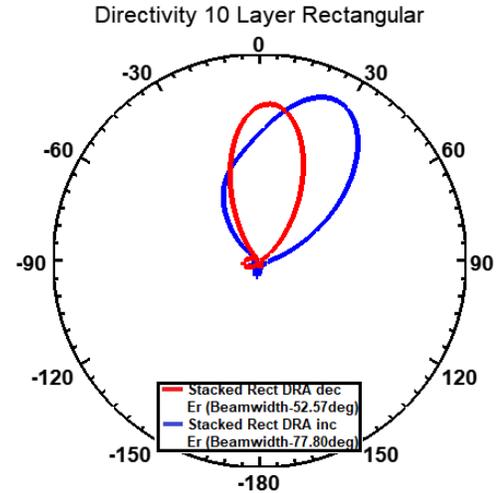


(b)

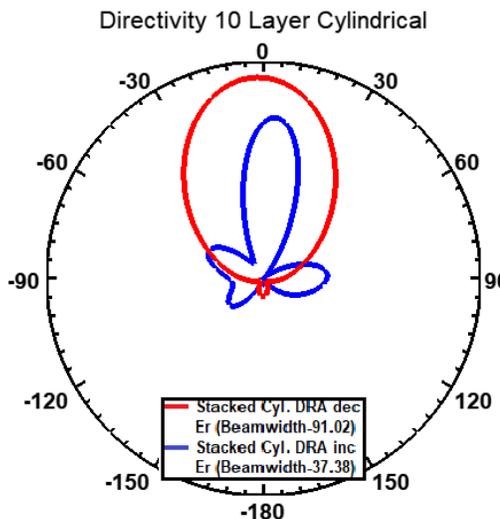


(c)

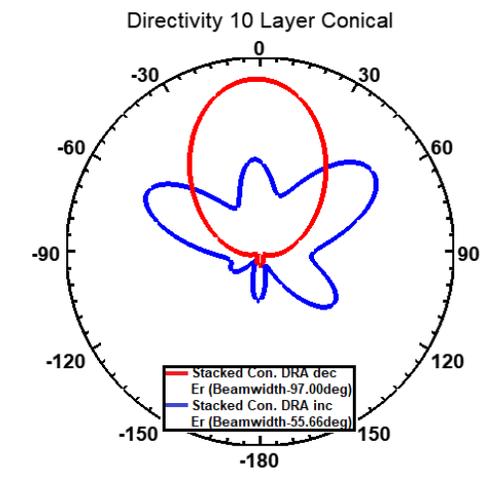
Fig. 2. S_{11} Vs Frequency (a) Rectangular (b) Cylindrical (c) Conical



(a)



(b)



(c)

Fig. 3. Directivity (a) Rectangular (b) Cylindrical (c) Conical.

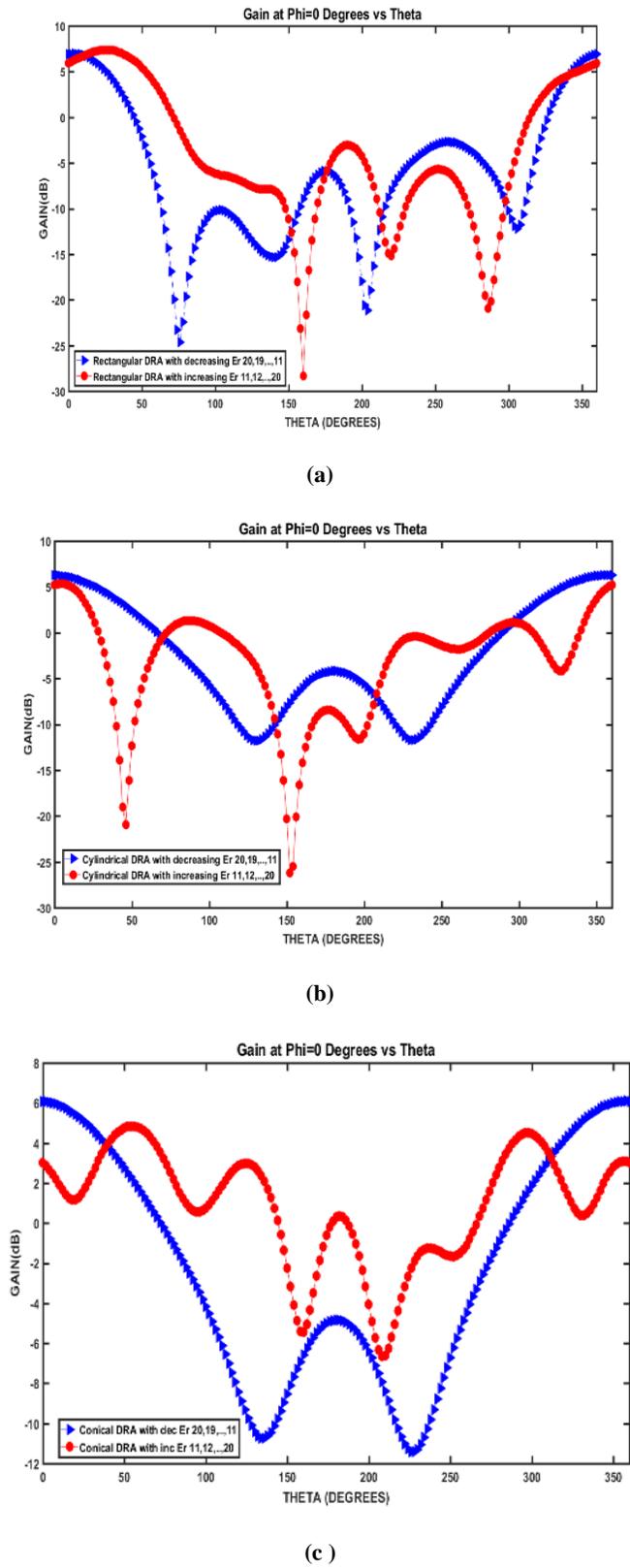


Fig. 4. Gain pattern (a) Rectangular (b) Cylindrical (c) Cone

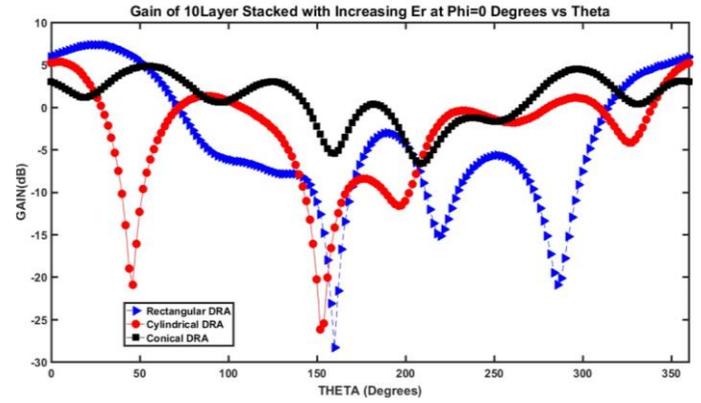
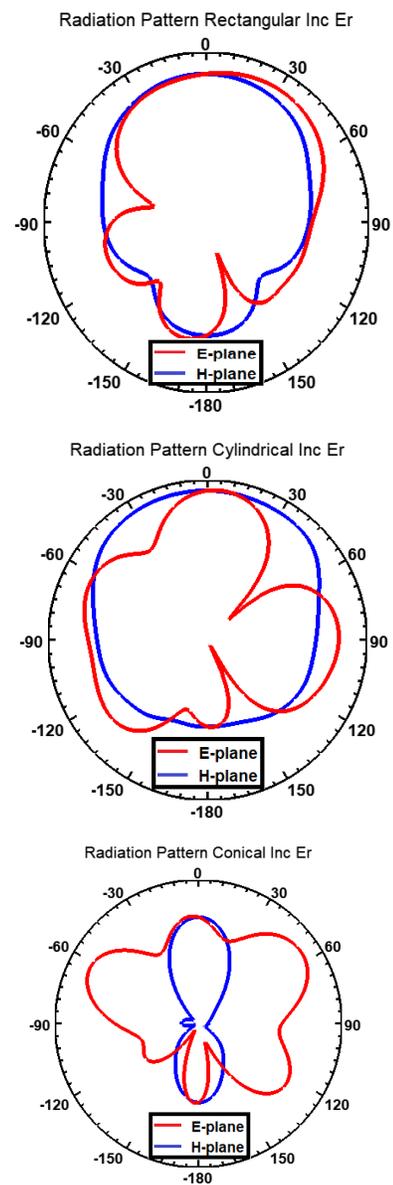


Fig. 5. Gain pattern Rectangular, Cylindrical, Cone



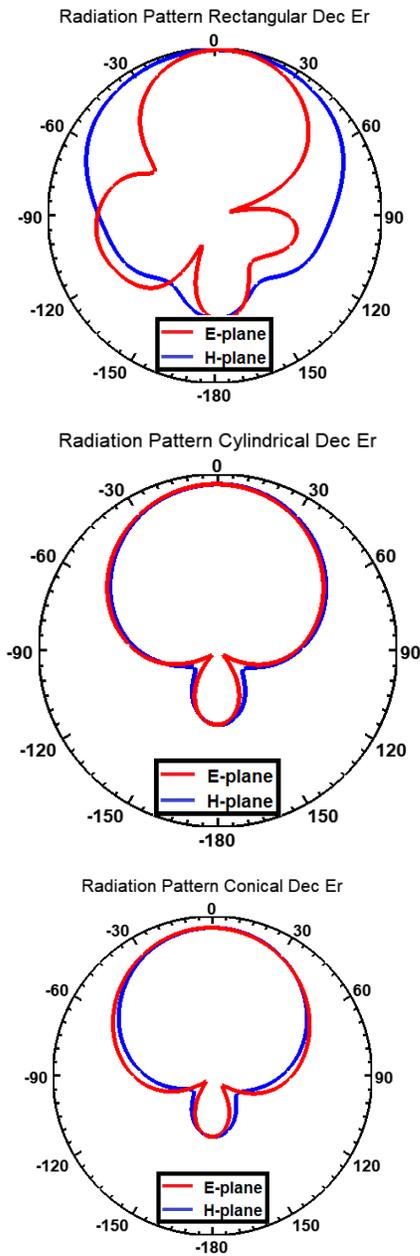


Fig.6 Radiation pattern Rectangular, Cylindrical, Cone

TABLE 2: Capable investigation for six differing geometries.

Configurations of DRA	S11 (GHz)	VS WR	GAIN (dB)	3 dB Beam width (dB 10)	BW (%)	Centre frequency (GHz)	Directivity (mag)
10 layers Increasing Rectangular Permittivity (11,12,...., 20)	6.3-6.56 6.72 -6.9 7.26 - 7.34	<2	5.93	77.80	4.04% 2.64% 1.09%	6.43 6.81 7.3	4.33

20) With height 1.5mm each							
10 layers Decreasing Rectangular Permittivity (11,12,...., 20) With height 1.5mm each	5.19 - 5.60 6.85 -7.0 7.6- 8.05	<2	6.9	52.57	7.59% 2.16% 5.75%	5.395 6.925 7.825	5.24
10 layers conical Increasing Permittivity (11,12,...., 20) With height 1.5mm each	6.72 - 6.76 7.70 - 7.76 8.88 - 9.08	<2	2.99	55.66	0.59% 0.77% 6% 2.22% 7%	6.74 7.73 8.98	2.324
10 layers Conical Decreasing Permittivity (11,12,...., 20) With height 1.5mm each	3.27 - 3.38 6.72 - 6.79 7.62 - 7.69 7.80 - 8.13	<2	6.08	97.00	3.30% 1.03% 0.91% 4.14%	3.325 6.755 7.965	4.43
10 layers Cylindrical Decreasing Permittivity (11,12,...., 20) With height 1.5mm each	3.33 - 3.47 5.74 - 5.83 7.46 - 7.64	<2	6.26	91.10	4.11% 1.55% 2.38%	3.40 5.785 7.55	4.86
10 layers Cylindrical Increasing Permittivity (11,12,...., 20) With height 1.5mm each	6.27 - 6.36	<2	5.20	37.38	1.42%	6.315	3.59

IV. CONCLUSION

A reasonable assessment for distinct stacked geometries rectangular DRA, cylindrical DRA, and conical DRA have been submitted to boost the gain of the antenna, along to make the beam more directive and subsequently diminishing the half power beamwidth. Dissimilar geometries have been researched and contrasted. 10 layers stacked rectangular geometry with decreasing permittivity represents the maximum gain (6.9 dBi) equated to any other geometry along with reasonably controlled beamwidth. 10-layer Cylindrical cumulative permittivity stacking structure with permittivity fluctuating from (11,12.....,20) with height 1.5mm each delivers narrow beamwidth

REFERENCES

- [1] S. A. Long, M. W. McAllister, and L. C. Shen, "The resonant cylindrical dielectric cavity antenna," *IEEE Trans. Antennas Propag.*, vol. AP-31, no. 3, pp. 406–412, May 1983.
- [2] K. M. Luk and K. W. Leung, *Dielectric Resonator Antennas*. Baldock, U.K.: Research Studies Press, 2003.
- [3] K. W. Leung, E. H. Lim, and X. S. Fang, "Dielectric resonator antennas: From the basic to the aesthetic," *Proc. IEEE*, vol. 100, no. 7, pp. 2181–2193, Jul. 2012.
- [4] Gupta, Richa, and Arti Vaish. "Deminiaturized Mode Control Rectangular Dielectric Resonator Antenna." *Progress In Electromagnetics Research* 86 (2016): 173-182.
- [5] Perron, A., Denidni, T.A., Sebak, A.-R.: 'High-gain hybrid dielectric resonator antenna for millimeter-wave applications: design and implementation', *IEEE Trans. Antennas Propag.*, Oct. 2009, 57, (10), pp. 2882–2892
- [6] Petosa, A., Thirakoune, S.: 'Rectangular dielectric resonator antennas with enhanced gain', *IEEE Trans. Antennas Propag.*, Apr. 2011, 59, (4), pp. 1385–1389
- [7] Nasimuddin Esselle, K.P.: 'A low-profile compact microwave antenna with high gain and wide bandwidth', *IEEE Trans. Antennas Propag.*, Jun. 2007, 55, pp. 1880–1883
- [8] Gupta, Richa, and Rajveer S. Yaduvanshi. "Embedded cylindrical magneto-hydrodynamic antenna." *International Journal of Ultra Wideband Communications and Systems* 3, no. 2 (2015): 68-74.
- [9] Gupta, R. and Yaduvanshi, R.S., 2015. High gain and wideband rectangular DRA. *International Journal of Ultra Wideband Communications and Systems*, 3(2), pp.107-114.
- [10] Gupta, Richa, and Rajveer Yaduvanshi. "Superstrate embedded hybrid MHD antenna." In *2015 Annual IEEE India Conference (INDICON)*, pp. 1-5. IEEE, 2015.
- [11] Fakhte, S., Oraizi, H., Matekovits, L.: 'High gain rectangular dielectric resonator antenna using uniaxial material at fundamental mode', in *IEEE Trans. Antennas and Propag.*, Jan. 2017, 65, (1), pp. 342–347
- [12] Fakhte, S., Oraizi, H., Matekovits, L., et al.: 'Cylindrical anisotropic dielectric resonator antenna With improved gain', in *IEEE Trans. Antennas and Propag.*, March 2017, 65, (3), pp. 1404–1409
- [13] Kim, T.-W., & Pak, S.-O. (2019). Enhanced gain and miniaturisation method of stacked dielectric resonator antenna using metallic cap. *IET Microwaves, Antennas & Propagation*, 13(8), 1198–1201
- [14] A. A. Kishk, Xiao Zhang, A. W. Glisson and D. Kajfez, "Numerical analysis of stacked dielectric resonator antennas excited by a coaxial probe for wideband applications," in *IEEE Transactions on Antennas and Propagation*, vol. 51, no. 8, pp. 1996-2006, Aug. 2003,
- [15] Kishk A. A., Zhang X., Glisson A. W., Kajfez D., "Numerical analysis of stacked dielectric resonator antennas excited by a coaxial probe for wideband application", *IEEE Transaction on Antenna and Propagation*, Vol. 51, No. 8, pp. 1996-2006, 2003.
- [16] Kishk A. A., Ahn B., and Kajfez D., "Broadband stacked dielectric resonator antennas", *IEEE Electronics Letters*, Vol. 25, No. 18, pp. 1232-1233, Aug 1989.
- [17] Rocha H. H. B., Freire F. N. A., Sohn R.S.T.M., da Silva M.G., Santos M.R.P., Junqueira C.C.M., Cordaro T., and Sombra A.S.B., "Bandwidth enhancement of stacked dielectric resonator antennas excited by a coaxial probe: an experiment and numerical investigation", *IET Microwave Antennas Propagation*, Vol. 2, No. 6, pp. 580-587. 2008.
- [18] Petosa A., *Dielectric Resonator Antenna Handbook*, Artech House, 25007, January 2007

Axial Ratio Bandwidth and Gain Enhancement of a Stacked Rectangular Dielectric Resonator Antenna

Richa Gupta¹, Deepshika Yadav²

^{1,2}Maharaja Surajmal Institute of Technology, GGSIPU, Delhi, India
¹richagupta@msit.in, ²deepshikha@msit.in

Abstract: A novel technique for the enhancement of axial ratio bandwidth, impedance bandwidth and high gain stacked rectangular dielectric resonator antenna (RDRA) is projected during this paper. Stacked RDRA with z form slot is projected to enhance the AR bandwidth and impedance bandwidth. Metal coated stacked RDRA with Z form slot ends up in higher gain. The performance of all the styles are documented by perceptive the results of reflection constant, bandwidth, gain, axial ratio. The projected style covers the frequency range from 5.02 GHz to 15.01 GHz. Metal coated stacked DRA provides the measured gain of 11.9 dB. The antenna provides the measured AR and impedance bandwidth of 76.24% to 85.02% respectively. The prototypes of antenna are invented within the research laboratory. The measured results are in close proximity of simulated results.

Keywords: Axial Ratio, Bandwidth, Metal coated, Stacked dielectric resonator antenna, High gain.

I. INTRODUCTION

Dielectric resonator antennas (DRAs) have received plenty of attention in antenna designing throughout past decade [1–3]. Because of its characteristics of small size, high radiation potency and low ohmic losses they're additional liable to work on higher frequencies like in RADARs and satellite applications.

Nowadays, compact, broadband, and high potency antenna styles are in the imperative want for contemporary wireless communication systems. Many techniques are reportable [4]-[13] to broaden the axial ratio bandwidths of single feed DRAs. The rotated-stacked technology has been proven to be an efficient approach to broaden the axial ratio bandwidth in [4] and [5]. However, the assembly of such antennas is difficult as a result of the DRs is created from many layers with rotation angles. The dual-mode operation inherent to all or any microstrip fed high ratio (height-to-width or height-to-length ratio) DRAs has been exploited for bandwidth improvement [6]-[8], however it additionally results in a large antenna size. In [9] and [10], changed cross-slot and traveling-wave slot are accustomed to excite the square DRAs, earning wide axial ratio bandwidths. Other broadband DRAs have additionally been incontestable by taking benefits of special DR shapes, like stair-shaped DR and formed DR [11]-[13]. Unfortunately, this type of antennas with non-conventional structures is troublesome to be in theory analyzed and accurately fabricated. Different methods have been proposed to enhance the gain [14-16]. A surface mounted short horn was use to make the gain of a cross

DRA higher than 9 dB [14]. A circular periodic EBG substrate based on the mushroom-like structure was applied for a cylindrical DRA to offer a gain enhancement of 3 dB [15]. The higher-order TE_{δ15} mode was excited in a very tall rectangular DRA to obtain a maximum gain of 9.1 dB [16]. However, these approaches increase the complexity or height of the DRAs. High profile DRAs are not suitable for applications that have limited space. Multi-segment DRA or stacked DRA has been proved to be an effective approach to broaden the impedance bandwidth [17-20]. It uses a combination of dielectric layers with different permittivity to function as a whole DRA.

Recently, a replacement quite dense material patch antenna (DDPA) has been investigated in [21]-[25], that reveals that the material patch antenna will give higher radiation potency, wider bandwidth and similar gain compared to microstrip patch antenna. A simplified theoretical model was conferred to investigate such quite flat material antenna, wherever the skinny high-permittivity material film was approximated to an ideal magnetic wall boundary.

This paper presents a novel design technique of metal coated stacked DRA for bandwidth and gain enhancement. DRA is fed with z shape slot. Three different antenna designs investigated are shown in Fig. 2. The first design (antenna1) proposed z shape slot fed DRA. The second design (antenna 2) consists of stacked DRA with Z slot and the third design (antenna 3) consists of metal coated stacked DRA. The various proposed DRA structures are analyzed using Ansoft high frequency Simulator HFSS. Furthermore, the antenna structure is simple and needs single feeding. The use of conductive coating at the DR is a simple and novel technique for the enhancement of gain. The prototype of antenna is developed in lab and tested on Vector Network Analyzer.

II. ANTENNA STRUCTURE

The geometry of proposed antenna is shown in Fig.1. The design consists of FR4 epoxy substrate with permittivity 4.4 and dimensions (lg *Wg) with height 0.8mm. The permittivity of ceramic material used for DRA is 12.8. For impedance matching stub of length s is used. SMA connector is used for RF EXCITATION. Fig.1(a) shows geometry of DRA with Z shape slot. Z shape slot is made by three rectangular shape slot of same DIMENSIONS. THE schematic design consists of three rectangular DRA is shown in Fig 1(b). TWO DRAs are made up of same

permittivity material with same cross section area and height to form stacked DRA. THE breadth of middle DRA is double of that other two DRAs to enhance the BANDWIDTH. THE total height of stacked DRA is the combination of the height of two DRA. THE field is coupled from the micro strip line to DRA through a Z shape slot in ground plane at the top of the substrate. In the third design DRA is coated with conductive material. This metal coating is the novel technique of gain enhancement. The metal coating works as a parasitic element by controlling the direction of beam from an antenna in a desired direction. All the optimized dimensions of antenna ARE SUMMARIZED in Table I.

The geometry of antenna is determined using equations developed from DVM model. The resonant frequency of DRA is given by

$$k_x^2 + k_y^2 + k_z^2 = \epsilon_r k_0^2$$

$$f_0 = \frac{c}{2\pi\sqrt{\epsilon_r}} \sqrt{k_x^2 + k_y^2 + k_z^2}$$

$$k_x = \frac{\pi}{a}; k_y = \frac{\pi}{b}$$

$$k_z (\tan \frac{k_z d}{2}) = \sqrt{(\epsilon_r - 1)k_0^2 - k_x^2 - k_y^2}$$

Where ϵ_r denotes dielectric constant of dielectric resonator antenna, c is the velocity of light, and k_0, k_x, k_y and k_z are wave numbers along x, y and z directions .

Since method of excitation of DRA is aperture coupling following equation have used as the starting point for designing slot dimensions.

Slot length,

$$L_s = \frac{0.4\lambda_0}{\sqrt{\epsilon_e}}$$

Where λ_0 is the wavelength and the effective permittivity is defined as:

$$\epsilon_e = \frac{\epsilon_r + \epsilon_s}{2}$$

Where ϵ_r and ϵ_s are the dielectric constant of the rectangular dielectric resonator and substrate respectively.

Slot width,

$$W_s = 0.2L_s$$

Stub length,

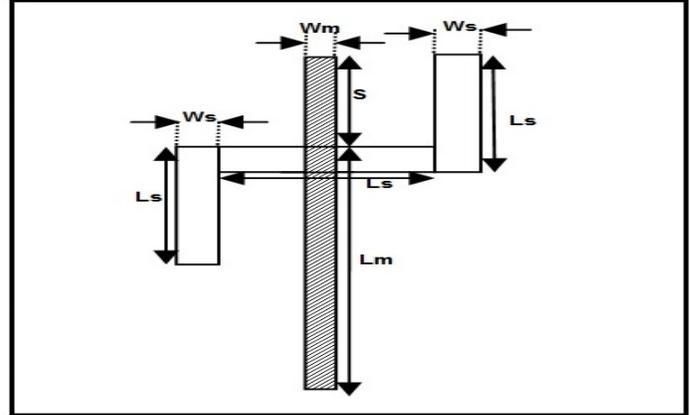
$$s = \frac{\lambda_g}{4}$$

Where λ_g is the guided wave in the substrate.

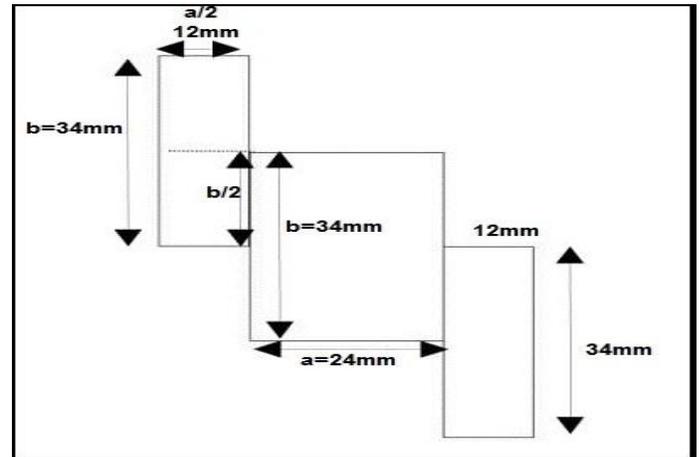
Where λ_g is the guided wave in the substrate.

III. RESULTS

The large bandwidth and high gain antenna is designed, fabricated and tested for demonstration. The three geometries of antenna are proposed and investigated.



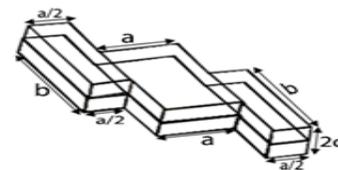
(a)



(b)

Fig. 1.(a-b) Geometry of proposed R DRA

The first antenna structure (antenna 1) contains three rectangular DRA with z shape slot. Z shape slot is made by 3 rectangular shape slots of same dimensions. The second antenna structure (antenna 2) contains 3 stacked rectangular DRA with z shape slot. In the third structure (antenna 3), the design consists of 3 stacked rectangular DRA with z shape slot coated with conductive material.



(a)

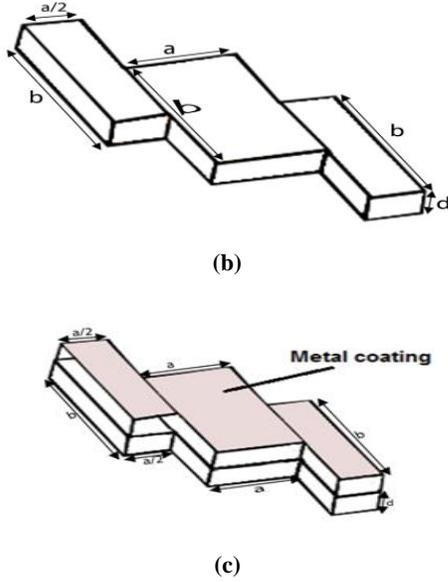


Fig. 2. Three antenna design (a) DRA, (b) Stacked DRA, (c) Metal coated Stacked

TABLE 1: Design Dimensions

Elements	Dimensions	Elements	Dimensions
a	24mm	L _g	80mm
b	34mm	W _g	80mm
d	6mm	L _s	13mm
s	2.1mm	W _s	1.5mm

It has been demonstrated that by metal coating the stacked DRA and properly choosing the permittivity of the two stacked layers, antenna having low profile, wide bandwidth, high gain and circularly polarized can be realized. The gain can be further enhanced by making use of DRA material with high permittivity. The prototype of the antenna has been designed and tested on Vector Network Analyzer and Anechoic Chamber. The simulated results are in close proximity of tested results. Fig.3. shows simulated and measured 10 dB impedance bandwidth response of all the three antennas. The performance of all three structures are summarized in Table II. In thecal proposed DRA TE₁₁₁ mode is generated in the direction of propogation. The simulated and measured impedance bandwidth for antenna structure 1 is 81.16% (5.08-12.02 GHz) and 77.9% (5.25-11.95 GHz) respectively. The antenna 2 provides the simulated and measured impedance bandwidth of 85.36 % (6.03-15.01 GHz) and 85.02 % (5.95-14.75 GHz). Stacking creates a air gap, which decreases the quality factor of DR that leads to slight increment in impedance bandwidth of antenna 2. The conductive coating on antenna 3 structure causes little increase in quality factor, hence impedance bandwidth of antenna 3 is less than antenna 2. The simulated impedance and measured bandwidth for antenna 3 is 82.88% (5.82-14.05 GHz) and 78.9% (5.75-13.25 GHz) respectively.

The simulated and measured axial ratio bandwidth of all three

antenna structures is shown in Fig.4, Table III shows the comparison of 3 dB axial ratio bandwidth of 3 antenna structure. The simulated and measured axial ratio bandwidth for antenna structure 1 is 75.31 % (5.02-10.97 GHz) and 70.12% (5.26-10.94 GHz). The antenna 2 provides the simulated and measured axial ratio bandwidth of 82.31 % (5.99-14.37 GHz) and 76.24 % (5.97-13.32 GHz). For antenna structure 3, simulated and measured axial ratio bandwidth of 75.02 % (5.02-11.05 GHz) and 69.20% (5.32 -10.95 GHz) .The conductive coating does not increase the structural complexity of antenna as it can be achieved by pasting the easily available copper tape.

The simulated and measured gain of all three antenna structure is shown in Fig 5. Table IV shows the comparison of gain of 3 antenna structures, simulated and measured gain is 9.7 dB and 8.9 dB. Stacking enhanced the simulated and measured gain of (antenna 2) to 10.7 dB and 9.8 dB. The conductive coating on (antenna 3) enhances the simulated and measured gain of an antenna to 12.7 dB and 11.9 dB. The peaks of the gain plot are shown in the frequency range in which antenna operated and decreases at other frequency. The conductive coating does not increase the structural complexity of antenna as it can be achieved by pasting the easily available copper tape. As can be observed, simulated results are in close proximity of experimental results. The measured results are generally lower than the simulated values as losses of the dielectric, connectors and cables are not taken into account in simulated results. In Fig 6 shows the radiation petterm in different design of DRA with multiple resonant frequency which is operated in application in the field of wireless communication. Fig.7 shows the e field distribution inside the proposed DRA. Rotation of E field distribution confirms the circular polarization operation of proposed antenna. The experimental setup of antenna for measuring return loss is shown in fig 8 .

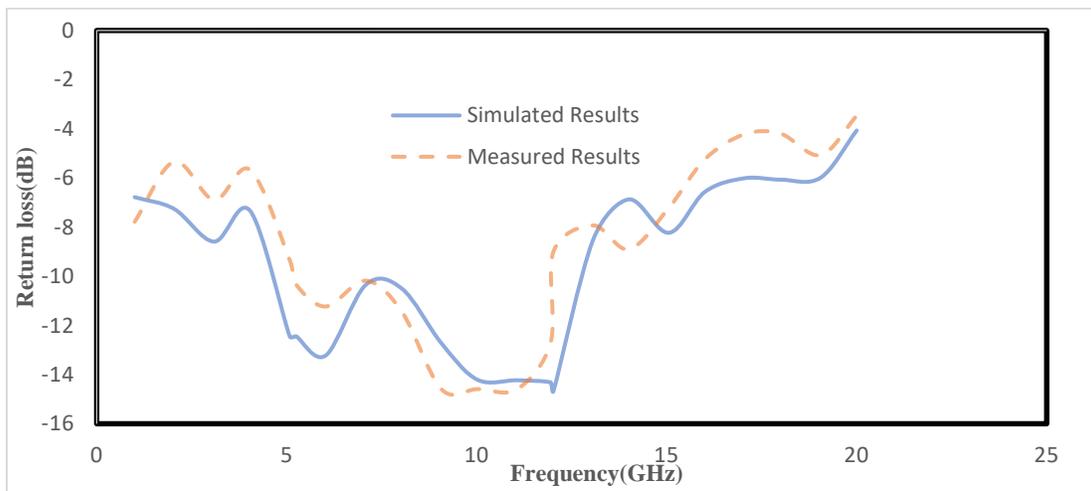
Fig 8 shows measurement setup of return loss with the variation of frequency in the specified range through VNA by connecting the SMA connection for providing feeding power to the DRA.

Table II: Comparison of 10 dB Impedance bandwidth

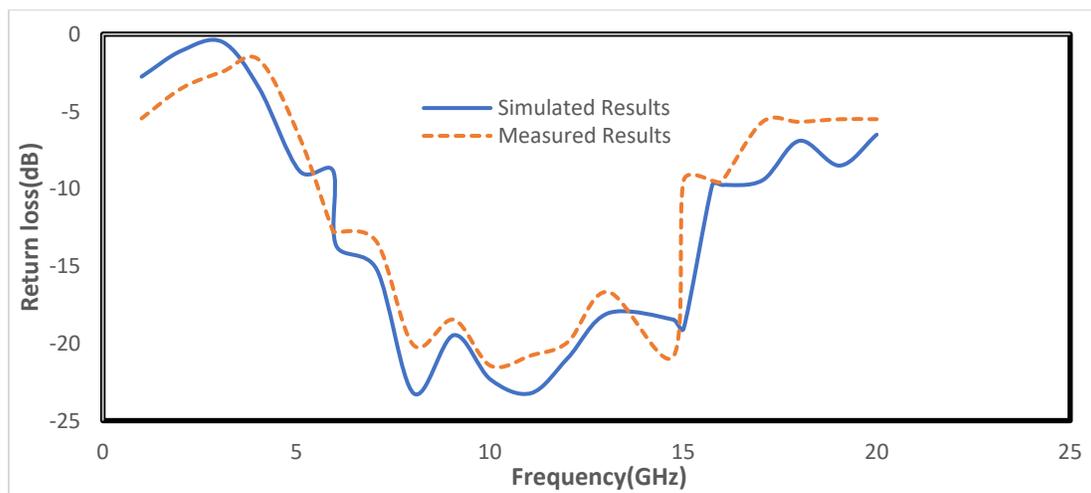
10 dB Impedance bandwidth		
	Simulated (GHz)	Measured (GHz)
Antenna 1	81.16% (5.08-12.02)	77.9% (5.25-11.95)
Antenna 2	85.36% (6.03-15.01)	85.02% (5.95-14.75)
Antenna 3	82.88% (5.82-14.05)	78.9% (5.75-13.25)

Table III: Comparison of Axial Ratio Bandwidth

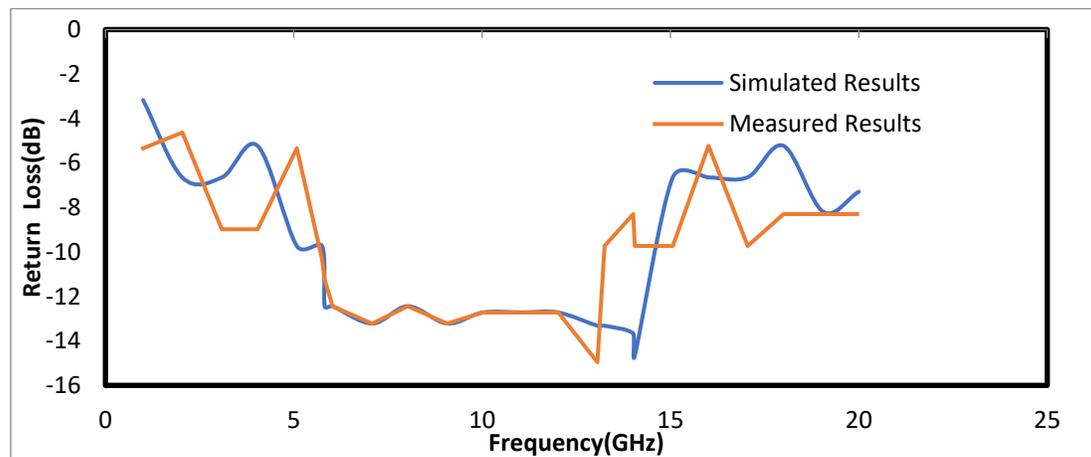
3 dB Axial Ratio Bandwidth		
	Simulated(GHz)	Measured(GHz)
Antenna 1	75.31%(5.02-10.97)	70.12%(5.26-10.94)
Antenna 2	82.31%(5.99-14.37)	76.24%(5.97-13.32)
Antenna 3	75.02%(5.02-11.05)	69.20%(5.32-10.95)



(a)

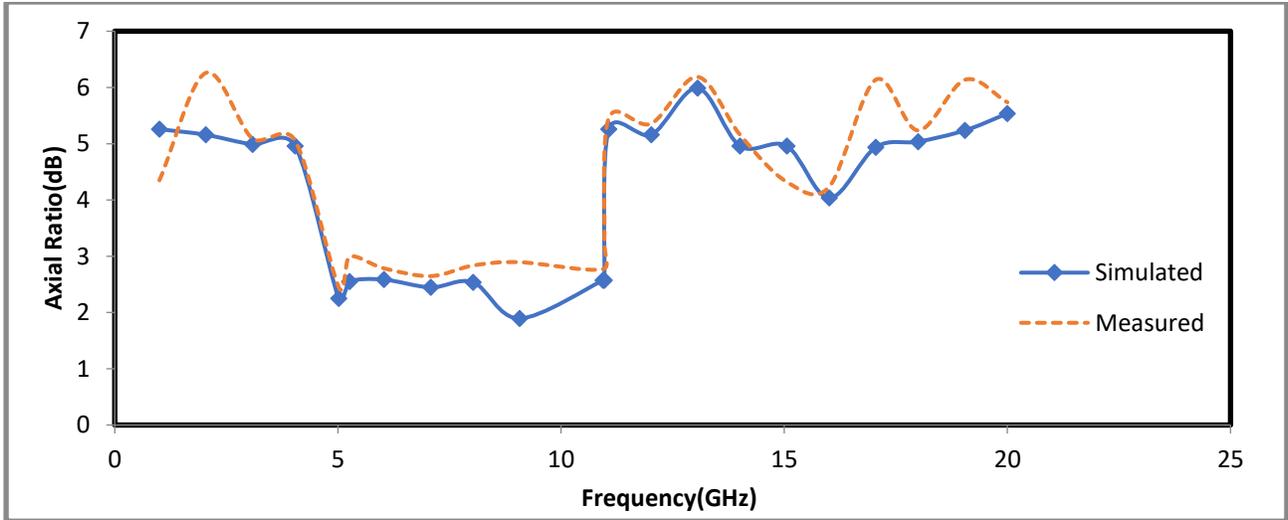


(b)

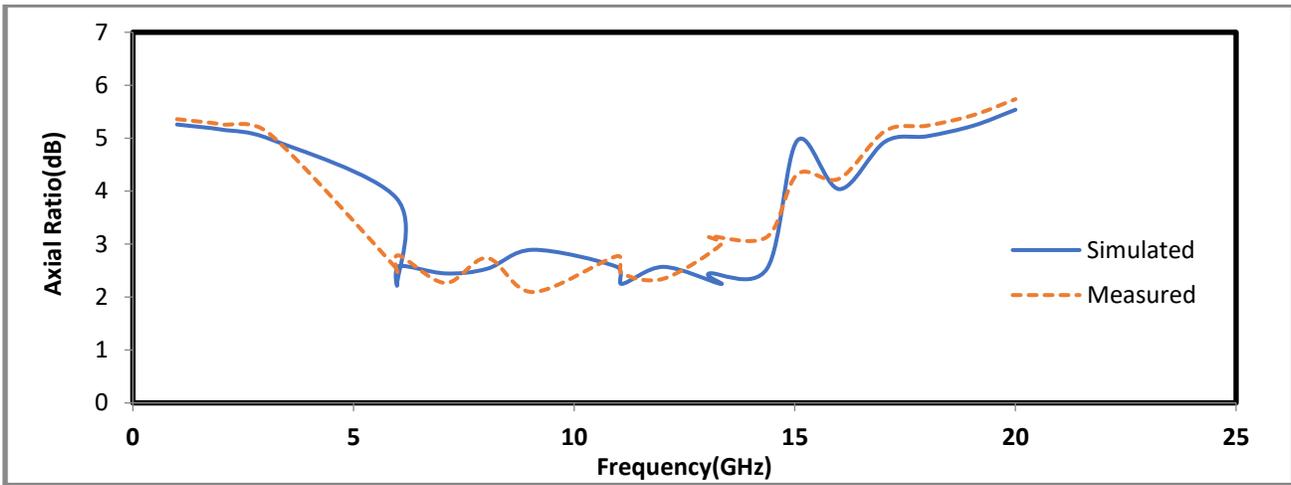


(c)

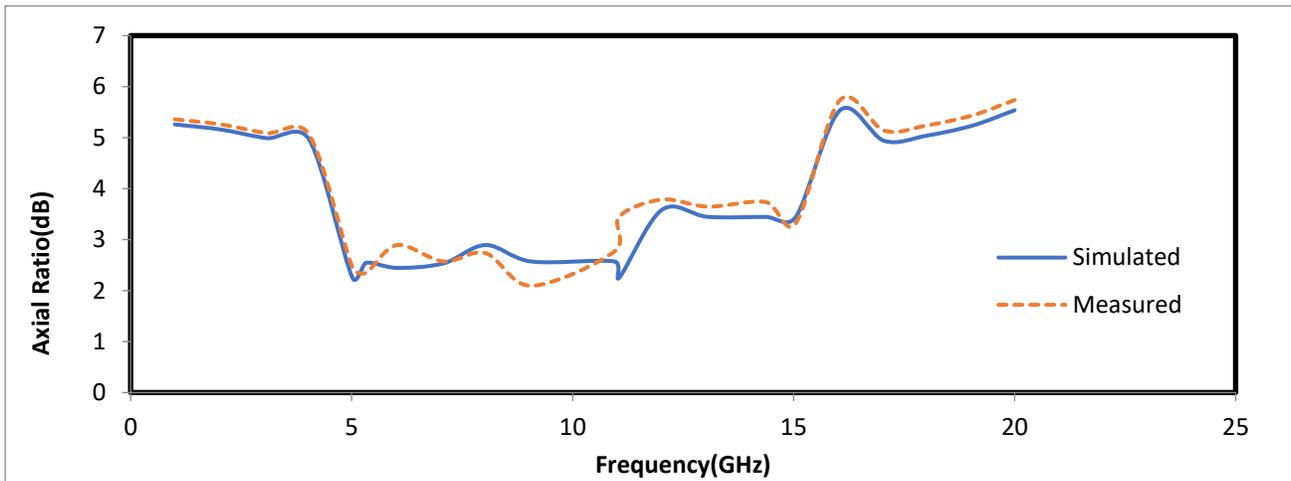
Fig. 3. S11 performance of (a) Antenna 1, (b) Antenna 2, (c) Antenna 3



(a)

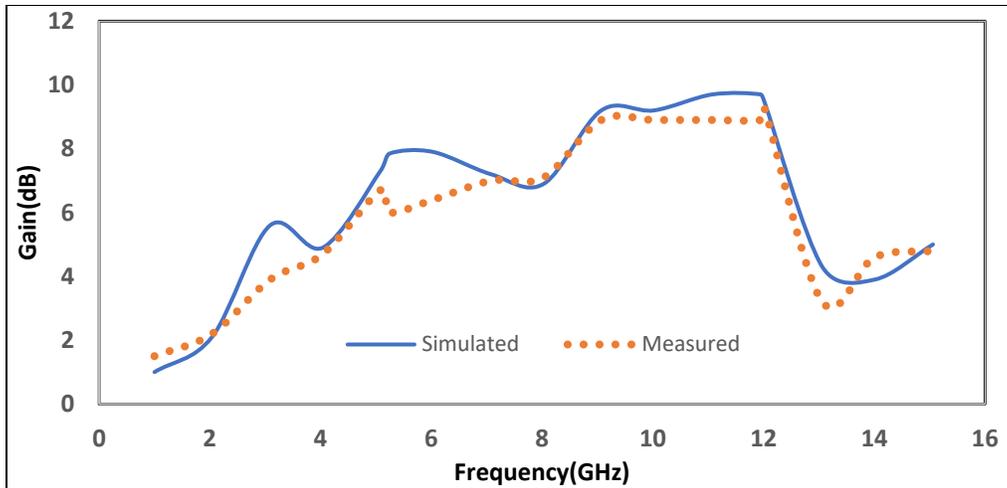


(b)

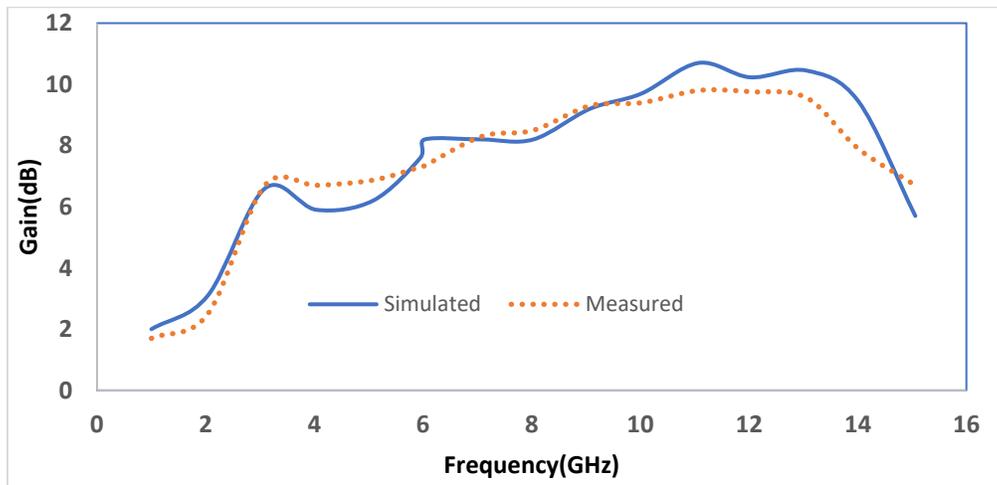


(c)

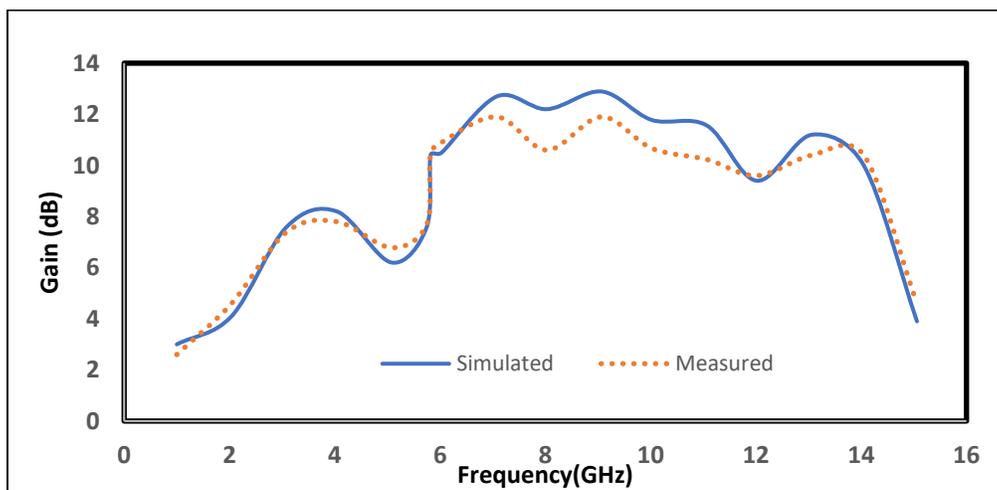
Fig. 4. Axial Ratio performance of (a) Antenna 1, (b) Antenna 2, (c) Antenna 3



(a)



(b)



(c)

Fig. 5. Gain performance of (a) Antenna 1, (b) Antenna 2, (c) Antenna 3

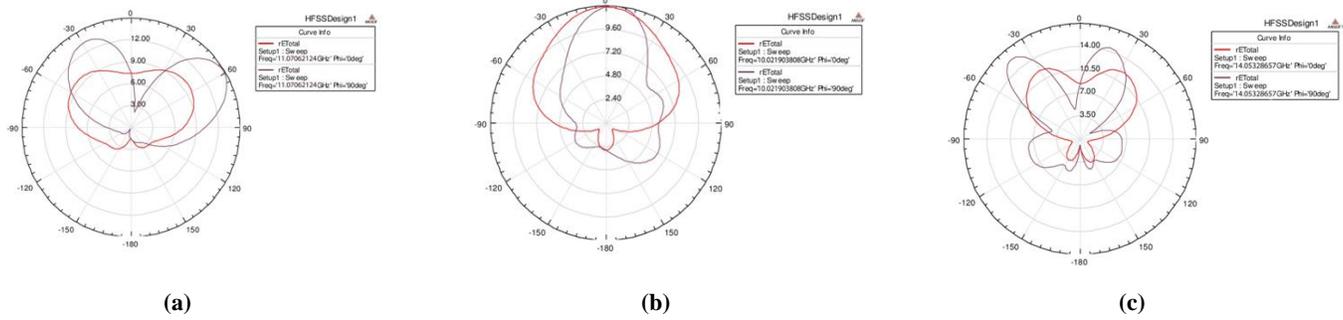


Fig. 6. Radiation Pattern of (a) Antenna 1, (b) Antenna 2, (c) Antenna 3

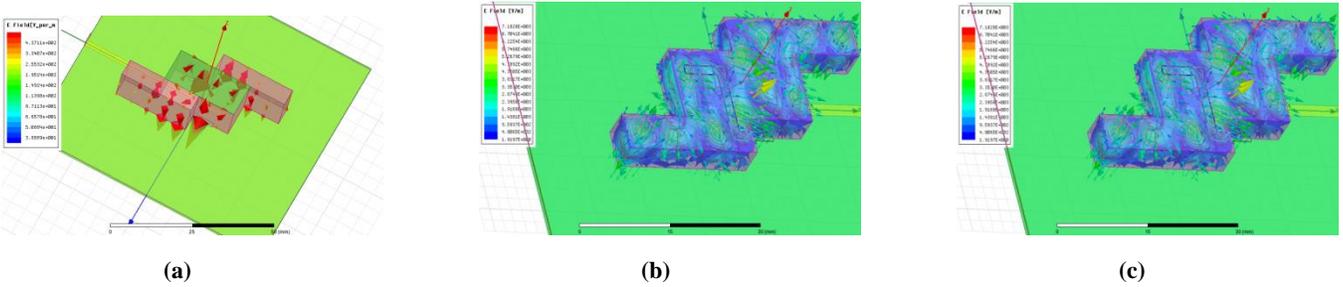


Fig.7. E field pattern at the top surface of DRA (a) Antenna 1, (b) Antenna 2, (c) Antenna 3

TABLE IV : Comparison of Gain

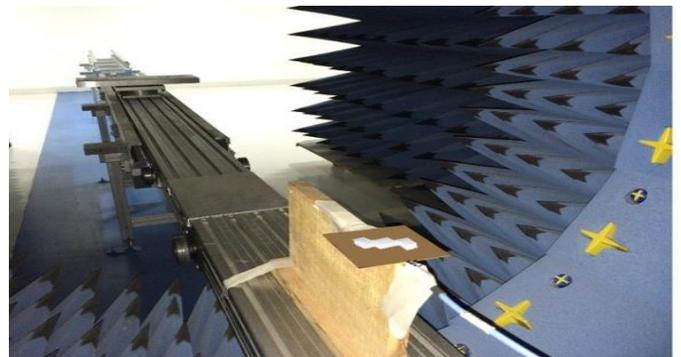
	Gain	
	Simulated(dB)	Measured(dB)
Antenna 1	9.7	8.9
Antenna 2	10.7	9.8
Antenna 3	12.7	11.9

IV. CONCLUSION

Stacked RDRA with z form slot is projected to enhance the AR bandwidth and impedance bandwidth. Metal coated stacked RDRA with Z form slot ends up in higher gain. The performance of all the styles are documented by perceptible results of reflection constant, bandwidth, gain, axial ratio. The projected style covers the frequency range from 5.02 GHz to 15.01 GHz. Metal coated stacked DRA provides the measured gain of 11.9 dB. The antenna provides the measured AR and impedance bandwidth of 76.24% to 85.02% respectively. The proposed design of RDRA can be used in C and X band application such as surveillance, weather radar, satellite communication and wireless computer network etc.



(b)

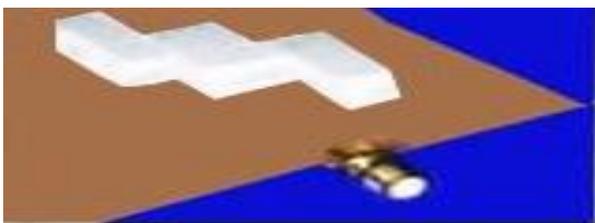


(c)

Fig 8(a-c) Fabricated Proposed Design of RDRA

REFERENCES

[1] Petosa, A. (2007). Dielectric resonator antenna handbook. Norwood, MA: Artech House.
 [2] Luk, K. M., & Leung, K. W. (Eds.). (2003). Dielectric resonator antennas. Baldock: Research Studies Press.



(a)

- [3] Petosa, A., & Ittipiboon, A. (2010). Dielectric resonator antennas: A historical review and the current state of the art. *IEEE Antennas and Propagation Magazine*, 52(5), 91–116.
- [4] K. X. Wang and H. Wong, “A circularly polarized antenna by using rotated-stair dielectric resonator,” *IEEE Antennas Wireless Propag. Lett.*, vol. 14, pp. 787–790, 2015.
- [5] S. Fakhte, H. Oraizi, and R. Karimian, “A novel low-cost circularly polarized rotated stacked dielectric resonator antenna,” *IEEE Antennas Wireless Propag. Lett.*, vol. 13, pp. 722–725, 2014.
- [6] Y. Pan and K. W. Leung, “Wideband circularly polarized trapezoidal dielectric resonator antenna,” *IEEE Antennas Wireless Propag. Lett.*, vol. 9, pp. 588–591, Jun. 2010.
- [7] A. Rashidian and D. Klymyshyn, “On the two segmented and high aspect ratio rectangular dielectric resonator antennas for bandwidth enhancement and miniaturization,” *IEEE Trans. Antennas Propag.*, vol. 57, no. 9, pp. 2775–2780, Sep. 2009.
- [8] P. Patel, B. Mukherjee, and J. Mukherjee, “Wideband circularly polarized rectangular dielectric resonator antennas using square-shaped slots,” *IEEE Antennas Wireless Propag. Lett.*, vol. 15, pp. 1309–1312, 2016.
- [9] M. Zou and J. Pan, “Wideband hybrid circularly polarised rectangular dielectric resonator antenna excited by modified cross-slot,” *Electron. Lett.*, vol. 50, no. 16, pp. 1123–1125, Jul. 2014.
- [10] M. Zou, J. Pan, and Z. Nie, “A wideband circularly polarized rectangular dielectric resonator antenna excited by an archimedean spiral slot,” *IEEE Antennas Wireless Propag. Lett.*, vol. 14, pp. 446–449, 2015.
- [11] G. Varshney, V. S. Pandey, R. S. Yaduvanshi, and L. Kumar, “Wide band circularly polarized dielectric resonator antenna with stair-shaped slot excitation,” *IEEE Trans. Antennas Propag.*, vol. 65, no. 3, pp. 1380–1383, Mar. 2017.
- [12] S. Fakhte, H. Oraizi, R. Karimian, and R. Fakhte, “A new wideband circularly polarized stair-shaped dielectric resonator antenna,” *IEEE Trans. Antennas Propag.*, vol. 63, no. 4, pp. 1828–1832, Apr. 2015.
- [13] L. Lu, Y.-C. Jiao, W. Liang, and H. Zhang, “A novel low-profile dual circularly polarized dielectric resonator antenna,” *IEEE Trans. Antennas Propag.*, vol. 64, no. 9, pp. 4078–4083, Sep. 2016.
- [14] Nasimuddin and K. P. Esselle, “A low profile compact microwave antenna with high gain and wide bandwidth,” *IEEE Trans. Antennas Propag.*, vol. 55, no. 6, pp. 1880–1883, 2007.
- [15] T. A. Denidni, Y. Coulibaly and H. Boutayeb, “Hybrid dielectric resonator antenna with circular mushroom-like structure for gain improvement,” *IEEE Trans. Antennas Propag.*, vol. 57, no. 4, pp. 1043–1049, Apr. 2009.
- [16] R. Gupta, R. Yaduvanshi “High gain and wide band Rectangular DRA, *International Journal of Ultra-wideband Communication*”, Inderscience, vol. 3, no. 2, pp. 107–114, 2015. ISSN online: 1758-7298
- [17] A. A. Kishk, X. Zhang, A. W. Glisson, and D. Kajfez, “Numerical analysis of stacked dielectric resonator antennas excited by a coaxial probe for wideband applications,” *IEEE Trans. Antennas Propag.*, vol. 51, no. 8, pp. 1996–2006, Aug. 2003.
- [18] A. Petosa, N. Simons, R. Siushansian, A. Ittipiboon and M. Cuhaci, “Design and analysis of multisegment dielectric resonator antennas,” *IEEE Trans. Antennas Propag.*, vol. 48, no. 5, pp. 738–742, May. 2000.
- [19] X. S. Fang and K. W. Leung, “Design of wideband omnidirectional two-layer transparent hemispherical dielectric resonator antenna,” *IEEE Trans. Antennas Propag.*, vol. 62, no. 10, pp. 5353–5357, Oct. 2014.
- [20] K. X. Wang and H. Wong, “A circularly polarized antenna by using rotated-stair dielectric resonator,” *IEEE Antennas Wireless Propag. Lett.*, vol. 14, pp. 787–790, 2015.
- [21] H. W. Lai, K. M. Luk, and K. W. Leung, “Dense dielectric patch antenna— A new kind of low-profile antenna element for wireless communications,” *IEEE Trans. Antennas Propag.*, vol. 61, no. 8, pp. 4239–4245, Aug. 2013.
- [22] M. Asaadi, and A. Sebak, “Gain and bandwidth enhancement of 2×2 square dense dielectric patch antenna array using a holey superstrate.” *IEEE Antennas Wireless Propag. Lett.*, vol. 16, pp. 1808–1811, 2017.
- [23] Y. Li and K. M. Luk, “Wideband perforated dense dielectric patch antenna array for millimeter-wave applications,” *IEEE Trans. Antennas Propag.*, vol. 63, no. 8, pp. 3780–3786, Aug. 2015.
- [24] A. Rashidian, L. Shafai, M. Sobocinski, J. Peräntie, J. Juuti, and H. Jantunen, “Printable planar dielectric antennas,” *IEEE Trans. Antennas Propag.*, vol. 64, no. 2, pp. 403–413, Feb. 2016.
- [25] Kumar, Gaurav, et al. “Design of Stacked Rectangular Dielectric Resonator Antenna for Wideband Applications.” *Wireless Personal Communications* (2019): 1-12.

Periodic Heating System to Investigate Pyroelectric Performance

Deepak Goyal

Department of Electronics and Communication Engineering Maharaja Surajmal Institute of Technology, New Delhi-110058, India
deepak.r.goyal@gmail.com

Abstract: A periodic heating system to continuous heat and cool the pyroelectric samples to investigate their performance has been designed. Different heating and cooling cycles ranging from 1-3 seconds was applied to BaTiO₃ and PZT. It is found that the temperature increases rapidly for high heating cycles in BaTiO₃ for the obvious reason. Also, the temperature does not drop back to initial temperature as there is no external cooling resulting in cumulative heating of the samples. It is seen that after certain number of cycles, the samples come to their equilibrium state and the temperature becomes almost constant. The steady state is achieved by BaTiO₃ and PZT in around 9 and 15 seconds respectively. BaTiO₃ sample gains equilibrium faster as compared to PZT sample because of its higher heat capacity. It is interesting that the gradient peaks for BaTiO₃ are maximum for 3 second cycles while in PZT it was observed for 1 second cycle because of their conductivities. It was found that for BaTiO₃ the maximum induced dynamic pyroelectric current was obtained for 3 second of heating cooling cycle because of higher absorption of heat in same time duration.

Keywords: Energy harvesting, Pyroelectric, BaTiO₃, PZT

I. INTRODUCTION

As a consequence of increasing energy crisis energy harvesting has currently become a topic of intense interest. Coal, oil and natural gas in all meet around 80% of the global energy requirement. Therefore, to bridge this demand- supply gap, researchers are actively investigating the alternative sources of energy which are sustainable[1–5]. Tidal, wind and solar are one of the most common alternative sources of energy of renewable energy. In the surroundings, thermal energy is ejected from almost all the physical systems in the form of low grade energy which needs to be harvested. Different methods like thermoelectric, solar power plants and photovoltaic cells have been devised to convert the thermal energy into electric energy[6]. Recently, pyroelectric materials have gained popularity in the research community for energy harvesting capabilities. These are the class of materials which produce electricity when subjected to temporal temperature gradient[7]. In addition, pyroelectric materials are well known for their actuation and sensing applications.

Pyroelectric materials have the potential to function with high thermodynamic efficiency when compared to thermoelectric generators and do not need large heat sinks to maintain the temperature gradient. Pyroelectric materials react to temporal temperature gradient which causes an internal strain and this, in turn, results in electrical charges on the material's surface.

Advances in materials and in thermal-electrical cycling methods are predictable to provide low cost and high-power-density electrical generators [8]. Pyroelectric element when subjected to a power density radiation (W) causing a temperature variation (dT) the induced charge (dQ) released by the electrode area

of the element due to a decrease in polarization is given as: [7], [9].

$$dQ = \eta P A dT \quad (1)$$

where η is the absorption coefficient of radiation and P (units: $\mu\text{Cm}^{-2} \text{K}^{-1}$) is the pyroelectric coefficient of the pyroelectric material.

$$P = \frac{dP_s}{dT} \quad (2)$$

$$i_p = \eta P A \frac{dT}{dt} \quad (3)$$

where P_s is the magnitude of the electrical polarization vector and i_p pyroelectric response current. Pyroelectric materials, such as flat-plate capacitors are sandwiched in between the top and bottom electrodes and poled along the axis perpendicular to the plates. P_s is perpendicular to the electrode surface and its magnitude is given as electrode charge density. Pyroelectric materials with high P value are considered for applications. Also, increasing the electrode area will be result in enhanced current under parity of incident thermal power density per unit area. It is difficult to experimentally determine the temperature gradient therefore finite element modeling is done to explore the temperature variation rate in pyroelectric materials with some designs of cavities created by wet etching, trenches made with a precision dicing saw, and grooves generated by a sandblast etching technique, in order to improve the energy conversion efficiency of BaTiO₃ and PZT cells by pyro-electricity [10–12].

Periodic heat energy harvesting mostly is used to convert temperature gradient into electricity. Periodic heating leads to continuous power generation over time and provides a means of continuously harvesting energy. It is necessary to design a periodic temperature profile and apply it to the pyroelectric elements to generate temperature variation rates. The factors affecting the periodic temperature profiles for improving the temperature variation rate in pyroelectric elements include the

frequency or work cycle, radiation power, properties and dimensions of the air layer, and the material properties, dimensions and structure of the pyroelectric elements, etc.

The rest of the paper is organized as follows. Material and methods used are explained in section II. Experimental results and discussion is done in section III. And final conclusion is in section IV.

II. MATERIALS AND METHOD

In the present study, the pyroelectric performance of BaTiO₃ and PZT has been explored using finite element method. For this purpose, finite element simulations were carried out. As a starting point, the transient heat transfer is carried out analysis to find out the temperature variation in the materials with temperature and other parameters. For the analysis purpose, cylindrical samples were considered with diameter of 24 mm and thickness of 3 mm as shown in Fig.1. The material properties are provided in Table 1.

TABLE 1 Material properties

Sample	Thickness (mm)	Area (mm ²)	Pyroelectric coefficient (μC/m ² K)	Specific heat ((J/(gK))	Thermal conductivity (W/(mK))	Density (g/cm ³)
BaTiO ₃	3	452	200	0.434	2.85	5.94
PZT	3	452	557	0.348	0.14	7.6

The temperature variation in samples is governed by the following differential equation:

$$\rho C_p \frac{\partial T}{\partial t} - \nabla \cdot (k \nabla T) = Q \tag{4}$$

Where ρ, C_p, k and Q are density, specific heat at constant pressure, thermal conductivity and heat flux respectively.

Here, the sample has been simulated in axially symmetric configuration i.e. the rotation of rectangular domain has been considered about the vertical axis as presented in fig.1. The bottom and side edges of the samples were exposed to room temperature in simulations while the periodic heat flux was given on the top surface. A heat flux of 50 W was given with different on off cycles and average variation in temperature on top surface of sample is monitored. At later stage, this temperature variation is related to the dynamic pyroelectric response current using equation 3.

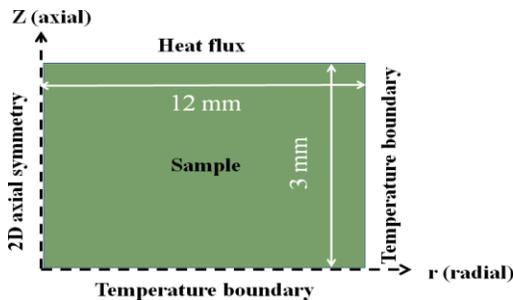


Fig. 1. Cylindrical sample

III. RESULTS AND DISCUSSIONS

Here, the Periodic heating system is designed to periodically heat and cool the samples so as to explore their pyroelectric performance. It is to be noted that with periodic heating the temperature change is smaller, however, over the time temperature change becomes higher and so the harvester energy [15]. As a starting point, different heating and cooling cycles of 1, 2 and 3 seconds were applied to BaTiO₃ and PZT. It is found that in BaTiO₃ the temperature increases rapidly for high heating cycles for the obvious reason. In addition, it is to be noted that for the same duration of cooling cycle the temperature does not drop back to initial temperature as there is no external cooling. This results in cumulative heating of the samples over the time as shown in fig. 2. However, similarity is not observed in PZT in terms of temperature rise with heating cooling cycles Owing to its lower thermal conductivity PZT is not able to dissipate heat as fast as it gains so for smaller duration of cycles its temperature increases at a higher rate. It can be seen that after certain number of cycles the samples come to their equilibrium state and the temperature becomes almost constant. The steady state is achieved by BaTiO₃ and PZT in around 9 and 15 seconds respectively. BaTiO₃ sample gains equilibrium faster as compared to PZT sample because of its higher heat capacity. After this, the temporal gradient of temperature was computed as presented in fig 3. It is interesting that the gradient peaks for BaTiO₃ are for maximum 3 second cycles while in PZT it was observed for 1 second cycle because of their conductivities.

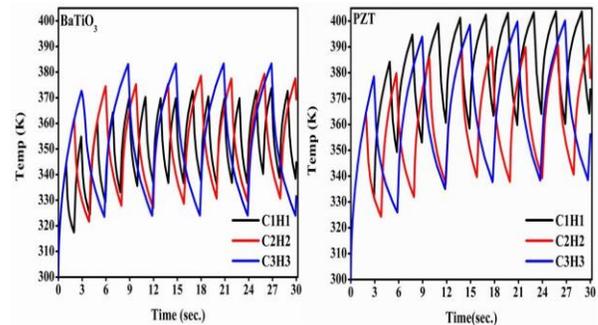


Fig. 2. Cumulative heating of the samples over the time.

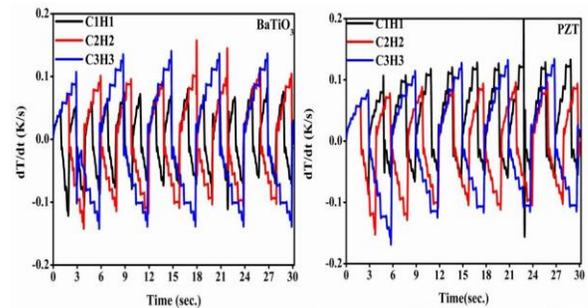


Fig. 3. Temporal gradient of temperature.

It is to be understood that upon being subjected to temporal temperature gradient charge (Q) is induced on the electrode

area. This charge (Q) can be calculated in accordance with equation 1. Charge collected on the electrode area was computed for different cycles for both the samples. It can be observed from fig.4 that for corresponding cycles the charge collected on the surface was much higher for PZT sample because of its higher pyroelectric coefficient. In addition, highest peaks were observed for heating cooling cycles of 2 seconds each because of high temperature gradient obtained. One step ahead, dynamic pyroelectric current response due to induced charge was also computed using equation 3 as shown in Fig. 5. It was found that for BaTiO₃ the maximum induced dynamic pyroelectric current was obtained for 3 second of heating cooling cycle because of higher absorption of heat in same time duration. On the other hand, because of lower thermal conductivity peaks were observed for 1 second cycle.

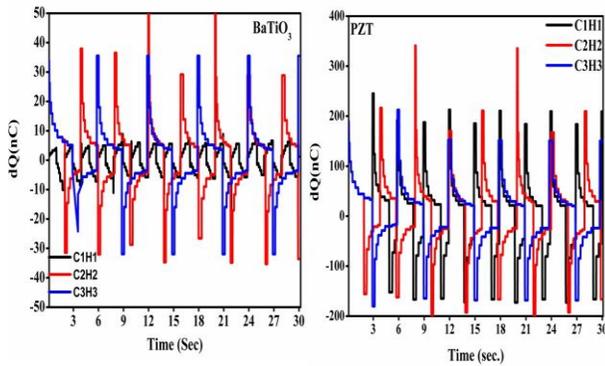


Fig. 4. Charge collected on the surface.

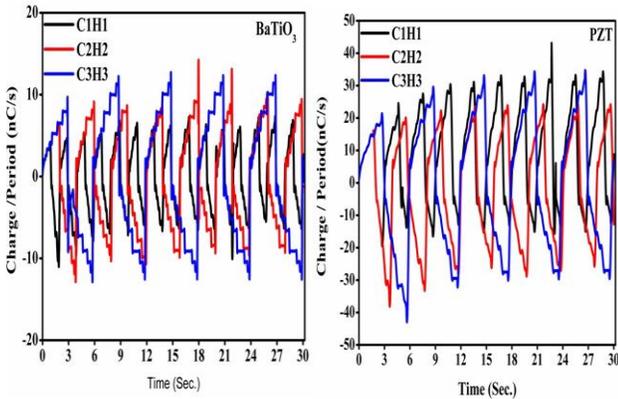


Fig. 5. Dynamic pyroelectric current response

IV. CONCLUSION

In the present scenario with increase in demand of energy it is

required to have an alternate energy harvesting system. From the above discussion it can be concluded that materials like to BaTiO₃ and PZT can serve the purpose of energy harvesting. PZT is found to have high charge collected on the surface whereas for BaTiO₃ the maximum induced dynamic pyroelectric current was obtained. Finally, it is concluded that that materials with property of higher absorption of heat and lower cooling at some extent can be used for energy harvesting.

REFERENCES

- [1] F. Orecchini. (2013). Energy sources of the future: Introduction. in *Handbook of Sustainable Engineering*, pp. 923– 925.
- [2] M. J. McCann, K. R. Catchpole, K. J. Weber, and A. W. Blakers (2001). A review of thin-film crystalline silicon for solar cell applications. Part 1: Native substrates. *Sol. Energy Mater. Sol. Cells*, 68(2), pp. 135–171.
- [3] Q. Zhang, A. Agbossou, Z. Feng, and M. Cosnier (2010). Solar micro-energy harvesting based on thermoelectric and latent heat effects. Part II: Experimental analysis. *Sensors Actuators, A Phys.*, vol. 163 (1), pp. 277–283.
- [4] J. P. Carmo, L. M. Goncalves, and J. H. Correia (2010). Thermoelectric microconverter for energy harvesting systems. *IEEE Trans. Ind. Electron.*, 57(3), pp. 861–867.
- [5] G. Sebald, D. Guyomar and A. Agbossou (2009). On thermoelectric and pyroelectric energy harvesting. *Smart Materials and Structures*, vol.18, 125006.
- [6] B. O'Regan and M. Grätzel (1991). A low-cost, high-efficiency solar cell based on dye-sensitized colloidal TiO₂ films," *Nature*, vol. 353, no. 6346, pp. 737–740, 1991.
- [7] R. W. Whatmore (1986). Pyroelectric devices and materials. *Reports on Progress in Physics*, vol. 49 (12), pp. 1335–1386.
- [8] R. B. Olsen, D. A. Bruno, and J. M. Briscoe (1985). Pyroelectric conversion cycles. *J. Appl. Phys.*, vol. 58 (12), pp. 4709–4716.
- [9] A. Cuadras, M. Gasulla, and V. Ferrari (2010). Thermal energy harvesting through pyroelectricity. *Sensors Actuators, A Phys.*, vol. 158 (1), pp.132–139.
- [10] C. C. Hsiao, J. C. Ciou, A. S. Siao, and C. Y. Lee (2011). Temperature field analysis for pzt pyroelectric cells for thermal energy harvesting. *Sensors*, vol. 11(11), pp. 10458–10473.
- [11] C. C. Hsiao, A. S. Siao, and J. C. Ciou (2012). Improvement of pyroelectric cells for thermal energy harvesting," *Sensors*, vol. 12, (1), pp. 534–548.
- [12] C. C. Hsiao and A. S. Siao (2013). Improving pyroelectric energy harvesting using a sandblast etching technique. *Sensors (Switzerland)*, vol. 13 (9), pp. 12113–12131.
- [13] Y. He (2004). Heat Capacity, Thermal Conductivity, and Thermal Expansion of Barium Titanate-Based Ceramics. *Thermochim. Acta*, vol. 419(1-2), pp. 135–141, 2004.
- [14] S. Yarlagadda, M. H. w Chan, H. Lee, G. A. Lesieutre, D. W. Jensen, and R. S. Messer (1995). Low Temperature Thermal Conductivity, Heat Capacity, and Heat Generation of PZT. *J. Intell. Mater. Syst. Struct.*, vol. 6 (6), pp. 757– 764, 1995.
- [15] P. Mane, J. Xie, K. K. Leang, and K. Mossi (2011). Cyclic energy harvesting from pyroelectric materials. *IEEE Trans. Ultrason. Ferroelectr. Freq. Control*, vol. 58(1), pp. 10–17.

Digital Newspaper with Voice Assistant Using Alan AI

Archana Balyan¹, Deepshikha Yadav²

^{1,2}Department of ECE Maharaja Surajmal Institute of Technology, New Delhi, India
¹archanabalyan@msit.in, ²deepshikha@msit.in

Abstract: Web Development is building and maintenance of websites is a vast and ever growing field. For making front-end of any website or page, a lot of designing and planning processes are undertaken to make a seamless user interface and provide satisfying user experience. The backend of the website is where the data is stored and it uses computer programs to ensure that the server, the application and the database run smoothly together. Here, we will discuss the idea of development and implementation of digital newspaper that uses modern technologies namely, Alan Studio, News API and React. In order to allow users to have a smooth and enjoyable experience, an artificial intelligence based voice assistance is provided in this application. The assistant can take voice commands from the user and respond accordingly. This system can help blind / visually impaired people or elderly people with weak eyesight to access online facilities, specifically -daily weather forecast and online news.

Keywords: Artificial Intelligence, Voice Assistants, React, NewsAPI, Alan AI.

I. INTRODUCTION

Information can sometimes be communicated very rapidly through the newspaper. One of the finest means for individuals to converse with one another and with world at large is via the social media. Weather forecasting has many purposes in daily life, notably guiding you chose what to wear and if you should bring an umbrella to work. Textual information occurs predominantly mostly in acquisition and dissemination of knowledge. There are many people, including blind, visually impaired, and other others with a diverse range of abilities who are youngsters, adults, and individuals of all ages, who may have severe visual disabilities and limb abnormalities. If blind individuals have adequate access to mass media, they will have the opportunity to obtain new skills and information [1-3]. With this wider perspective, they will now find themselves on a more even playing field with their friends, family, workplace, and opponents. Less observable, but possibly even more crucial, is the ability of blind and differently abled citizens to participate in social concerns enabled by availability to the newspaper [4-5]. You gain power if you are given access to the newspaper. These fantastic prospects to grow and develop, however, are restricted to those who are blind.

In order to help the visually impaired and differently abled people, we propose to create a web app which is voice assistant enabled digital newspaper- “Newsosphere”, where they can give out voice commands to get the information regarding present weather, latest news and even recommendation to what all

essential things they need to carry if they are planning on going outdoors.

The distinct feature of “Newsosphere” that makes it special is that it has a voice assistant. Modern web technologies such as React JS and Alan AI are used in the development of the web app in this work.

II. TECHNOLOGY

The choice of technologies used was based on how suitable they are in the modern web development, how vast is the technology community behind it, its simplicity and implementation. This is because, having an active developer community behind a technology will assure doubt support and continuous evolution of the technology. Therefore, we chose the following technologies in our work:

- a) React JS (Developed and maintained by Facebook engineers) for the front-end.
- b) Alan AI for handling the voice commands and interaction.

2.1 React JS

It is a front-end component-based open-source library that is only in charge of the application's view layer [6]. The view layer in the Model View Controller (MVC) architecture is in charge of how the application appears and functions. The aadvantages of ReactJS are as below [7]:

- a) *Intuitive:* ReactJS provides interaction to just about any UI layout and is extremely simple to utilize. Secondly, it allows for the creation of applications and services quite well.
- b) *Declarative:* ReactJS, which prompts designated components of the interface to adapt automatically, supports relevant data alterations.
- c) *Provides Reusable Components:* The developers already have liberty to use components designed for one application in the other with related functionalities attributable to this platform. This assures seamless execution while involving least effort while development phase.

- d) *JavaScript library:* One of the operations in the JS library essentially is to integrate HTML elements into required functionalities and improves the project across the entire project.
- e) *Components Support:* ReactJS basically demonstrates the perfect fusion between HTML core elements and JavaScript. The document object model is a massive array of information that could be effectively handled through HTML elements and JS scripts.

2.2 Alan AI

Alan provides a fully server-less environment that makes it possible to create sophisticated and dependable in-app voice assistants. The majority of the work is done by the Alan AI backend when using the advanced tool known as Alan Studio to add a voice interface to a web application [8–9]. JavaScript is used to build voice scripts, which gives them a tonne of flexibility. In figure 1, AlanAI's operation is shown.

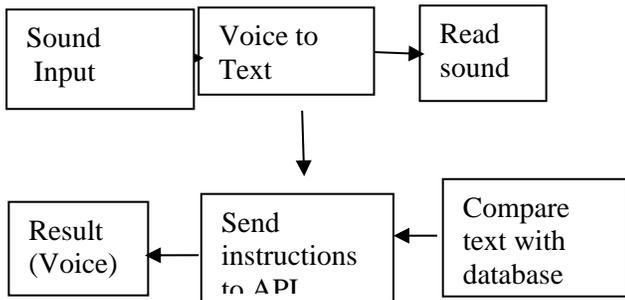


Fig. 1. Working of Alan AI

III. DIGITAL NEWSPAPER – NEWSOSPHERE : DEVELOPMENT PROCESS

Newsosphere is a web-based application built using React.JS (A frontend JavaScript library) integrated with voice assistant. The development process can be divided into following tasks i.e., (i) Start (ii) Ideation (iii) Designing/Prototyping (iv) Building (v)Refactoring (vi) Deploying (vii) Finish. The development process is discussed below.

Ideation

The idea of the Digital Newspaper (Newsosphere) is a web-based application backed with AI voice assistant which tells us weather and news based on the location of the user or according to the search input. Apart from that, user can also view the latest news or news based on certain keywords or source. All this is enveloped by an AI voice assistant, so that the user can interact with the app using voice commands. Figure 2 shows the basic user flow and interaction process for AI interface. This app can be accessed from web browser present on device of any dimensions and hence it needs to be made responsive. Not only just responsive, but we have aimed for making it a PWA (Progressive Web Application) which is easily installable and is

fast due to its data caching technique.

Prototyping and Designing

In essence, a website prototype is a high-fidelity visual representation of the site that enables you to link between screens and show how the website would function before actually building it.

The interaction map in Figure 3 shows the planned screens and how they will be connected with each other. This map helps in connecting and linking various pages of the website during the coding and building phase. The interaction map shows the various pathways that can be followed by the user. This interaction map also helps in developing an understanding of how a user might navigate through the web application.

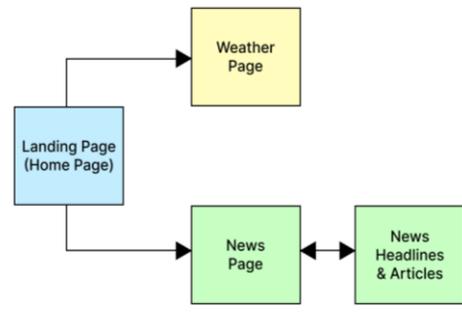


Fig. 2. Basic user flow and interaction map of the application

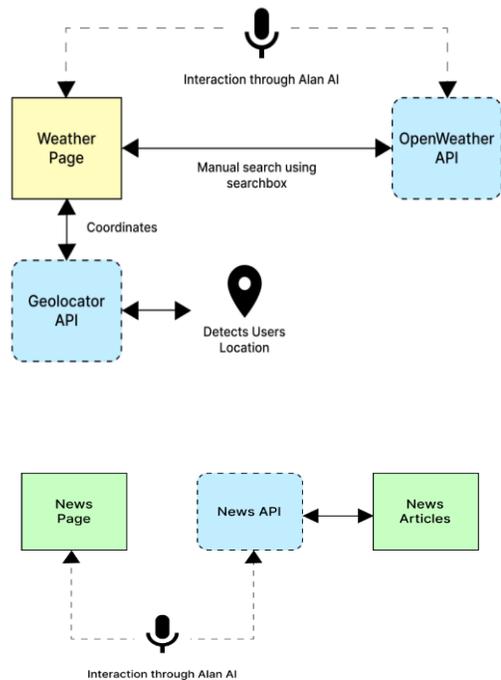


Fig. 3. Basic interaction map of the News Page

This provides further scope of studying about the user experience which is important to keep the user hooked up with the application without losing interest.

After designing the interaction map and refining it in accordance with the best user experience, it is time to build a basic **wireframes** for different screens of the website. Figure 4 shows the starter wireframe. The wire framing and prototyping tool used is Figma (figure 5). Creating the wireframes first before actually diving into the coding part allows the developers to get a prior idea about the designs and the different views.

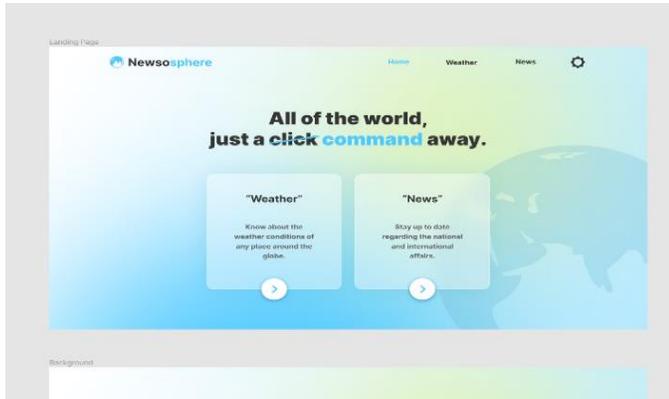


Fig. 4. Starter wireframe



Fig. 5. Prototyping using Figma

IV. BUILDING THE APPLICATION

Following the prototyping and designing process, we start towards building up the application wherein the application actually begins to take shape. Considering the interaction map, we decided that we need to build multiple screens that is one main container component which would be used to enclose the react router connecting various screens.

Using ReactJS, we created the application's front end. CSS is used for style, adding layout, and positioning (Cascading Style Sheets). CSS specifies how HTML elements should appear on screens or in other types of media. A lot of work is saved via CSS. It can manage the design of several web pages simultaneously. CSS files are used to store external style sheets.

We were able to divide the complicated application into smaller, reusable components by using react. In order to get started, we need to enter the following command into the terminal to create a folder with ready-to-use startup code for a react application:

```
$ yarn create-react-app newsosphere
```

After that change into the above created directory

```
$ cd newsosphere
```

This command will create the starter application, after opening which we will see a src directory, this is where the majority of the code will go. Inside this, we made a components directory, which will contain all the components. To keep the code clean and well organized, each component has its own folder. Some of the major components and its sub-components along with their functionalities are mentioned below:

HOME

The home component is the first stop for a new visitor, it acts as a landing page, and it sets the look and the feel of the application along with links to navigate to other pages of the app. The main sub components of the home component can be categorised as follows in table I:

TABLE I: CHILD COMPONENTS OF HOME

Component	Functionality/Purpose
Home.jsx	Parent Component
Navbar.jsx	Navigation Bar displaying the links for the login and register page
Card.jsx	A component whose main functionality is to display the content within a card
RoundButton.jsx	RoundButton Component is just a round button with a svg arrow within it. As the name suggests, it is a button

Weather

The weather component is accessed after hitting the weather route from the home component. It displays weather related data and components, such as, map of the current location, current weather, hourly and daily forecast and required things. In table II below, are the major sub-components of the weather component.

TABLE II: CHILD COMPONENTS OF WEATHER

Component	Functionality/Purpose
Weather.jsx	Parent Component
Navbar.jsx	Navigation Bar displaying the links for the home and login page
WeatherInfo.jsx	WeatherInfo component has three main functionalities. Firstly, it displays the current weather details in card. Apart from that, it also displays hourly and daily forecast.
MyMap.jsx	This component displays the map with the help of react-leaflet

RequiredItems.jsx	This component displays all the suggested items that a user should carry outside based on the weather conditions outside.
-------------------	---

News

The news component is rendered when the user hits the news route from the home or weather page. The sole purpose of this component is to initially display some cards which suggests users to give some valid voice commands. Once the user gives the voice commands to fetch the news, the components gets re-rendered with the fetched data. Table III below lists the components related to news component.

TABLE III: CHILD COMPONENTS OF NEWS

Component	Functionality/Purpose
News.jsx	Parent Component
Navbar.jsx	Navigation Bar displaying the links for the home and register page
NewsCards.jsx	This component displays the valid voice commands the user can give.
NewsCard.jsx	This component displays the individual card for news headline and the corresponding article.

Other major components

The other major components are as follows:

Connecting everything using react router

The one page application will be up and running as desired with the help of react router which allows different components to be rendered when the user hits different routes without re-rendering the entire application. Hence it is extremely fast. The app.jsx which is the main component is where the react router is defined and used.

Using APIs

As mentioned earlier, we will be collecting and extracting data from a bunch of APIs (Application Programming Interface(s)). With the help of these pre-built APIs we would then be able to send requests to resources and get responses based on that request in real time. The main APIs we are using are as follows:

- **OpenWeather API:** The OpenWeather Ltd.-owned web service OpenWeatherMap offers global weather data through API, including real-time weather information, forecasts, nowcasts, and historical weather information for every place. For any place, the firm offers a minute-by-minute hyperlocal precipitation forecast.
- **News API:** The News API is a straightforward, user-friendly REST API that offers JSON search results for

recent and old news stories published by more than 80,000 sources worldwide.

- **API Autocomplete:** When inputting a city or location name into the react search box on the weather page, this API assists in auto-completing the field.

Now to integrate the APIs in our application, we need an API key, which is used as an environment variable for security reasons. Following is an example:

Adding ALAN AI voice assistant

We can easily add a speech interface to our app thanks to Alan, an excellent voice AI platform. Instead of a team of Machine Learning and Dev Ops professionals, Alan allows a single developer to create and develop a voice experience for our app. The Alan Studio interface can be shown in Figure 6.

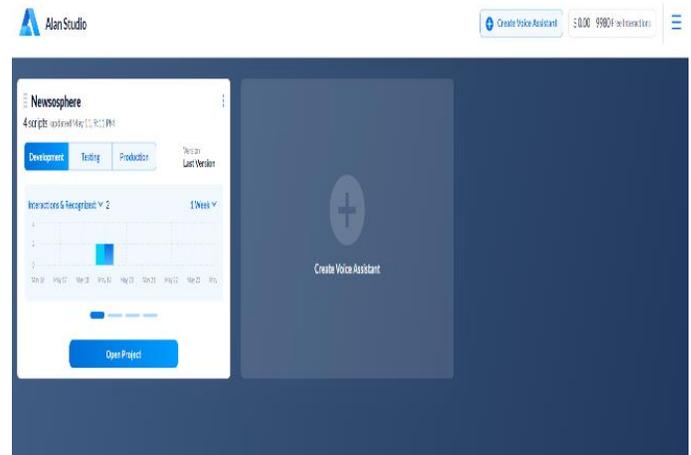


Fig. 6. Alan Studio

V. RESULTS

Figure 7 below shows the final look of the interface page for proposed digital newspaper, Newsosphere.

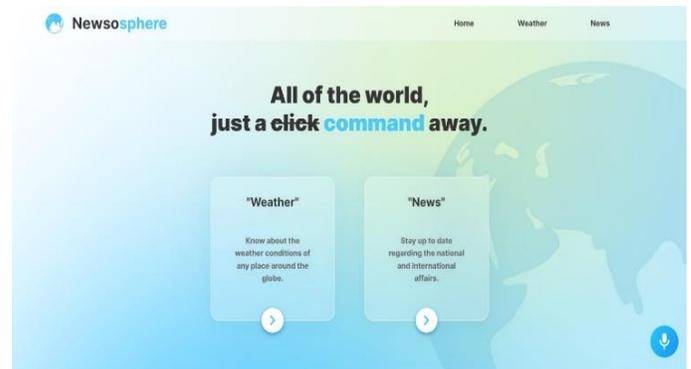


Fig. 7. Home (Landing) Page

As depicted in figures 8-13, the home page allows user to select the city and provides the daily and hourly weather forecast as well.

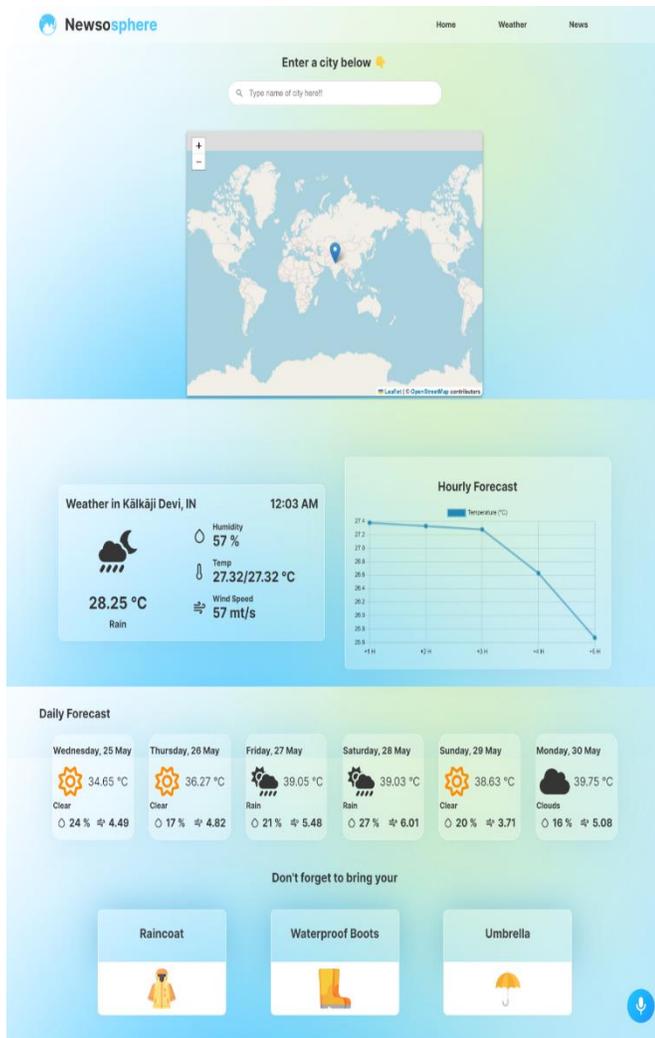


Fig. 8. Weather Page

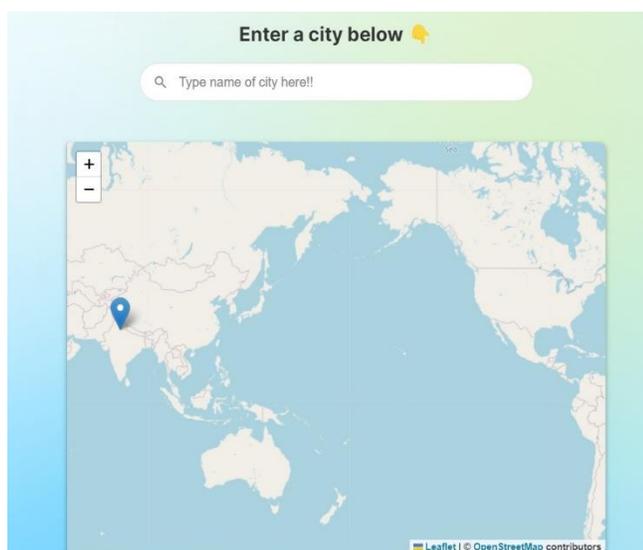


Fig. 9. Map displaying location in Weather Page



Fig. 10. Current Weather Card

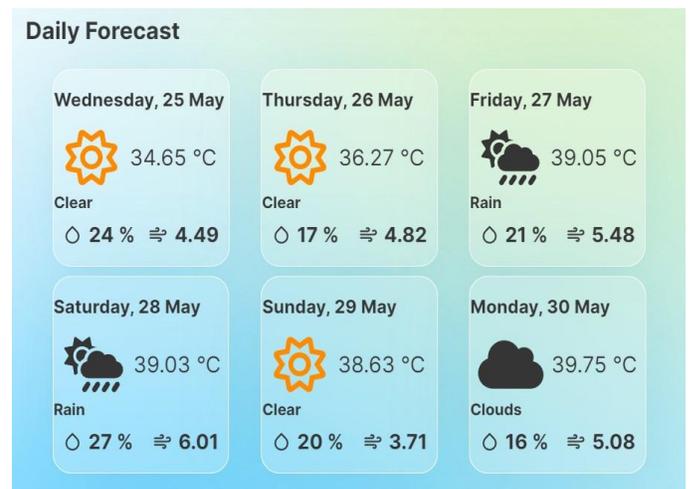


Fig. 11. Six-Day Forecast

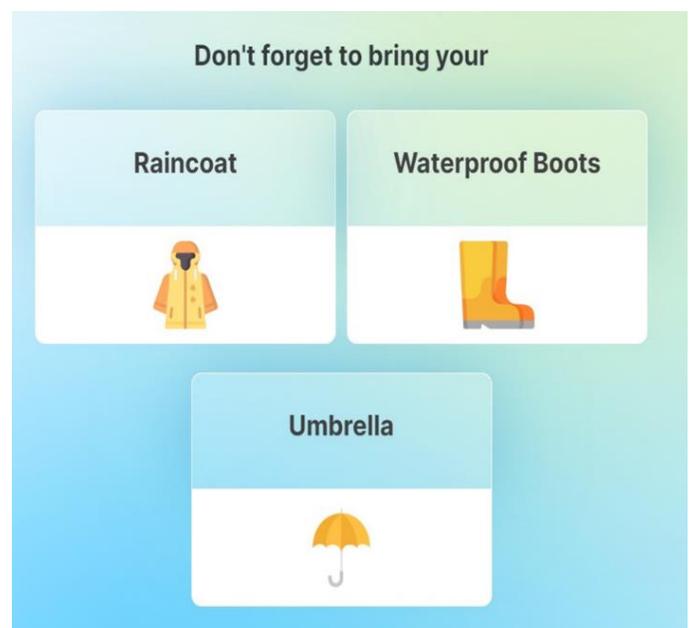


Fig. 12. Required Things



Fig. 13. Hourly Forecast in graphical format

Along with weather forecast Newsosphere also successfully displayed other related news articles as shown in figure 14 below.

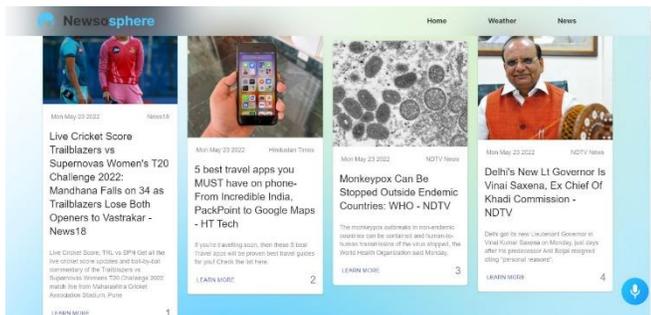


Fig. 14. News Articles

All the application code can be accessed from the online repository hosted on GitHub at: <https://github.com/Newsosphere/Newsosphere-app>

The Figma designs and wireframes along with prototypes can be viewed at: <https://www.figma.com/file/8e5yg8qBBPYLh5IDig4bS1/Newsosphere?node-id=0%3A1>

The final Netlify hosted version of the application can be viewed at: <https://newsosohere.netlify.app/>

VI. CONCLUSION

This paper examines the creation and use of a digital newspaper that makes use of contemporary tools including Alan Studio, News API, and React. The application offers voice help powered by artificial intelligence to ensure users have a seamless and engaging experience. The user can issue vocal commands to the assistant, and it will carry them out as instructed. This technique can make it easier for older persons or those who are blind or visually impaired to access internet resources, particularly the daily weather prediction and online news.

REFERENCES

- [1] A. Abdulrahmani, R. Kuber, and A. Hurst, "An empirical investigation of the situationally-induced impairments experienced by blind mobile device users," In Proceedings of the 13th Web for All Conference (W4A'16), vol. 21, pp. 1—8, 2016.
- [2] A. Abdulrahmani, R. Kuber, and S. M. Branham, "Siri talks at you: An empirical investigation of voice-activated personal assistant (VAPA) usage by individuals who are blind," In Proceedings of the 20th International ACM SIGACCESS Conference on Computers and Accessibility (ASSETS'18), pp. 249—258, 2018.
- [3] J. Albuouys-Perrois, J. Laviolle, C. Briant, and A. M. Brock, "Towards a multisensory augmented reality map for blind and low vision people: A participatory design approach," In Proceedings of the CHI Conference on Human Factors in Computing Systems (CHI'18). ACM, New York, NY, vol. 629, pp. 1—629, 2018.
- [4] L. Anthony, Y. Kim, and L. Findlater, "Analyzing user-generated YouTube videos to understand touchscreen use by people with motor impairments," In Proceedings of the SIGCHI Conference on Human Factors in Computing Systems, pp. 1223—1232, 2013.
- [5] M. Baldauf, R. Bösch, C. Frei, F. Hautle, and M. Jenny, "Exploring requirements and opportunities of conversational user interfaces for the cognitively impaired," In Proceedings of the 20th International Conference on Human-Computer Interaction with Mobile Devices and Services Adjunct, pp. 119—126, 2018.
- [6] S. Aggarwal, "Modern web-development using reactjs," International Journal of Recent Research Aspects, vol. 5(1), pp. 133-137, 2018.
- [7] M.F.S Lazuardy and D. Anggraini, "Modern Front End Web Architectures with React. Js and Next. Js," Research Journal of Advanced Engineering and Science, vol. 7(1), pp. 132-141, 2022.
- [8] S. Muggleton, "Alan Turing and the development of Artificial Intelligence," AI communications, vol. 27(1), pp. 3-10, 2014.
- [9] G.F. Luger and C. Chakrabarti, "From Alan Turing to modern AI: practical solutions and an implicit epistemic stance," AI & SOCIETY, vol. 32(3), pp. 321-338, 2017.
- [10] Z.F.F. Putra, H. Ajie, and I.A. Safitri, "Designing A User Interface and User Experience from Piring Makanku Application by Using Figma Application for Teens," IJISTECH (International Journal of Information System and Technology), vol. 5(3), pp. 308-315, 2021.

Future of Software Development Methods and Tools in A Hybrid, Post Covid World

Kirti Dahiya

*Assistant Professor, CSE MSIT
Maharaja Surajmal Institute of Technology, New Delhi, India*

Abstract: Businesses shut down and sent employees home due to the COVID-19 outbreak, resulting in a massive natural experiment. Many supervisors were worried that their engineers wouldn't be able to or wouldn't be motivated to work successfully from home, that they'd lose control, and that they wouldn't even notice when things went wrong. The subject of what is expected of software engineers who work from home is becoming more pressing as many organizations have established permanent remote-work or hybrid home/office policies in the wake of the COVID outbreak.

Agile methodology's use by businesses continues to rise. However, these businesses frequently employ a so-called hybrid development approach, which combines agile and plan-based methods. However, it is challenging for firms to establish these methods because agile and plan-based methods generally adhere to diametrically opposed ideals. Companies need to resolve the tensions between agile and plan-based techniques if they want to get the benefits of both approaches at the same time. Whether or not agile and plan-based methodologies clash is determined by the desired outcomes. However, there is no summary of the specific objectives sought after by hybrid techniques and the associated difficulties and contradictions. As a result, we decided to map out the objectives and obstacles of hybrid development strategies. The literature presenting the actual requirements and objectives of businesses and projects is the primary subject of the mapping analysis. Our findings reveal the elements that contribute to hybrid approaches' inherent tensions, and we offer solutions for dealing with them.

This study is concerned with improving how software is developed in modern Information Technology (IT) companies. The purpose of this paper is to bridge the gap between the many hybrid approaches to software development and the established practices that underpin them. Through the use of a survey questionnaire and the examination of preexisting research articles and papers on software development practices, this study aims to collect data from software professionals and gain insight into how current practices in the software development industry have contributed to the productivity of employees and the IT organization. To help IT organizations boost productivity and provide commercial value beyond customer expectations, this study proposes a conceptual model centered on a contemporary hybrid approach to software development, rather than a singular software development strategy. Software development approaches can be integrated to cut down on development costs and speed up the process of bringing a product or service to market. An organization's success in today's market can be aided by adopting the most effective software development processes, frameworks, and models for their specific values and bodies of knowledge. The overarching goal of the conceptual model is to narrow the chasm that exists between the many hybrid software development techniques and the established practices that aid in the software development process.

At the end of the article, we discuss the advantages of the hybrid approach to software development and encourage IT firms to embrace it in accordance with their own needs and those of their clients.

Keywords: Agile; Design Thinking; hybrid software development; Information technology; Application development

I. INTRODUCTION

As a result of the rapid evolution of markets, software and system developers must contend with a wide range of difficulties. To overcome these difficulties, businesses and projects have turned to hybrid development strategies that use a combination of rigorously planned, all-encompassing methods and adaptable agile practices. Despite this, there is a plethora of options, and research suggests that actual process construction is often done in ad hoc fashion. This document presents findings from a survey of hybrid methods for creating software. We investigate the prevalent methods, the ways in which they are integrated, and the contextual factors that affect the usage and mixing of hybrid approaches in software development.

We demonstrate that most mixtures adhere to a pattern wherein a classic process model acts as a framework into which other fine-grained (agile) methods are inserted. We also demonstrate that the size of the organization and external triggers have little bearing on the viability of hybrid software development methodologies. We draw the conclusion that such methods are the outcomes of a naturally occurring evolutionary process that is primarily motivated by experience, learning, and pragmatism.

Methodologies for Developing Hybrid Software. The following is what we've done in our research on hybrid approaches to software development: A hybrid approach to software development is one that takes elements from both agile and more traditional (plan-driven or rich) methods, and modifies them to fit the specific demands of the organization (e.g., application domain, culture, processes, project, organizational structure, techniques, technologies, etc.).

A. Problem Statement

Water-Scrum-Fall was first proposed in 2011 by West et al. [24] who also predicted the widespread adoption of hybrid development practices. Theocharis et al. [20] conducted a comprehensive literature search to gather evidence supporting West's assertion. As a result, they brought to light a void in the

literature: while there is a plethora of studies on agile software development, traditional techniques have been mostly overlooked in recent studies. As a result, there is a dearth of information (and evidence) on the patterns of combination and the contextual elements that lead to the development of hybrid approaches, such as how standards affect the deployment of agile methodologies or whether or not firm size and industrial sector are relevant?

B. Objective

Our study's primary objective is to fill this knowledge vacuum by collecting information that will be useful in identifying combination patterns; that is, which development approaches are really implemented and how they are combined in company- or project-specific development strategies. We also hope to determine what kinds of environmental conditions prompt the development of hybrid strategies. We also hope to learn what kind of software development issues lead to the adoption of hybrid methodologies, and whether or not these adoptions are successful.

II. LITERATURE REVIEW

Miller et al. (2021) reports on an extension of the survey work begun by Bao et al. (2020) at Microsoft. We didn't include it since the authors looked at team productivity, whereas we're interested in individual productivity. The research presents findings from a July 2020 survey measuring team productivity in addition to the second survey featured in Bao et al. Following the findings that only 20% of respondents say that WFH has had a positive impact on their team's productivity, 56% say it has had no effect, and 23% say it has had a negative impact, the new analysis provides rich insight into various aspects of communication and collaboration that explain the results.

Neto et al. (2020) conducted a survey of 279 professionals from 32 countries and found that, overall, productivity and job completion times were not affected by the pandemic. The authors' focus on negative changes or the lack thereof precludes any assessment of positive effects on respondents, hence we do not include this study in our analysis (which is important for our analysis).

Finally, Bezerra et al. (2020) rated the current productivity during the pandemic and not on changes in the state of practice of WFH in Brazilian software firms in May 2020 on a scale of bad, regular, good, and excellent. Therefore, we did not include this study in our evaluation. The authors discovered that most people felt they were productive, and that how productive they were was affected by things like outside distractions, willingness to change, and general happiness.

The use of agile techniques like incremental testing and continuous integration has made agile software development (ASD) a mainstream practice. Even though the software industry is becoming increasingly competitive, new processes and technologies are always being developed that help software

development organizations provide commercial value to their clients. When it comes to agile software development, Scrum is a popular framework [11]. Kanban, Extreme Programming, Feature Driven Development, and so on are all examples of other Agile software development paradigms. Kanban is a useful tool for visualizing and managing the progress of various implementation tasks [12]. Agile methods of software development are characterized by their ability to swiftly adjust to shifting needs and other factors. [13].

It's common practice for agile software development to employ multi-disciplinary teams. The teams have been able to work together more effectively thanks to the agile methods. Software development in Agile frameworks like Scrum occurs in iterative sprints with an emphasis on incremental delivery of the product [14]. Users' stories, or needs for a business solution, are the primary emphasis of Scrum's Product Backlog. In a sprint, these user stories contribute to a smaller increment of a business solution given to a customer [15].

Gaining efficiency is essential for finishing any task or undertaking. The composition of the team, dependency on external factors, and staff turnover are crucial parameters that affect productivity in the Agile Software development approach. When planning an agile team, it's important to think about things like team size, skill sets, team dynamics, and the amount of time each team member will have to devote to the project. [16].

Productivity can be impacted by a variety of project elements, including project limitations and development tools [17]. The duration of a project is often estimated and monitored in relation to the phases of design, development, and testing. But it's also important to think about everything that goes into finishing a project, such as consulting, training, and anything else that might be needed [18]. In order to maintain a competitive edge in the information technology market, the quality of a software product has taken center stage [19]. Effective practices in project management, systematic development, and testing techniques [20] are major contributors to the success of IT projects. In the Agile method of developing software, the process for keeping the program up to date is treated as a separate activity. [21].

The Maintenance mechanism or process of software can be simplified with the help of DevOps, a practice that bridges the gap between the Development Team and the Operations Team [22]. Both Continuous Integration (CI) and Continuous Delivery (CD) are key to DevOps' methodology (CD). With the help of DevOps, previously siloed teams may work together to create business solutions more efficiently. As a result, it can facilitate faster problem solving and less misunderstanding. [23].

DevOps makes it easier to ship software builds quickly, which is crucial in today's cutthroat business environment. There is little difficulty in combining DevOps and the Scrum

Framework. The integration process needs to run well, hence several tools are needed for that [24]. CI/CD is facilitated by tools such as GIT, Jenkins, and Maven [25]. DevOps rely heavily on log management solutions like Log4j [26] to keep track of any issues that may arise. Scrum and DevOps are two examples of Agile software development approaches that can be combined for optimal results [27]. This approach has been demonstrated to increase deployment frequency, decrease the amount of defects, and increase the number of user stories completed by a team within a sprint. For DevOps to be successful in an organization, the required infrastructure must be in place.

Companies like Google and Amazon have been able to reduce their cycle time to the minutes with the help of DevOps [28]. Since frequent software releases are a standard practice on the Cloud, DevOps approaches have found a natural home there. Measuring the results of software development processes is crucial for modern-day iterative improvement. Mean Time to Repair (MTTR) and similar metrics can assist a company see how much progress it has made in terms of reducing repair times[29].

The importance of DevOps' security measures has been recognized in recent years. DevSecOps is the term for this methodology. The primary objective is to prioritize security at the solution design phase and throughout the whole development process. In the beginning stages, security needs to be prioritized. During solution development, making ensuring all security concerns are addressed can be expensive. A business must also make sure that non-functional requirements are secure. Focusing on security concerns related to non-functional needs early on in the solution development process is what's known as "shifting security left".

DevSecOps was created so that different departments, such as development, security, and operations, could stop working in isolation from one another. DevSecOps processes can benefit from the use of source code quality management tools like Sonar Cube. A DevSecOps approach is the creation of automation test scripts that can verify the security features of a business solution. In order to avoid spending a ton of money patching security holes later on, it's important to minimize those holes throughout the design phase [30]. Innovations in both methodology and tools are constantly being developed. Micro services is another emerging pattern; it's an architectural approach that emphasizes creating a service (a collection of software capabilities) that caters to a specific business process. For constantly updated software systems, the advantages of microservices have been demonstrated. The cloud-based software system has also benefited from this design.

Exciting new avenues for software creation are made possible by the plethora of ideas and developments made possible by DevOps and Micro services. Since the fundamental principles of frequent deployment are present in DevOps practice and employed for providing Micro services, this method can be

highly beneficial to a business. It's not uncommon for software solutions to be intricate, requiring integration with a wide variety of other systems and services. When done correctly, an enterprise architecture (EA) can assist a company more effectively manage its IT solutions and aid in its efforts to modernize its business operations. The enterprise architecture of a company should help it develop its strategy, guarantee that all of its initiatives and programs work together, and realize its long-term goals.

EA artifacts can help a company decide where to invest in IT and gain important strategic insights. EA is a very important link between IT and business for a company. The more experienced an organization is at using EA, the more it can get out of it and make good use of its IT investments. EA can help an organization streamline its business processes, use its IT infrastructure well, integrate its business units well, and speed up the delivery of software solutions. EA is very important when it comes to IT Governance.

Organizations can benefit from the combination of IT Governance and EA in their pursuit of their many enterprise-wide objectives. Microservices are becoming important because of their ability to speed up a company's digital transformation; they also aid with gap analysis, the identification of old systems, and the improvement of software solutions. Due to the ever-changing nature of both technology and project needs, it is becoming increasingly vital to carefully consider the software development processes and practices that will be used to create today's business solutions. Companies frequently employ a number of different approaches within a single project. Combining methods in this way is what's known as a "hybrid approach" in the field of software development.

Other considerations in selecting a hybrid methodology include the project's criticality and available resources (high, medium, or low). To some extent, a company's familiarity with different types of IT projects and the breadth of its team members' professional experiences in the IT business are also factors in the decision to use a hybrid strategy. Reasons for opting for a hybrid approach to software development include the need to work within existing business, organizational, and customer restrictions while simultaneously increasing the agility of operations and adapting current processes. The adoption of a hybrid strategy is a result of its inherent strengths as both traditional and modern approaches. The hybrid approach to software development is gaining traction in the IT sector because it helps organizations better balance the needs of their many stakeholder groups.

Design Thinking (DT) is a methodology for identifying problems, establishing customer empathy, defining insights, generating creative ideas, prototyping those solutions, and testing them with actual customers. This method can be repeated as needed. With design thinking, the focus is on the people who will be using the solution. From the customer's perspective, businesses can better identify problems and develop prototype

solutions. Integrating Design thinking with agile software development approaches can help businesses better comprehend issues and create workable solutions. The iterative and adaptable nature of design thinking makes it a natural fit for agile frameworks like Scrum and extreme programming.

A company's digital transformation can also benefit from the application of design thinking in tandem with agile software development practices. Since it can improve the efficiency with which needs are gathered from a customer, design thinking is a useful tool for the requirements collecting phase of agile processes. The benefits of the design thinking approach are not confined to the requirements collecting and design phase of a software project; rather, they can be extended to cover the entirety of the software lifecycle with the help of Agile-based software development methods. Current methods of software development should not be abandoned in favor of design thinking. Instead, it's a method that, when combined with standard software engineering processes, may help a company gain an edge in the marketplace by producing customer-focused, perception-driven business solutions.

III. HYBRID SOFTWARE DEVELOPMENT METHOD

Researchers have indicated that large and complicated projects can also benefit from adequately designed agile development methods [8, 10, 20, 21], despite the fact that agile methods have primarily been used in relatively small-scale and basic projects as described in the introduction. Combining the Scrum approach with the RUP approach is one way to address this problem. Scrum is flexible enough to work with projects of any size [31], and RUP can be easily streamlined [2]. In Figure 1 is shown a proposed hybrid model.

TABLE 1. Disciplines of Hybrid Model and RUP

Hybrid	RUP
Business Modeling	Business Modeling
Analysis & Design	Requirements
Implement	Analysis & Design
Testing	Implement
Deployment	Testing
Configuration	Deployment
	Configuration & Change Management
	Project Management
	Environment

The new approach is broken down into its four primary phases and disciplines, as indicated in Figure 1. In order to simplify the procedure, the nine RUP principles have been condensed into seven disciplines. All seven fields can be used throughout all stages, however only the most important ones are shown in Figure 1. During the brainstorming stage, business modeling is crucial. The elaboration phase makes heavy use of analysis and design. The disciplines of implementation and testing center on the building stage, while those of deployment and configuration are concerned with the ensuing stage of change. The nine

original RUP disciplines are shown with the seven hybrid model disciplines in Table 1.

Scrum's ceremonies (the Daily Scrum meeting and the Sprint meeting), roles (the Scrum Master, the development team, and the product owner), and artifacts (the product backlog, the sprint backlog, and the burndown chart) may be seamlessly integrated into an RUP's iterative development process. At any point during the RUP process, you can hold a daily Scrum meeting, a daily Scrum of Scrums meeting, a Sprint planning meeting, and a Sprint review meeting. As part of the business modeling process, the product owner might develop the product log. The SM is free to take on any of the standard Scrum roles. The daily Scrum meeting and the Sprint meeting are where the tasks defined in the product backlog and the Sprint backlog are worked on and tracked.

Phase diagram of a typical hybrid model is shown in Figure 2. The product backlog and Burndown chart are displayed in Figure 2's leftmost column. These Scrum artifacts are available for use by several Sprints, as shown at the top of each column. There are two meetings per Sprint, the planning meeting and the review meeting. Each of the seven RUP disciplines can be tracked in the daily Scrum meeting. The seven RUP disciplines are utilized in different ways depending on where a project is in its lifecycle. In the genesis phase, the business modeling discipline may receive more attention than the others during the first Sprint. However, the analysis/design and implementation/testing processes may play a larger role in the second and third Sprint. For example, in Figure 2, a typical phase includes several Sprints, but depending on the scope of the project, a single phase may only include one or two Sprints. The four main steps of RUP are maintained in our hybrid approach, as indicated in Figures 1 and 2. This allows us to deliver a simple, methodical, and structured process. However, because Scrum is so flexible, the hybrid approach sacrifices some of the predictability, stability, and high assurance of RUP. Another benefit of the hybrid approach is that it can adapt to ever-shifting business needs. With the hybrid approach's increased flexibility comes the hope of fewer instances of going over budget or falling behind schedule. Scrum's rituals, roles, and artifacts can provide management and tracking methods, while RUP's four primary phases and seven disciplines can serve as a method platform in the new hybrid model/approach.

A Hybrid Software Development Method for Large-Scale Projects

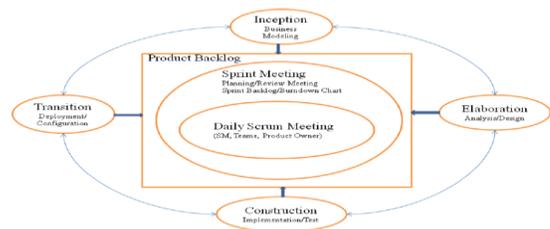


Fig. 1. A Hybrid Model

	Sprint 1	Sprint 2	...	Sprint n
Product Backlog - Breakdown Chart	Sprint Planning Meeting (Sprint Backlog)	Sprint Planning Meeting (Sprint Backlog)	...	Sprint Planning Meeting (Sprint Backlog)
	Daily Scrum Meeting	Daily Scrum Meeting	...	Daily Scrum Meeting
	Business Modeling	Business Modeling	...	Business Modeling
	Analysis/Design	Analysis/Design	...	Analysis/Design
	Implementation/Testing	Implementation/Testing	...	Implementation/Testing
	Deployment/Configuration	Deployment/Configuration	...	Deployment/Configuration
	Sprint Review Meeting	Sprint Review Meeting	...	Sprint Review Meeting

Fig. 2 A Typical Phase of Hybrid Model

IV. METHODOLOGY

The importance and influence of the numerous practices, approaches on the agile software development methodology were better understood after reviewing the relevant research papers and publications. The results of hybrid approaches to software development were evaluated using both qualitative and quantitative measures. To quantitatively test the hypothesis "Organization's comfort level to adopt and employ hybrid - a hybrid approach affects its production," a t-test was conducted with independent samples. Questionnaires were used to collect data for both quantitative and qualitative studies. We used Google Forms to distribute the survey to IT experts in the field. An online survey link was sent over various social media. This discussion centered on the experts who have implemented the Agile Software Development methodology in their companies. Questions in the questionnaire covered a wide range of topics, such as job titles and types of projects undertaken by respondents. Agile methods, DevOps, DevSecOps, Enterprise Architecture, and Design thinking were all discussed, with an emphasis on their practicality, effectiveness, and public image. Participants were also questioned about the ways in which their organizations encourage the adoption of new technologies and the maintenance of high quality standards. In addition to answering questions on their experience with agile software development and DevOps, participants were asked to detail the frameworks used by their firm. The questionnaire was also used to account for respondents' perceptions of the ease with which they could learn about the productivity gain associated with hybrid software development, as well as the factors that would prompt the adoption of such a strategy. Using the Five-Point Likert Scale, criteria were established for evaluating the participants' thoughts on using various technological methods. "The scale created is as follows: Strongly Disagree (1), Disagree (2), Neutral (3), Agree (4), Strongly Agree (5). Also, utilizing Design Thinking was rated on a scale of Five: Never (1), Occasionally (2), Sometimes (3), Often (4), Always (5)".

V. RESULTS AND DISCUSSION

Assessing the impact of hybrid approaches on productivity:

A) The benefits of combining DevOps and Agile in

project management: The majority of our respondents (70.37%) said that combining DevOps and Agile techniques was beneficial to their projects. Organizations can reap the benefits of this hybrid strategy with proper training and the development of proof of concept sample projects. The improved productivity of a project as a result of a combined DevOps and Agile methodology is represented in Figure 3.

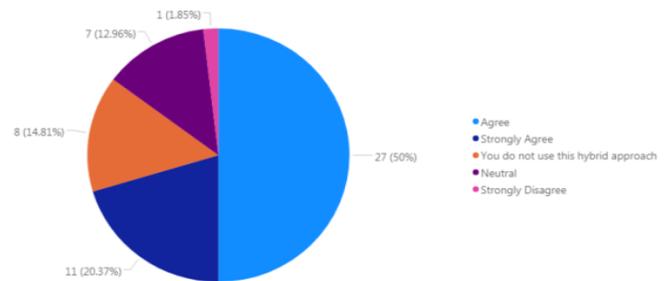


Fig. 3. Assessing Project's productivity improvement from using a hybrid approach of DevOps and Agile Methodology

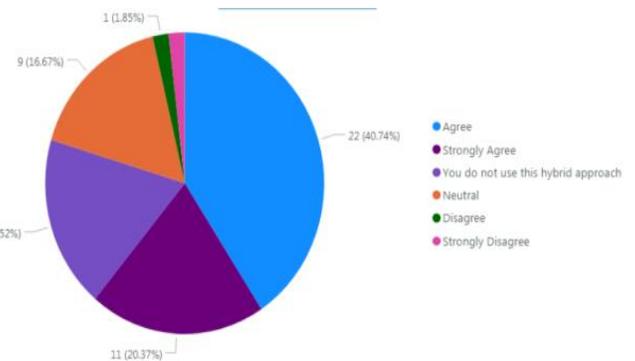


Fig. 4. Assessing Project's productivity improvement from using a hybrid approach of Design Thinking and Agile Methodology

B) Evaluation of the Combined Effects of Design Thinking and Agile Methodology on Project Efficiency: The majority of our respondents (61.11%) felt that combining Design Thinking with Agile has increased their project's efficiency. It's likely that the value of Design Thinking could be enhanced with formal training in the method. In addition to time and money constraints, other factors can play a role in deciding whether or not to use this hybrid technique. In Figure 4, we can see how the Assessing Project benefited from a combination of Design Thinking and Agile Methodology and how much more productive it became as a result.

VI. SUGGESTION

Over the years, software teams have gradually become more dispersed as technology advancements facilitated hybrid work and allowed teams to collaborate, create and innovate remotely. However, this trend accelerated and became more of a mainstream norm over the last two years during the COVID-19

pandemic, requiring newly dispersed teams to develop a more streamlined hybrid approach to the development process.

When seeking to implement a hybrid environment, it's important for development leaders to consider how best to coordinate a distributed workforce across time zones, how to track projects effectively and ensure accountability. To be effective in a hybrid environment, we adopted certain processes and tools that facilitated open communication and cross-collaboration no matter the location. After evaluating various hybrid methods, here are five best practices that stand out.

A. *Adapt the development process to suit a hybrid setting*

Estimating work, refining issues, and planning sprints can be difficult to do in a consistent manner in a mixed work setting. Due to the time-sensitive nature of many software projects, it is often a waste of time to try to coordinate schedules across numerous time zones and a number of different calendar systems. Moreover, many developers are highly creative and want fewer coordinated meetings and more time to contribute when they want, at their own pace.

To navigate these challenges, program managers can adapt the development process to be less regimented and more flexible. Asynchronously coordinating team activities like estimating, sprint planning, and backlog refinement in a digital workspace can help remote workers feel included, make their voices heard, and receive constructive criticism from colleagues. Such programs can also enable an automatic way to log decisions and house required software documentation.

B. *Establish a single source (or tool) of truth*

The problem of having project data in different applications is one that many businesses can relate to. Misalignment can arise in a hybrid setting when the development team uses one set of tools to monitor day-to-day operations while other stakeholders use an altogether separate set of tools to monitor goals and team key performance indicators.

To address this issue, development teams can implement a centralized repository for past, present, and future projects that can be accessed by all members of the team for reference and collaboration. Managers of both the development and the program management teams can benefit from this tool's ability to serve as a centralized hub of information and so increase both teams' visibility and alignment.

C. *Enable full transparency in decision making*

Our team at Lenovo follows a strict process of documenting the decisions taken throughout the development process and we make that documentation available for all team members to access within the team workspace.

This can be a beneficial practice for project managers that want to strengthen accountability. Encouraging such transparency enables team members and stakeholders to reference the

reasoning behind a specific decision, especially if concerns arise later in the project life cycle process. The result is better alignment across the organization.

D. *Establish a facilitator for each ritual*

To maintain a healthy hybrid environment, assigning an owner to each Agile event can make all the difference. By serving as a facilitator, that owner would then be responsible for aligning everyone to a pre-meeting agenda and goal, allowing teams to prepare and review issues and tickets ahead of time. This added organizational step can result in a more streamlined meeting cadence and more productive discussions.

E. *Automate and leverage efficient tools*

Finding the right combination of tools to support a team's specific collaboration needs is imperative to a successful hybrid development environment. Seamless and automated collaboration is the key, but there is no one-size-fits-all solution mix. Development leaders should consider tailoring their portfolio of tools around specific needs and look for programs that can help keep a dispersed team on track and synchronized (via direct messaging, ongoing team conversation chats or face-to-face virtual meetings, for example), as well as those that can ensure visibility and improve efficiencies. Whatever external programs are selected, however, should be hosted internally behind the company firewall and VPN for added security.

The modern workplace has changed dramatically in the last two years—in many ways permanently—with flexible, remote and hybrid work driving the greatest transformation of collaboration for software development teams across all sectors. By adapting to new hybrid development strategies, enabling transparency in decision-making and leveraging automation for greater efficiency, the development teams of today and tomorrow will be well equipped to more easily adapt to future disruptions in the workplace.

VII. CONCLUSION

The results of the study demonstrated that hybrid methods to software development can boost productivity. Business vision and goals can only be realized if an organization is able to comfortably adopt hybrid software development approaches, which in turn requires a continually evolving set of business processes and technology. Leveraging an organization's current software development methods is the goal of the conceptual framework, which incorporates the benefits of Agile software development methodology, DevOps, DevSecOps, Enterprise Architecture, and Design thinking. The power of the hybrid approach can help businesses since it allows for more adaptability in business operations and guarantees success and customer satisfaction in the final business solution. In order to meet the needs of their clients, businesses, and employees, IT departments are being asked to use hybrid software development strategies.

REFERENCES

- [1] Allshuqayran, N., Alli, N., & Evans, R. (2016). In microservice architecture, a systematic mapping study was conducted. *Proceedings - 2016 IEEE 9th International Conference on Service-Oriented Computing and Applications, SOCA 2016*, 44–51. <https://doi.org/10.1109/SOCA.2016.155>
- [2] Armmour, F. J., & Kaaisler, S. H. (2001). Transition and deployment of enterprise architecture in an agile manner. *IT Professional*, 3(6), 31–36. <https://doi.org/10.1109/6294.9777769>
- [3] Advanced Development Methods, Inc. (2007). Scrum, Retrieved March 19, 2008, from <http://www.controlchaos.com>.
- [4] Ambler, S. (2005). A manager's introduction to the Rational Unified Process (RUP). Retrieved Feb 20, 2009, from <http://www.ambysoft.com/downloads/managersIntroToRUP.pdf>
- [5] Bohh, W. F., & Yeellin, D. (2006). Managing information infrastructure using enterprise architecture principles. *Journal of Management Information Systems*, 24(3), 161–207. <https://doi.org/10.2753/MIS0742-12222303307>
- [6] Carter, K. (2017). Farancois Raynaud on DsevSecOps. *IEEE Software*, 33(5), 92–96. <https://doi.org/10.1109/MS.2017.32571578>
- [7] Cesaar, J., & Reusso, R. D. F. S. M. (2018). ScienceDirect is a website dedicated to science. *Design Thinking in Agile Software Development: A Systematic Literature Review Design Thinking in Agile Software Development: A Systematic Literature Review. Procedia Computer Science*, 138, 775–782. <https://doi.org/10.1016/j.procs.2018.10.1001>
- [8] Coohen, D., Lindvall, M., & Cossta, P. (2004). Introduction to Agile Method. *Advances in Computers*, 62(C), 1–66. [https://doi.org/10.1016/S0065-2458\(03\)62001-2](https://doi.org/10.1016/S0065-2458(03)62001-2)
- [9] Diaz, J., Peerez, J. E., M. A., Meena, G. A., & Yagaue, A. (2019). Self-Service Cybersecurity Monitorings as Enabler for DeevSecOps. *IEEE Access*, 7, 100283–100295. <https://doi.org/10.1109/access.2019.29300000>
- [10] Dingssøyr, T., Nerrur, S., Ballijepally, V., & Moe, N. B. (2012). Towards describing agile software development after a decade of agile methodologies. *Journal of Systems and Software*, 85(6), 1213–1221. <https://doi.org/10.1016/j.jss.2012.02.0033>
- [11] Doobrigkeit, F., & Dea Paaula, D. (2019). Understanding the manifestations of design thinking in software engineering is essential to understanding design thinking in practice. *ESEC/FSE 2019 - Proceedings of the 2019 27th ACM Joint Meeting European Software Engineering Conference and Symposium on the Foundations of Software Engineering*, 1059–1069. <https://doi.org/10.1145/3338906.33400451>
- [12] Dooležel, M. (2018). Potential applications of institutional theory to the study of hybrid software development principles and practices. *Lecture Notes in Computer Science (Including Subseries Lecture Notes in Artificial Intelligence and Lecture Notes in Bioinformatics)*, 11271 LNCS, 441–448. https://doi.org/10.1007/978-3-030-03673-7_35
- [13] Dummitriu, D., & Poopescu, M. A. (2020). IT Management Enterprise Architecture Framework Design In IT management, Enterprise Architecture Framework Design is a must. *Procedia Manufacturing*, 46, 932–940. <https://doi.org/10.1016/j.promfg.2020.05.011>
- [14] Ebbert, C., Galardo, G., Herenantes, J., & Serrano, N. (2016). DevOps. *IEEE Software*, 33(34), 944–1000. <https://doi.org/10.1109/MS.2016.688>
- [15] Häger, F., Kowaark, T., Krügser, J., Vedterli, C., Übefnickel, F., & Uflaacker, M. (2015). DT@Scrum: Integrating Design Thinking with Software Development Process. In *Design Thinking Research: Building Innovators (Vol. 2, Issue 2, pp. 263–289)*. https://doi.org/10.1007/978-3-3109-06823-7_014
- [16] Hidalgo, E. S. (2019). Adapting the scrum frameworks for agile projects and management system in science : a case study of a distributed research initiative. *Heliyon*, July 2018, e01447.
- [17] Jaabbari, R., Alli, N., & Peetersen, K. (2016). What is DevOps? A Systematic Mapping Study on Definition and Practice. *ACM XP '16 Workshops: Proceedings of the Scientific Workshop Proceedings of XP2016*. <https://doi.org/https://doi.org/10.1145/2962695.2962707>
- [18] Kuhhrmann, M., Diebold, P., Muinch, J., Teell, P., Garorusi, V., Feldderer, M., Trektser, K., McCaffery, F., Linssen, O., Hanser, E., & Prause, C. R. (2017). Hybrid software system development: Waterfall, Scrum, and beyond. *ACM International Conference Proceeding Series, Part F1287*, 30–39. <https://doi.org/10.1145/3084100.3084104>
- [19] Kuhhrmann, M., Diebold, P., Munvch, J., Tesll, P., Trektser, K., MewCaffery, F., Gwarousi, V., Feelderer, M., Leinssen, O., Haanser, E., & Prrause, C. R. (2019). Hybrid Software Development Approach in Practice: A European Perspective. *IEEE Software*, 36(4), 20–31. <https://doi.org/10.1109/MS.2018.1210161245>
- [20] Kuhrmanen, M., & Fwernandez, D. M. (2015). Systematic Software Development: A State of the Practice Report from Germany. *Proceeding - 2015 IEEE 10th International Conference on Global Software Engineering, ICGSE 2015*, 51–60. <https://doi.org/10.1109/ICGSE.2015.11>
- [21] Lee, J. S. (2018). The DevOps and Agency Theory and revolution. *Proceedings - 29th IEEE International Symposium on Software Reliability Engineering Workshops, ISSREW 2018*, 243–244. <https://doi.org/10.1109/ISSREW.2018.00013>
- [22] Lindberg, T., Köoppen, E., Rauuth, I., & Meeinel, C. (2012). On the Perception, Adoption, and providing of Thinking in the IT Industry. In *Design Thinking Research (pp. 229–240)*. Springer Berlin Heidelberg. https://doi.org/10.1007/978-3-642-21643-5_13
- [23] Luccena, P., Brasz, A., Cheicoria, A., & Tizezei, L. (2017). IBM's software development platform for design thinking. *Communications in Computer and Information Science*, 680, 98–109. https://doi.org/10.1007/978-3-319-55907-0_9
- [24] Papadopoulos, G. (2015). Traditional Software Development Methodologies to Agile Software Development Methodologies On large, distributed projects, as well. *Procedia - Social and Behavioral Sciences*, 175, 455–463. <https://doi.org/10.1016/j.sbspro.2015.01.12233>
- [25] Praddhan, S., Nannaiyur, V., Mellanahalli, P., Pallaa, M., & Chullani, S. (2019). A Case Study of Quality Metrics for Hybrid Software Development Organizations. *Proceedings - Companion of the 19th IEEE International Conference on Software Quality, Reliability and Security, QRS-C 2019*, 505–506. <https://doi.org/10.1109/QRS-C.2019.00097>
- [26] Sammarawickrama, S. S., & Perrera, I. (2017). Continuous Scrum is a method for incorporating DevOps into Scrum. *17th International Conference on Advances in ICT for Emerging Regions, ICTer 2017 - Proceedings*, 2018-Janua, 18–25. <https://doi.org/10.1109/ICTER.2017.82578808>
- [27] Shoukoourian, A., & Daneilyan, E. (2011). How to Measure “ Soft ” Things ? 2011 7th Central and Eastern European Software Engineering Conference (CEE-SECR), 7–10. <https://doi.org/10.1109/CEE-SECR.2011.61888466>
- [28] Terrán, C., Torrees, J., & Flores, P. (2018). Under an Agile Methodological Approach, a Productivity Model for Software Development Factories is developed. *Proceedings - 2017 International Conference on Computational Science and Computational Intelligence, CSCI 2017*, 1039–1042. <https://doi.org/10.1109/CSCI.2017.1880>
- [29] van dene Besrg, M., Sllot, R., van Stenbergen, M., Faase, P., & van aVliet, H. (2019). How does enterprise architecture help you make better IT investment decisions?. *Journal of Systems and Software*, 152, 134–150. <https://doi.org/10.1016/j.jss.2019.02.053>
- [30] Vijayassarathy, L. R., & Buttler, C. W. (2016). Can Organizational, Project, and Team Characteristics Influence Software Development Methodologies? *IEEE Software*, 33(5), 86–94. <https://doi.org/10.1109/MS.2015.26>
- [31] Watson, R. T., Kelly, G., Galliers, D., & Brancheau, C. (1997). Key issues in informationsystems management: An internationalperspective. *Journal of Management InformationSystems*, 13(4), 91-115.
- [32] Williams, L. & Cockburn, A. (2003, June). Agilesoftware development: It's about feedback andchange. *IEEE Computer*, 36(6), 39-43.

Designing of Photovoltaic MPP System with MATLAB Simulation

Monu Malik

Department of Electrical Engineering
Maharaja Surajmal Institute of Technology
msmalikmonu@msit.in

Abstract: This paper presents the determination of unknown parameters from the given parameters of a solar panel data sheet by using the iterative method i.e. Newton-Raphson method. The values obtained from the above are used to calculate the voltage-current and voltage-power characteristics of a solar panel at different radiation and temperature conditions. The maximum power point tracking (MPPT) operation and control is developed. The Matlab/simulink set-up of PV-module gives power and the power output of module is fed to the load through a dc-dc boost converter to track the maximum power output. The Matlab/simulink arrangement of Incremental conductance algorithm is responsible for driving the dc-dc boost converter to track maximum power point (MPP). In this paper the MPP tracking is made for

- A battery charging of 24 volts with varying radiation and temperature conditions.
- A battery charging along with a dc load of 10 watts at standard temperature and radiation conditions (STC).
- A battery discharging along with a dc load of 40 watts at standard radiation and temperature conditions (STC).

I. INTRODUCTION

A solar cell is a device that converts sunlight into direct current using the photovoltaic effect. The photovoltaic (PV) cells available in the commercial market are classified into two categories: (i) In crystalline silicon cells like Mono crystalline and multi-crystalline are the available technologies

(ii) In thin film cells as amorphous silicon, Cadmium- Telluride, Copper-indium-gallium-arsenide (CIGS), Gallium- arsenide (GaAs) etc are the available technologies. In the past the prices of PV modules were the major contribution to the cost of the total system. A downward tendency is now seen in the price for the PV modules due to a massive increase in the production of PV-modules. Considering the cost and efficiency of the total system it's always desirable to operate the system at its maximum power output. The maximum power output tracking is basically divided into two ways:

- Mechanical tracking.
- Electrical tracking.

1) *Mechanical Tracking:* In the mechanical tracking, the PV systems are driven by stepper motors, which are controlled in order to ensure the optimal positioning of the panel relatively

to the sun position on the sky dome. As the position of the sun changes throughout the day, the PV system must be adjusted so that it always aimed precisely at the sun and as a result produces maximum possible power [1,2,3]. Observing the geometrical relation between the sun and earth, the following two motions can be considered.

- Earth describes a rotational motion on elliptical trajectory around the sun in a year, which generates the seasons.
- Earth also has a daily motion around its own axis that is responsible for the succession of days and nights.

Single axis tracking system is responsible for moving the receiver surface from east to west in a day. The dual axis solar trackers combine above two motions, so that they can follow precisely the sun trajectory along the whole year.

In actuating system there are two types of solar trackers:

- Passive-trackers: Based on thermo sensitive fluids that adjust the position of the receiver along with the sun position.
- Active-trackers: Consists of linkages, gear mechanisms, chain or belt transmissions which are driven by controlled motor and actuators.

2) *Electrical Tracking:* The voltage-current and voltage-power characteristics of the solar panel changes with change in solar radiation and temperature conditions. In un-control mode, the power output of the panel will depend on the load characteristics which are not desirable. The panel should supply the maximum power available on any particular radiation and temperature to the load side irrespective of the load. This type of panel control is called electrical tracking and gives the maximum efficiency. This is achieved by maximum power point tracking. Different electrical MPP tracking algorithms are available to track the maximum power point operation [4,5]. These algorithms should operate close to MPP when it is subjected to changing in environmental conditions to provide high conversion efficiency.

This paper presents the development of the mathematical model of a PV array by using Matlab/simulink and the power output from the PV array is fed to the boost converter and to the load. A Matlab/simulink arrangement of Incremental conductance

algorithm is prepared for MPPT and is responsible for tracking the maximum power output from the given panel at different temperature and radiation conditions as well as for different loading conditions.

The characteristics are exactly matching with the given panel parameter values.

TABLE 1: Comparison of graphical values with the panel-data sheet values.

Given parameters	Panel data at STC	Calculated graphical values	Calculated unknown parameters of PV by Newton-Raphson method are R_s , R_{sh} , A used for Matlab program & graphs are plotted. Graphical results are identical to the panel data at STC
V_{mpp}	17 volts	17volts fig(2)	
I_{mpp}	2.05 amps	2.05amps fig(2)	
P_{mpp}	35 watts	35 watts fig(5)	
V_{oc}	21 volts	21 volts fig(2)	
I_{sc}	2.25amps	2.25 amps(2)	

II. PV PANEL WITHOUT MPP TRACKING

The Matlab/Simulink arrangement is as shown in figure-8 to represent the PV panel without MPP. This panel of Matlab is considered for two case studies with 10 watts dc load and 40 watts dc load. The characteristic diagrams of 10 watts are simulated in figure-9 for current and figure-10 for voltage respectively. The characteristic diagrams of 40 watts are simulated in figure-11 for current and figure-12 for voltage respectively[9].

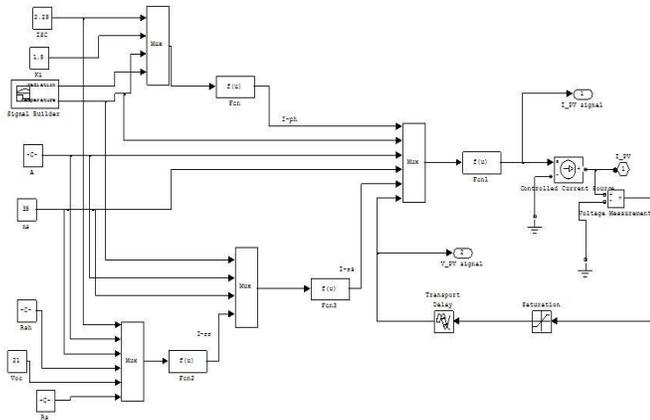


Fig. 8. Matlab/Simulink setup of PV array.

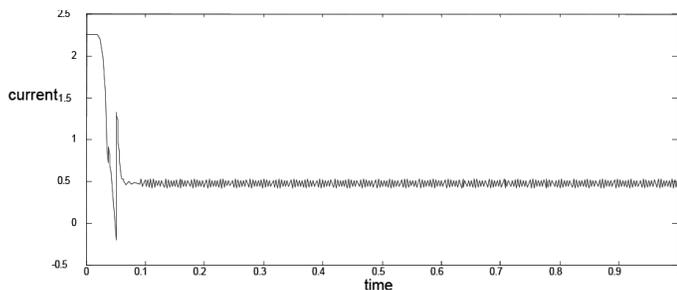


Fig. 9. Current output of a PV array for 10 watts dc load without MPPT.

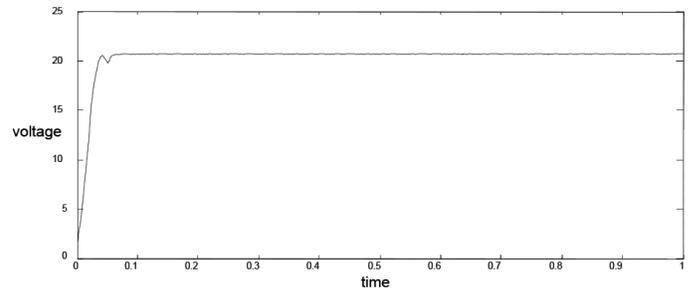


Fig. 10. Voltage output of a PV array for 10 watts dc load without MPPT

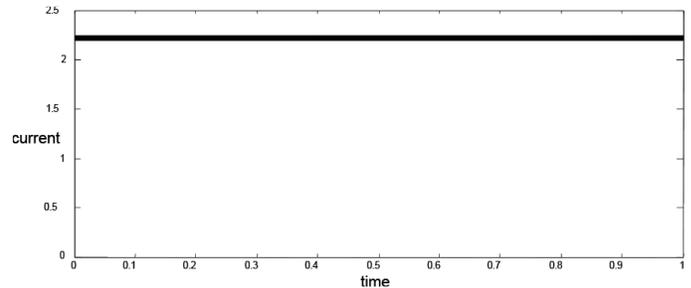


Fig. 11. The current output of a PV array for 40 watts dc load without MPPT.

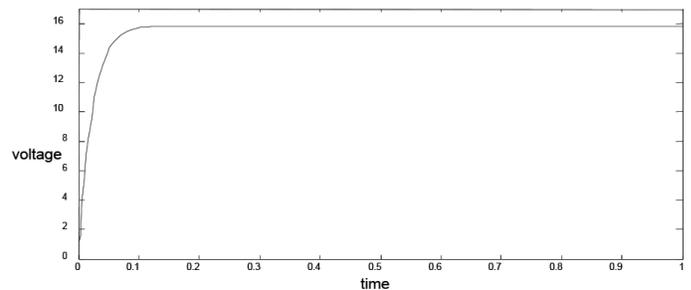


Fig. 12. The voltage output of a PV array for 40 watts dc load without MPPT.

A. Observation of panel on under-load and over-load:

It is observed in graphically that: (i) the power output= 20 volts * 0.5 amperes=10 watts. Therefore 35 watts (STC)-10watts=25watts of panel power is wasting without any use due to lower load is proved graphically.

Similarly it is observed in graphically that: (ii) the power output = 15.9 volts*2.15ampers=34.1 watts. Therefore for a 35 watts panel at STC cannot supply more than 35 watts panel value and the output is decreases as the load is increases from the panel value. Thus the output characteristics of the PV panel are dependent on load characteristics and situations. This is not desirable for maximum power tracking.

III. DESIGN OF MPP TRACKING WITH INCREMENTAL CONDUCTANCE ALGORITHM

The power output characteristics of the solar panel changes with (i) solar radiation, (ii) temperature conditions and (iii) load

characteristics. In this case for any load characteristics maximum power tracking desires. As seen from the power-voltage characteristics figure-5 of the panel there exists a single maximum point for each radiation and temperature conditions. It is desirable to operate the module at the peak power point so that the maximum power can be delivered to the load side [10].

A maximum power point (MPP) tracker is designed by the combination of incremental conductance algorithm [4, 11] which triggers the duty cycle of the DC/DC converter. By changing the duty cycle of converter, the PV panel will deliver the maximum power to the load. The Matlab/simulink model of Incremental conductance algorithm to track maximum power output, along with a DC/DC boost converter is shown in figure-16.

A. Maximum Power output of the Panel:

The maximum power operating point (MPOP) is shown in figure-13 and other two points left and right sides are:

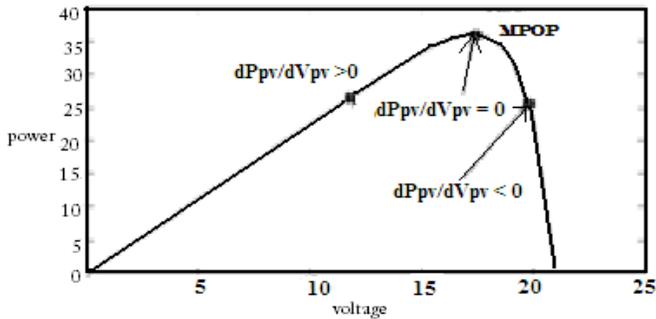


Fig. 13. Typical power-voltage characteristics of PV array.

From the power equation (4) of PV array:

Where

Hence the PV array terminal voltage can be adjusted the voltage in case of $\partial P_{pv} / \partial V_{pv}$ less than zero to select the MPPT.

B. Boost converter and load relation:

In normal boost converter, the power transfer depends on source and load. For variable power transfer, (i) at constant voltage load (battery), the load current should be voltage should be maximized and for (iii) any other type of loads either the output voltage or output current of DC/DC converter should be maximized. Most of the cases the boost converter output is treated as voltage type load i.e. battery, so the output current of converter is maximized. The duty cycle of the dc/dc converter should adjust with above situations i.e. load and hence it is not a MPP tracking. In MPP tracking, MPP deciding the duty cycle of the converter and not by the load.

C. Parameters of Boost Converter:

In continuous conduction mode of operation the output voltage of boost converter [12, 13] is defined as shown in figure-15:

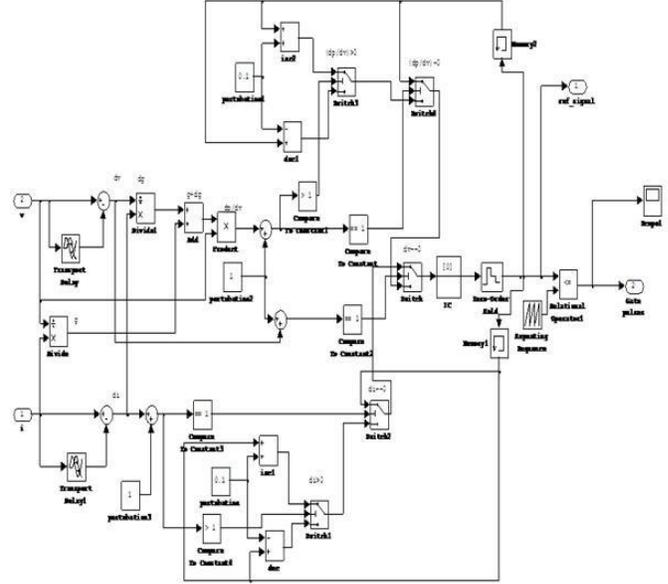


Fig. 15. Boost converter in circuit.

The critical inductance of boost converter is the boundary edge between continuous and discontinuous conduction modes and is defined as:

The total set-up of Matlab/simulink [14,15] arrangement of the PV array, boost converter along with the incremental conductance algorithm to supply a dc load and a battery (charging/discharging modes) is as shown in figure-8.

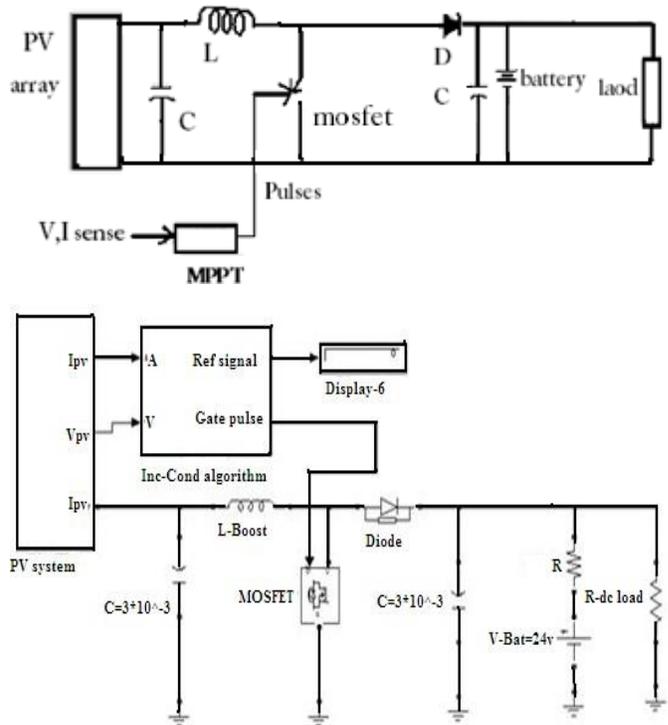


Fig. 16. The MPP tracking of PV array.

IV. TESTING AND RESULTS

In Simulation following cases are considered for MPP tracking and control:

A. 24 volts battery charging without load by varying solar radiation and temperature conditions:

The figure-17A is considered with 600w/m², 1000w/m², and 800w/m² radiations. The figure-17B is considered with 25⁰c, 45⁰c, 40⁰c temperatures. The effect of figure17A and figure-17B is observed on current, voltage and power characteristics as shown in figure-17C, 17D and 17E.

It is observed that at MPP of figure-2, current values are 1.2 amperes for 600w/m² and 25⁰c, 2.05 amperes for 1000w/m² and 25⁰c and are identical to figure-17C in first two stages.

Similarly at MPP of figure-4, current values are 2.07 amperes for 1000w/m² and 45⁰c and 1.65 amperes for 800w/m² and 40⁰c and are identical to figure-17C in next two stages.

Similarly in figure-17D the MPP voltage values are 16.5 volts, 17 volts and identical to figure-2 in first two stages, 15.8volts and 16.1 volts and identical to figure-4 in next two stages.

The MPP power variations in figure-17E, in above four cases of radiation and temperature are 20.81 watts, 35 watts, 33.7 watts and 26.8 watts and are identical to figure-5 in first two cases and are identical to figure-7 in next two cases.

The battery charging of four stages are shown in figure- 17F. Thus MPP power of panel at any particular radiation and temperature is tracking by the MPP tracker with battery as a load.

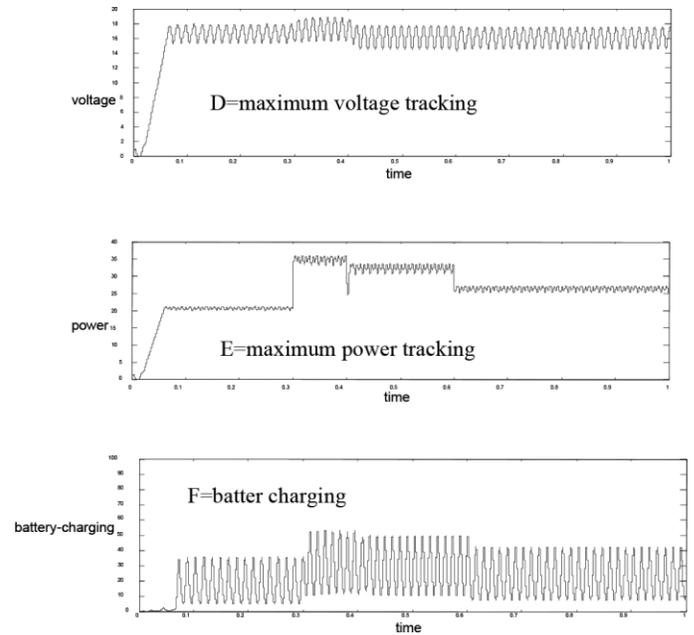
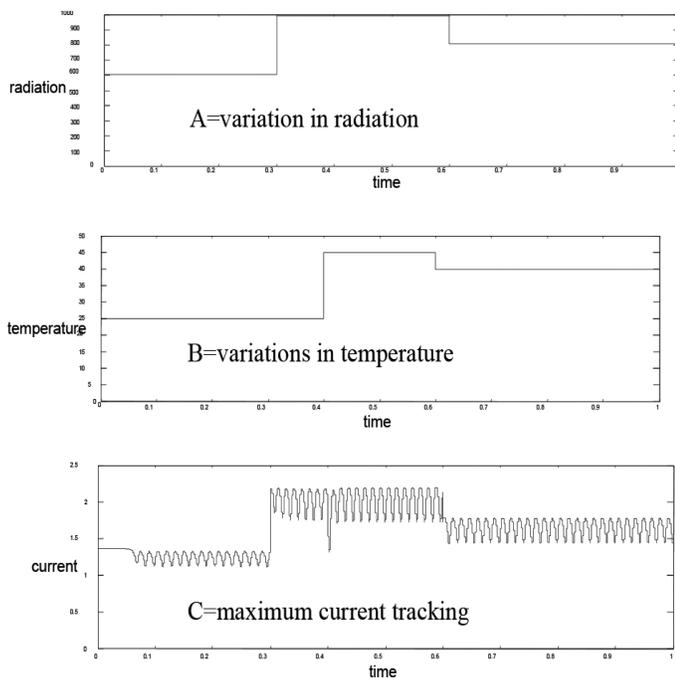


Fig. 17. Battery charging with varying solar radiation and temperature conditions.

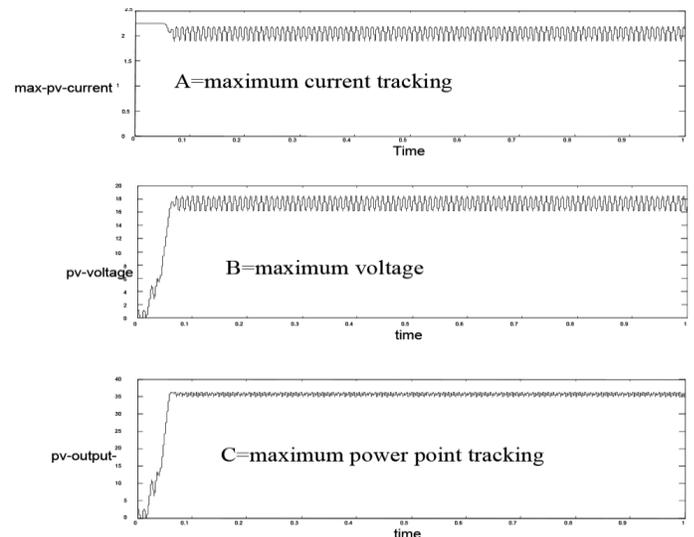
A. 24 volts battery charging with 10 watts dc load at STC:

In this case, 1000w/m² radiation and temperature 25⁰c (STC) is considered. The figure-18A, 18B and 18C are represents maximum current, maximum voltage and maximum power at MPP tracking at 10 watts load and along with a 24 volt battery.

The maximum current of 2.05 amperes (STC) at MPP of figure-18A is identical to figure-2 at MPP.

The maximum voltage of 17 volts at MPP of figure-18B is identical to figure-2 at MPP.

The maximum power of 35 watts (STC) at MPP of figure-18C is identical to figure-5 at MPP.



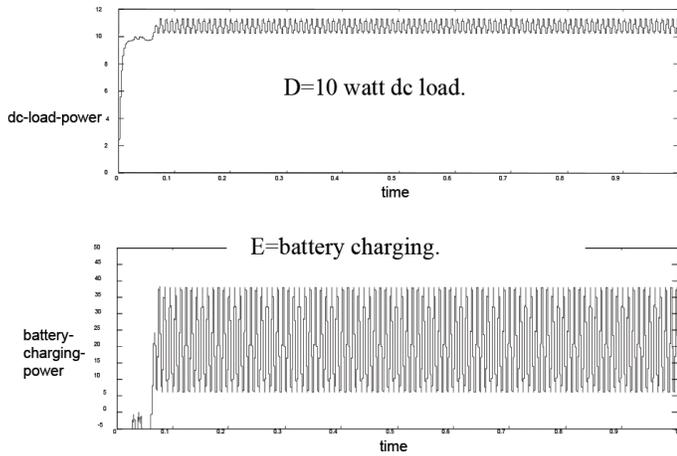


Fig. 18. A 10 watts dc load connected across a PV array with MPPT.

Thus it is observed that in MPP tracking load has no effect. The extra 25 watts of PV panel is charging the battery as shown in figure-18E (taking average of highest value 39 watts and lowest 8 watts= 23.5 watts). The input power of the load will gradually increase in case if battery charging failure in MPP tracking as shown in figure 19.

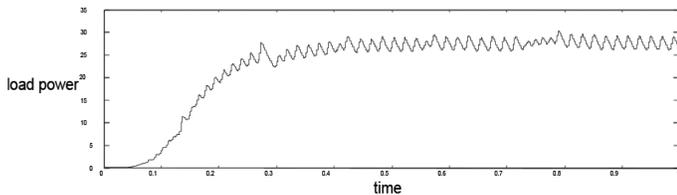


Fig. 19. 10 watts load and battery charging failure.

C. 24 volts battery charging with 40 watts dc load at STC:

In this case, 1000w/m² radiation and temperature 25⁰c (STC) is considered.

The figure-20A, 20B and 20C are represents maximum current, maximum voltage and maximum power at MPP tracking at 40 watts load and along with a 24 volt battery.

The maximum current of 2.05 amperes (STC) at MPP of figure-20A is identical to figure-2 at MPP.

The maximum voltage of 17 volts at MPP of figure-20B is identical to figure-2 at MPP.

The maximum power of 35 watts (STC) at MPP of figure-20C is identical to figure-5 at MPP.

Thus it is observed that in MPP tracking load has no effect. The PV panel is supplying 35 watts maximum power (STC) and extra required load power of 5 watts is discharging by battery as shown in figure-20E (taking average of -22 watts and 10 watts=-6 watts). In case of higher load than the MPP power of the PV panel will supply MPP power only and load has no effect on the panel even failure of battery discharging as shown in figure-21.

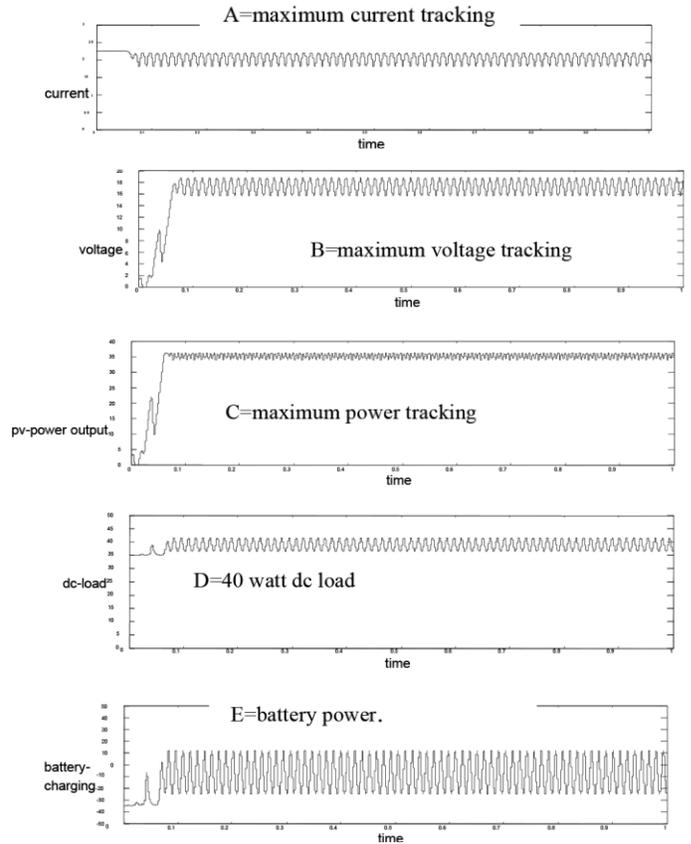


Fig. 20. A 40 watts dc load connected across a PV array with MPPT.

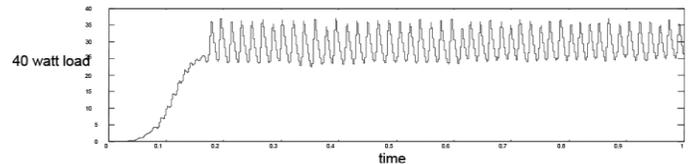


Fig. 21. 40 watts load and battery charging failure

A comparative study on tracking with MPP and without MPP is shown in table-2. It is observed that voltage is decreasing and current is increasing as load increases without MPP tracking.

TABLE 2: Comparison between PV arrays output connected to the load, with and without MPP arrangement.

load	Without MPPT at STC		With MPPT at STC along with battery			
	PV current	PV voltage	PV current	PV voltage	PV power	Battery charge/discharge
10 watt	0.5A figure (9)	20v figure (10)	2.05A figure (17)	17v figure (17)	35watt figure (17)	25watt charge figure(17)
40 watt	2.12A figure (11)	16v figure (12)	2.05A figure (18)	17v figure (18)	35watt figure (18)	5watt discharge figure (18)

V. CONCLUSION

The paper presented the MPP tracking of solar energy. The critical analysis of parameters of PV panel is presented with the help of Newton-raphson method. Matlab/simulation is utilised

to find the ideal characteristics of PV panel at various radiation and temperature conditions. In the ideal characteristics demonstrating the ideal MPPs at different radiation and temperature conditions. The design of MPP tracker using incremental conductance algorithm with Matlab/simulink at optimal duty cycle adjustments for MPP is presented. It is verified by the simulation and graphs that (i) for any radiation and temperature conditions the MPP tracking is able to track that particular MPP watts. (ii) in lower load, MPP tracking continue to track that MPP power and as a result battery charging is necessary. (iii) in higher load, MPP tracking will continue to track the MPP watts and as a result a battery for discharging is necessary. Thus, MPP power is tracking in all cases without any effect of load. In future microcontroller based system for MPP tracking is developing for implementation.

REFERENCES

- [1] Catalin Alexandru, Mihai Comsit, "The energy balance of the photovoltaic tracking systems using virtual prototyping platform" 978- 1-4244-1744-5/08/\$25.00 ©2018 IEEE
- [2] Rajiv K. Varma, V. Khadkikar, and Ravi Seethapathy, "Night-Time Application of PV Solar Farm as STATCOM to Regulate Grid Voltage" IEEE PES ,2019
- [3] M. Cosmit and I. Visa, "Design of the linkages type tracking mechanisms of the solar energy conversion systems by using multi body systems method" 12th IFTOMM world congress, Besancon (France), June 18-21, 2017.
- [4] Hardik P.Desai and H.K.Patel, "Maximum power point algorithm in PV generation: an overview" in IEEE PEDS pp: 624-630-2007.
- [5] Trishan Eram, Patrick L. Chapman, "Comparison of photovoltaic array maximum power point tracking techniques" National science foundation ECS-01-34208.
- [6] Dezso Sera, Remus Teodorescu, Pedro Rodriguez, "PV panel model based on data sheet values" IEEE transactions pp-2392-2396, September-2021.
- [7] C. L. Wadhawa, "Electrical Power System" New age international publishers, fourth edition-2020.
- [8] S. Rahman, M. A. Khallat, and B. H. Chowdhury, "A discussion on the diversity in the applications of photovoltaic system," IEEETrans.
- [9] Energy Conversion, vol. 3, pp. 738–746, Dec. 2020
- [10] Yushaizad yusof, siti Hamizah sayuti, Muhammad Abdul Latif and Mohd. Zamri che Wanik, "Modeling and simulation of maximum power point tracker for photovoltaic system" National power and energy conference 2004 proceedings, kuala Lumpur, Malaysia.
- [11] Caisheng Wang, M. Hashem Nehrir, "Power Management of a Stand-Alone Wind/Photovoltaic/Fuel Cell Energy System", IEEE Transaction on Energy Conversion, Vol. 23, NO. 3, September 2008.
- [12] K.H.Hussein, I.Muta, T.Hoshino, M.Osakada, "Maximum photovoltaic power tracking for rapidly changing atmospheric conditions" IEE proc, vol.142, No.1, pp. 59–64,January 2001.
- [13] B. M Hasaneen and Adel A. Elbaset Mohammed, "Design and simulation of dc-dc boost converter" IEEE Transactions 2008.
- [14] Soren Baekhoej Kjaer, John K. Pedersen and Frede Blaabjerg, "A review of single-phase grid-connected inverters for photovoltaic modules" IEEE Transactions on industry applications, vol. 41,no. 5,sept.-2005.
- [15] Michael E. Ropp, and Sigifredo Gonzalez, "Development of a MATLAB/Simulink Model of a Single-Phase Grid-Connected Photovoltaic System"IEEE Transaction on Energy Conversion,2020
- [16] 'Matlab/Simulink user's guide' the math works, version-7.0.1.24704.

A High-Performance Stand-alone Solar PV Power System for Led Lights

Rakhi Kamra¹, Monu Malik², Annu Dagar³, Shilpam Malik⁴

^{1,2,3,4}Department of Electrical Engineering
Maharaja Surajmal Institute of Technology, New Delhi, India

Abstract: The present study developed a high-performance solar PV power technology for the LED lighting of a solar home system. The nMPPO (near-Maximum-Power-Point- Operation) design is employed in system design to eliminate MPPT. A feedback control system using pulse width modulation (PWM) technique was developed for battery charging control which can increase the charging capacity by 78%. For high-efficiency lighting, the LED is directly driven by battery using a PWM discharge control to eliminate a DC/DC converter. Two solar-powered LED lighting systems (50W and 100W LED) were built. The long-term outdoor tests have shown that the loss of load probability for full-night lighting requirement is zero for 50W LED and 3.6% for 100W LED.

Keywords: LED; Power System; Solar Energy

I. INTRODUCTION

The solar home system requires a high-performance stand-alone solar-powered system for lighting and other utilization, including high-efficiency power generation of PV, battery charging and discharging. The present study has developed a high-performance solar PV power technology for the LED lighting of a solar home system.

II. SYSTEM DESIGN BASED ON NMPPPO

For high-efficiency PV power generation, the nMPPO (near-Maximum-Power-Point-Operation) design [1] is employed in the system design, instead of using MPPT, to reduce the conversion loss of MPPT at non-full load operation.

III. BATTERY CHARGING CONTROL

To charge the battery to its full capacity, a three-stage charge algorithm can be used (Fig.1). The first phase is to directly charge the battery from solar PV until the battery voltage reaches its overcharge point and then stops. The nMPPO design [1] can maintain the charge current near the maximum-power-point (MPP) current and the battery charger does not control the charging current in Phase 1.

Thus, only 70~80% state of charge (SOC) can be charged into the battery at Phase 1. Phase 2 is to maintain the battery voltage at the overcharge point to replenish the remaining capacity. Phase 3 is to make up the internal current leakage to maintain 100% SOC for the battery. In both Phase 2 and Phase 3 the charge current generated from PV needs to be reduced in order to maintain a set voltage to protect the battery.

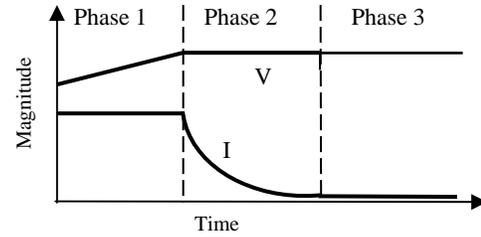


Fig. 1. Battery charging process

A feedback control system using pulse width modulation (PWM) technique (Fig.2) was thus developed in the present study to control the charge current from PV in Phase 2 and Phase 3.

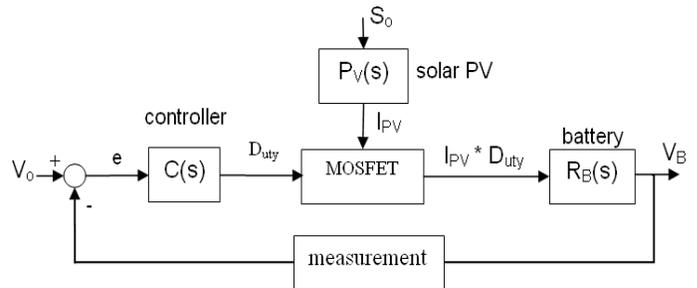


Fig. 2. Battery charging control system

Fig.3 shows that the controller performs very well. The charging current starts to decrease when the battery voltage reaches the overcharge point. The voltage is kept constant at the overcharge voltage during the charging process. Fig.4 shows that the PWM charge control can increase the battery charge capacity by about 78%.

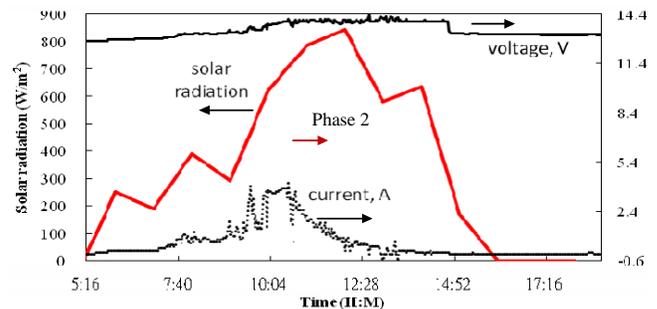


Fig. 3. Charging process of solar system.

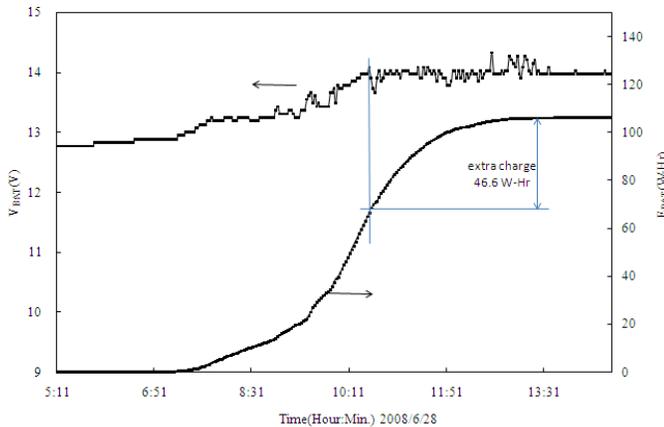


Fig. 4. Field test results of solar battery charging

IV. LED LIGHTING CONTROL SYSTEM

The lead-acid battery is widely used in stand-alone solar power systems. The lead-acid battery usually operates at 11.3–12.7 V with a state-of-charge (SOC) from 10% to 100%. The discharge controller in a stand-alone solar-powered light-emitting diode (LED) lighting system usually consists of a DC/DC converter that converts the floating battery voltage into a constant current which in turn drives the LED. A 15% energy loss of the DC/DC converter is then introduced. The DC/DC converter may also increase system costs and reduce system reliability due to the additional components. As shown in Fig.5, the current-voltage (I-V) curve of an LED indicates that the LED will be easily overdriven and damaged by the voltage variation from the battery and the junction temperature of the LED.

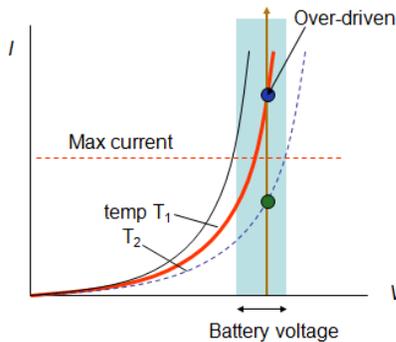


Fig. 5. Variation of LED driving current.

The LED can be driven using the pulse width modulation (PWM) technique to maintain an average current below its rated value (e.g., 350 mA) (Fig. 6). The battery output current is switched by a metal-oxide-semiconductor field-effect transistor (MOSFET) according to the PWM signal that is generated by a feedback control system that maintains an average current. Fig.7 shows the constant current PWM (CCPWM) driving control system in which the controller is implemented in a microprocessor to output a PWM signal. This signal triggers the MOSFET to deliver a PWM current to an LED which in turn generates light.

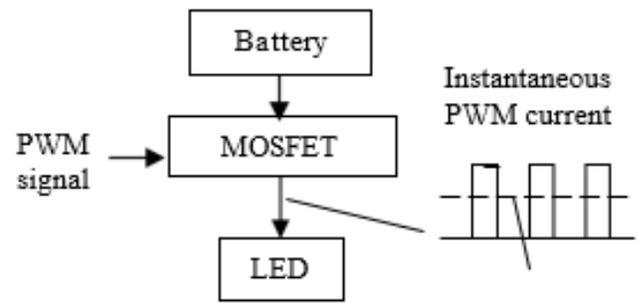


Fig. 6. Variation of LED driving current.

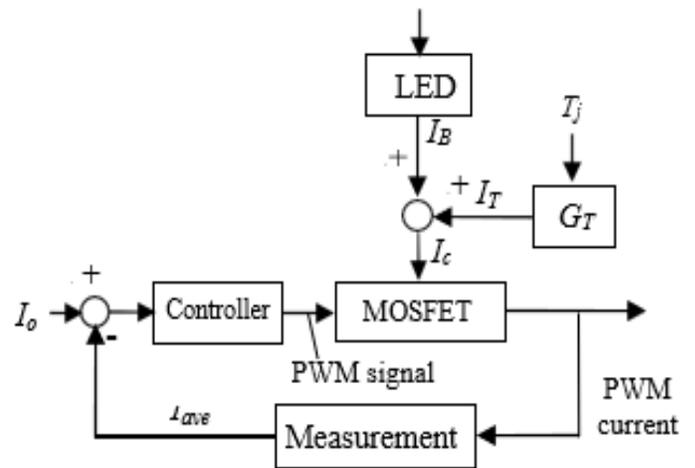


Fig. 7. Constant-current PWM (CCPWM) driving control system.

The I-V curve of the LED is sensitive to the junction temperature (T_j). Therefore, the coefficient G_T in Fig.7 represents the relation between the variation in the driving current and the junction temperature. The PWM current is measured and analyzed to determine the average current (I_{ave}) feedback control according to the average current setting (I_o) for the CCPWM direct driving control system. Therefore, the control system in Fig.7 can maintain a constant average current to drive the LED. Daniel L. Barton [2] has shown that an LED can be driven using high current stress, while M. Meneghini [3,4] has shown that an LED can operate at an instantaneous current less than five times the rated current. The present study focuses on the design of the PWM LED direct driving controller that will drive the LED luminaire using the PWM current while rejecting the effect of variation in the battery voltage and the junction temperature.

When the LED is driven by the constant-current PWM, the instantaneous driving current will be larger which is at $1/D$ times (D : duty cycle, %). Fig.8 shows the variation of duty cycle with voltage for a constant-current PWM. Higher battery voltage will cause larger instantaneous current through LED.

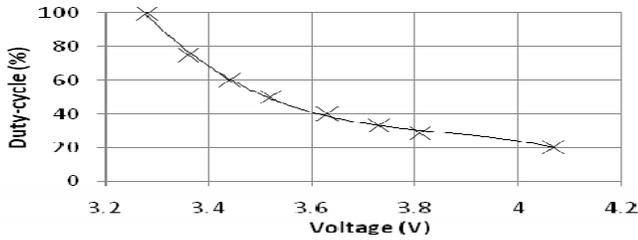


Fig. 8. Constant-current PWM duty cycle vs voltage

As shown in Fig.7, the feedback control system feeds back the average current to the controller to generate a PWM signal that triggers the MOSFET and drives the LED luminaire using the PWM current. Therefore, a constant average current can be produced directly from the battery output to drive the LED luminaire.

The PI controller was adopted in the CCPWM feedback system design. The PI controller for the LED luminaire should be robust with respect to the output current that results from the variation in the battery’s output voltage and the junction temperature. A sensitivity function, or $S_I(s)$, was defined for the closed-loop transfer function with respect to the variation of the output current, as is shown in Eq. (1).

$$S_I(s) = \frac{G(s) I_c}{I_c G(s)} \frac{K_p T_I (T_p s + 1) s}{I (K_I s + K_I) (K_I I s + K_I) (K_I I s + K_I) (K_I I s + K_I)} \quad (1)$$

A system simulation for the feedback control system was carried out to determine the controller parameters. The controller design is shown in Eq.(2).

$$C(s) = 0.7 \left(1 + \frac{1}{8s} \right) \quad (2)$$

The test result of Fig 9 shows that the controller can reject the influence of the LED junction temperature variation and suppress the influence of the variation in the input voltage.

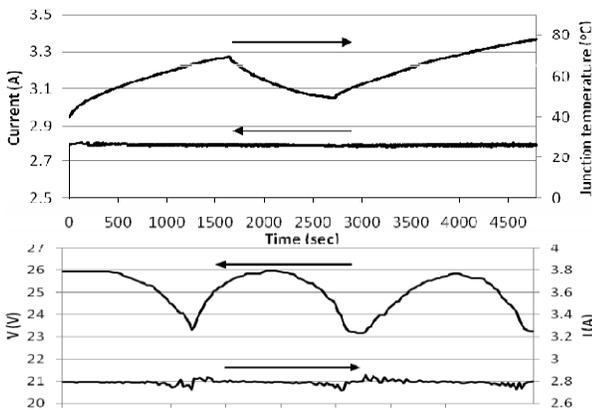


Fig. 9. Test result of CCPWM controller

In the worst-case scenario, the maximum deviation when

compared to the set driving current was -2.75% when the input voltage was varied. This shows that a stand-alone solar-powered LED lighting system allows for removal of the traditional DC/DC converter and can drive an LED luminaire directly from the battery output. This increases the reliability and reduces the cost.

V. SOLAR LED LIGHTING SYSTEM OUTDOOR TEST

Two solar-powered LED lighting systems (50W and 100W LED) were designed and built in the present study. The 50W solar-powered LED lighting system consists of a 50W LED luminaire, a 360Wp solar PV module, a 48V 100Ah lead-acid battery, and a controller developed in the present study. The 100W solar-powered LED lighting system consists of a 100W LED luminaire, a 400Wp solar PV module, a 48V 100Ah lead-acid battery, and a controller developed in the present study. The long-term outdoor field test results have shown that the system performance is satisfactory. The loss of load probability for full-night lighting in the 50W solar LED system is zero from Jan 7 to May 13, 2009 (Fig.10). For the 100W solar LED system, the loss of load probability is 3.6 % in spring.

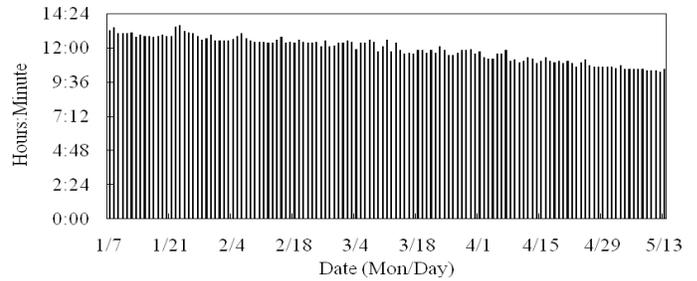


Fig. 10. Daily lighting time of 50W solar LED system.

ACKNOWLEDGMENT

This publication is based on the work supported in part by Award No.KUK-C1-014-12, granted by King Abdullah University of Science and Technology (KAUST).

REFERENCES

- [1] M. Yamaguchi et al., “Minority-Carrier Injection Annealing of Electron Irradiation-Induced Defects in InP Solar Cells”, Appl. Phys. Lett. 44, 2017, pp. 432-434.
- [2] B.J. Huang, F.S. Sun, R.W. Ho, “Near-maximum- power-point-operation (nMPPO) design of photovoltaic power generation system”, Solar Energy 80, 2016, 1003- 1020.
- [3] Daniel L. Barton, Marek Osinski, Piotr Perlin, Petr G. Eliseev, Jinhyun Lee, “Single-quantum well InGaN green light emitting diode degradation under high electrical stress”, Microelectronics Reliability 39, 2009, pp. 1219- 1227.
- [4] Meneghini, M., Morelli A., Pintus, R., Meneghesso, G., Vanzi, M., Zanoni, E., “High brightness GaN LEDs degradation during dc and pulsed stress”, Microelectronics Reliability 46, 2006, pp. 1720-1724.
- [5] Meneghini, M., Trevisanello, L., Podda S., Buso, S., Spiazzi, G., Meneghesso, G., Zanoni, E., “Stability and performance evaluation of High Brightness Light Emitting Diodes under DC and pulsed bias conditions”, SPIE, Sixth International Conference on Solid State Lighting, 2016, Vol. 63370R, 63370R-1.

High-Efficiency Battery Charging with Switching Resonant Converter

Monu Malik¹, Rakhi Kamra²

Department of Electrical Engineering, Maharaja Surajmal Institute of Technology, New Delhi, India

Abstract: The high-frequency resonant converter has numerous well-known advantages over the traditional hard-switching converters. The most important advantage is that it offers a lower switching loss and a higher power density. Additionally, the soft-switching current waveform characterizes a lower electromagnetic interference (EMI). This study presents the circuit configuration with the least components to realize a highly efficient solar energy battery charger with a zero-voltage-switching resonant converter. The optimal values of the resonant components are determined by applying the characteristic curve and the electric functions derived from the circuit configuration. The experiment demonstrates the switching on and off of the main switches in a solar energy battery charger with a zero-voltage-switching resonant converter, wherein the switches are all operated using zero-voltage switching. The circuit efficiency in the overall charging process exceeds 80%.

Keywords: Battery charger, photovoltaic array, resonant converter, soft-switching, zero-voltage-switching (ZVS).

I. INTRODUCTION

RAPID technological changes have led to power electronic products playing a crucial role in daily life. Energy storage equipment is a commonly used form of power electronic products. However, the conventionally adopted battery chargers produce power losses that incur power dissipation during charging. Therefore, the charging method is especially important. Various charging approaches engender various charging efficiencies and also indirectly influence the life of a battery charger. This study analyzes the charging losses and power dissipation of a buck zero-voltage-switching resonant solar battery charger, and then, improves the charging efficiency. Additionally, Taiwan is located in a subtropical zone that is close to the equator, and southern Taiwan, particularly, is full of sunshine during summer. Consequently, the energy collected on photovoltaic arrays is utilized as the source of a battery charger for saving energy. However, the output voltage of photovoltaic arrays varies with the sunshine. Unstable output voltage shifts the operating point of a zero-voltage-switching resonant converter. Consequently, this study designs a novel approach in which the output terminal of photovoltaic arrays is in series with a closed-loop buck converter to stabilize the input voltage of the zero-voltage-switching resonant converter, and prevent the operating point of the charger from varying with the sunshine. Fig. 1 illustrates the whole system block diagram of the zero-voltage-switching resonant converter for photovoltaic arrays.

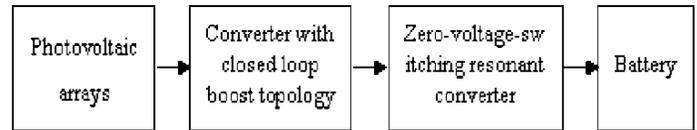


Fig. 1. The system block diagram of zero-voltage-switching resonant converter for photovoltaic arrays.

Batteries are extensively used in various applications, including telecommunication power supply, electric vehicles, uninterruptible power supplies, photovoltaic systems, portable electronics products, and others. Photovoltaic arrays are presently employed to supply electricity to remote or inaccessible areas. A battery charger is crucial in a photovoltaic array and the charge mode markedly affects battery life and capacity. Topologies with high switching frequencies are used to reduce the charging current ripple and extend the battery life. However, as the switching frequency further increases, switching losses and electromagnetic interference (EMI) noise arise. Hence, to solve this problem, the switching frequency is increased by reducing the switching losses through a so-called zero-voltage-switching (ZVS) circuit.

The traditional battery charger, which extracts power from an ac-line source, requires a thyristor ac/dc converter rectifier, with an equivalent series resistance, to control the power flow to charge the battery system. Such a charging circuit necessarily draws a high ripple charging current. This shows notoriously low efficiency, and is associated with a large volume. Accordingly, as the concern about the quality of a charger grows, a charging circuit for reducing the ripple and extending the battery life becomes more important in designing the battery storage systems. Several charging circuits have been proposed to overcome the disadvantages of the traditional battery charger. The linear power supply is the simplest. A 60-Hz transformer is required to deliver the output within the desired voltage range. However, the linear power supply is operated at the line frequency, which makes it large both in size and weight. Besides, the system conversion efficiency is low because the transistor operates in the active region. Hence, when higher power is required, the use of an overweighted and oversized line-frequency transformer makes this approach impractical.

The high-frequency operation of the conventional converter topologies depends on a considerable reduction in switching losses to minimize size and weight. Many soft-switching techniques have been proposed in recent years to solve these

problems. Unfortunately, switching losses in these new circuits can be reduced only at the expense of substantially increased

voltage and current stresses in the power switches, resulting in a considerable increase in the conduction loss. However, flexible control techniques can be used to realize switching-mode converters with small circuit components of high efficiency and low cost. In switch-mode topologies, controllable switches are operated under hard-switching conditions, resulting in increased switching losses, switching noise, and electromagnetic interference. In an attempt to overcome these shortcomings, much effort has been made to find a less expensive filtering approach and topology of the charging circuit, to be able to offer a competitive price in the consumer market. This work considers the application of zero-voltage-switching to a charger to minimize the switching losses, switching noise, and high-frequency electromagnetic interference. In the developed approach, a resonant tank is inserted between the input and the battery. With the zero-voltage-switching topology, a charger with high efficiency can be achieved without an additional power switch or sophisticated control circuit.

II. COMPARISONS BETWEEN THE RESONANT CONVERTER AND THE TRADITIONAL PULSE WIDTH MODULATOR (PWM) CONVERTER

In the conventionally adopted power converters, the switching frequency must be increased to lower the volume and weight in order to enhance the power density. Paradoxically, this also leads to an increase in the switching losses, switching stress, and EMI. The snubber circuit is parallel to the switch in the conventional solution for reducing the dv/dt surge resulting from the switching-off, while the switching-on buffer circuit is in series with the switch to reduce the di/dt surge resulting from the switching-on. Although snubber circuits can reduce the switching losses, switching stress, and EMI, the whole loss remains unchanged, and efficiency becomes a significant concern. The resonant converter is developed by using the series or parallel combination of inductor and capacitor to generate the resonance situation. The switch is switched to achieve zero-voltage or zero-current switching in the resonant situation, to effectively solve the switching losses, switching stress, and EMI.

A. Traditional PWM Power Converter

Switching losses are produced by the current linearly increases owing to the switching-on operation in the active region, when the transistor is generally adopted as the switch of the converter. The traditional PWM power converter is designed to use the power transistor as the switching switch, and be operated in a switching-on and switching-off model to control the power transistor duty cycle to achieve the buck/boost topology. Four main circuit configurations have been developed: 1) buck converter, 2) boost converter, 3) buck-boost converter, and 4)

Cuk converter. Although the traditional PWM power converter enhances the low efficiency shortcoming of the conventionally adopted linear power converter, the converter switching frequency must be increased to reduce the volume and weight, simultaneously increasing the switching losses, switching stress, and EMI.

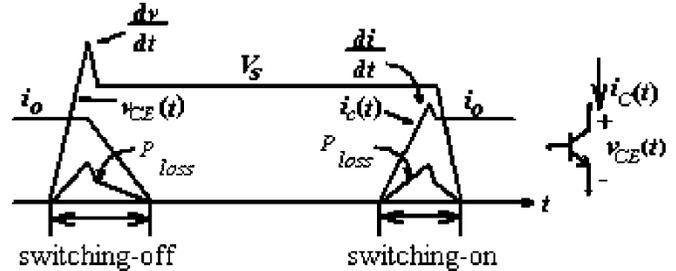


Fig. 2. Switching loss and EMI in a traditional PWM power converter.

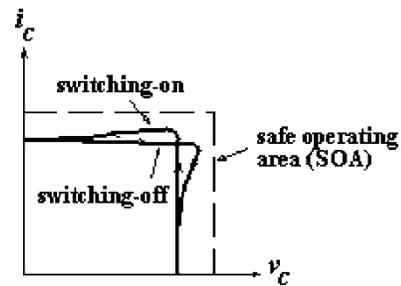


Fig. 3. $v_c - i_c$ switching path in a switched power converter.

1) *Switching Loss*: The switch must withstand the input terminal voltage, and during switching-off, the switch current must immediately reduce to zero. In practice, the increase of voltage $V_{CE}(t)$, and the decrease of current $i_c(t)$, both exhibit a slope form, the switch voltage and switch current overlap in the form of a cross, owing to the existence of these slopes. The generated power P_{loss} at the intersection is the switching loss. Switching losses increase with the increase in switching frequency. Fig. 2 shows the switching losses and EMI in a traditional PWM power converter. $V_{CE}(t)$ is the voltage drop between the collector and emitter of transistors, and $i_c(t)$ is the current flow from the collector.

2) *EMI*: The dv/dt is generated in the voltage waveform at the instance of switching-off, because of the stray inductance during switching-off. The di/dt is generated at the instance of switching-on, owing to bad reverse recovery characteristics during the switching-on period. These two situations are the source of EMI. EMI also appears increasingly serious with increasing switching frequency.

3) *Switching Stress*: Fig. 3 displays the switching path in the $v_c - i_c$ plane in a switched power converter. The switch must withstand the switching stress within a safe operating area (SOA), because of the high voltage and large current in the switch during switching. Power semiconductor elements

withstand large switching stress and certainly have some effect on performance.

B. Resonant Power Converter

The resonant power converter utilizes the resonance theory by incorporating a LC resonant circuit from the conventionally adopted PWM converter. The switching-on and switching-off conditions, both operate in zero-voltage to reduce the switching.

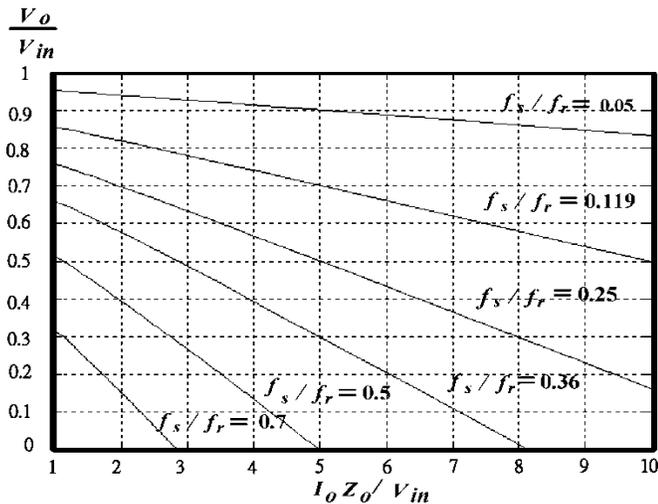


Fig. 11. Conversion ratio for buck ZVS.

TABLE I CIRCUIT PARAMETERS

Input voltage V_{in}	24V
Resonant inductor L_f	50 μ H
Resonant capacitor C_f	0.2 μ F
Characteristic impedance Z_o	16 Ω
Switching frequency f_s	18KHz
Resonant frequency f_r	50KHz
Charging voltage V_o	15V
f_s/f_r	0.36
Open circuit voltage of the battery	11V
Initial charging current I_o	2A

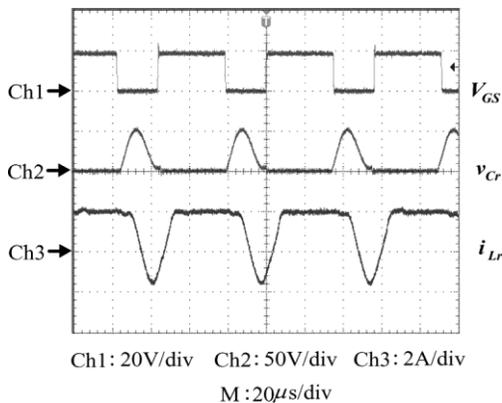


Fig. 12. Waveforms of the switching signal V_{GS} , the resonant voltage v_{Cr} , and the resonant current i_{Lr} .

The voltage ratio of the buck ZVS was numerically determined, as plotted in Fig. 11, with f_s/f_r as the running parameter. Fig. 11 plots the dc voltage-conversion-ratio characteristics of the buck ZVS as functions of normalized output current $I_{on} = I_o Z_o / V_{in}$. The first step in designing the converter is to determine f_s/f_r , based on a set of dc characteristics curves for various f_s/f_r in Fig. 11.

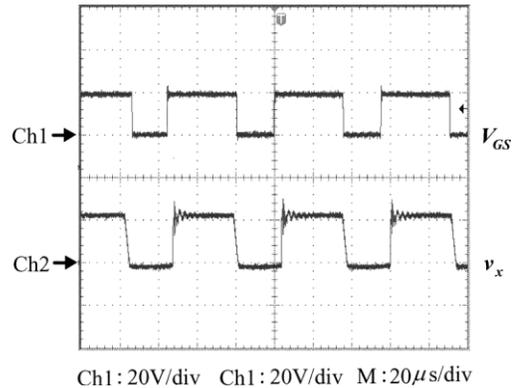


Fig. 13. Waveforms of switching signal V_{GS} , and voltage v_x , of the free-wheeling diode.

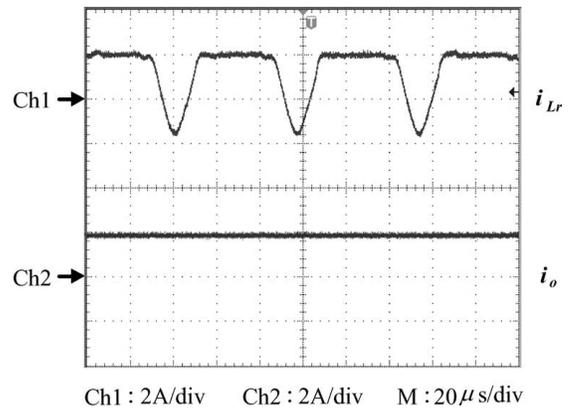


Fig. 14. Waveforms of the charging current I_o , and the resonant current i_{Lr} .

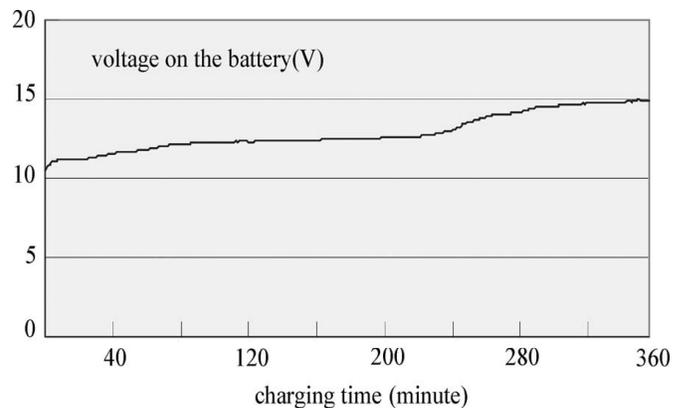


Fig. 15. Charging voltage curve.

III. EXPERIMENTAL RESULTS

A prototype of the buck converter with zero-voltage-switching resonant topology was established in a laboratory to confirm the functional operations. The developed charging circuit is applied to a 12 V, 4 Ah lead-acid battery. Table I lists the circuit parameters of the experiment results in the developed novel high-efficiency battery charger with a buck zero-voltage-switching resonant converter. The resonant capacitance $C_f = 0.2\mu\text{F}$, and resonant inductance $L_f = 50\mu\text{H}$, are determined using (24) and (25).

Fig. 12 displays the waveform of the switch signal, the resonant voltage, and the resonant current i_{Lr} . Fig. 13 presents the waveform of the switching signal V_{GS} , and the voltage v_x during freewheeling while Fig. 14 plots the waveform of charging

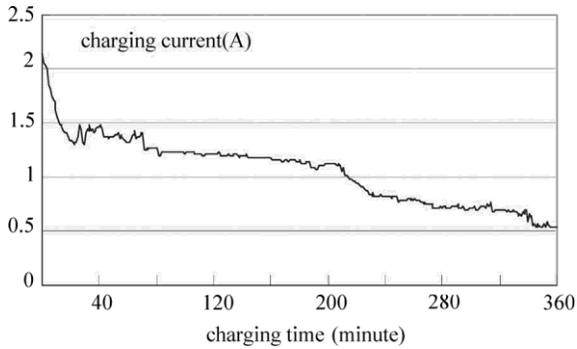


Fig. 16. Charging current curve.

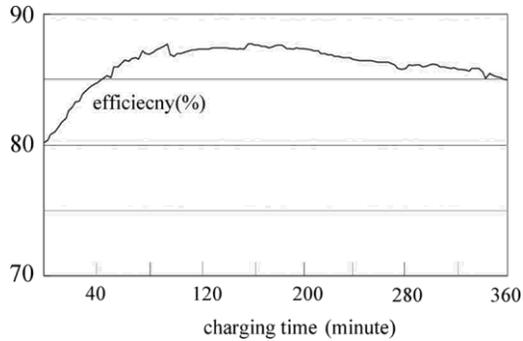


Fig. 17. Charging efficiency curve.

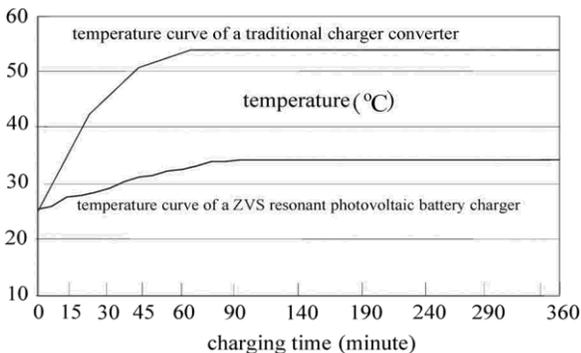


Fig. 18. Comparison of power switching temperatures.

current i_o and resonant current i_{Lr} . Fig. 15 displays the voltage variation curve of the charger. The charging of the battery from 11 to 15 V takes 360 min. Figs. 16 and 17 plot the charging current and the charging efficiency, respectively. The charging current takes 300 min to fall below 0.7 A. The minimal and maximal efficiencies are around 81% and 87%, respectively, and the mean charging efficiency of the charger is 84%. Moreover, Fig. 18 compares power switching temperatures between the developed zero-voltage-switching resonant battery charger and the conventionally adopted PWM hard-switching converter. Under the same operating conditions, the measured temperature of the power switches in the presented battery charger with ZVS is maintained at 34 °C, much lower than that of the traditional pulse-width-modulation (PWM) converter at 54 °C. Experimental results also show that the switching loss in the developed battery charger with ZVS is significantly lower than that for the traditional hard-switching charger.

IV. CONCLUSIONS

This study presents the photovoltaic battery charger with ZVS technology for use in the charging test of a lead-acid battery charger, to demonstrate the effectiveness of the developed methodology. Under the same operating conditions, the measured temperature of power switches in the proposed battery charger with ZVS is maintained at 34 °C and is much lower than that of the traditional pulse-width-modulated (PWM) converter at 54 °C. The proposed battery charger with ZVS indeed reduces the temperature of the switch, reducing the switching losses. The circuit efficiency of the overall charging process exceeds 80% and greatly exceeds the 68% efficiency, of traditional converters.

REFERENCES

- [1] N. Mohan, T. M. Undeland, and W. P. Robbins, *Power Electronics: Converters, Applications and Design*, 3rd ed. New York: Wiley, 2021.
- [2] K. H. Liu and F. C. Lee, "Zero-voltage switching technique in DC/DC converters," *IEEE Trans. Power Electron.*, vol. 5, no. 3, pp. 293–304, 2000.
- [3] W. A. Tabisz and F. C., "Zero-voltage-switching multi-resonant technique—A novel approach to improve performance of high frequency quasi-resonant converters," in *Proc. Power Electron. Spec. Conf.*, 2014, vol. 1, no. 11–14, pp. 9–17.
- [4] J. G. Cho, J. W. Baek, G.-H. Rim, and I. Kang, "Novel zero voltage transition PWM multi-phase converters," *Proc. 11th Annu. Appl. Power Electron. Conf. Exposition (APEC'96)*, vol. 1, no. 3–7, pp. 500–506, Mar. 3–7, 2016.
- [5] R. W. Erickson, *Fundamental of Power Electronics*, 2nd ed. Norwell, MA: Kluwer, 2021.

Wireless Charging in Electric Vehicles

Monu Malik¹, Rakhi Kamra², Jagriti Krishnan³

^{1,2,3}Department of Electrical Engineering

Maharaja Surajmal Institute of Technology, New Delhi, India

¹monumalik@msit.in, ²rakhikamra@msit.in, ³jagritikrishnan@gmail.com

Abstract: One of the most exciting and growing advancements in the forthcoming technological world is wireless charging. Everything is regulated by wireless charging technologies, from household appliances to automobiles. This charging method has enabled adaptability, user-friendliness, energy efficiency, durability, the creation of smaller gadgets, and fast charging. These strategies are becoming increasingly popular among the world's population. This paper discusses the various aspects and discusses the practical application of wireless charging in electric vehicles. There are three sections to this paper. The first delves into the many forms of wireless charging, as well as the terminology used, electric vehicles, and the techniques used to charge an electric vehicle. To gain a deeper and clearer understanding of the concept, the second section presents a tiny project that uses the static wireless charging method for an electric way. The third section examines existing wireless charging applications in various industries, as well as the primary benefits. The study, as well as the project, might be expanded to include a dynamic charging technique for charging a moving electric vehicle. This wireless charging technology is highly handy in today's fast-paced, ever-changing environment. It is big time to use this charging method in the majority of areas, as practically everything nowadays is built on and dependent on energy and technology.

Keywords: wireless charging, electric vehicle, static wireless charging, dynamic wireless charging, energy.

I. INTRODUCTION

Wireless charging may be defined as a technique that uses a variety of methods to charge device batteries without the usage of a charging connection or an AC adapter. Wireless charging, also known as wireless power transfer, is a technique that allows a power source to send electromagnetic energy through an air gap to an electrical load without the use of cables. Because of its simplicity and improved user experience, this technology is attracting a wide range of applications, from low-power toothbrushes to high-power electric automobiles.

Wireless charging is fast moving from a concept to a function on commercial items, particularly mobile phones and portable smart gadgets. Wireless charging is used to charge batteries in a range of devices such as laptop computers, cellphones, and tablets. Furthermore, wireless chargers are employed for bigger equipment such as electric automobiles and other electronic gadgets.[1]

Wireless charging has many advantages over the traditional methods of charging. Some of them are discussed below:

- It promotes user-friendliness by eliminating the

inconvenience of connecting cables. Wired charging necessitates dragging a lengthy data wire, which is unsightly and devoid of any technological sense. The sole requirement for wireless charging is to gently lean the phone against the charger, and the electricity will be continually charged into the phone.

- The same charger may be used for devices of many manufacturers and models. To achieve wireless charging, most mobile phones on the market rely on the idea of electromagnetic induction. Between the charger and the phone, there is no interaction. A receiving coil is built within the phone, while a transmitting coil is installed into the charger. They use electromagnetic induction to charge the phone using electricity. It doesn't matter what phone brand is; as long as it's compatible with the charging head's wireless charging standard, it can be charged.
- It improves versatility, particularly for devices where replacing batteries or charging cords is expensive, dangerous, or impossible (e.g., body implanted sensors). The wear and tear on the data interface of the mobile phone will be greatly minimized since wireless charging does not require repeated plugging and unplugging of the charging connection. At the same time, the coil for wireless phone charging is not exposed to the air, which helps to prevent oxidation and corrosion of the charging unit. The wired charging is often plugged in and out, resulting in wear and tear, and the interface is exposed, making it susceptible to oxidation and corrosion.
- It allows for the design and manufacture of considerably smaller gadgets that do not require the use of batteries.
- It improves the durability of contact-free devices (e.g., waterproof and dustproof).
- Wireless charging is more versatile and energy-efficient since it can give electricity required by charging devices on-demand.

II. TYPES OF CHARGING

Onboard and off-board chargers are defined by the physical placement of the components that convert grid electricity to the power required by the car battery. Onboard chargers are built into the device, and their size and power output are limited by the amount of space available. Outside the device, off-board chargers allow additional flexibility in terms of the amount of power that can be provided. Both types of charging devices must

include control circuits and be able to interact with the car battery in real-time. This is to guarantee that the battery is charged as efficiently as possible, preventing any battery damage caused by overcharging. An onboard charger is used for AC charging, while an off-board charger is used for DC charging and battery swapping. In the event of an inductive charger, you'll need both an onboard and off-board charger.

Wireless charging may be classified into three types[2]:

1. Radio Charging
2. Inductive Charging
3. Resonance Charging

A. RADIO CHARGING

This sort of wireless charging is used to power gadgets with small batteries and low power consumption. Wireless keyboards, wireless mouse, cellphones, medical gadgets, hearing aids, watches, music players, and much more are among the devices. These are gadgets that already send and receive wireless signals through radio waves. For electrical transmission, they function similarly. Once sent, a radio wave propagates in all directions until it reaches an antenna set to the correct frequency.

Two units are designed to broadcast and receive radio waves for energy transmission. In order to create radio waves, wireless radio charging requires a transmitter that is linked to a socket. The transmitter broadcasts a low-power radio wave at a predetermined frequency. Any low-power device can be fitted with the receiver. When the transmitter and receiver are tuned to the same frequency, the gadget is powered and the battery is charged.

B. INDUCTIVE CHARGING

Charging by induction is the technique of charging an uncharged object by bringing another charged object close to it but not touching it.[3] This charging method is employed in electric vehicles.

Consider an example of an uncharged metal sphere and a negatively charged plastic rod. Charge separation happens when a negatively charged plastic rod is brought close to an uncharged sphere. The positive charges in the sphere are drawn to the plastic rod and migrate to one end of the sphere that is closest to it. Negative charges, meanwhile, are repelled by the plastic rod and migrate to the other end of the sphere, further away from it. As a result, the sphere's charges rearrange themselves so that all positive charges are closer to the plastic rod and all negative charges are farther away. When this sphere is linked to the ground via the wire, the sphere's free electrons flow to the ground. Induction causes the sphere to become positively charged.

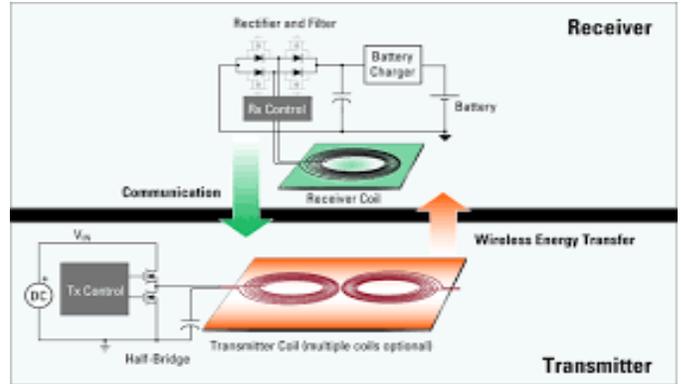


Fig. 1. Inductive Charging

C. RESONANCE CHARGING

Resonance charging is a distinct sort of wireless charging that is utilized for high-power gadgets. A huge computer, an electric automobile, a vacuum cleaner, or a robot are examples of this equipment. Resonant wireless charging has several advantages, including increased user-friendliness (a device may be put anywhere within 30 mm of the transmitter) and the ability to charge numerous devices of varied sizes and power at the same time. Its frequency is 6.78 MHz. Bluetooth Low Energy is used by resonant wireless charging devices, whereas proprietary resonant solutions use in-band communication.

The frequency of resonant wireless charging is high. Standard silicon power methods in transmitter and receiver devices face substantial hurdles as a result, particularly in higher-power systems. The most common topologies for resonant wireless charging systems are class-D zero voltage switching (ZVS) and differential class-E. Both methods decrease switching losses by transitioning power devices between on and off switching states at zero volts across the power switch.

A copper coil is attached to the gadget that has to be charged, and another copper coil is coupled to a power source in resonance charging. When both copper coils are set to the same electromagnetic frequency, wireless charging is possible. This allows you to charge the device's battery directly from the power supply. Only limited distances are covered via wireless resonance charging.

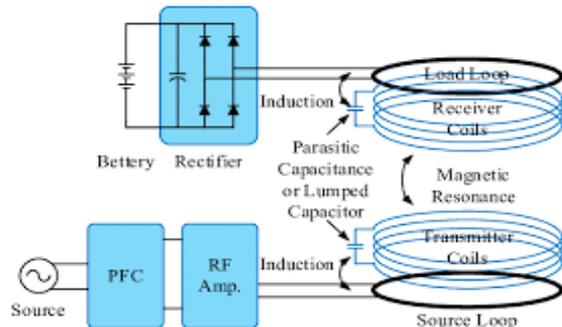


Fig. 2. Resonance Charging

III. WIRELESS CHARGING OF ELECTRIC VEHICLE

A. Electric Vehicle

An electric vehicle (EV) is a vehicle that runs on electricity rather than gasoline or diesel. As a result, such a vehicle is being considered a viable replacement for current-generation vehicles to solve issues such as rising pollution, global warming, natural resource depletion, and so on. [4] Over the last decade, the development of electric cars has accelerated significantly. Part of this is due to cities' desire to move away from petrol-diesel-powered cars to help offer cleaner cities, especially in light of global urbanization, and partially due to electric vehicles becoming more efficient and cost-competitive.

The cars' batteries, on the other hand, maybe charged wirelessly without the need for a socket. The likelihood of charging automobiles using the plug-in technique will be lowered with wireless charging equipment fitted into vehicles. To charge the vehicle's battery, the traveler merely needs to park over a coil put on the ground. Wireless charging systems have an advantage over plug-in charging systems in terms of dependability, simplicity, and adaptability. The battery may be charged both when the vehicle is stopped and when it is moving with this technique. [5]

B. Wireless Charging

Wireless Charging allows electric energy from the main supply to be transported without the need for wires to a vehicle's high-voltage battery. Similar to that of a transformer, for wireless charging, there are transmitters and receivers in wireless charging. A 220V 50Hz AC supply is transformed into a high-frequency alternating current, which is then supplied to the transmitter coil, which creates an alternating magnetic field that cuts the receiver coil and causes Alternating Current power output in the receiver coil. However, maintaining the resonance frequency between the transmitter and receiver is highly significant for efficient wireless charging. Compensation networks are implemented on both sides to preserve the resonant frequencies. Finally, this AC power is rectified to DC at the receiver and delivered to the battery via the Battery Management System (BMS).

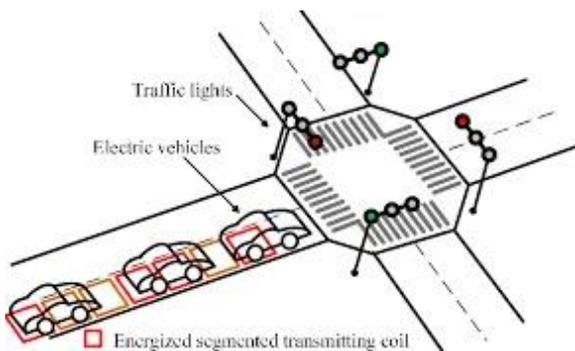


Fig. 3. Electric Vehicles

C. Types of Wireless Charging for Electric Vehicles

Wireless charging systems for electric vehicles may be divided into two groups based on the application.[6]

1. Static Wireless Charging
2. Dynamic Wireless Charging

1) STATIC WIRELESS CHARGING

When the car remains still, it is charged. So we could just park the EV in a parking area or in a garage that is connected to WCS. The transmitter is installed beneath the earth, while the receiver is installed beneath the car. Align the transmitter and receiver before leaving the vehicle to charge. The charging time is determined by the AC supply power level, transmitter and receiver distance, and pad sizes. This Static Wireless Charging Station is best suited for regions where electric vehicles are parked for an extended period.

The charging time of an electric car is determined by the size of the charging pad, the amount of power supplied, and the distance (air gap) between the transmitter and receiver.

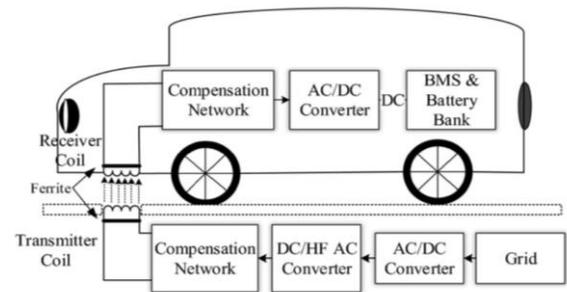


Fig. 4. Static Wireless Charging

2) DYNAMIC WIRELESS CHARGING

The car is charged while in motion, as the name implies. A stationary transmitter transmits electricity over the air to a moving vehicle's reception coil. [7]With DWCS, an electric vehicle's range might be extended by continuously charging its battery while traveling on roads and highways. It eliminates the need for significant energy storage, thus reducing vehicle weight.

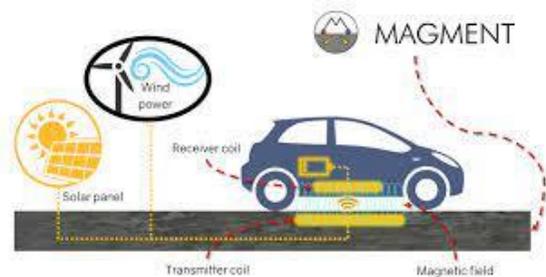


Fig. 5. Dynamic Wireless Charging

IV. PROJECT

A. AIM

The goal of this mini-project is to charge an electric vehicle using the static wireless charging method. A receiving coil from an electric car will be put over the charging port's built-in transmitting coil. The LED above the car will flash when electricity is given, indicating static charging is successful.

B. COMPONENTS USED

1. *Three Transformers of 220V 500mA* - A transformer is a device that changes voltage levels from high to low or from low to high. The mutual induction principle, commonly known as Faraday's Law of Electromagnetic Induction, governs the operation of a transformer. The experiment employed a step-down transformer, which transforms high voltage electricity into low voltage power. A step-down transformer is one that has a higher number of turns in the primary winding and a lower number in the secondary winding. [8] When the main number of turns is more than the secondary number of turns, the EMF generated in the secondary is less than the primary input, resulting in a low voltage in the secondary coil of a transformer.
2. *Two LED* - When an electric current runs through a Light Emitting Diode (LED), it emits light. Light is produced when holes from p-type semiconductors recombine with electrons from n-type semiconductors. When the electric car is put over the transmitting coil, an LED is utilized to signal that it is charging.
3. *Two Coils - Transmitting Coil and Receiving Coil* - The transmitter and receiver coils combine to form a system of magnetically connected inductors. A magnetic field is created by an alternating current in the transmitter coil, which produces a voltage in the reception coil. This voltage is utilized to power a gadget or charge a battery in this scenario.



Fig. 6. Step-down Transformer



Fig. 7. LED

C. PROCEDURE

Inductive charging is based on the usage of two electromagnetically connected coils. The static wireless charging method is used in this project. The primary coil is installed on the road surface in a pad-like structure that is connected to the power grid. The secondary coil is mounted on the electric vehicle, preferably on the bottom or top. Within the offboard charging station, the grid's Alternating Current power is rectified to Direct Current and then transformed to a high-frequency Alternating Current power. Electromagnetic induction then transfers this high-frequency power to the Electric Vehicle side. The car's coils convert this high-frequency AC electricity back to DC, allowing the onboard charger to charge the EV.

The vehicle's batteries may be charged autonomously while it is parked in static mode, with the transmitter contained with the primary coil. The transmitter coil transmits an AC signal. The AC is received by the receiver coil, which is enclosed with the secondary coil and positioned on the vehicle's underbelly. Two LED bulbs are attached to the top of the vehicle to respond when the vehicle charges.

Three primary transformers are connected in parallel and their secondary component is connected in the series with a coil. When power is supplied to the circuit, the coil is energized and as a result of it, magnetic flux is produced. Then due to the effect of electromagnetic induction, the coil placed under the car is also energized and an alternating current is developed in it. As a result, the LED bulb attached to the top of the car glows, as a response to charging.

D. CIRCUIT DIAGRAM

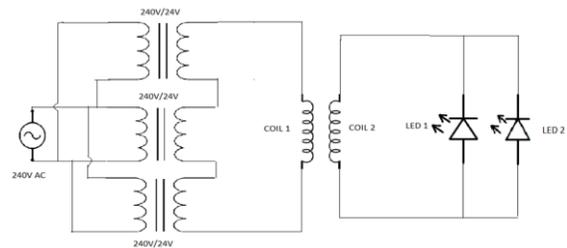


Fig. 8. Circuit Diagram

The three step-down transformers, each having a voltage of 220V and a current of 500mA, are linked in parallel so that they have the same potential difference between them. These transformers are connected to the power source. These transformers are linked in series with the primary coil (Coil 1), commonly known as the transmitting coil. The secondary coil(Coil 2), also known as the receiving coil, is linked in series with two LEDs that are connected in parallel.

E. OBSERVATIONS

As soon as the electric car's receiving coil makes contact with the transmitting coil beneath it, the LED linked to the electric vehicle illuminates. This method of charging is convenient to use and extremely user-friendly. It is an excellent method of charging the self-driven cars which are gaining high demand in today's world.

F. PROBLEMS FACED

With advancement comes difficulties, stated below are just a few difficulties that this mini-project faced. [9]

1. One of the issues that were evident was that on a larger scale, this method of charging large financial investments is needed. Setting up charging pads, and designing these cars require a huge amount of resources.
2. Charge pads that hold the transmitting coil require a limited amount of area and are heavy. Due to this reason, these charging pads cannot be moved from place to place. The vehicle should be brought to the charging pad rather than moving the pad.
3. There should be a high tolerance for misalignment between the car and the charging pad. When a car is parked, it should be aligned properly over the charging pad, otherwise, the charging process wouldn't take place properly and efficiently. [10] Self-tuning methods have been devised to overcome this issue.
4. In comparison to conductive charging, there are power losses and a reduced efficiency with the inductive charging method.
5. In this charging method, a high risk of exposure to electromagnetic radiation is involved. Hence, high care should be taken while handling.
6. Electric vehicles need long-lasting batteries so that they can last longer for long distances or by the time they reach their destination.[11]

G. RESULT

The LED attached to the electric vehicle glows as soon as the receiver coil in the electric vehicle comes in contact with the transmitting coil placed beneath.

V. APPLICATIONS

Wireless charging technology has swiftly surpassed traditional charging methods. Not only that but it's now being used in industries where it wasn't even considered decades before.

Some of its efficient and life-changing applications are discussed below:

1. Norway is placing charge plates on the road that connect to energy receivers in the taxis themselves to implement the wireless taxi charging system. The objective is to make charging electric taxis as simple as possible, as it is currently inconvenient, time-consuming, and costly. Taxis can be charged at a taxi rank, which is a slow-moving queue where cabs line up to wait for customers, using induction, which is more energy-efficient.
2. The most popular wireless standard is Qi. The Wireless Power Consortium (WPC) established Qi as a standard for inductive charging across distances of up to 40mm. Several major smartphone manufacturers use the Qi wireless charging standard, including Samsung, Apple, Sony, LG, HTC, Huawei, Nokia (HMD), Motorola, and Blackberry. It has a frequency of 110-22 kHz and a power of under 100 watts. In-vehicle charging, phone chargers, infrastructure charges, home robotics, laptop computers, and speakers all use this standard.
3. The Ki cordless kitchen standard was launched by the Wireless Power Consortium (WPC) in 2019. This standard covers cordless kitchen gadgets that use up to 2.2kW of power, such as low-voltage juicers, kettles, and other heating appliances. The gadgets are powered by inductive charging technology. This standard is used in devices that require up to 2200W of power and have a frequency of 13.56MHz 50-60kHz.
4. The Society of Automotive Engineers (SAE) has established a wireless power transfer (WPT) standard for electric vehicles (SAE). Resonant inductive coupling is the charging mechanism employed in this system. According to Forbes, the SAE revealed that wireless charging over a 10-inch air gap may achieve up to 94% efficiency. The Ground Assembly (GA), which links the charging hardware to the grid, and the Vehicle Assembly (VA), which is a form of on-vehicle equipment located on the opposite side of the vehicle, make up the WPT system.

VI. CONCLUSION

Wireless charging is becoming more popular in many sectors nowadays. Because it comes with several advantages: The following are the key benefits of this method of charging:

- Infrastructure expenses of wireless charging methods are lower compared to wireless methods.

- High-efficiency power transfer is obtained by wireless charging methods.
- High-speed charging is a possibility that can be attained in wireless charging but it would further increase costs.
- Maintenance needs are minimal in wireless charging methods.
- There are hardly any electromagnetic emissions. Therefore, causing no harm to anyone.

The popularity of wireless charging technologies has increased the demand for electric vehicles. It has the following advantages which have made them popular in today's society.

- They save money on petrol because no fuel is necessary.
- They are eco-friendly since they do not release toxins. Electric car drivers have cut CO₂ emissions by more than 177,758,804 kg.
- Because of the efficient electric motor, there is less maintenance. Electric motors feature fewer parts than typical non-electric vehicles, resulting in less damage and lower running costs.
- Electric vehicles are not only lighter, but they also accelerate more quickly.

With these benefits in mind, this project may be further by using the dynamic charging approach and making more adjustments to the circuitry and process. In practical life, dynamic charging for electric vehicles involves intelligent routing[12] inroads for effective charging of these vehicles and leading a healthy and pollution-free environment.

REFERENCES

[1] Feng, Hao; Tavakoli, Reza; Pantic, Zeljko; Onar, Omer C. (2020).

Advances in High-Power Wireless Charging Systems: Overview and Design Considerations. *IEEE Transactions on Transportation Electrification*

[2] Shinohara, N. (2019). Wireless Power Transmission: Inductive Coupling, Radio Wave, and Resonance Coupling. *Advances in Energy Systems: The Large-scale Renewable Energy Integration Challenge*, 211-220.

[3] Wu, H. H., Gilchrist, A., Sealy, K., Israelsen, P., & Muhs, J. (2011, May). A review on inductive charging for electric vehicles. In *2011 IEEE international electric machines & drives conference (IEMDC)* (pp. 143-147). IEEE.

[4] Jang, Y. J. (2018). Survey of the operation and system study on wireless charging electric vehicle systems. *Transportation Research Part C: Emerging Technologies*, 95, 844-866.

[5] Sun, X., Li, Z., Wang, X., & Li, C. (2019). Technology development of electric vehicles: A review. *Energies*, 13(1), 90.

[6] Panchal, C., Stegen, S., & Lu, J. (2018). Review of static and dynamic wireless electric vehicle charging systems. *Engineering science and technology, an international journal*, 21(5), 922-937.

[7] R. Tavakoli and Z. Pantic, "Analysis, Design, and Demonstration of a 25-kW Dynamic Wireless Charging System for Roadway Electric Vehicles," in *IEEE Journal of Emerging and Selected Topics in Power Electronics*, vol. 6, no. 3, pp. 1378-1393, Sept. 2018, doi: 10.1109/JESTPE.2017.2761763.

[8] S. Bhattacharya and Y. K. Tan, "Design of static wireless charging coils for integration into electric vehicle," 2012 IEEE Third International Conference on Sustainable Energy Technologies (ICSET), 2012, pp. 146-151, doi: 10.1109/ICSET.2012.6357389.

[9] Sanguesa, J. A., Torres-Sanz, V., Garrido, P., Martinez, F. J., & Marquez-Barja, J. M. (2021). A review on electric vehicles: Technologies and challenges. *Smart Cities*, 4(1), 372-404.

[10] A. Kamineni, G. A. Covic and J. T. Boys, "Self-Tuning Power Supply for Inductive Charging," in *IEEE Transactions on Power Electronics*, vol. 32, no. 5, pp. 3467-3479, May 2017, doi: 10.1109/TPEL.2016.2590571.

[11] K. N. Mude, "Battery charging method for electric vehicles: From wired to on-road wireless charging," in *Chinese Journal of Electrical Engineering*, vol. 4, no. 4, pp. 1-15, Dec 2018, doi: 10.23919/CJEE.2018.8606784.

[12] D. Kosmanos et al., "Route Optimization of Electric Vehicles Based on Dynamic Wireless Charging," in *IEEE Access*, vol. 6, pp. 42551-42565, 2018, doi: 10.1109/ACCESS.2018.2847765.

Verilog Code Tester using Microcontroller

Najeeb Mohammad Khan, Aahan Bhargava, Karan Kumar

Electronics & Communications Engg. Department
Maharaja Surajmal Institute of Technology

Abstract: Digital logic designing is a course where students learn to design digital logic design using Hardware Description Languages (HDL) like Verilog, VHDL etc. In such courses, we need to use Field Programmable Gate Array (FPGA) for the implementation and debugging of HDL code via the use of hardware.

Such FPGA boards are costly to purchase, and hence out of reach of a regular student. We aim to develop an inexpensive hardware solution using micro-controller, which could be used in place of FPGA for the purpose of testing the Verilog (HDL Code) via test bench. This will include the emulation of the working of FPGA to display the output of the Verilog Code onto the output devices like LEDs, Seven Segment Displays, Buzzers etc.

I. INTRODUCTION

After the completion of digital logic designing via HDL code is done, the verification of the logic could be performed via two options (as we are aiming to develop solution for novice students, we are excluding the professional methods where we make use System Verilog, verification methodologies etc.):

- 1) Output Waveform Method
- 2) Hardware Implementation Method

In Output Waveform Method, we use a testbench for compilation and creation of an output waveform of the HDL code (through a software compiler like Icarus Verilog Tool). A testbench is an HDL code written to drive the digital logic by providing the input to the input ports and reading the corresponding output on the output port of the logic design code. Such waveforms could be viewed using any waveform viewer (such as GTK Wave Software Tool). Despite not being an efficient method, it is the easiest way to produce the output to verify the logic. Logic verification using reading of waveforms is a slow process with higher possibilities of making mistakes and confusion.

Such drawbacks are overcome using hardware implementation of HDL code onto the devices like FPGA boards.

In the method of Hardware Implementation, we can directly implement the output onto the hardware to view that output using the LEDs, Buzzers and other output displaying devices. This process of verification significantly reduces the time to validate the output and possibility of any error.

Implementation of the HDL code onto the hardware can be achieved either by providing the input using test bench HDL code or by using the buttons/switches present on the hardware board. We will be using the implementation using test bench

code as it is much easier and simpler.

This paper describes the method we will use to implement this idea for the creation of an inexpensive hardware solution.

II. AIMS / OBJECTIVES

We aim to make an embedded system-based solution where a stm32 based micro-controller will be used for emulating the working of Verilog HDL code inside the FPGA Board with the help of Verilog testbench.

III. LITERATURE SURVEY

Semiconductor devices that are built around a matrix of configurable logic blocks (CLBs) connected via programmable interconnects are called FPGA. After production, it can be reprogrammed to meet specific applications/features. They are frequently accessed for applications that include streaming, data processing and heavy dataflow because of low power and high computing density. They are being capitalized by many cloud service providers (CSPs) to speed up network encryption, deep learning, memory caching, etc.

Uses of FPGA

- Designing ASICs using FPGA
- Improvement in automotive experience like cruise control, blind spot warning, etc.
- Supporting real time systems
- Usage in software design networks
- Used in data centers and cloud
- In computer vision system such as facial recognition

Use of Verilog Code Testing incorporates software design networks feature of FPGA as well as it comes within the permissible limits of its consumers due to reduction in cost.

We will be using open-source software tools along with readily available hardware components to make a fully functional hardware solution. It is to be noted that FPGA is a very complex integrated circuit with multiple use cases, we will be emulating only the Verilog code testing part with the help of a test bench.

Software Components used

- 1) Icarus Verilog synthesis tool.
=> Used for compiling the Verilog code and generating output.

- 2) GTK wave.
=> Used for viewing the waveform of the generated output.
- 3) ARM Cross Compiler.
=> Used for generating the binary file which is to be uploaded into micro-controller.
- 4) GNU Make.
=> For automating the compilation and testing process of micro-controller code.

Hardware Components to be used

- 1) Stm32f103 based micro-controller (MCU) board.
=> Used for controlling the Seven Segment Displays and LEDs.
- 2) St-Link Programmer.
=> Used for programming stm32 based micro-controller board.
- 3) Seven Segment Displays (SSD).
=> Used for displaying output.
- 4) Max7219 Seven Segment Display Driver IC
=> Used for controlling SSDs
- 5) 74HC595 Serial-In Parallel-Out Shift Register IC.
=> Used for controlling LED Array.
- 6) 5mm Light Emitting Diodes (LED)
=> Used for displaying output.
- 7) Logic Analyzer.
=> Used for debugging the communication protocols.
- 8) Resistors and Capacitors.
=> Used for limiting and stabilizing the current & voltage within the circuit.

IV. METHODOLOGY / MATERIALS

In analytical reports, like business reports, this would include a description of survey methods, participants, focus groups and the use of secondary sources. In scientific reports it would include a description of participants, materials, equipment, design and procedure.

This section is important and should be written concisely and clearly so that a fellow researcher will be able to reproduce your work and arrive at similar results by reading and following your reported methodology. Therefore, all the steps used must be presented clearly, so that they can be reproduced by others seeking to build on your research.

Where appropriate, describe your selection of experimental samples and controls, and the reasons for selecting them. Describe the methods and tools or apparatus used to carry out your experiment or survey, giving references to published methods you have followed. If you have developed your own methods or tools, refer to the literature which the ideas were based. Illustrations, if applicable, are very useful to help describe and illustrate the experimental set-up you adopted.

Present the degree of precision and accuracy obtained using the methods you have employed.

V. RESULTS / DISCUSSION

Present your results and findings in a logical sequence of text, tables and figures, in a clear, concise manner. Do not repeat, in your text, all the data given in the tables and figures; **instead emphasise or summarise the important observations from the tables and figures**

Present your error analysis and your estimates for any measurements made.

Only original results must be submitted. All figures should be digitally created with the exception of biological drawings, which may be drawn by hand.

The significance and interpretation of the results of your study should be clearly presented in your discussion. Emphasise any new and important aspects that have been identified as a result of the study, and any conclusions you can draw that follow from these findings.

Include in your discussion the implications of the findings, and the limitations, and related to your observations to other relevant studies covered in your literature survey.

Link the conclusion of your discussion with the aims or goals of your study. Avoid unqualified statements and conclusions not completely supported by your data.

You may choose to merge your results and discussion, presenting them concurrently under the heading RESULTS and DISCUSSION or separately by inserting another heading for DISCUSSION.

VI. CONCLUSION

Advantages

- 1) It is an inexpensive hardware solution for testing/verifying those logic designs implemented using Verilog HDL code with the help of test bench.
- 2) Easy to use and provides much comprehensive understanding of the digital logic designed by the students.

Disadvantages

- 1) As this implementation is based on testbench code, we can't use switches and buttons for the provision as an input to our digital logic design. This restricts the user's ability to test the code for various orders of inputs sequences to verify the overall functioning.

Even though the user can provide all the possible input combinations but disdain in changing the sequence of such inputs while running of program onto the hardware. For such alterations, the user had to make

such variations in test bench to organize and transfer the code containing the new input sequence into the micro-controller.

This drawback can be resolved if the user had ability to apply any input at any point of time. Such capability is provided if switches and buttons can be used for providing the input to the HDL code. This way of implementation needs the handling of Verilog to C compiler which is out of scope for this paper.

- 2) Speed of operation is much slower with respect to the actual FPGA., this is due to the fact that we are

operating micro-controller to emulate the FPGA working and micro-controllers works at much lower operating clock speed as compared to FPGA clock speeds. Hence, we should use this hardware solution for designs which don't require any high-speed computations.

REFERENCES

- [1] <https://www.logic-fruit.com/blog/fpga/what-is-fpga/>
- [2] <https://www.fpga-key.com/technology/details/fpga-history-current-situation-and-future>
- [3] <https://digilent.com/blog/history-of-the-fpga/>

Theorem of L_p -Norm by Linear Combination for Baskakov Durrmeyer Operators

Man Singh Beniwal

Department of Applied Sciences
Maharaja Surajmal Institute of Technology
Janakpuri, New Delhi – 110058
mansingh@msit.in

Abstract: In recent past I studied basic results [5] and one direct result [6] for L_p -Norm by linear combination for certain Baskakov-Durrmeyer operators. I extended the study to prove one more direct result for L_p -Norm for linear combinations for certain Baskakov-Durrmeyer operators.

Keywords: Linear positive operators; Baskakov-Durrmeyer operators; Basic Results.

I. INTRODUCTION

Gupta et al [9] introducing the following Baskakov-Durrmeyer operators as

For $f \in C_\alpha[0, \infty) \equiv f \in C[0, \infty); |f(t)| \leq M(1+t)^\alpha$, for some $M > 0, \alpha > 0$, [9] are defined as

$$B_n(f(t), x) = \sum_{v=1}^{\infty} p_{n,v}(x) \int_0^{\infty} b_{n,v}(t) f(t) dt + p_{n,0}(x) f(0)$$

$= \int_0^{\infty} W_n(x, t) f(t) dt$ where

$$p_{n,v}(x) = \binom{n+v-1}{v} \frac{x^v}{(1+x)^{n+v}},$$

$$b_{n,v} = \frac{1}{B(n+1, v)} \frac{y^{v-1}}{(1+t)^{n+v+1}}$$

and

$$W_n(x, t) = \sum_{v=1}^{\infty} p_{n,v}(x) b_{n,v}(t) + p_{n,0}(x) \delta(t),$$

and $\delta(t)$ being the Dirac-delta function.

The space $C_\alpha[0, \infty)$ is normed by

$$\|f\|_{C_\alpha} = \sup_{0 \leq t < \infty} |f(t)(1+t)^{-\alpha}|.$$

Let $d_0, d_1, d_2, \dots, d_k$ be $k+1$ arbitrary but fixed distinct positive integers. Then, the linear combination

$B_n(f, k, x)$ of $B_{d_j n}(f, x), j = 0, 1, 2, \dots, k$ is given by

$$B_n(f, k, x) = \sum_{j=0}^k C(j, k) B_{d_j n}(f, x),$$

where $C(j, k) = \prod_{\substack{i=0 \\ i \neq j}}^k \frac{d_j}{d_j - d_i}, k \neq 0$ and $C(0, 0) = 1$.

These linear combinations were first used by May [2]

And later by Kasana [3] so exponential operators.

Direct Theorem

Theorem 2.1 Let $f \in L_1[0, \infty)$. If f has $2k+1$ derivatives on I_1 with $f^{(2k)} \in A.C.(I_1)$ and $f^{(2k+1)} \in B.V.(I_1)$, then for all n sufficiently large

$$\|B_n(f, k, \cdot) - f\|_{L_1(I_2)} \leq M n^{-(k+1)} \left(\|f^{(2k+1)}\|_{B.V.(I_1)} + \|f^{(2k+1)}\|_{L_1(I_2)} + \|f\|_{L_1[0, \infty)} \right)$$

where M is a constant independent of f and n .

Proof. By the given assumptions on f , for almost all $t \in I_1$ and for all $x \in I_2$,

we have

$$f(t) = \sum_{i=0}^{2k+1} \frac{(t-x)^i}{i!} f^{(i)}(x) + \frac{1}{(2k+1)!} \int_t^x (t-w)^{2k+1} df^{(2k+1)}(w) \phi(t) + F(t, x)(1-\phi(t))$$

where $\phi(t)$ denotes the characteristic function of I_1

$$\text{and } F(t, x) = f(t) - \sum_{i=0}^{2k+1} \frac{(t-x)^i}{i!} f^{(i)}(x),$$

for almost all $x \in I_2$ and for all $t \in [0, \infty)$.

Thus, by using linear combination (4.2), we have

$$B_n(f, k, x) - f(x) = \sum_{i=1}^{2k+1} \frac{f^{(i)}(x)}{i!} B_n((t-x)^i, k, x) + \frac{1}{(2k+1)!} B_n\left(\int_x^t (t-w)^{2k+1} df^{(2k+1)}(w)\phi(t), k, x\right) + B_n(F(t, x)(1-\phi(t)), k, x) = J_1 + J_2 + J_3 .$$

Applying Lemma 2.3 [8] and [6], we obtain

$$\|J_1\|_{L_1(I_2)} \leq M n^{-(k+1)} \left(\|f\|_{L_1(I_2)} + \|f^{(2k+1)}\|_{L_1(I_2)} \right).$$

Further, to estimate J_2 , we proceed as follows:

$$K \equiv \left\| B_n\left(\int_x^t (t-w)^{(2k+1)} df^{(2k+1)}(w)\phi(t), x\right) \right\|_{L_1(I_2)} \leq \int_{a_2}^{b_2} \int_{a_1}^{b_1} W_n(x, t) |t-x|^{2k+1} \left| \int_x^t df^{(2k+1)}(w) \right| dt dx$$

For each n there exist a non-negative integer r ,

which depends on n such that $rn^{-1/2} \leq \max(b_1 - a_2, b_2 - a_1) \leq (r+1)n^{-1/2}$.

Then, we have

$$K \leq \sum_{i=0}^r \int_{a_2}^{b_2} \left\{ \int_{x+\ln^{-1/2}}^{x+(l+1)n^{-1/2}} \phi(t)W_n(x, t) |t-x|^{2k+1} \left(\int_x^{x+(l+1)n^{-1/2}} \phi(w) |df^{(2k+1)}(w)| \right) dt + \int_{x-\ln^{-1/2}}^{x-\ln^{-1/2}} \phi(t)W_n(x, t) |t-x|^{2k+1} \left(\int_{x-(l+1)n^{-1/2}}^x \phi(w) |df^{(2k+1)}(w)| \right) dt \right\} dx$$

Let $\phi_{x,c,d}(w)$ denote the characteristic function of the interval $[x - cn^{-1/2}, x + dn^{-1/2}]$

where c, d are non-negative integers. Then, we have

$$K \leq \sum_{l=1}^r \int_{a_2}^{b_2} \left\{ \int_{x+\ln^{-1/2}}^{x+(l+1)n^{-1/2}} \phi(t)W_n(x, t) l^{-4} n^2 |t-x|^{2k+5} \left(\int_x^{x+(l+1)n^{-1/2}} \phi(w)\phi_{x,0,l+1}(w) |df^{(2k+1)}(w)| \right) dt \right.$$

$$\left. + \int_{x-(l+1)n^{-1/2}}^{x-\ln^{-1/2}} \phi(t)W_n(x, t) l^{-4} n^2 |t-x|^{2k+5} \left(\int_{x-(l+1)n^{-1/2}}^x \phi(w)\phi_{x,l+1,0}(w) |df^{(2k+1)}(w)| \right) dt \right\} dx + \int_{a_2}^{b_2} \int_{-n^{-1/2}}^{a_1+n^{-1/2}} \phi(t)W_n(x, t) |t-x|^{2k+1} \left(\int_{x-n^{-1/2}}^{x+n^{-1/2}} \phi(w)\phi_{x,1,1}(w) |df^{(2k+1)}(w)| \right) dt dx \leq \sum_{l=1}^r \left\{ l^{-4} n^2 \int_{x+\ln^{-1/2}}^{x+(l+1)n^{-1/2}} \phi(t)W_n(x, t) |t-x|^{2k+5} \left(\int_{a_1}^{b_1} \phi_{x,0,l+1}(w) |df^{(2k+1)}(w)| \right) dt + \int_{x-(l+1)n^{-1/2}}^{x-\ln^{-1/2}} \phi(t)W_n(x, t) |t-x|^{2k+5} \left(\int_{a_1}^{b_1} \phi_{x,l+1,0}(w) |df^{(2k+1)}(w)| \right) dt dx \right\} + \int_{a_2}^{b_2} \int_{-n^{-1/2}}^{a_1+n^{-1/2}} \phi(t)W_n(x, t) |t-x|^{2k+1} \left(\int_{a_1}^{b_1} \phi_{x,1,1}(w) |df^{(2k+1)}(w)| \right) dt dx$$

By using Lemma 2.1 [8] and Fubini's theorem in the next step we proceed as follows:

$$K \leq M n^{-(2k+1)/2} \left\{ \sum_{l=1}^r l^{-4} \left(\int_{a_2}^{b_2} \int_{a_1}^{b_1} \phi_{x,0,l+1}(w) |df^{(2k+1)}(w)| dx + \int_{a_2}^{b_2} \int_{a_1}^{b_1} \phi_{x,l+1,0}(w) |df^{(2k+1)}(w)| dx \right) + \int_{a_2}^{b_2} \int_{a_1}^{b_1} \phi_{x,1,1}(w) |df^{(2k+1)}(w)| dx \right\} \leq M n^{-(2k+1)/2} \left\{ \sum_{l=1}^r l^{-4} \left(\int_{a_1}^{b_1} \left(\int_{w-(l+1)n^{-1/2}}^w dx \right) |df^{(2k+1)}(w)| + K \right) \right.$$

$$\left. \text{where } K = \int_{a_1}^{b_1} \left(\int_w^{w+(l+1)n^{-1/2}} dx \right) |df^{(2k+1)}(w)| \right\} + \int_{a_1}^{b_1} \left(\int_{w-n^{-1/2}}^{w+n^{-1/2}} dx \right) |df^{(2k+1)}(w)| \leq M n^{-(k+1)} \|f^{(2k+1)}\|_{B.V.(I_1)} .$$

Hence

$$\|J_2\|_{L_1(I_2)} \leq M n^{-(k+1)} \|f^{(2k+1)}\|_{B.V.(I_1)},$$

where the constant on right hand side depends on k .

Finally, we estimate J_3 .

For all $t \in [0, \infty) \setminus [a_1, b_1]$ and all $x \in I_2$, we can choose a $\delta > 0$ such that $|t-x| \geq \delta$.

Thus,

$$\begin{aligned} & \|B_n(F(t, x)(1 - \phi(t)), x)\|_{L_1(I_2)} \\ & \leq \int_{a_2}^{b_2} \int_0^\infty W_n(x, t) |f(t)| (1 - \phi(t)) dt dx \\ & + \sum_{i=0}^{2k+1} \frac{1}{i!} \int_{a_2}^{b_2} \int_0^\infty W_n(x, t) |f^{(i)}(x)| |t - x|^i (1 - \phi(t)) dt dx \\ & =: J_4 + J_5. \end{aligned}$$

For sufficiently large t there exist positive constants such that

$$\frac{(t - x)^{2k+2}}{t^{2k+2} + 1} > M \text{ for all } t \geq M, x \in I_2.$$

By Fubini's theorem and Lemma 2.1 [8], we get

$$\begin{aligned} J_4 & = \left(\int_0^{M} \int_{a_2}^{b_2} + \int_M^\infty \int_{a_2}^{b_2} \right) W_n(x, t) |f(t)| (1 - \phi(t)) dx dt \\ & \leq M n^{-(k+1)} \left(\int_0^{M_0} |f(t)| dt \right) \\ & + \frac{1}{M} \int_{M_0}^\infty \int_{a_2}^{b_2} W_n(x, t) \frac{(t - x)^{2k+2}}{(t^{2k+2} + 1)} |f(t)| dx dt \\ & \leq M n^{-(k+1)} \|f\|_{L_1[0, \infty)}. \end{aligned}$$

Further using Lemma 2.1 [8] and [6]

$$J_5 \leq M n^{-(k+1)} \left(\|f\|_{L_1(I_2)} + \|f^{(2k+1)}\|_{L_1(I_2)} \right).$$

Combining the estimates of J_4 and J_5 , we get

$$\|J_3\|_{L_1(I_2)} \leq M n^{-(k+1)} \left(\|f\|_{L_1[0, \infty)} + \|f^{(2k+1)}\|_{L_1(I_2)} \right).$$

The result follows, by combining the estimates of $J_1 - J_3$.

This completes the proof of Theorem 2.1

REFERENCES

- [1] A. Zygmund, Trigonometrical series, Dover Publications, Inc. N.Y. (1955)
- [2] C. P. may, Saturation and Inverse theorems for combinations of a class of exponential type operators, Canad. J. Math. 28(1976), 1224-1250.
- [3] H.S. Kasana and P.N. Agarwal, On sharp estimates and Linear Combinations of Modified Bernstein polynomials, Bull. Soc. Math. Belg. Ser. B40(1)(1988), 67-71.
- [4] Man singhbeniwal, Basic results for Lp-Approximation by Linear Combination for certain Baskakov-Durrmeyer type operators, Satyam Vol. 7(2018-19), 14-18.
- [5] Man Singh Beniwal, "Basic results for L p- Approximation by Linear Combination for Certain Baskakov-Durrmeyer Type Operators", MSIT Journal of Research, Satyam, Vol 7(2018-19), 14-18.
- [6] Man Singh Beniwal, "Direct Theorem for L p- Norm by Linear Combination for Baskakov-Durrmeyer Operators", MSIT Journal of Research, Satyam, Vol 9(2020-21), 28 - 29.
- [7] O. Agratini, An asymptotic property of integral type operator, Mathematica 40 (63) (1998), 3 - 8.
- [8] S. Goldberg and A. Meir, Minimum moduli of ordinary differential operators, Proc. London Math. Soc. 23(3) (1971), 1 - 15.
- [9] V. Gupta, M.A. Noor, M.S. Beniwal and M.K. Gupta On Simultaneous approximation for certain Szasz-baskakovDurrmeyer type Operators. J. Inequal Pure and Appl Math, 7(4) ASRT. 125, 2006.

Price Prediction Application on AWS

Sandeep Kumar¹, Jay Seth², Khushi³

^{1,2,3}Department of Computer Science and Engineering,
Maharaja Surajmal Institute of Technology, New Delhi, India

Abstract: This research paper proposes a means of constructing a prediction-based machine learning with high accuracy and leveraging the model to predict accurate flight prices in real-time, this is achieved by building a user interface using flask and taking live inputs, which are then sent to the model and an accurate prediction is made. The key differentiator of this project is that it is made publicly available through AWS cloud's EC2 Virtual Machine Service. This is done by ensuring industry standard best practices for networking, security and availability. The machine learning model is constructed, trained and validated on AWS SageMaker, thus making our complete approach open-sourced and highly agile.

Keywords: AWS; Cloud Computing; Machine Learning; python.

II. INTRODUCTION

A. Machine Learning

Machine Learning tells us the potential of a particular system to acquire knowledge with the help of observations on a massive scale which in flip enables the system to make itself higher and improve, instead of being programmed with expertise. The call for artificial intelligence turned into a given start by way of John McCarthy in 1956. Since then, artificial intelligence has developed into a field that is particularly complex with numerous uses. Some of the popular make use of AI are smartphones around us, and pinnacle groups make use of AI inside their chips. AI performs a big position in healthcare, and it enables the reduction of medical expenses which have been on an upward fashion for a long term. Humans often think systems gaining knowledge of and synthetic Intelligence are equal matters, however, it's not the case. You can say that synthetic Intelligence is a massive discipline, and that gadget getting to know is a subset of synthetic Intelligence. The main gist of a device gaining knowledge is to equip a system with a massive quantity of data so that it can reflect decisions which could have been made via a human. There were a few demanding situations in the area of device studying, one such arguable issue is what's going to happen whilst machines will triumph over human intelligence. Will it ever happen? If it does then it'll create a variety of inquiries to be replied to, one such query is who will be held responsible in case a coincidence occurs in a self-driving car. Those questions can only be spoken back with time and with any luck with greater development in those fields.

Some of the popular packages of device studying are the applications within the field of finance, many systems along with Betterment and Numerai have made a significant impact in finance.

B. Prediction using Machine Learning

Generating unseen values based on data from the past is called prediction. Using machine learning, we derive different algorithms to take in the raw data related to the aim and predict based on the variations and trends of the past.

C. Cloud Computing

Cloud Computing is a rising version that has turned out to be famous in nearly every commercial enterprise. It consists of the idea of demand services this means that by using cloud resources in which needed, we can rate assets in keeping with every need. Cloud computing surely offers endless advantages and is a powerful model. Cloud computing has emerged as an important device not only for the enterprise global but also for each day activities. Many organizations have opted to use cloud computing as it is far taken into consideration relaxed and exceptionally dependable particularly for tracking property. Cloud computing is the provision of on-demand offerings that include information and tasks that can be easily deleted and retrieved. Amazon is a leading company of cloud-computing offerings internationally the use of a carrier referred to as Amazon web offerings (AWS).

Recognition of the human face is a critical region in numerous disciplines which includes safety, authentication, attendance, and many others. It is presently utilized in human-pc interaction, monitoring, detection systems, and different such applications to call. Every enterprise makes use of an exclusive technique to maintain a record of the users.

D. Amazon Web Services

Amazon Web Services (AWS) is a form of cloud carrier provided using Amazon. The user is supplied with constructing blocks that can assist to build various varieties of cloud programs. They may be built in a specific way where they could paintings with each differently.

E. AWS SageMaker

Amazon Sage Maker is a cloud-based system-gaining knowledge of platform that helps customers create, design, train, song, and install gadget-getting-to-know models in production-equipped hosted surroundings. The AWS SageMaker comes with a pool of blessings. It is a service used to assist users to construct numerous sorts of fashions quite simply and at an excessive speed. It includes various modules that can without problems be utilized in sync or one by one

to construct system-studying models.

As soon as your model is skilled and tuned SageMaker uses the EC2 to expand a practical gadget mastering model. It also provides aid for the famous Jupyterpocket book which helps customers to percentage code.

Textbooks have applications and libraries for in-depth reading forums and frameworks. Engineers can put into effect a pre-constructed notebook, that's supplied through AWS for diverse purposes.

Algorithms which can be constructed based totally on necessities which might be written on the ML frames can be used. Statistics saved in S3 can be extracted, this is because there may be no data-set length restriction.

F. AWS EC2

Amazon EC2 gives the subsequent features of digital computer systems, known as instances Pre-custom designed templates on the situation, known as Amazon gadget pics (AMIs), which % the portions you want for your server (which includes operating device and additional software program). diverse CPU configurations, reminiscence, garage, and networkability in your environment, known as instance sorts. Protecting your login records with the use of key pairs (AWS maintains the key public and keeps the key non-public in a comfortable location). temporary statistics garage volumes which can be eliminated while quitting, dozing, or disconnecting your occasion, referred to as shop volumes. Volumes of continuous storage of your facts using the Amazon Elastic Block save (Amazon EBS), additionally referred to as Amazon EBS volumes.

III. LITERATURE REVIEW

Counselled study [1] plane fee forecast using machine learning strategies, through studies paintings statistics set comprising 1814 Aegean airlines facts planes was gathered and used to teach the machine learning version. A distinct range of functions has been used to train different models to expose how the choice of features may want to exchange the accuracy of the model.

In the study [2] by William Grove an agent turned into a brought who ought to improve the acquisition time on behalf of customers. The partial reversal technique is used to construct the model.

In work done by S. Rajendran, S. Srinivas, and T. Grimshaw, a comprehensive analysis of air taxi aviation has been done using Machine Learning algorithms.

A study by Santos [3] analyzed flights from Madrid to London, Frankfurt, New York and Paris within a few months. The model provides an acceptable number of days before purchasing a plane ticket. Tianyi Wang [5] is a proposed framework wherein two websites are combined with macroeconomic records and machine studying strategies which include vector help, XGBoost is used to model price ticket rates primarily based on

source pairs and destination. The body achieves a maximum accuracy of zero.869 with adjusted R + square overall performance metrics. In a study, the preferred model is used using the Linear Quantile Blended Regression method of the San Francisco – New York study where daily flight expenses are provided on an online website [6]. Two factors such as the number of days of travel and the fact that travel on weekends or during the week is considered to improve the model.

IV. APPROACH

We have managed to set up a lightweight and reusable infrastructure on AWS Cloud for our ML Model using Amazon SageMaker and S3.

- S3 is responsible for storing and providing the dataset.
- SageMaker has been configured to build and train the Machine Learning Model by setting up the development environment beforehand.
- Jupyter Notebook has been configured by installing packages and setting up the Kernel for python 3 Environment.
- Jupyter Notebook Instance also acts as the interface between the Virtual EC2 CPUs which perform the computational functionalities of our Model.
- The Dataset import and provisioning are enabled via Amazon’s Native APIs.

A. SageMaker Setup

From the AWS Console, we can go to the SageMaker service from where we can Navigate to Notebook Instance under Images and create a new Notebook Instance.

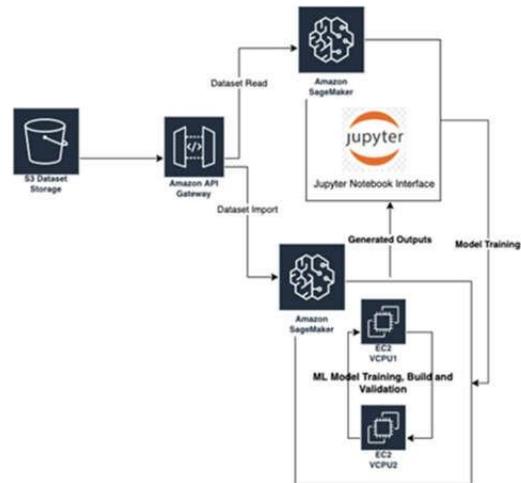


Fig. 1. SageMaker Setup.



Fig. 2. Notebook Setup.

B, Notebook Instance Setup

The Notebook Instance needs to be configured for low-cost and high-CPU memory, since we have not included the Dataset directly in our notebook thus, we can optimize higher CPU Memory by cutting down on the storage requirement.

We have decided to use the ml.t2.medium instance which has 2 Virtual 4GB CPUs dedicated solely to our Notebook, this is also the lowest cost option for our model costing less than 0.05/hr. Also, we have enabled root user access to our Notebook Enabling access to the S3 bucket where our Dataset is stored.

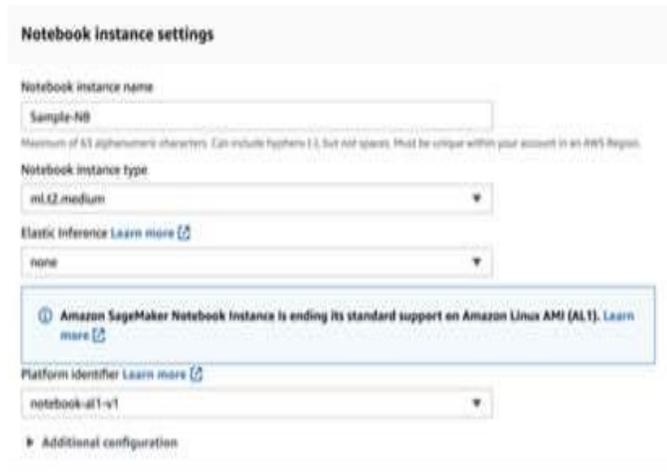


Fig. 3. Notebook Instance Setup.

After the setup, we observe that our Notebook Instance is now **InService**.

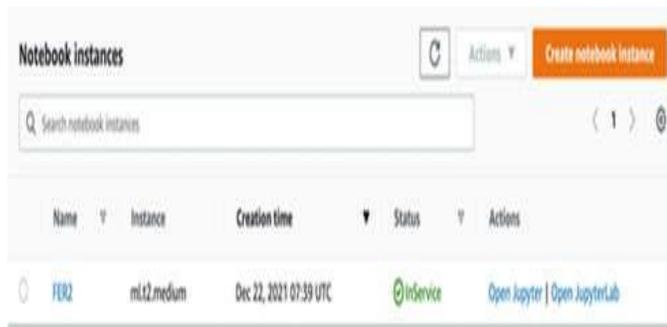


Fig.4 Jupyter Notebook Created in SageMaker.

C. Model Integration

After the Notebook setup, we have Single Click access to our dedicated Jupyter Notebook on AWS SageMaker.

To integrate our Model, we need to upload the Jupyter Notebook containing our Machine Learning Model in this setup, after the add, we configure the Kernel to Python3 and we use the import command to install crucial frameworks and libraries along with NumPy, pandas, matplotlib and seaborn.



Fig. 5. Kernel Setup.

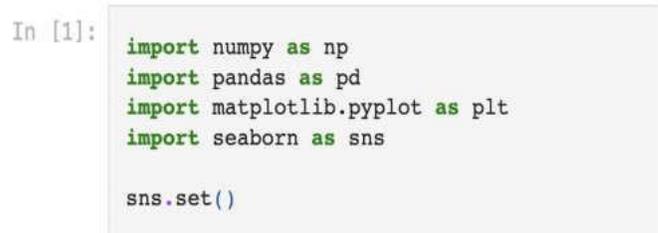


Fig. 6. Importing Packages.

A. Dataset Storing and Importing

Since our focus was to achieve higher computation with our Jupyter Notebook Instance we have decided to store the dataset in AWS S3 Bucket i.e. Simple Storage Service offered by Amazon for object storage at low costs since our Dataset is less than 1GB and is a .csv file our cost is less than \$0.023 which falls into the free tier, making this option highly in our favour.

Storing the Dataset in the S3 also allows easy updates, re-usability and rollback enablement for our ML Model.

To import our Dataset in the Model we use the s3uri to connect to our bucket and access the file using the file key variable, finally, we read the CSV file using pandas read.

In this project, a machine getting to know cycle to create a web application that would predict flight charges using a device gaining knowledge of algorithms from flight records using python libraries such as Pandas, NumPy, Matplotlib, seaborn and sklearn.

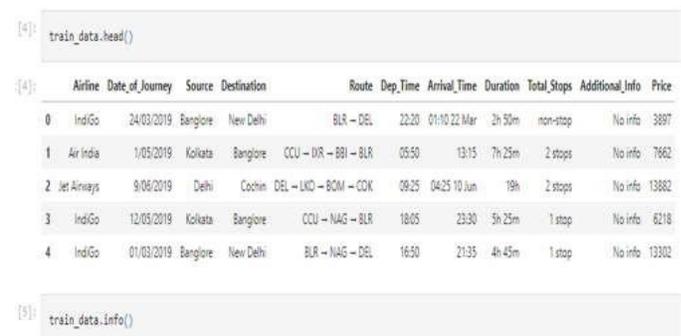


Fig. 7. Data import and read.

In the range Index, there were 10683 entries, 0 to 10682 and 11 columns.

```
<class 'pandas.core.frame.DataFrame'>
RangeIndex: 10683 entries, 0 to 10682
Data columns (total 11 columns):
#   Column                Non-Null Count  Dtype
---  ---
0   Airline                10683 non-null   object
1   Date_of_Journey       10683 non-null   object
2   Source                 10683 non-null   object
3   Destination            10683 non-null   object
4   Route                 10682 non-null   object
5   Dep_Time              10683 non-null   object
6   Arrival_Time          10683 non-null   object
7   Duration              10683 non-null   object
8   Total_Stops           10682 non-null   object
9   Additional_Info        10683 non-null   object
10  Price                 10683 non-null   int64
dtypes: int64(1), object(10)
memory usage: 918.2+ KB
```

Fig. 8. Data training output.

The next step is a preliminary analysis of the data in which we noted that most of the data was present in the character string format. Data on each aspect is extracted as day and month are issued on the day of the trip in full format, and hours and minutes are issued in travel time. Factors such as the source and destination need to be converted into values as they have been classified.

Data selection is the first step in which flight history data is collected so that the model can predict values. Our database contains over 10,000 records of related aircraft and their prices. Other features of the source data are location, departure date, departure time, stop value, arrival time, prices and a few more.

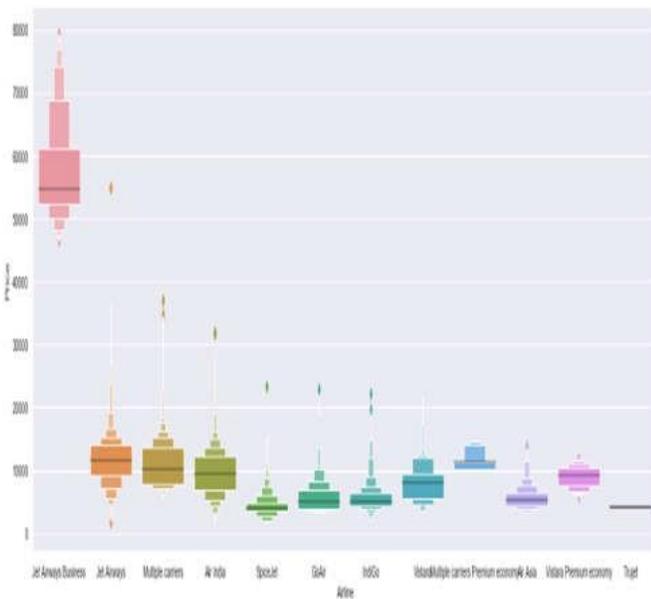


Fig. 9. Data analysis output.

Jet Airways Business has the highest Price from the above visualization result. Apart from the first Airline, almost all are having similar median.

One Hot Encoding is a way to process the functions of the types of machines studying models. This form of coding creates a new binary function for each feasible category and gives a value of one in every pattern function corresponding to its unique class.

One hot encoded copy is a very important part of the feature engineering process in training learning strategies. For example, having our variables such as colours and labels “red,” “green,” and “blue,” we could code each of these labels as a binary vector of three things such as Red: [1, 0, 0], Green: [0, 1, 0], Blue: [0, 0, 1]. Category statistics at the same time as processing, must be converted to a numeric form. One-hot encoding is regularly used to represent complete data. right here the integer encoded variables are removed, and new binary variables are delivered to every integer price. During the process, it takes a column with category data, labelled code and divides the next column into multiple columns. Numbers are changed to 1 and 0 randomly, depending on which column has a value. Although the method is useful in some ordinal cases, some input data does not have the category value level, and this can lead to problems with guessing and poor performance.

E. Feature Selection

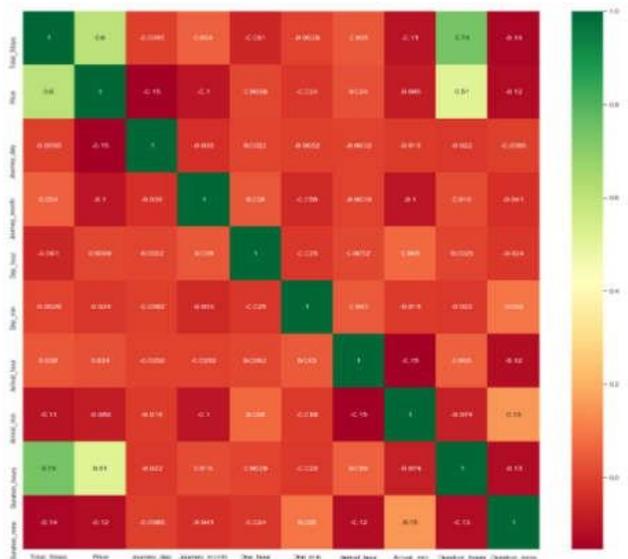


Fig. 10. Heat Map.

Feature Selection is the technique of lowering the variable in the model by using relevant data and eliminating noise in records. It's far from the technique of mechanically selecting relevant capabilities for the machine studying version primarily based on the form of hassle the model is attempting to resolve. This is achieved via which includesor excluding important features without converting them. It helps in cutting down the noise in the model and decreasing the scale of entering

information. Descent models are used to explain the connection between structured and impartial variables. The machine learning algorithms we will use in our project are Linear Regression, Decision Tree, Random Forest, Performance Metrics, MAE, MSE, RMSE and Flask.

A. Saving Model in Flask using pickle

The trained model is saved to the disk using the pickle library. Saved the model so that it can be used by the server. So, save the object regressor to the file named model.pkl.

```
from flask import Flask, request, render_template
from flask_cors import cross_origin
import sklearn
import pickle
import pandas as pd

app = Flask(__name__)
model = pickle.load(open("flight_rf.pkl", "rb"))
```

Fig. 11 Flask using pickle.

B. HTML Form with Flask

For predicting the profits from various attributes, we first need to gather the statistics (new attribute values) after which the model uses the random forest version we built.

Consequently, so one can accumulate the information we create an HTML form which could comprise all of the exclusive alternatives to pick from every characteristic.

```
<form action="/predict" method="post">
  <div class="row">
    <div class="col-sm-6">
      <div class="card">
        <div class="card-body">
          <h5 class="card-title">Departure Date</h5>
          <!-- Departure -->
          <input type="datetime-local" name="Dep_Time" id="Dep_Time" required="required">
        </div>
      </div>
    </div>
    <div class="col-sm-6">
      <div class="card">
        <div class="card-body">
          <h5 class="card-title">Arrival Date</h5>
          <!-- Arrival -->
          <input type="datetime-local" name="Arrival_Time" id="Arrival_Time" required="required">
        </div>
      </div>
    </div>
  </div>
  <br>
  <br>
  <div class="row">
    <div class="col-sm-6">
      <div class="card">
        <div class="card-body">
          <!-- Source -->
          <h5 class="card-title">Source</h5>
          <select name="Source" id="Source" required="required">
            <option value="Delhi">Delhi</option>
            <option value="Kolkata">Kolkata</option>
            <option value="Mumbai">Mumbai</option>
            <option value="Chennai">Chennai</option>
          </select>
        </div>
      </div>
    </div>
  </div>
</form>
```

Fig. 12. HTML form output.

Integrate the form in our flask app.py script as follows:

```
@app.route("/predict", methods = ["GET", "POST"])
@cross_origin()
def predict():
    if request.method == "POST":
        # Date_of_Journey
        date_dep = request.form["Dep_Time"]
        Journey_day = int(pd.to_datetime(date_dep, format="%Y-%m-%dT%H:%M").day)
        Journey_month = int(pd.to_datetime(date_dep, format="%Y-%m-%dT%H:%M").month)
        # print("Journey Date : ",Journey_day, Journey_month)

        # Departure
        Dep_hour = int(pd.to_datetime(date_dep, format="%Y-%m-%dT%H:%M").hour)
        Dep_min = int(pd.to_datetime(date_dep, format="%Y-%m-%dT%H:%M").minute)
        # print("Departure : ",Dep_hour, Dep_min)

        # Arrival
        date_arr = request.form["Arrival_Time"]
        Arrival_hour = int(pd.to_datetime(date_arr, format="%Y-%m-%dT%H:%M").hour)
        Arrival_min = int(pd.to_datetime(date_arr, format="%Y-%m-%dT%H:%M").minute)
        # print("Arrival : ", Arrival_hour, Arrival_min)
```

Fig. 13. Integration of form with flask script.

Define the route as “/predict” and we collect the input values as model values in a flask function “predict”.

H. Generating Prediction Output using Flask Web App

After collecting and feeding the model input values, predict the flight price by calling our pickle model object and providing the input values as attributes to the model object.

```
prediction=model.predict([
    Total_stops,
    Journey_day,
    Journey_month,
    Dep_hour,
    Dep_min,
    Arrival_hour,
    Arrival_min,
    dur_hour,
    dur_min,
    Air_India,
    GoAir,
    IndiGo,
    Jet_Airways,
    Jet_Airways_Business,
    Multiple_carriers,
    Multiple_carriers_Premium_economy,
    SpiceJet,
    Trujet,
    Vistara,
    Vistara_Premium_economy,
    s_Chennai,
    s_Delhi,
    s_Kolkata,
    s_Mumbai,
    d_Cochin,
    d_Delhi,
    d_Hyderabad,
    d_Kolkata,
    d_New_Delhi
])

output=round(prediction[0],2)

return render_template("home.html",prediction_text="Your Flight price is Rs. {}".format(output))

return render_template("home.html")
```

Fig. 14 Prediction outputs using Flask.

Use “model.predict” to perform and store the prediction value in an array “prediction”. Then round the output value to the closest decimals and store the output in the “output” variable. Now the output value is rendered in the html page and displayed to the user.

I. AWS EC2 Setup

To publicly deploy a model, we create a Windows 2019 Server Instance using the AWS EC2 service, with the following configurations:

1. Instance Configurations

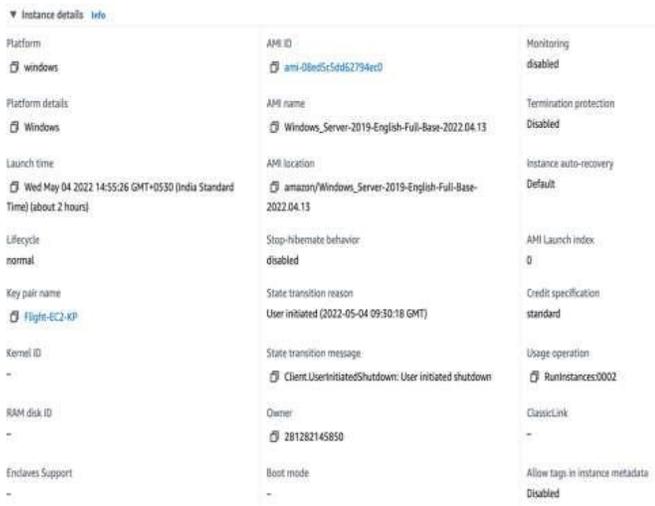


Fig. 15. Instance Configuration.

The Instance is Windows Server 2019, with a key pair to decrypt the RDP password, to connect to the machine.

2. Networking Configurations

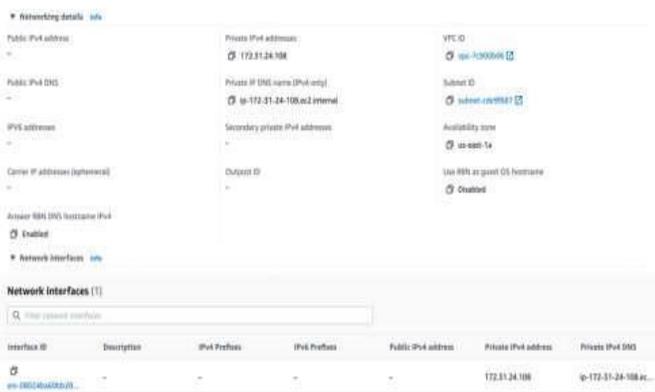


Fig. 16. Network configuration.

Attach a network interface which connects our EC2 Server to a Subnet, inside of a Virtual Network to isolate our machine and it is traffic. The Network Interface also attaches a Public and Private IP, to connect to and access the Server and also make it publicly available.

3. Security Configurations

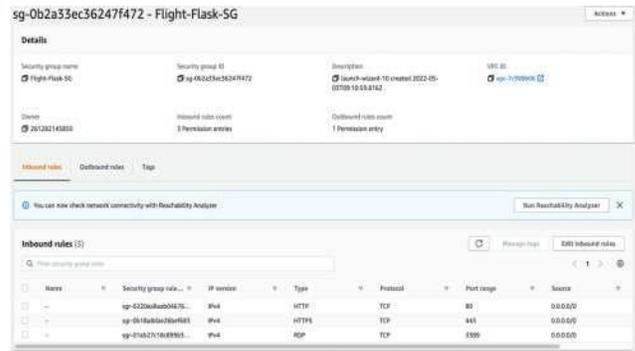


Fig. 17 Security Configuration.

Attach the following Security Group to our Instance’s Network Interface. This security group manages the inbound and outbound traffic for our machine, it allows RDP Connections and HTTP/HTTPS requests made onto the machine ports, making our machine secure and publicly accessible. All other traffic is denied.

Connecting to the machine

Connect to EC2 machine using Windows Remote Desktop Protocol.

In our Instance we choose the connect option and download the rdp client, it connects as administrator to the machine and for the password, we use our previously generated key-pair to decrypt the RDP Password.

Configuring EC2 Windows Server for hosting Flask Web App

There are a set of prerequisites which are required to create and run a Flask Application. As Flask is a micro web framework designed in Python, we need to install python first into the system. We Download the executable file and install Python in the “C:\Python” folder and add “C:\Python\” and “C:\Python\Scripts” to the system environment variables. We can verify the installation by using the command prompt (CMD).

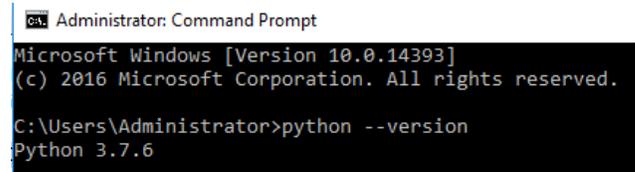


Fig. 18 Install python.

To run a flask application in the IIS server, the “flask” and “wfastcgi” libraries are needed. Install the Python libraries by executing the “pip” command in CMD.

After this step, install git on the server, to clone the web app repository onto our machine. Clone the repository and save its path for future use.

The Flask application connects with the FastCGI module of the server to expose the microservice APIs. So, install the IIS feature in the Windows server and enable the CGI role. Open Server Manager and select Manage > Add Roles and Features and select “Role-based or feature-based installation”.

Select “Web Server (IIS)”, and select “Add Features”.

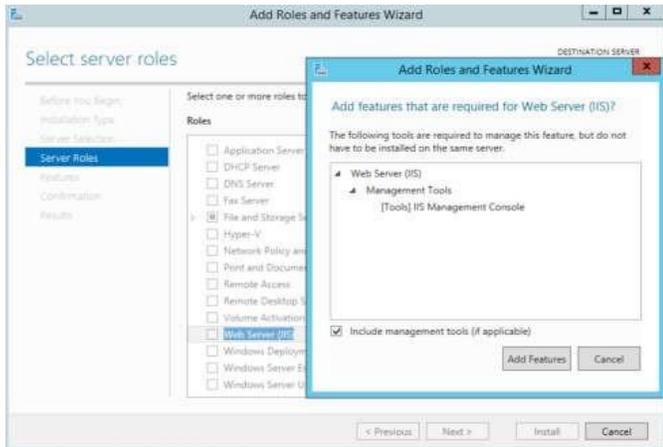


Fig. 19 Installation Wizard.

Select “CGI” under “Application Development”.

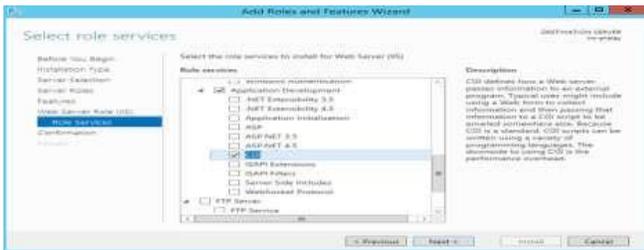


Fig. 20 CGI Feature.

Accept the default configurations and select “Install”.

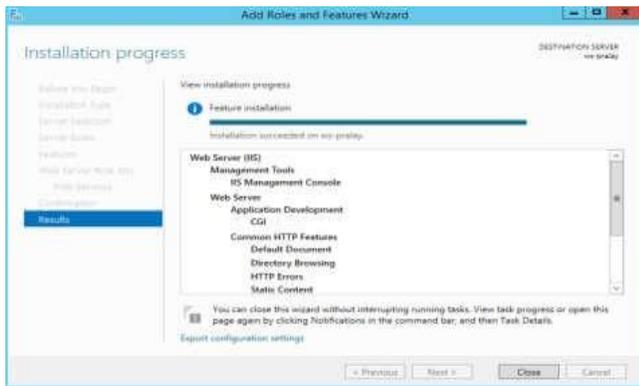


Fig. 21 Installing Features.

After the installation is complete, close the wizard.

Launch the IIS Manager by executing the following command

in Windows Run (Win + r)



Fig. 22 IIS Manager Launch.

This will launch the IIS Manager in the system. Microsoft Web Platform helps to install the Python and FastCGI modules which we have already installed earlier.

In the path “C:\Python\Scripts” execute the “wfastcgi-enable.exe” file. This will enable the FastCGI module and attach it with the IIS server.

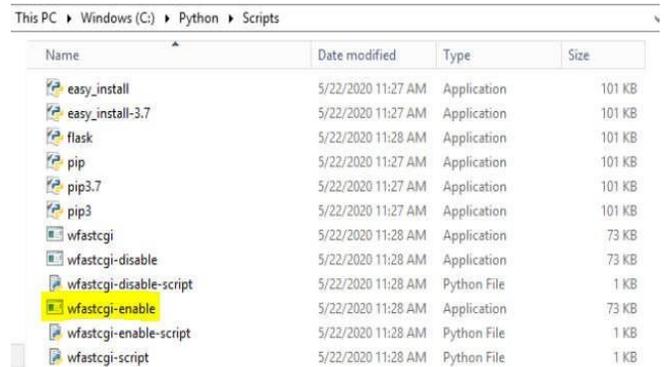


Fig. 23 Enabling FastCGI Module.

This should create an entry for FastCGI pointing to the wfastcgi module in IIS Server. Verify the entry under FastCGI Settings in IIS Manager root server.

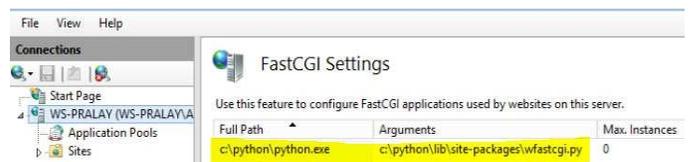


Fig. 24 Verifying FastCGI Setting.

6. Copy the Flask Application

The Previously cloned repository is copied to a directory under “C:\inetpub\wwwroot\” named “FlaskApp”. Inside FlaskApp folder, we also copy the “wfastcgi.py” file from “C:\Python\Lib\site-packages\” directory and paste it to “C:\inetpub\wwwroot\FlaskApp\” directory.

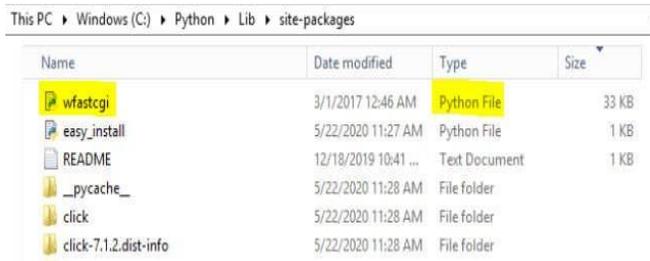


Fig. 25 Copying Flask Application.

Provide a few permissions to IIS so that it can access the FlaskApp directory. Open a CMD and change the directory to FlaskApp and execute the following commands:

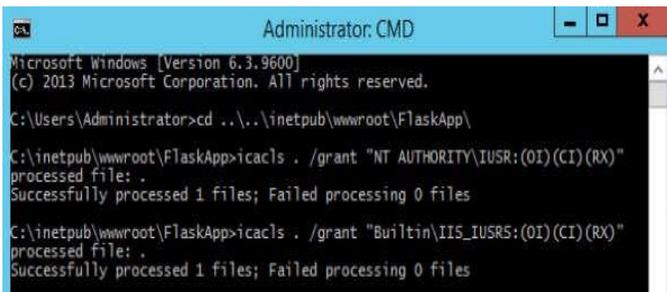


Fig. 26 Administrator CMD.

Now, as the permissions are added, it is ready to deploy the Flask application in the IIS server.

7. Create a Website in IIS Manager

To host the Flask Application, create a website using IIS Manager that can serve our application. Open IIS Manager> Sites > Default Web Site (Default Web Site must display the FlaskApp folder).

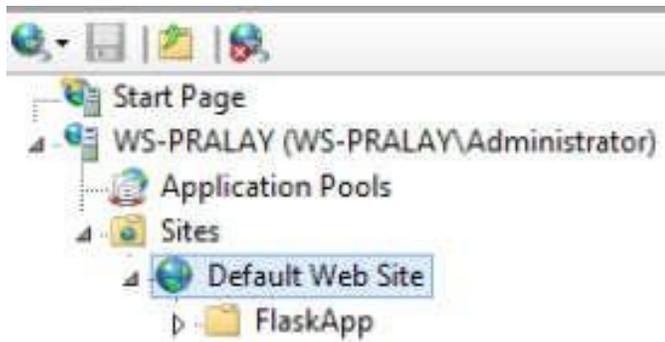


Fig. 27 IIS Manager.

Change the Default Web Site folder mapping, In Default Web Site's Advanced Settings, we update the Physical Path value by "C:\inetpub\wwwroot\FlaskApp" and select "OK". This should update the Physical Path of the Default Web Site which should now point inside the "FlaskApp" directory. Selected "Handler Mappings" in Default Web Site Home screen and Add Module Mapping as below:

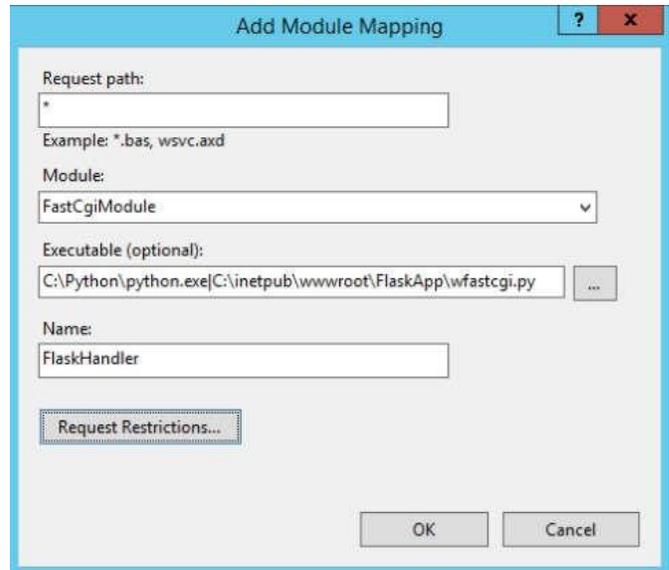


Fig. 28 Module Mapping.

In "Request Restrictions" uncheck "Invoke handler only if request is mapped to:" checkbox. Now, verify the module mapping in FastCGI Settings in the root server. This should create an entry in FastCGI Settings.



Fig. 29 FastCGI Settings.

In the application entry in FastCGI settings edit the application and select "Environment Variables".

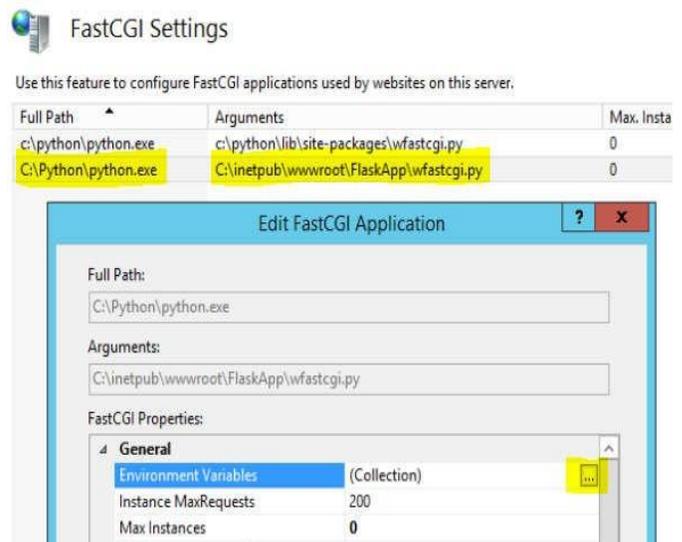


Fig. 30 FastCGI Application.

Open the “Environment Variables Collection Editor”, and add the below entries:

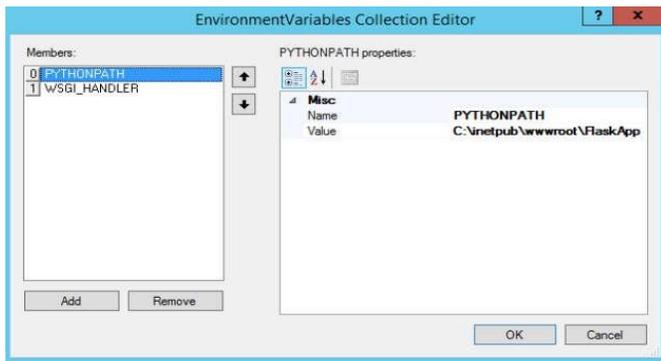


Fig. 31 Python path.

The PYTHONPATH points to the directory containing the Flask Application.

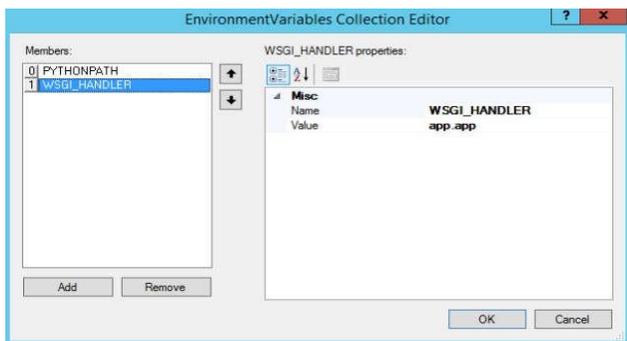


Fig. 32 WSGI properties.

The WSGI_HANDLER points to the application name followed by “.app”. In our case, the application name is “app.py” so WSGI_HANDLER is pointing to “app.app”.

8. **Host the Application on machine IP address**

In the IIS Manager Bindings and in the “http” entry select the Machine IP Address under IP Address drop down.

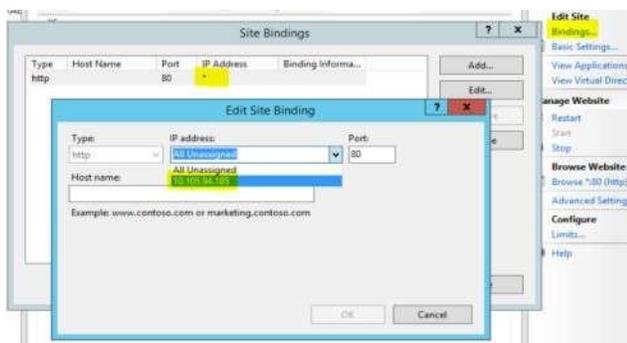


Fig. 33 Edit site binding.

Now the Flask Application is hosted on the EC2 Machine's IP Address.

V. **RESULTS AND ANALYSIS**

Proposed flight prediction model gave the highest accurate model out of all models and for further implementation we integrated our flask-based web application with it. Following are the major parameters in the algorithm inside the model:

1. The number of trees in the proposed algorithm is selected using numpy linspace,
`n_estimators = [int(x) for x in np.linspace(start = 100, stop = 1200, num = 12)]`
2. The number of features to consider at every split in flightprediction algorithm
`max_features = ['auto', 'sqrt']`
3. Maximum number of levels in tree in proposed algorithm
`max_depth = [int(x) for x in np.linspace(5, 30, num = 6)]`
4. Minimum number of samples required to split a node
`min_samples_split = [2, 5, 10, 15, 100]`
5. Minimum number of samples required at each leaf
`min_samples_leaf = [1, 2, 5, 10]`

Proposed flight prediction model results:MAE: 1172.55
 MSE: 4347276.16
 RMSE: 2085.012268

Compared to the following models:Logistic Regression
 MAE:1872.6485727655593
 MSE:10734864.158165652
 RMSE:3276.4102548621186

KNeighbors Regression:
 MAE:1700.4507253158633 MSE:6653493.631445953
 RMSE:2579.436688784191

Decision Tree:
 MAE: 1254.5940570893777
 MSE: 5054622.88482036
 RMSE: 2248.2488485086255

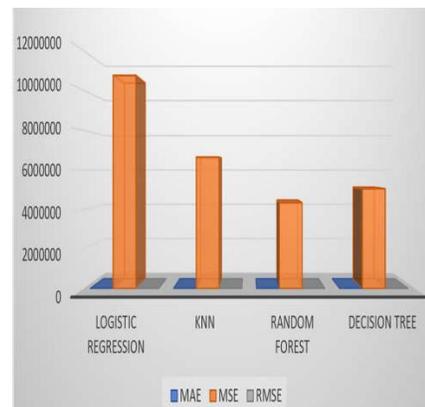


Fig. 34 Comparing results.

The following graph shows the relation between the predicted and test set output i.e., price values.

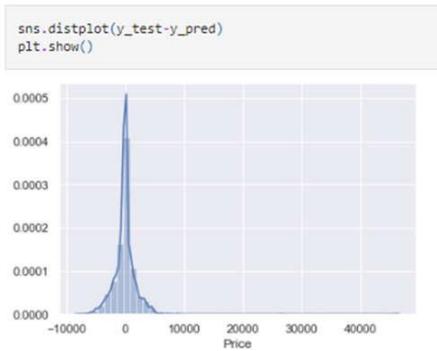


Fig. 35 Outcome-test vs Outcome-predict.

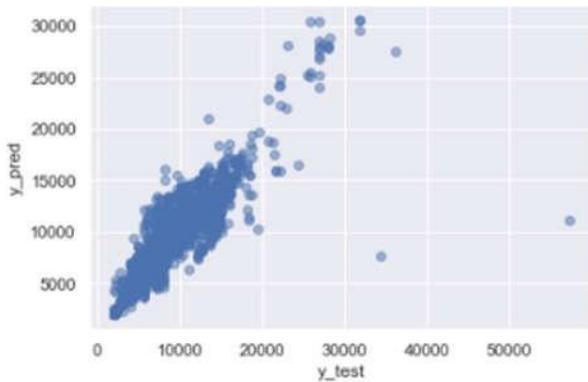


Fig. 36 Output Plot.



Fig. 37 EC2 setup.

Observe that once we have the EC2 setup for the flask web app, whenever the instance is in the running state, we can access the web app using either the instance Public IPv4 or the Public IPv4 DNS.

Access the app and now we can interact with the website and provide input values to get real time predictions.



Fig. 38 Output of web application.

VI. CONCLUSION

The purpose of this work has been to design an accurate prediction model built, trained, and validated on the AWS cloud using SageMaker, converted into a reusable object and embedded as code in a flask web application, which is then securely deployed onto a Windows 2019 Server on the AWS Cloud’s EC2 machine, making it a publicly accessible tool capable of performing real time predictions using user inputs. The accuracy of these predictions is at least 80% when compared to the actual ticket prices, and in the future, this can be increased with more research, testing and computation. The complete web app can also be enhanced in terms of the user interface, and we can make use of persistent data to further personalize each user’s journey and a recommendation layer on top of the application to retain more users. This can also be converted to an API which can then be integrated into a more comprehensive application with multiple user-friendly features. From a cloud perspective if we were to build this tool as a production product for public use, we can make use of modernized services such as containers and Kubernetes for deployment and run data analytic stacks on top of that such as ELK and grafana to get deep insights and points of improvement.

REFERENCES

- [1] K. Tziridis, T. Kalampokas, G. A. Papakostas and K. I. Diamantaras, "Airfare prices prediction using machine learning techniques," 2017 25th European Signal Processing Conference (EUSIPCO), 2017, pp. 1036-1039, doi: 10.23919/EUSIPCO.2017.8081365.
- [2] W. Groves and M. Gini, "An agent for optimizing airline ticket purchasing," in 12th International Conference on Autonomous Agents and Multiagent Systems 2013, AAMAS 2013, 2013, vol. 2, pp. 1341–1342.
- [3] J. S. Domínguez-Menchero, J. Rivera, and E. Torres-Manzanera, "Optimal purchase timing in the airline market," *J. Air Transp. Manag.*, vol. 40, pp. 137–143, 2014, doi: 10.1016/j.jairtraman.2014.06.010.
- [4] S. Rajendran, S. Srinivas, and T. Grimshaw, "Predicting demand for air taxi urban aviation services using machine learning algorithms," *J. Air Transp. Manag.*, vol. 92, p. 102043, May 2021, doi: 10.1016/j.jairtraman.2021.102043.
- [5] T. Wang et al., "A Framework for Airfare Price Prediction: A Machine Learning Approach," 2019 IEEE 20th International Conference on Information Reuse and Integration for Data Science (IRI), 2019, pp. 200-207, doi: 10.1109/IRI.2019.00041.
- [7] T. Janssen, "A Linear Quantile Mixed Regression Model for Prediction of Airline Ticket Prices," *cs.ru.nl*, 2014.

Reviewers

<p>Dr. Vijander Singh Professor, Department of Instrumentation and Control Engineering, Netaji Subhash University of Technology vijaydee@nsut.ac.in</p>	<p>Dr. Navin Rajpal Professor, University School of Information & Communication Technology GGSIPIU, New Delhi navin.rajpall@ipu.ac.in</p>
<p>Dr. Jaya Srivastava Senior Programmer IIT Delhi jsrivastava@rgipt.ac.in</p>	<p>Dr. Balarama Ravindra Professor, Department of Computer Science Engineering Indian Institute of Technology, Madras ravi@cse.iitm.ac.in</p>
<p>Dr. Charu Gupta Associate Professor, Department of Computer Science Engineering Bhagwan Parshuram Institute of Technology, New Delhi charugupta@bpitindia.com</p>	<p>Dr. A L Sangal Professor & Head, Department of Computer Science Engineering Dr. B. R. Ambedkar National Institute of Technology, Jalandhar, Punjab sangalal@nitj.ac.in</p>
<p>Dr. Lokendra Kumar Professor, Department of Mathematics Jaypee Institute of Information Technology lokendma@gmail.com</p>	<p>Dr. Manisha Bharti HOD, Electronics & Communications Engineering Department, NIT Delhi manishabharti@nitdelhi.ac.in</p>
<p>Dr. Amrish Aggarwal Operations Research and Numerical Technique Jaypee Institute of Information Technology amrish.aggarwal@jiit.ac.in</p>	<p>Dr. Jagdish Kumar Professor & Head, Department of Electrical Engineering Punjab Engineering College, University of Technology (PEC Chandigarh) jagdishkumar@pec.edu.in</p>
<p>Dr. Vishwambhar Nath Mishra Professor & Head of Department Department of Electronics Engineering, Indian Institute of Technology, Uttar Pradesh, India vnmishra.ece@iitbhu.ac.in</p>	<p>Dr. Soumitra Das Professor-HOD, Electrical and Electronics Engineering National Institute of technology Goa (NIT Goa) hod.eee@nitgoa.ac.in</p>
<p>Dr. RamaKoteswara Rao Alla Associate Professor Department of Electrical and Electronics Engineering, RVR & JC College of Engineering, Andhra Pradesh, India ramnitkkr@gmail.com</p>	<p>Dr. P Ramani, Assistant Professor, Electronics & Communications Engineering SRM University, Gurugram, India</p>
<p>Mr Ravita Saraswat JRF EE Dept NIT Kurukshetra ravita.saraswat009@gmail.com</p>	<p>Dr. Rajesh Mehta Assistant Professor, Department of Computer Science Engineering Thapar Institute of Engineering and Technology rajesh.mehta@thapar.edu</p>

<p>Mr. Saurabh Gulati Test Manager Robert Bosch Engineering and Business Solutions Private Limited saurabh.gulati@bosch.com</p>	<p>Dr. Manoj Kumar Professor, University School of Information & Communication Technology (IPU) GGSIPU, New Delhi manojtaleja@ipu.ac.in</p>
<p>Dr. Archana Sandhu Associate Professor Geeta Engineering College Panipat, Haryana asandhu@geeta.edu.in</p>	<p>Dr. V.P. Vishwakarma Professor, University School of Information & Communication Technology (IPU) GGSIPU, New Delhi vpv@ipu.ac.in</p>
<p>Dr. Vahida Zakirhusen Attar Computer & IT Department College of Engineering Pune vahida@comp.ac.in</p>	<p>Dr A L Sangal Professor (HAG) & Head Computer Science & Engineering (CSE) Dr B R Ambedkar National Institute of Technology, sangalal@nitj.ac.in</p>
<p>Dr. Amita Malik Professor-Computer Science Engineering (CSE) Deenbandhu Chhotu Ram University of Science and Technology Murthal Sonepat (Haryana) amitamalik@dcrustm.ac.in</p>	<p>Dr. Tajinder Singh Arora Assistant Professor, Electronics & Communications Engineering National Institute of Technology, Uttarakhand tajarora@gmail.com</p>
<p>Dr. Kavita Khanna, Professor and HOD - CSE The NorthCap University Gurugram kavitakhanna@ncuindia.edu</p>	<p>Dr. Jyotsna Yadav Assistant Professor, University School of Information & Communication Technology (IPU) GGSIPU, New Delhi jyotsnayadav@ipu.ac.in</p>
<p>Dr. Sanjay Kr. Malik Professor, University School of Information & Communication Technology (IPU) GGSIPU, New Delhi skmalik@ipu.ac.in</p>	<p>Dr. Pawan Kumar Dahiya Department of Electronics & Communications Engineering Deenbandhu Chhotu Ram University of Science & Technology, Murtha pawandahiya@gmail.com</p>
<p>Dr. Ashish Bhardwaj HOD, CSE, GTBIT aashish@gtbit.org</p>	<p>Dr. Amit Kumar Singh Assistant Professor, Department of Instrumentation & Control Engg. Dr B R Ambedkar National Institute of Technology, Jalandhar, Punjab singhak@nitj.ac.in</p>
<p>Dr. Akhilesh Singh Assistant Professor, NPS Engineering Institute, Government College, Uttrakhand</p>	<p>Dr Rajneesh Singh Assistant Professor, ECE IIIT, Nagpur rsingh@iiitn.ac.in</p>

<p>Dr. Jayshree Goswa Assistant Professor, Law Institute Alipore, Kolkata, jgjayshreegoswami@gmail.com</p>	<p>Dr. Varsha Assistant Professor, Chandigarh University varshae10453@cumail.in</p>
<p>Dr. Mahak Singh Associate Professor, mahaksingh@ramjas.du.ac.in</p>	<p>Dr. Akhilesh Singh Assistant Professor, NPS Engineering Institute, Government college, Utrakhand</p>
<p>Dr. H.C. Nagaraj Professor and Principal, NMIT, Bengaluru nagaraj.hc@nmit.ac.in, NMIT</p>	<p>Dr. Chinna Ayya Swami Assistant Professor, NIT Calicut, swamy@nitc.ac.in</p>
<p>Dr. Rohit Beniwal Assistant Professor, IT dept., DTU dr.rohitbeniwal@gmail.com</p>	<p>Dr Anu Saini Assistant Professor, CSE dept., GB Pant Inst. of Tech., anuanu16@gmail.com</p>
<p>Dr. Indu Kashyap Professor, MRIIRS indu.kashyap82@gmail.com</p>	<p>Dr. Niranjnamurthy M Assistant Professor, Dept. of ISE, BMSIT, Bangalore niruhsd@gmail.com</p>
<p>Dr Janpreet Singh Lovely Professional University, Punjab janpreet.singh@lpu.co.in</p>	<p>Dr Amita Seehra HOD, ECE GNDEC, Ludhiana</p>
<p>Dr. Shweta Singhal, miss.shweta.singhal@gmail.com</p>	<p>Dr. Deepa Gupta Sen. Lect, CSE, Amity University, Noida dgupta@amity.edu</p>
<p>Dr. Rama Koteswara Rao Alla Associate Professor Department of Electrical and Electronics Engg, RVR &JC College of Engineering, Guntur, Andhra Pradesh, India</p>	<p>Dr.M.Gulam Nabi Alsath Associate Professor, ECE Department, SSN Institutions, Chennai. gulamnabialsathm@ssn.edu.in</p>
<p>Dr. Amit Sharma Associate Prof., IT Department, IMSEC Ghaziabad. amit.faculty@gmail.com</p>	<p>Dr.Pushpendra Singh Associate Prof., IT Department, Raj Kumar Goel Institute of Technology, Ghaziabad pushpit@rkgit.edu.in</p>
<p>Dr. Yogendra Arya Associate Professor, EEE, YMCA, Faridabad yarya@jcboseust.ac.in</p>	<p>Dr. S. Anita Shanthi Associate Professor, Mathematics, Anna Malai University shanthi.anita@yahoo.com</p>
<p>Dr. Pooja Singh Assistant Professor, BCA, MSI Pooja.asm@gmail.com</p>	<p>Mr. Dhyan Pachnanda Business Analyst, Connect Compusys Pvt. Ltd</p>
<p>Dr Preeti Nagrath Associate Professor, Bharati Vidyapeeth, New Delhi preeti.nagrath@bharativedyapeeth.edu</p>	<p>Dr. Jude Hemanth Professor, ECE, Karunya University</p>

<p>Dr Parveen Poon Terang Electrical Engineering Dept., Associate Professor JSSATE, Noida, India ppterang.eed@jssaten.ac.in</p>	<p>Dr Neha Gupta Assistant Professor/Programme Director EE School of Engineering & Technology. Sushant University, Gurgaon guptaneha2207@gmail.com</p>
<p>Dr. Lokendra Kumar Professor, Department of Mathematics, Jaypee Institute of Information Technology</p>	<p>Dr Amrish Kumar Aggarwal Professor, Department of Mathematics, Jaypee Institute of Information Technology</p>
<p>Dr. Puneet Rana Assistant Professor, Mathematics Wenzhou Kean University</p>	<p>Prof. Hardeo Thakur Professor Bennett Univeristy hardeokumar@gmail.com</p>
<p>Dr. Archana Balyan Professor, ECE Department, MSIT</p>	<p>Dr. Alka Singhla Snr. Assistant PProfessor CS Department, IIIT, Noida alkasinghal83@gmail.com</p>
<p>Dr Meena Tushir Professor, EEE Department, MSIT</p>	<p>Dr. Anupama Kaushik, HOD, IT Department, MSIT</p>
<p>Prof. Man Singh Beniwal HOD, Department of Applied Sciences, MSIT</p>	<p>Dr Puneet Azad Associate Professor, ECE Department, MSIT</p>
<p>Dr Kavita Sheroan Associate Professor, CSE Department, MSIT</p>	
<p>Dr Shaifali M. Arora Associate Professor, ECE Department, MSIT</p>	<p>Dr. Rakesh Chikara Assistant Professor, Dept of Applied Science, MSIT</p>
<p>Dr Sudesh Pahal Associate Professor, ECE Department, MSIT</p>	<p>Dr Meena Rao Associate Professor, ECE Department, MSIT</p>
<p>Dr Sunil Gupta Associate Professor, EEE Department, MSIT</p>	<p>Dr. Pradeep Sangwan Associate Professor, ECE Department, MSIT</p>
<p>Dr Neeru Rathee Associate Professor, ECE Department, MSIT</p>	<p>Dr Amita Yadav, Associate Professor, CSE Department, MSIT</p>
<p>Dr. Tripti Sharma Associate Professor, IT, MSIT tripti_sharma@msit.in</p>	<p>Dr Deepti Assistant Professor, ECE Department, MSIT</p>
<p>Dr Anshul Pareek Assistant Professor, ECE Department, MSIT</p>	<p>Dr. Poonam Assistant Professor, ECE Department, MSIT</p>
<p>Dr Geetika Associate Professor, CSE Department, MSIT</p>	<p>Dr. Sitender Assistant Professor, IT Department, MSIT</p>
<p>Dr. Monu Malik Assistant Professor, EEE, Department, MSIT</p>	<p>Dr. Rakhi Kamra Assistant Professor, EEE Department, MSIT</p>